NAVAL POSTGRADUATE SCHOOL
Monterey, California

THESIS

MISSILE MISDISTANCE REDUCTION:
AN INSTRUCTIVE METHODOLOGY FOR DEVELOPING
TERMINAL GUIDANCE CONTROL SYSTEMS TO
MINIMIZE MISSILE MISDISTANCE

by

Gregory George Voulgarakis

October 1982

Thesis Advisor: Daniel J. Collins
Co-advisor: George Thaler

Approved for public release; distribution unlimited

REPORT DOCUMENTATION PAGE		READ INSTRUCTIONS BEFORE COMPLETING FORM
1. REPORT NUMBER	2. GOVT ACCESSION NO.	3. RECIPIENT'S CATALOG NUMBER
4. TITLE (and Subtitle) Missile Misdistance Reduction: An Instructive Methodology for Developing Terminal Guidance Control Systems to Minimize Missile Misdistance		5. TYPE OF REPORT & PERIOD COVERED Master's Thesis October 1982 6. PERFORMING ORG. REPORT NUMBER
7. AUTHOR(s) Gregory George Voulgarakis		8. CONTRACT OR GRANT NUMBER(s)
9. PERFORMING ORGANIZATION NAME AND ADDRESS Naval Postgraduate School Monterey, California 93940		10. PROGRAM ELEMENT, PROJECT, TASK AREA & WORK UNIT NUMBERS
11. CONTROLLING OFFICE NAME AND ADDRESS Naval Postgraduate School Monterey, California 93940		12. REPORT DATE October 1982 13. NUMBER OF PAGES 260
14. MONITORING AGENCY NAME & ADDRESS(if different from Controlling Office)		15. SECURITY CLASS. (of this report) Unclassified 15a. DECLASSIFICATION/ DOWNGRADING SCHEDULE

16. DISTRIBUTION STATEMENT (of this Report)

Approved for public release; distribution unlimited

17. DISTRIBUTION STATEMENT (of the abstract entered in Block 20, if different from Report)

18. SUPPLEMENTARY NOTES

19. KEY WORDS (Continue on reverse side if necessary and identify by block number)

Missiles
Missile Control Laws
PN and Augmented PN
State Variable Control

20. ABSTRACT (Continue on reverse side if necessary and identify by block number)

The present thesis is an instructive methodology for developing and improving guidance control systems, in order to minimize the missile misdistance. The complexity of the system which is under development depends heavily upon the defined assumptions, scenarios, specifications, current technology and cost effectiveness. It depends on the designer or the expert,

to weigh up the advantages and disadvantages of all the above, according to their availability, for obtaining best results.

Approved for public release; distribution unlimited

Missile Misdistance Reduction: An Instructive Methodology for Developing Terminal Guidance Control Systems to Minimize Missile Misdistance

by

Gregory George Voulgarakis
Lieutenant, Hellenic Navy
B.S., Naval Postgraduate School, 1980

Submitted in partial fulfillment of the
requirements for the degrees of

MASTER OF SCIENCE IN ELECTRICAL ENGINEERING
and
MASTER OF SCIENCE IN AERONAUTICAL ENGINEERING

from the

NAVAL POSTGRADUATE SCHOOL
October 1982

ABSTRACT

The present thesis is an instructive methodology for developing and improving guidance control systems, in order to minimize the missile misdistance. The complexity of the system which is under development depends heavily upon the defined assumptions, scenarios, specifications, current technology and cost effectiveness. It depends on the designer or the expert, to weigh up the advantages and disadvantages of all the above, according to their availability, for obtaining best results.

TABLE OF CONTENTS

ACKNOWLEDGMENT

I would like to express my very deep gratitude to professors D. J. Collins and G. Thaler, whose knowledge, guidance and help enabled me to complete this study.

This document is dedicated to the Greek tax payers, whose contribution supported my studies, and to my beloved wife Jinny.

I. INTRODUCTION

A missile is an unmanned sophisticated airframe design, carrying a warhead and aimed to kill a target.

In order to kill the target when the warhead explodes, a guidance system is needed to get the missile close enough to the target. Therefore, an appropriate measure of guidance performance is miss-distance, which is defined as the minimum distance between the missile and the target. Miss-distance is the measure of homing performance, and miss-distance is affected by the following three main guidance parameters:

(a) Used guidance law

(b) Relative stability

(c) Response time.

Two other important causes of miss-distance due to target's characteristics are:

(a) Random target maneuver

(b) Glint noise.

The required flight control system properties of the missile are affected by:

(a) The type of target-sea vessel, ground vehicle or airframe (i.e. airplane, missile)

(b) The aerodynamic properties of the missile, whether it is stable or unstable, winged or wingless

(c) The aerodynamic characteristics of the missile (aerodynamic coefficients)

(d) The zone of performance required--short, medium or long range, low or high speed, low, medium or high altitude and other operational characteristics of a possible scenario

(e) The type and quality of used instrumentation

(f) Many other interdiscipline design factors that occur during the missile design development work.

The type of target determines the maneuver capability required by the missile and in conjunction with the type of sensor and background environment, determines the noise that contaminates the target signal needed for homing. For instance a ship gives a strong radar return, but its complex shape generates much radar noise. The relatively low maneuverability of the ship and its sea level location minimize the maneuverability and the extent of the altitude versus Mach envelope required by the missile. The tank target is similar but with different noise and clutter properties than those of the ship. The aircraft target is quite different. Its high maneuverability and fast response in conjunction with its daily improving survivability, and the large flight envelope of modern aircraft, further burdens the missile aerodynamic and flight control system design.

Today, the trade-off in missile design is towards the reduction of missile size and consequently weight, by developing guidance systems leading to minimum possible miss distances. This magnifies the importance of guidance component imperfections and dictates relatively stringent control

of the flight control system dynamics--acceleration gain, time constant and relative stability.

This study deals with the antiairframe missile control system. Specifically it deals with the terminal guidance as it is developed in the following.

II. EQUATIONS OF MOTION

A. GENERAL EQUATIONS OF MOTION

It is well known that on each material body there are acting forces and moments.

Newton's law, concerning an inertial system states that:

$$\sum \vec{F} = m\vec{\gamma} \qquad \text{(II.A-1)}$$

It is also known that in the case of a kinematic system, the following is valid:

$$\left(\frac{d}{dt}\right)_{\text{inertia}} = \frac{d}{dt}(\ ) + \omega\times(\ ) \qquad \text{(II.A-2)}$$

Thus in case of a freely maneuvering body, the application of equation (II.A-2) into equation (II.A-1) gives:

$$\sum \vec{F} = m\left[\frac{d}{dt}(\vec{V}_m) + \vec{\omega}\times\vec{V}_m\right] \qquad \text{(II.A-3)}$$

where: $\sum \vec{F}$: total force acting on a missile

$\vec{V}_m$: vector velocity of a missile

$\vec{\omega}$: angular rate of a missile

m: mass of a missile (it is considered as constant for simplification reasons)

$\frac{d}{dt}(\vec{V}_m)$: linear acceleration

$\vec{\omega}\times\vec{V}_m$: centripical acceleration

The total force acting on a missile is given by:

$$\sum \vec{F} = m\vec{g} + \vec{F}_T + \vec{F}_A \qquad \text{(II.A-4)}$$

where: $m\vec{g}$: missile weight

$\vec{F}_T$: vector thrust of missile motor

$\vec{F}_A$: missile vector aerodynamic force.

$\vec{F}_T$ and $\vec{F}_A$ are controllable applied to the missile forces while $m\vec{g}$ is uncontrollable existing force.

In this study, the missile is considered as moving into the perceivable three-dimensional (3-D) space. Thus, utilizing an orthogonal 3-D Cartesian coordination system with the X-axis along the missile longitudinal axis, and making use of international notation, the following expressions are derived:

$$\vec{V}_m = U\vec{i} + V\vec{j} + W\vec{k} \qquad \text{(II.A-5)}$$

$$\vec{\omega} = P\vec{i} + Q\vec{j} + R\vec{k} \qquad \text{(II.A-6)}$$

$$\vec{g} = g_x\vec{i} + g_y\vec{j} + g_z\vec{k} \qquad \text{(II.A-7)}$$

$$\vec{F}_T = F_{T_x}\vec{i} + F_{T_y}\vec{j} + F_{T_z}\vec{k} \qquad \text{(II.A-8)}$$

$$\vec{F}_A = F_{A_x}\vec{i} + F_{A_y}\vec{j} + F_{A_z}\vec{k} \qquad \text{(II.A-9)}$$

where: F_{A_x}: drag force (II.A-9a)

F_{A_y}: side (II.A-9b)

F_{A_z}: lift (II.A-9c)

$$\vec{F} = F_x\vec{i} + F_y\vec{j} + F_z\vec{k} \qquad \text{(II.A-10)}$$

$$F_x = F_{T_x} - F_{A_x} + mg_x = X + mg_x \qquad \text{(II.A-10a)}$$

$$F_y = F_{T_y} + F_{A_y} + mg_y = Y + mg_y \qquad \text{(II.A-10b)}$$

$$F_z = F_{T_z} + F_{A_z} + mg_z = Z + mg_z \qquad \text{(II.A-10c)}$$

$$\vec{\omega} \times \vec{V}_m = \begin{vmatrix} \vec{i} & \vec{j} & \vec{k} \\ P & Q & R \\ U & V & W \end{vmatrix} \qquad \text{(II.A-11)}$$

Expanding equation (II.A-3) in 3-D and utilizing equations (II.A-4) - (II.A-11), the following three force equations are derived:

$$F_x = m\left[\frac{d}{dt}U + QW - RV\right] \qquad \text{(II.A-12a)}$$

$$F_y = m\left[\frac{d}{dt}V + RU - PW\right] \qquad \text{(II.A-12b)}$$

$$F_z = m\left[\frac{d}{dt}W + PV - QU\right] \qquad \text{(II.A-12c)}$$

It is also well known that the absolute rate of change of the moment of momentum (with respect to flight path axis), for a freely maneuvering body in 3-D, is given by:

$$\frac{d\vec{h}_{abs}}{dt} = \frac{d\vec{h}}{dt} + \vec{\omega} \times h \qquad \text{(II.A-13)}$$

Making use of international notation, the following expressions are derived:

$$\frac{d\vec{h}_{abs}}{dt} = L\vec{i} + M\vec{j} + N\vec{k} \qquad \text{(II.A-14)}$$

$$\vec{h} = h_x\vec{i} + h_y\vec{j} + h_z\vec{k} \qquad \text{(II.A-15)}$$

$$h_x = PI_{xx} - QI_{xy} - RI_{xz} \qquad \text{(II.A-16a)}$$

$$h_y = -PI_{yx} + QI_{yy} - RI_{yz} \qquad \text{(II.A-16b)}$$

$$hz = -PI_{zx} - QI_{zy} + RI_{zz} \qquad \text{(II.A-16c)}$$

Moments of inertia: $I_{xx} = \int (y^2 + z^2)\,dm$ (II.A-17a)

$$I_{yy} = \int (z^2 + x^2)\,dm \quad \text{(II.A-17b)}$$

$$Izz = \int (x^2 + y^2)\,dm \quad \text{(II.A-17c)}$$

Products of inertia: $I_{xy} = I_{yx} = \int xydm$ (II.A-17d)

$$I_{yz} = I_{zy} = \int yzdm \quad \text{(II.A-17e)}$$

$$I_{zx} = I_{xz} = \int zxdm \quad \text{(II.A-17f)}$$

$$\vec{\omega} \times \vec{h} = \begin{vmatrix} \vec{i} & \vec{j} & \vec{k} \\ P & Q & R \\ h_x & h_y & h_z \end{vmatrix} \quad \text{(II.A-18)}$$

Expanding equation (II.A-13) in 3-D and utilizing equation (II.A-14) up to (II.A-18), the following three moment equations are derived, which in matrix notation are:

$$\begin{vmatrix} L \\ M \\ N \end{vmatrix} = \begin{vmatrix} I_{xx} & -I_{xy} & -I_{xz} \\ -I_{yx} & I_{yy} & -I_{yz} \\ -I_{zx} & -I_{zy} & I_{zz} \end{vmatrix} \begin{vmatrix} \dot{P} \\ \dot{Q} \\ \dot{R} \end{vmatrix} + \begin{vmatrix} 0 & -I_{yz} & I_{yz} \\ I_{xz} & 0 & -I_{xz} \\ -I_{xy} & I_{xy} & 0 \end{vmatrix} \begin{vmatrix} P^2 \\ Q^2 \\ R^2 \end{vmatrix}$$

$$+ \begin{vmatrix} -I_{xz} & (I_{zz} - I_{yy}) & I_{xy} \\ I_{yz} & -I_{xy} & (I_{xx} - I_{zz}) \\ (I_{yy} - I_{xx}) & I_{xz} & -I_{yz} \end{vmatrix} \begin{vmatrix} PQ \\ QR \\ RP \end{vmatrix} \quad \text{(II.A-19)}$$

The three force equations (II.A-12) and the three moment equations (II.A-19) are the six equations which describe the

motion of any body with six degrees of freedom in the 3-D orthogonal Cartesian coordinate system. Actually, these equations are not linear.

Up to this point of derivations, the only assumption that has been made is that the missile mass remain constant.

B. NOTATION AND CONVENTIONS

It is accepted internationally that the missile 3-D orthogonal Cartesian coordination system be centered on its center of gravity and fixed in the body as follows:

x-axis, called the roll axis, forwards, along the axis of symmetry if one exists, but in any case in the plane of symmetry.

y-axis, called the pitch axis, outwards and to the right if viewing the missile from behind.

z-axis, called the yaw axis, downwards in the plane of symmetry to form a right handed orthogonal system with the other two.

The forces and moments acting on the missile, the linear and angular velocities, and the moments and products of inertia are shown in Fig. (II.B-1) and their notation is summarized in Table (II.B-1).

The yaw plane is the xoy plane and the pitch plane is the xoz plane.

In the missile study, the following angles are defined:

α: incidence in the pitch plane. It is called angle of attack and is equal to $\alpha = w/u$

β: incidence in the yaw plane. It is called side slip angle and is equal to $\beta = v/u$

λ: incidence plane angle

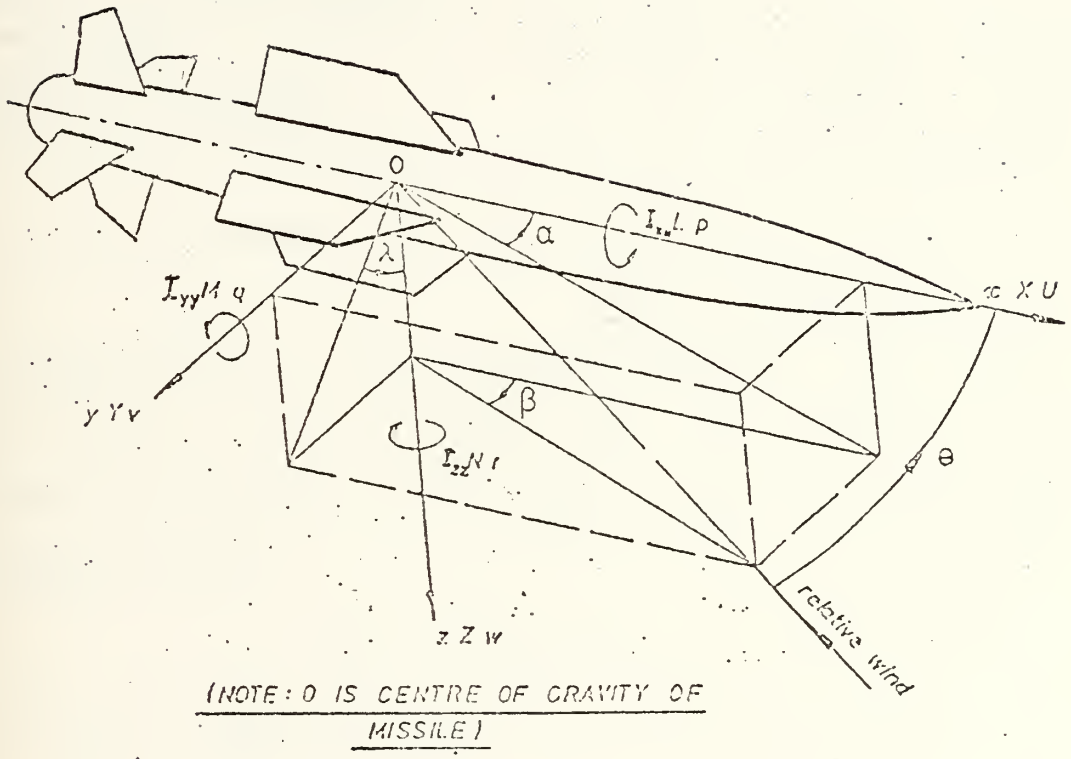

(NOTE: O IS CENTRE OF GRAVITY OF MISSILE)

Figure II.B-1 Forces, Moments, etc. Conventions

Table II.B-1. Notation

Axis	Roll x	Pitch y	Yaw z
Angular rates	P	Q	R
Component of missile velocity along each axis	U	V	W
Component of force acting on missile along each axis	X	Y	Z
Moments acting on missile about each axis	L	M	N
Moments of inertia about each axis	I_{xx}	I_{yy}	I_{zz}
Products of inertia	I_{yz}	I_{xz}	I_{xy}

θ: Total incidence, such that: $\tan \alpha = \tan \theta \cos \lambda$

$\tan \beta = \tan \theta \sin \lambda$

In any body and for any plane of symmetry, two out of three products of inertia become zero. For instance, for a projectile like missile (as in Fig. II.B-1), if xz is a plane of symmetry, then:

$$I_{xy} = I_{yz} = 0$$

$$\text{but} \quad I_{zx} \neq 0$$

C. FURTHER DEVELOPMENT OF MOTION EQUATIONS

It is plainly obvious, that no one missile has undisturbed flight, due to a lot of reasons; for instance, atmospheric variations, target motion, jittering, glint, etc.

Thus, at any moment, the velocity and angular rate vector components will be:

$$U = U_0 + u \rightarrow \dot{U} = \dot{u} \qquad \text{(II.C-1a)}$$

$$V = V_0 + v \rightarrow \dot{V} = \dot{v} \qquad \text{(II.C-1b)}$$

$$W = W_0 + w \rightarrow \dot{W} = \dot{w} \qquad \text{(II.C-1c)}$$

$$P = P_0 + p \rightarrow \dot{P} = \dot{p} \qquad \text{(II.C-2a)}$$

$$Q = Q_0 + q \rightarrow \dot{Q} = \dot{q} \qquad \text{(II.C-2b)}$$

$$R = R_0 + r \rightarrow \dot{R} = \dot{r} \qquad \text{(II.C-2c)}$$

where the component subscripted with zero represents the steady state vector component and the unsubscripted component represents the perturbation of the vector component along each axis.

The steady state of the missile orientation will result in the following gravitational force components:

$$g_x = -g \sin \theta_0 \qquad \text{(II.C-3a)}$$

$$g_y = g \cos \theta_0 \sin \phi_0 \qquad \text{(II.C-3b)}$$

$$g_z = g \cos \theta_0 \cos \phi_0 \qquad \text{(II.C-3c)}$$

where:

$$\vec{g} = g_x\vec{i} + g_y\vec{j} + g_z\vec{k} \qquad \text{(II.C-3)}$$

ϕ_0: angle of vehicle lateral axis with respect to local horizontal

θ_0: angle of vehicle longitudinal axis with respect to local horizontal

ψ_0: angle of vehicle vertical axis with respect to local horizontal.

Also, due to instant perturbations, there will be:

$$\Phi = \phi_0 + \phi \qquad \text{(II.C-4a)}$$

$$\Theta = \theta_0 + \theta \qquad \text{(II.C-4b)}$$

$$\Psi = \psi_0 + \psi \qquad \text{(II.C-4c)}$$

The general Direction Cosine Matrix is:

$$[\text{Cosine Matrix}] = \begin{vmatrix} \cos\theta\cos\psi & \cos\theta\sin\psi & -\sin\theta \\ \left(\begin{matrix}\cos\psi\sin\theta\sin\phi \\ -\sin\psi\cos\phi\end{matrix}\right) & \left(\begin{matrix}\cos\psi\cos\phi \\ +\sin\psi\sin\theta\sin\phi\end{matrix}\right) & \cos\theta\sin\phi \\ \left(\begin{matrix}\cos\psi\sin\theta\cos\phi \\ +\sin\psi\sin\phi\end{matrix}\right) & \left(\begin{matrix}\sin\psi\sin\theta\cos\phi \\ -\cos\psi\sin\phi\end{matrix}\right) & \cos\theta\cos\phi \end{vmatrix} \qquad \text{(II.C-5)}$$

Then:

$$[A'] = [\text{Cosine Matrix}][A] \qquad \text{(II.C-6)}$$

where [A'] is the (3x1) matrix of the components of any force that acts along the axis of the air frame at any instant.

[A] is the (3x1) matrix of the components of any force that acts along the steady state flight path Eurelian axes.

The relations between instantaneous Angular Velocities and their rates due to instantaneous changes in Eurelian axes orientation are:

$$\begin{vmatrix} P \\ Q \\ R \end{vmatrix} = \begin{vmatrix} 1 & 0 & -\sin\theta \\ 0 & \cos\phi & \sin\phi\cos\theta \\ 0 & -\sin\phi & \cos\phi\cos\theta \end{vmatrix} \begin{vmatrix} \dot{\phi} \\ \dot{\theta} \\ \dot{\psi} \end{vmatrix} \qquad \text{(II.C-7)}$$

$$\begin{vmatrix} \dot{\phi} \\ \dot{\theta} \\ \psi \end{vmatrix} = \begin{vmatrix} 1 & \tan\theta \sin\phi & \tan\theta \cos\phi \\ 0 & \cos\phi & -\sin\phi \\ 0 & \frac{\sin\phi}{\cos\theta} & \frac{\cos\phi}{\cos\theta} \end{vmatrix} \begin{vmatrix} P \\ Q \\ R \end{vmatrix} \qquad \text{(II.C-8)}$$

Combining equations (II.C-1) up to (II.C-8) with the equations (II.A-12) and (II.A-19) and after minor manipulations, equations (II.A-13) and (II.A-19) turn into:

$$\frac{X}{m} = [\dot{u} + wQ_0 + qW_0 + qw - vR_0 - rV_0 - rv - g'_x] + [Q_0W_0 - R_0V_0 - g\sin\theta_0 \cos\theta] \qquad \text{(II.C-9a)}$$

$$\frac{Y}{m} = [\dot{v} + uR_0 + rU_0 + ru - wP_0 - pW_0 - pw - g'_y] + [R_0U_0 - P_0W_0 - g\cos\theta_0 \sin\phi_0] \qquad \text{(II.C-9b)}$$

$$\frac{Z}{m} = [\dot{w} + vP_0 + pV_0 + pv - uQ_0 - qU_0 - qu - g'_z] + [P_0V_0 - Q_0U_0 - g\cos\theta_0 \cos\phi_0] \qquad \text{(II.C-9c)}$$

$$L = I_{xx}\dot{p} - I_{xz}\dot{r} - I_{xz}(qP_0 + pQ_0 + pq) + (I_{zz} - I_{yy})(rQ_0 + qR_0 + qr) + [(I_{zz} - I_{yy})Q_0R_0 - I_{xz}P_0Q_0] \qquad \text{(II.C-10a)}$$

$$M = I_{yy}\dot{q} + I_{xz}(2pP_0 + p^2 - 2rR_0 - r^2) + (I_{xx} - I_{zz})(rP_0 + pR_0 + rp) + [I_{xz}(P_0^2 - R_0^2) + (I_{xx} - I_{zz})R_0P_0] \qquad \text{(II.C-10b)}$$

$$N = I_{zz}r + (I_{yy} - I_{xx})(pQ_0 + qP_0 + qp)$$
$$+ I_{xz}(qR_0 + rQ_0 + qr - p)$$
$$+ [(I_{yy} - I_{xx})P_0Q_0 + I_{xz}Q_0R_0] \qquad \text{(II.C-10c)}$$

Applying Taylor's series expansion around the operating point, the first parts of equations (II.C-9) and (II.C-10) turn into the general following form:

$$A = A_0 + dA + H.O.T. \qquad \text{(II.C-11)}$$

where A_0: the steady state component

dA: the first order perturbation around the operating point

H.O.T.: High Order Terms of perturbation, which are considered negligible and thus omitted for the rest of this study.

If there are not perturbations, which means

$$u = v = w = p = q = r = 0$$

then equations (II.C-9) and (II.C-10) turn into:

$$\frac{X_0}{m} = Q_0W_0 - R_0V_0 - g\sin\theta_0\cos\theta_0 \qquad \text{(II.C-12a)}$$

$$\frac{Y_0}{m} = R_0U_0 - P_0W_0 - g\cos\theta_0\sin\phi_0 \qquad \text{(II.C-12b)}$$

$$\frac{Z_0}{m} = P_0V_0 - Q_0U_0 - g\cos\theta_0\cos\phi_0 \qquad \text{(II.C-12c)}$$

$$L_0 = (I_{zz} - I_{yy})Q_0R_0 - I_{xz}P_0Q_0 \qquad \text{(II.C-13a)}$$

$$M_0 = I_{xz}(P_0^2 - R_0^2) + (I_{xx} - I_{zz})R_0P_0 \qquad \text{(II.C-13b)}$$

$$N_0 = (I_{yy} - I_{xx})P_0Q_0 + I_{xz}Q_0R_0 \qquad \text{(II.C-13c)}$$

Equations (II.C-12) and (II.C-13) are called "trim equations" and concern the absolute stability of the missile around the operating point.

Subtracting the "trim equations" from equations (II.C-9) and (II.C-10) correspondingly, the following equations result:

$$\frac{dX}{m} = \dot{u} + wQ_0 + qW_0 + qw - vR_0 - rV_0 - rv - g'_x \qquad \text{(II.C-14a)}$$

$$\frac{dY}{m} = \dot{v} + uR_0 + rU_0 + ru - wP_0 - pW_0 - pw - g'_y \qquad \text{(II.C-14b)}$$

$$\frac{dZ}{m} = \dot{w} + vP_0 + pV_0 - pv - uQ_0 - qU_0 - qu - g'_z \qquad \text{(II.C-14c)}$$

$$dL = I_{xx}\dot{p} - I_{xz}\dot{r} - I_{xz}(qP_0 + pQ_0 + pq) + (I_{zz} - I_{yy})(rQ_0 + qR_0 + qr) \qquad \text{(II.C-15a)}$$

$$dM = I_{yy}\dot{q} + I_{xz}(2pP_0 + p^2 - 2rR_0 - r^2) + (I_{xx} - I_{zz})(rP_0 + pR_0 + rp) \qquad \text{(II.C-15b)}$$

$$dN = I_{zz}\dot{r} + (I_{yy} - I_{zz})(pQ_0 + qP_0 + qp) + I_{xz}(qR_0 + rQ_0 + qr - \dot{p}) \qquad \text{(II.C-15c)}$$

These equations (II.C-14) and (II.C-15) are called "perturbation equations" and will be the subject of concern for the rest of this study.

At this point, it can be written that:

Equations of motion = (trim equations) + (perturbation equations)

D. FURTHER DEVELOPMENT OF PERTURBATION EQUATIONS

It is possible for a missile to look like an aeroplane. Thus, its hull may have all or some of the following controllable mechanisms:

Elevator

Ailerons

Rudders

Flaps

Dive brakes

Controllable directionally thrust vector

Controlling the above mechanisms a deflection angle is created as follows:

E: Elevator deflection angle

A: Aileron deflection angle

R: Rudder deflection angle

F: Flap deflection angle

B: Dive brakes deflection angle

T: Thrust deflection angle

These deflections result in perturbation quantities, the effects of which depend upon the design characteristics of each one part. These perturbating quantities are usually noted as:

$$\delta_j \quad \text{where } j \text{ is E or A,R,F,B,T.}$$

For the rest of this study, the effect of all these perturbation quantities due to deflections will be denoted as δ.

Furthermore the thrust vector will be considered steady and acting along the fuselage axis.

Any one of the components X,Y,Z,L,M,N is a function of u,v,w,p,q,r and their rates. In general, any one of the above quantities can be denoted as follows:

$$A \triangleq A(u,v,w,p,q,r,\delta,\dot{u},\dot{v},\dot{w},\dot{p},\dot{q},\dot{r},\dot{\delta}) \qquad \text{(II.D-1)}$$

and

$$dA \triangleq dA(u,v,w,p,q,r,\delta,\dot{u},\dot{v},\dot{w},\dot{p},\dot{q},\dot{r},\dot{\delta}) \qquad \text{(II.D-1a)}$$

The expansion of equation (II.D-1a) gives:

$$dA = \frac{\partial A}{\partial u}du + \frac{\partial A}{\partial v}dv + \frac{\partial A}{\partial w}dw + \frac{\partial A}{\partial p}dp + \frac{\partial A}{\partial q}dq + \frac{\partial A}{\partial r}dr + \frac{\partial A}{\partial \delta}d\delta$$
$$+ \frac{\partial A}{\partial \dot{u}}d\dot{u} + \frac{\partial A}{\partial \dot{v}}d\dot{v} + \frac{\partial A}{\partial \dot{w}}d\dot{w} + \frac{\partial A}{\partial \dot{p}}d\dot{p} + \frac{\partial A}{\partial \dot{q}}d\dot{q} + \frac{\partial A}{\partial \dot{r}}d\dot{r} + \frac{\partial A}{\partial \dot{\delta}}d\dot{\delta} \qquad \text{(II.D-1b)}$$

In perturbation theory, the perturbating quantities are assumed very small, thus:

$$u,v,w,p,q,r,\delta << 1$$

and consequently:

$$du,dv,dw,dp,dq,dr,d\delta << 1$$

After all the above, with reasonable accuracy it can be considered:

$$\begin{aligned} u &= du \quad & v &= dv \quad & w &= dw \\ p &= dp \quad & q &= dq \quad & r &= dr \quad & \delta &= d\delta \\ \dot{u} &= d\dot{u} \quad & \dot{v} &= d\dot{v} \quad & \dot{w} &= d\dot{w} \\ \dot{p} &= d\dot{p} \quad & \dot{q} &= d\dot{q} \quad & \dot{r} &= d\dot{r} \quad & \dot{\delta} &= d\dot{\delta} \end{aligned} \qquad \text{(II.D-2)}$$

For convenient notation it is introduced:

$$\frac{1}{m}\frac{\partial F}{\partial r} = F_r \qquad \text{(II.D-3a)}$$

$$\frac{1}{I_{hh}}\frac{\partial H}{\partial r} = H_r \qquad \text{(II.D-3b)}$$

where F: x/x X,Y,Z

H: x/x L,M,N

r: x/x $u,v,w,p,q,r,\delta,\dot{u},\dot{v},\dot{w},\dot{p},\dot{q},\dot{r},\dot{\delta}$

h: x/x x,y,z

Introducing equations (II.D-2) and (II.D-3) into equation (II.D-1b) the last equation turns into:

$$\frac{1}{m}dF = F_u u + F_v v + F_w w + F_p p + F_q q + F_r r + F_\delta \delta + F_{\dot{u}}\dot{u} + F_{\dot{v}}\dot{v} + F_{\dot{w}}\dot{w} + F_{\dot{p}}\dot{p} + F_{\dot{q}}\dot{q} + F_{\dot{r}}\dot{r} + F_{\dot{\delta}}\dot{\delta} \qquad \text{(II.D-4a)}$$

$$\frac{1}{I_{hh}}dH = H_u u + H_v v + H_w w + H_p p + H_q q + H_r r + H_\delta \delta + H_{\dot{u}}\dot{u} + H_{\dot{v}}\dot{v} + H_{\dot{w}}\dot{w} + H_{\dot{p}}\dot{p} + H_{\dot{q}}\dot{q} + H_{\dot{r}}\dot{r} + H_{\dot{\delta}}\dot{\delta} \qquad \text{(II.D-4b)}$$

The coefficients F_r or H_r are called aerodynamics derivatives or coefficients. These are normalized quantities and their magnitudes depend upon the aerodynamic characteristics of the missile. Hopefully, in practical aspects, some of these coefficients can be ignored as very small and thus negligible quantities.

The aerodynamic derivatives are devices enabling the control engineers to obtain transfer functions defining the

response of a missile to its aileron, elevator or rudder deflections.

At this point, it must be recalled that "the missile aerodynamic forces are relative to the atmosphere and NOT to the inertial space." Thus, if there exists atmospheric turbulence or motion, terms representing the gust loading (turbulence) must be added to equation (II.D-4) as follows:

$$\frac{1}{m}dF = F_u((u - u_g) + F_v(v - v_g) + \ldots \qquad \text{(II.D-4a.1)}$$

$$\frac{1}{I_{hh}}H = H_u(u - u_g) + H_v(v - v_g) + \ldots \qquad \text{(II.D-4b.1)}$$

The derivation of aerodynamic derivatives is beyond the scope of this study. Thus, these are not derived but used in the rest of this study.

After all the above, the perturbation equations in full expansion are shown in table (II.D-1).

Often it is required to express the equations in terms of the angle of attack α and side slip angle β rather than in terms of w and v.

Since $\alpha = W/U_0$ and $\beta = v/U_0$ it follows:

$$w = \alpha U_0 \quad \rightarrow \quad \partial w = U_0 \partial \alpha$$

$$v = \beta U_0 \quad \rightarrow \quad \partial v = U_0 \partial \beta$$

$$F_w w = \frac{1}{m}\frac{\partial F}{\partial w} w = \frac{1}{m}\frac{\partial F}{\partial \alpha}\frac{1}{U_0}\alpha U_0 = F_\alpha \alpha$$

$$F_v v = \frac{1}{m}\frac{\partial F}{\partial v} v = \frac{1}{m}\frac{\partial F}{\partial \beta}\frac{1}{U_0}\beta U_0 = F_\beta \beta$$

Table II.D-1. Perturbation equations in full expansion. For α missile with one plane of symmetry.

$$u + wQ_0 + qW_0 + qw - vR_0 - rV_0 - rv - g'_x = X_u u + X_v v + X_w w + X_p p + X_q q + X_r r + X_\delta \delta$$
$$X_\beta \beta \quad X_\alpha \alpha$$
$$+ X_{\dot{u}} \dot{u} + X_{\dot{v}} \dot{v} + X_{\dot{w}} \dot{w} + X_{\dot{p}} \dot{p} + X_{\dot{q}} \dot{q} + X_{\dot{r}} \dot{r} + X_{\dot{\delta}} \dot{\delta}$$
$$X_{\dot{\beta}} \dot{\beta} \quad X_{\dot{\alpha}} \dot{\alpha}$$

$$v + uR_0 + rU_0 + ru - wP_0 - pW_0 - pw - g'_y = Y_u u + Y_v v + Y_w w + Y_p p + Y_q q + Y_r r + Y_\delta \delta$$
$$Y_\beta \beta \quad Y_\alpha \alpha$$
$$+ Y_{\dot{u}} \dot{u} + Y_{\dot{v}} \dot{v} + Y_{\dot{w}} \dot{w} + Y_{\dot{p}} \dot{p} + Y_{\dot{q}} \dot{q} + Y_{\dot{r}} \dot{r} + Y_{\dot{\delta}} \dot{\delta}$$

$$w + vP_0 + pV_0 + pv - uQ_0 - qU_0 - qu - g'_z = Z_u u + Z_v v + Z_w w + Z_p p + Z_q q + Z_r r + Z_\delta \delta$$
$$Z_\beta \beta \quad Z_\alpha \alpha$$
$$+ Z_{\dot{u}} \dot{u} + Z_{\dot{v}} \dot{v} + Z_{\dot{w}} \dot{w} + Z_{\dot{p}} \dot{p} + Z_{\dot{q}} \dot{q} + Z_{\dot{r}} \dot{r} + Z_{\dot{\delta}} \dot{\delta}$$

$$\dot{p} - \frac{I_{xz}}{I_{xx}} (r + qP_0 + pQ_0 + pq) + \left(\frac{I_{zz} - I_{yy}}{I_{xx}} \right) (rQ_0 + qR_0 + qr) = L_u u + L_v v + L_w w$$
$$L_\beta \beta \quad L_\alpha \alpha$$
$$+ L_p p + L_q q + L_r r + L_\delta \delta + L_{\dot{u}} \dot{u} + L_{\dot{v}} \dot{v} + L_{\dot{w}} \dot{w} + L_{\dot{p}} \dot{p} + L_{\dot{q}} \dot{q} + L_{\dot{r}} \dot{r} + L_{\dot{\delta}} \dot{\delta}$$

$$\dot{q} + \frac{I_{xz}}{I_{yy}} (2pP_0 + p^2 - 2rR_0 - r^2) + \left(\frac{I_{xx} - I_{zz}}{I_{yy}} \right) (rP_0 + pR_0 + rp) = M_u u + M_v v + M_w w$$
$$M_\beta \beta \quad M_\alpha \alpha$$
$$+ M_p p + M_q q + M_r r + M_\delta \delta + M_{\dot{u}} \dot{u} + M_{\dot{v}} \dot{v} + M_{\dot{w}} \dot{w} + M_{\dot{p}} \dot{p} + M_{\dot{q}} \dot{q} + M_{\dot{r}} \dot{r} + M_{\dot{\delta}} \dot{\delta}$$

$$\dot{r} + \left(\frac{I_{yy} - I_{xx}}{I_{zz}} \right) (pQ_0 + qP_0 + qp) + \frac{I_{xz}}{I_{zz}} (qR_0 + rQ_0 + qr - \dot{p}) = N_u u + N_v v + N_w w$$
$$N_\beta \beta \quad N_\alpha \alpha$$
$$+ N_p p + N_q q + N_r r + N_\delta \delta + N_{\dot{u}} \dot{u} + N_{\dot{v}} \dot{v} + N_{\dot{w}} \dot{w} + N_{\dot{p}} \dot{p} + N_{\dot{q}} \dot{q} + N_{\dot{r}} \dot{r} + N_{\dot{\delta}} \dot{\delta}$$

$$H_w w = \frac{1}{I_{hh}} \frac{\partial H}{\partial w} w = \frac{1}{I_{hh}} \frac{\partial H}{\partial \alpha} \frac{1}{U_0} \alpha U_0 = H_\alpha \alpha$$

$$H_v v = \frac{1}{I_{hh}} \frac{\partial H}{\partial v} v = \frac{1}{I_{hh}} \frac{\partial H}{\partial \beta} \frac{1}{U_0} \beta U_0 = H_\beta \beta$$

These terms $F_\alpha\alpha$, $F_\beta\beta$, $H_\alpha\alpha$, $H_\beta\beta$ are shown underneath their equivalent terms in table (II.D-1).

The equations shown in table (II.D-1) are the six equations of motion of a body with one plane of symmetry and six degrees of freedom. The first three of these equations are force equations while the remaining three are moment equations. All six equations are not linear. These are also coupled to each other. For instance, the term "pw" says that there is a force in the y direction due to incidence in pitch (α = w/U) and roll motion. In other words, the pitching motion of the missile is coupled to the yawing motion on account of roll rate. The term "pv" also says that yawing motion induces forces in the pitch plane if rolling motion is present. This is most undesirable as it is required for these two "channels" to be completely uncoupled. Ideally speaking, rudder movements should produce forces and moments in the yaw plane and result in yawing motion only; elevators should result in a maneuver in the pitch plane. Cross-coupling between the planes contribute to system inaccuracy. To reduce these undesirable effects, the roll rates must be kept as low as possible.

At this point it is desirable to recall that "all three products of inertia (I_{xy}, I_{yz}, I_{zx}) are zero if there are two axes of symmetry, while two will be zero and the third will be small if there is one axis of symmetry and the missile is reasonably symmetrical about another axis."

E. LINEARIZATION AND DECOUPLIZATION OF MISSILE MOTION EQUATIONS

To simplify the study, a projectile like missile is assumed. Such a missile has two axes of symmetry and two planes of symmetry (rotational symmetry). Thus, there will be a correlation between some aerodynamic derivatives and inertia terms as in table (II.E-1) is shown.

Table II.E-1. Some relations due to the rotational symmetry of a projectile like missile.

$I_{xy} = I_{yz} = I_{zx} = 0$		
$I_{yy} = I_{zz}$		
$Y_{\beta} = Z_{\alpha}$	$N_{\beta} = -M_{\alpha}$	$q = -r$
$Y_{\dot{\beta}} = Z_{\dot{\alpha}}$	$N_{v} = -M_{w}$	$v = w$
$Y_{v} = Z_{w}$	$N_{\dot{\beta}} = -M_{\dot{\alpha}}$	
$Y_{r} = -Z_{q}$	$N_{r} = -M_{q}$	
	$N_{\dot{v}} = -M_{\dot{w}}$	

The two planes of symmetry that are used to study the missile motion are the:

a. XOZ plane or longitudinal or pitching motion plane with variables to be examined; $u, w, q, \alpha = w/U_0$, $q = \dot{\theta}$

b. XOY plane or lateral or yawing motion plane with variables to be examined; $v, p, r, \beta = v/U_0$, $p = \dot{\phi}$, $r = \dot{\psi}$

Decouplization of missile motion equations means to delete all the terms (variables) which are not mainly concerned.

For further simplification and in order to facilitate the linearization process, it is assumed that:

a. There is no wind side effect, that is: $W_0 = V_0 = 0$

b. The order of products and squares of perturbating quantities is negligible; thus:

$$qw = rv = ru = pw = pv = qu = qp = rq = p^2 = r^2 = rp = 0$$

c. The order of the following aerodynamic derivatives is negligible:

$$X\dot{w} = Xv = Xp = Xq = Xr = 0$$

$$Yu = Yw = Yp = Yq = Yr = 0$$

$$Z\dot{w} = Zq = Zv = Zp = Zr = 0$$

$$Lu = Lw = Lq = 0$$

$$Mp = Mr = 0$$

After the above assumptions, which from a practical point of view are acceptable, the six equations of missile motion are decoupled, linearized and organized in two sets of equations which are given in a state variable form as follows:

a. Longitudinal Equations

$$\begin{vmatrix} \dot{u} \\ \dot{w} \\ \dot{q} \\ \dot{\theta} \end{vmatrix} = \begin{vmatrix} X_u & X_w & 0 & -g \\ Z_u & Z_w & U_0 & 0 \\ M_u + M_{\dot{w}} Z_u & M_w + M_{\dot{w}} Z_w & M_q + M_{\dot{w}} U_0 & 0 \\ 0 & 0 & 1 & 0 \end{vmatrix} \begin{vmatrix} u \\ w \\ q \\ \theta \end{vmatrix} + \begin{vmatrix} X_\delta \\ Z_\delta \\ M_\delta + M_{\dot{w}} Z_\delta \\ 0 \end{vmatrix} \delta$$

and auxiliary relationship:

$$\alpha_z = \dot{w} - \dot{\theta}U_0 = -\ddot{h}$$

b. Lateral Equations

$$\begin{vmatrix} \dot{\beta} \\ \dot{p} \\ \dot{r} \\ \dot{\phi} \end{vmatrix} = \begin{vmatrix} Y_\beta & 0 & -1 & g/U_0 \\ L'_\beta & L'_p & L'_r & 0 \\ N'_\beta & N'_p & N'_r & 0 \\ 0 & 1 & 0 & 0 \end{vmatrix} \begin{vmatrix} \beta \\ p \\ r \\ \phi \end{vmatrix} + \begin{vmatrix} Y^*_{\delta_a} & Y^*_{\delta_r} \\ L'_{\delta_a} & L'_{\delta_r} \\ N'_{\delta_a} & N'_{\delta_r} \\ 0 & 0 \end{vmatrix} \begin{vmatrix} \delta_a \\ \delta_r \end{vmatrix}$$

where: a: aileron

r: rudder

ϕ: angle due to roll from vertical position.

Equation $\dot{\beta} = Y_\beta\beta - r + g\phi/U_0 + Y^*_{\delta_a}\delta_a + Y^*_{\delta_r}\delta_r$ can be re-replaced by its equivalent $\dot{v} = Y_v v - U_0 r + g\phi + Y_{\delta_a}\delta_a + Y_{\delta_r}\delta_r$ with auxiliary relationships:

$p = \dot{\phi}$ banking rate

$r = \dot{\psi}$ yawing rate

$$\alpha_{y_{c.g.}} = U_0\dot{\beta} - g\phi + U_0 r = \dot{v} - g\phi + U_0 r \qquad (\dot{v} = \dot{\beta}U_0)$$

Note: If the missile has only one plane of systems then:

$$L'_i = \frac{L_i + I_{xz}N_i/I_{xx}}{1 - I^2_{xz}/I_{xx}I_{zz}}$$

$$N'_i = \frac{N_i + I_{xz}L_i/I_{zz}}{1 - I^2_{xz}/I_{xx}I_{zz}}$$

Some control engineers prefer to work with transfer functions. These transfer functions can be derived by applying Laplace transform to the above sets of equations.

F. SUMMARY OF UTILIZED ASSUMPTIONS

The following assumptions were used during the derivation of the decoupled sets of longitudinal and lateral equations.

1. Rigid body with constant mass
2. Projectile-like missile with two planes of symmetry
3. Small perturbation theory
4. In a Taylor series expansion around the operating point, the second and higher order terms are negligible
5. Lots of Aerodynamic coefficients are deleted as negligible quantities
6. No wind side effect
7. The order of products and squares of perturbation quantities are deleted as negligible quantities
8. The terms (variables) which are not mainly concerned in the study of motion in each plane of symmetry are considered as zero.

III. GUIDANCE LAWS

A. DEFINITION OF GUIDANCE LAW

Guidance law is the mathematical modeling of a physical or logical relation between certain perceivable parameters, which enables appropriate missile flight path dynamics to be determined so that some mission objectives might be achieved in an efficient manner.

There have been developed many guidance laws, which have been categorized in two major subsets, the "classical" and the "modern" guidance laws.

Each one of the guidance laws is characterized by varying degrees of performance, complexity and seeker/sensor requirements. The increased accuracy requirements and more dynamic tactics of modern warfare render contemporary guidance laws unsatisfactory in many cases. This is especially true at the last moments of air to air missile engagements. Improving performance involves a trade-off between more sophisticated hardware or more sophisticated software. Increased hardware sophistication almost always results in increased costs. With the advent of new theoretical methods and low cost/high speed microprocessing techniques, the potential exists for tremendous increases in missile brain power with little or no corresponding increase in cost.

B. FLIGHT STAGES OF A MISSILE

The total flight history of any missile can be divided into the following three stages/phases:

1. From Launch Up to Full Activation of All Subsystems

Depending on the designer-manufacturer and safety reasons there are missiles that take a few seconds until all their subsystems become fully activated and capable of functioning.

2. Mid-Course or Stand-off Guidance

This is the phase from the end of previous phase until the missile seeker "locks-on" the target. It is required when the missile is launched at such long ranges from the target that either the missile seeker cannot "see" the target or, if it can, the available guidance information is of sufficiently poor quality that it is unusable. In such a case, the guidance law usually consists of some pre-programmed strategy such as "maintain launch heading and a constant altitude" or "fly directly to where it is believed that the target might be." (In some cases tactical missiles do not have seekers and the complete trajectory can be thought of as a type of mid-course guidance.)

Mid-course guidance is primarily an energy management and inertial instrumentation problem. Although advanced control and estimation techniques are applicable to this problem as well, the objectives are sufficiently different from the objectives of the terminal guidance and control

problem. The study of mid-course is not within the scope of this study.

3. Terminal Guidance

This is the phase where a terminal seeker is "locked-on" to a target and provides reliable tracking data (short-range combat). The dynamic requirements of terminal guidance are usually more stringent because all the trajectory errors which have accumulated must be corrected in a vary short time.

All the above three phases are shown in Fig. III.B-1.

C. TERMINAL GUIDANCE LAW

The terminal guidance law as a part of a guidance loop (Fig. III.C-1) represents an essential component in the design of guided missile systems. The information which is needed to perform the guidance task of missile-target intercept, determines basically the configuration of necessary sensors and information processing.

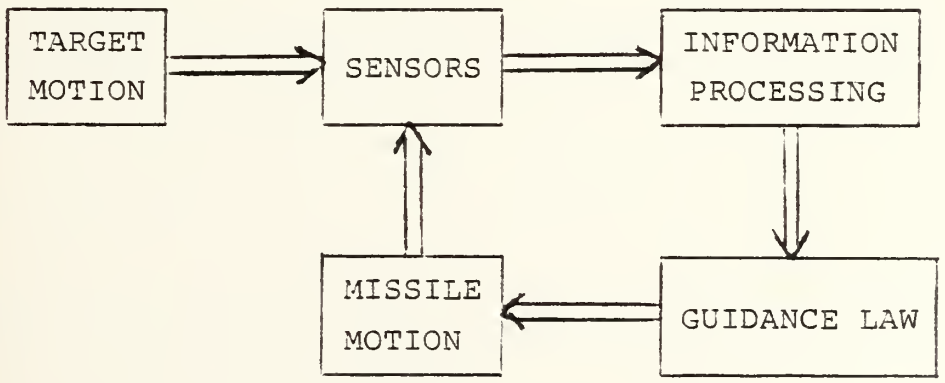

Fig. III.C-1. Structure of information flow in missile guidance loops.

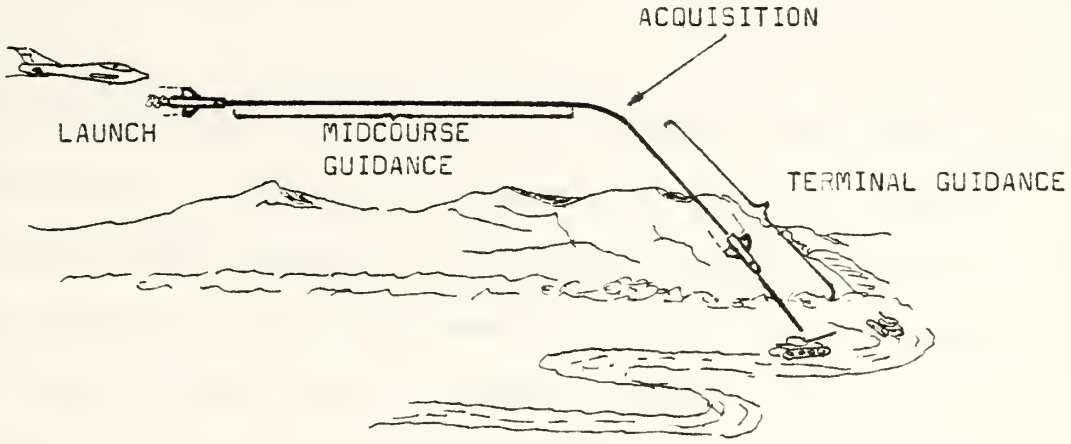

Fig. III.B-1. Typical Tactical Missile Trajectory

The objective of any terminal guidance law is to obtain as small a miss distance as possible. The demands on the missile accelerating capability as an important system parameter depend strongly on the kind of used terminal guidance law.

D. DESIGN PRINCIPLES FOR CLASSICAL GUIDANCE AND CONTROL LAWS

The guidance and control laws used in current tactical missiles are based largely on classical control design techniques. These control laws came into being over 35 years ago and have evolved into fairly standard design procedures. Though the specific guidance and control law varies from one missile to another (depending on its size, weight, cost and manufacturer), the following basic characteristics are common to all of the missiles:

a) The overall control of the missile is divided into two or more loops. The outer guidance loop controls translational degrees of freedom, while the inner, autopilot loop controls missile attitude.

b) Proportional feedback is used to correct missile course in the outer loop (commonly referred to as proportional navigation or "pro-nav"). Pro-nav is quite successful against nonmaneuvering targets.

c) In the inner loop, the roll, pitch and yaw channels are uncoupled and are typically controlled independently of each other.

d) Sensors typically measure aspect angles in pitch and yaw planes and rates may also be available. Advanced sensors may measure other variables.

e) No explicit state estimators are used and the signals are filtered to reject high frequency noise.

f) All commands are amplitude or torque constrained to ensure autopilot and missile stability.

Classical controllers have two major advantages, simplicity in design and simplicity in implementation; but they also have several problems. Table III.D-1 indicates how characteristics of classical short-range missile terminal guidance and control laws lead to advantages and disadvantages in design and implementation.

E. CLASSICAL TERMINAL GUIDANCE AND CONTROL LAWS

Quite a few guidance laws have been developed based upon classical control methods and used widely in missile control over the last 40 years.

There are many factors involved in the selection of a guidance law; i.e. cost, complexity, reliability, type and scenario of engagement, etc. The most popular classical terminal guidance laws are:

1. Command to Line-of-Sight

Strictly speaking, it is not a terminal guidance law because it requires no terminal missile seeker. According to this law, the launcher merely tracks the target, tracks or computes the missile position and sends steering commands to the missile, which are proportional to the angle the missile is off the line-of-sight, in order to guide it along the launcher to target L.O.S. This law is implemented in missiles of generally short range, from several hundred yards to a few miles. A speed advantage of the missile is needed since there is no anticipation or lead in the tracking. The

Table III.D-1. Major Advantages and Disadvantages of Classical Guidance and Control Designs

FEATURE OF CLASSICAL MISSILE CONTROLLER	ADVANTAGES	DISADVANTAGES
Pro Nav Guidance	(1) Requires only LOS rate information from the seeker. LOS rate is often available from somewhere in the seeker tracking loops. (2) This information is used in a simple, easy to implement manner. Also autopilot design becomes more universal; more independent of the properties of the seeker.	(1) Much more information about the pursuit/evation problems is known or available. Not using this information in the guidance law degrades performance.
Uncoupling of Steering and Roll Motions	(1) Can use classical control theory to select autopilot gains. Effects of variations in parameters is well understood. (2) The resulting autopilot design is not very involved. The autopilot can be implemented with either digital or analog circuits.	(1) The missile angle of attack, and thus the missile's maneuverability, is limited by the autopilot. These limits are imposed to keep the missile flight stable, but the limits could be raised of a different method of autopilot design were used.
Dither-Adaptation Scheme	(1) Allows a larger flight envelope, but still is easy to implement. Can be implemented with analog or digital circuits.	(1) Only partially adaptive. Other adaptive methods, perhaps more involved, could be used that would improve missile performance.
Direct Use of Sensor Data	(1) Reduces on-line data processing requirements.	(1) An optimal control law will require use of information that is not directly measurable.
Burning All the Engine Fuel at Once	(1) Engine design is simpler.	(1) May not be optimal solution for minimizing miss distance.

avionics of the missile are relatively simple. The missile must be able to distinguish left-right from up-down commands (roll stabilization or resolver). Commands are sent either by a wire attached to the missile or by a rear antenna on the missile. It is necessary to have the launcher reference system or personnel in the loop continually from launch to impact. So, "launch and forget" is not possible.

2. Pursuit

According to this law, steering commands are generated to drive the angle between the line-of-sight (L.O.S.) and missile velocity vector to zero. That is, the missile steers to head straight for the target. Pursuit navigation can be likened to "dog chasing a rabbit".

This law works well for non-moving or slowly moving targets but it degrades seriously in case of fast targets, such as those found in the air-to-air environment. In the air-to-air mission, the trajectories are clearly suboptimal and usually end in tail chases. However, this guidance law does have the advantage of being relatively insensitive to system noise.

This law can be implemented on medium range missiles. The target is required to give back a good homing signature. It can be used as a "launch and forget at lock-on" method. Its implementation requires, as avionics, homing sensors, simple processing scheme and maybe an observer.

3. Proportional Navigation (P.N.)

The development of this law was a major break-through in homing missile guidance. In P.N. law, steering commands are given so as to drive the line-of-sight rate to zero.

Subsequent studies using optimal control theory have found P.N. to be an "optimal" guidance law when the missile and target have constant velocity, the missile is inertia-less, and the only optimal criterion is to minimize terminal mis-distance. However, assuming constant missile velocity is a serious assumption that neglects considerable thrust and drag effect. Because thrust and drag are present, P.N. is not optimal even against constant velocity targets. Moreover, the targets seldom have constant velocities.

Despite its short-comings, P.N. is easy to implement and, for many years, provided satisfactory missile performance.

P.N. is implemented in "launch and forget upon lock-on" methods of missile steering.

Therefore, it has seen considerable use, although it is somewhat sensitive to unfiltered system noise.

Due to its popularity, P.N. is studied extensively in the next part of this study.

4. Proportional Navigation and Pursuit

There have been several attempts to combine the good features (while simultaneously eliminating the bad ones) of P.N. and pursuit guidance into an overall composite guidance law. The combination of P.N. with reduced navigation gain

and a parallel channel of body pointing pursuit provides a degree of compromise between the two guidance laws. In this case, guidance signals are computed based on both laws, and providing a time varying weighting factor for each one, the resulting signals are summed. Such an application usually weights pursuit guidance heavily at long ranges where the noise problem is most severe and the accuracy requirements less severe. Of course, a knowledge of time-to-go or range is required.

The above concept exhibits a greater tolerance to seeker scale factor errors than P.N. and a greater tolerance to boresight errors than pursuit. The most significant shortcoming of this technique is the relatively poor performance in the presence of wind, target motion and gravity compensation errors. The only situations for which this combination law performs better than P.N. is for large initial offsets and for large scale factor errors. The ability of the pursuit body attitude loop to zero the inital offset results in uniformly good performance for all offsets.

5. Dynamic Lead

This guidance law provides results similar to the weighting technique but for different reasons. At small L.O.S. rate frequencies (which typically occur at long ranges), it behaves like P.N. The advantage is that no estimate of range or time-to-go is necessary; the behavior transitions "automatically" based upon the frequency of the

input signal. It also has the advantage of better performance in a typical situation (e.g. large line-of-sight rates at long ranges). However, stability problems can occur if significant noise is still present when the guidance law transitions to a P.N. type behavior.

In the following table III.E-1 are summarized the advantages and disadvantages of each of the above guidance laws when they are used in combination with classical low pass noise filters.

F. SENSITIVITY COMPARISON OF CLASSICAL TERMINAL GUIDANCE LAWS

The primary purpose of the guidance law is to insure a minimum as possible mis-distance. Several studies, preliminary in nature, have been conducted to investigate the sensitivity of existing classical terminal guidance laws implemented in several scenarios of engagement. The parameters which were studied as a function of the guidance law were:

a. Initial heading of target

b. Target speed

c. Magnitude of target acceleration

d. Sensor bias in measurement of L.O.S. rate

e. Sensor noise caused by two different levels of target generated noise

f. Effect of wind gust.

The results of such studies, although generally valid, give the tendency of each law sensitivity and can be summarized as in table III.F-1 is shown.

Table III.E-1. Comparison of Classical Guidance Laws

GUIDANCE LAW	ADVANTAGES	DISADVANTAGES
1. Command-to-Line-of-Sight Guidance	No terminal seeker required.	Very inaccurate against moving targets and with winds. Data link required.
2. Pursuit	Noise insensitive. Easy to use with strapdown seekers.	Inaccurate against moving targets and with winds.
3. Proportional	Accurate against constant velocity targets.	Inaccurate against accelerating targets. Stability is sensitive to noise.
4. Pursuit + Pro Nav	Between 2 and 3 in terms of accuracy.	Between 2 and 3.
5. Dynamic Lead	Between 2 and 3 in terms of accuracy. Easy to use with strapdown seekers.	Between 2 and 3. Stability problems if transition to pro nav occurs when significant noise is present.

Table III.F-1. Sensitivity Comparison of Classical Guidance Laws

LAW	CLASSIFICATION	TARGET PARAMETERS			MISSILE PARAMETERS		
		HEADING	SPEED	ACCELER	BIAS	NOISE	GUSTS
L.O.S.	GOOD		*			*	
	AVERAGE				*		*
	POOR	*		*			
PURSUIT	GOOD		*			*	*
	AVERAGE				*		
	POOR	*		*			
P.N.	GOOD	*	*	*	*		*
	AVERAGE						
	POOR					*	

It is easily seen that P.N. rates well in all categories except that of noise. Angle rate, measurement noise, homing sensor noise and target noise all have their effect; thus arises the need for very good filtering.

The selection of proportional navigation constant must involve a trade-off between high gain necessary for high maneuvering targets and lower gains needed for noisy situations.

IV. GUIDANCE LAW OF CLASSICAL PROPORTIONAL NAVIGATION

A. GENERAL

This section is intended to present the basic concepts associated with the classical proportional navigation guidance law, and through a number of simplified cases to provide homing missile as it engages a target. In order to intercept a target a missile must be capable of maneuvers. These are accomplished by producing an acceleration normal to the velocity vector resulting in a turn maneuver. Acceleration, therefore, is one of the most important system parameters, and because of practical limitations is one of the major constraints in accomplishing an intercept. Acceleration is not the only parameter of interest; therefore other quantities such as turning rate, trajectory, and miss-distance are also considered. The analysis is generalized by normalizing many of these parameters to permit curves to be used that may be applied to different problems. Thus, for the cases considered, a reader can apply all of the results derived to any set of initial conditions and obtain information on the resulting trajectory.

To permit an analytical treatment of this type, several simplifications must be made. It has been the general practice to introduce proportional navigation by discussing the constant bearing course and then considering perturbations

about this idealized case. Constant missile and target speed are assumed to avoid having to contend with non-linear differential equations. This assumption is fairly good in many cases, where the intercept time is short, and the speeds do not have time to change significantly. A two-dimensional problem is also assumed, again to permit the effects of various parameter variations to be shown without becoming involved in unnecessarily complex mathematical manipulation. The discussion will cover some of these, as well as other assumptions made in various derivations. Full investigation of the resulting general differential equation for P.N. is not of primary interest. Thus representative cases will be studied.

It is believed that the approach taken, although somewhat idealized, will provide the reader with an understanding and feel for proportional navigation. It also provides a means for rapidly determining values of missile parameters required to achieve an intercept under ideal conditions, and thus shows the best performance that can be attained based upon the classical techniques.

Although proportional navigation has proved to be of value against aircraft targets of limited maneuverability, advances in aircraft design have increased their capability to the point where proportional navigation can no longer generate the missile commands necessary to insure a hit. This has led to the application of modern control theory for

the generation of optimal guidance laws, requiring more complex sensors and signal processors. The development of optimal control laws for guidance systems is receiving considerable attention, especially with the advent of high speed digital logic in the form of microprocessors, which can provide tremendous calculating power in a very small space. This area is beyond the scope of this study and is mentioned in passing to alert the reader to the fact that such work is being conducted.

For the following study, initially the missile will be considered to be ideal, in that it has no mass (unlimited acceleration) and there are no time lags (no time constants). Missile acceleration requirements and missile lateral displacement will be derived for cases of initial missile heading errors and for a maneuvering target. Then, the analysis can be extended to include a system having a single time constant, an acceleration bias, acceleration limiting and various combinations of these.

Missile acceleration curves are important because they show the missile response to the initial conditions as well as the maximum missile acceleration required to intercept a target under the conditions imposed.

The analytical derivation of differential equations of P.N. for the several cases will be based upon plain geometry and small perturbation theory and geometry in order to derive and deal with linear differential equations instead of

non-linear which are harder to be handled, analyzed and implemented into computer programs.

B. FUNDAMENTALS OF PROPORTIONAL NAVIGATION

1. Constant Bearing Course

The explanation of constant bearing course concept is considered as a prerequisite understanding before developing the Proportional Navigation concept.

A constant bearing course is a course in which the line-of-sight from the missile to the target maintains a constant direction in space and thus remains parallel to itself during a target/missile engagement. It is generally associated with constant missile and target speeds, which are assumptions made in this study to simplify the analysis. The constant bearing course results in an intercept and is the so-called collision course.

Figure IV.B-1 shows the geometry for a constant bearing course. The line-of-sight (LOS) between missile and target is at an angle ψ relative to an inertial space reference for all times of the flight. The missile velocity vector is at an angle L relative to the LOS, and the target velocity vector is at an angle A relative to the LOS. The relative closing velocity between missile and target ($\dot{r}$) is

$$\dot{r} = V_t \cos A - V_m \cos L \qquad \text{(IV.B-1)}$$

where $V_t \cos A$ and $V_m \cos L$ are the velocity components along the LOS.

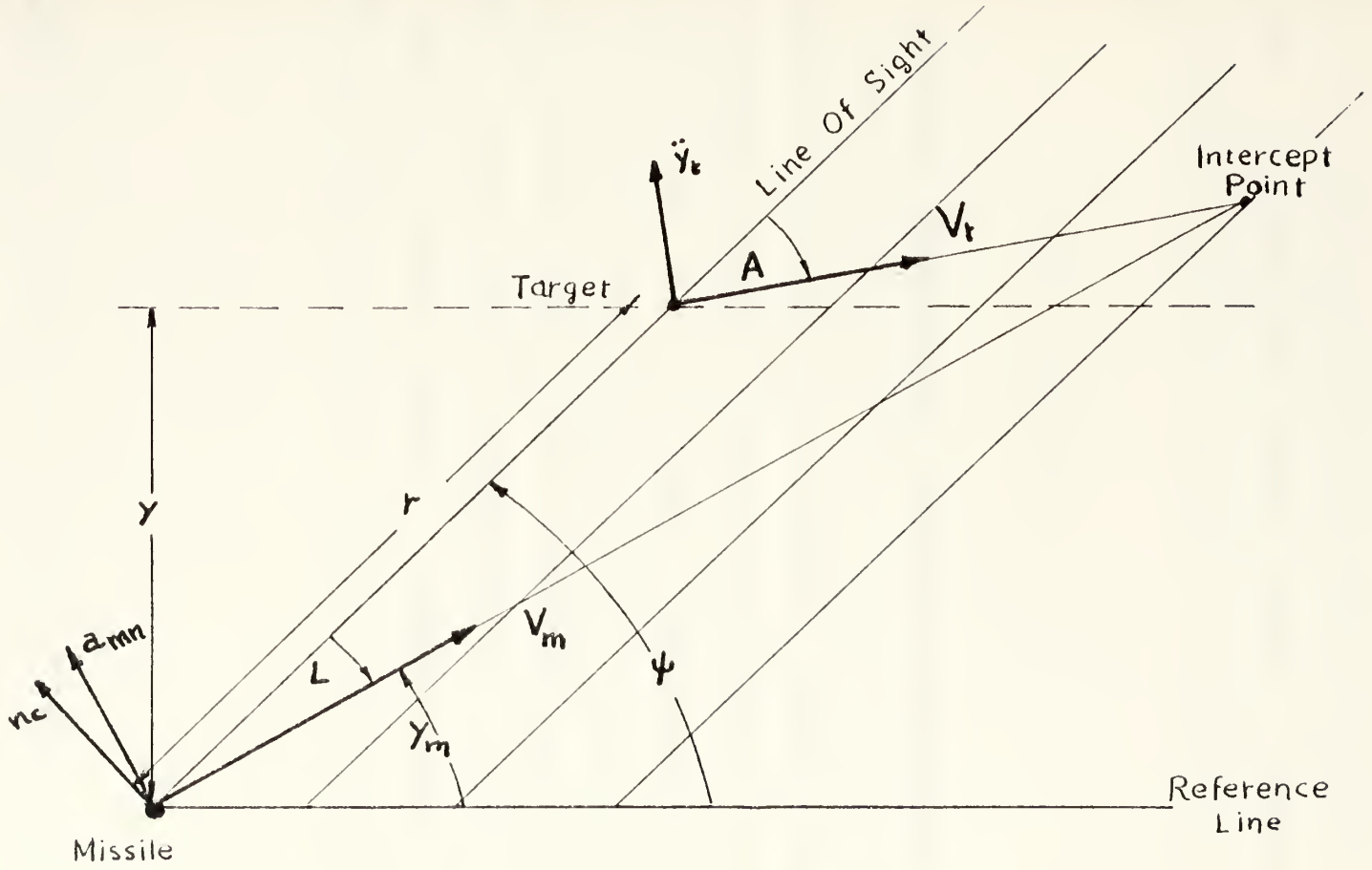

Fig. IV.B-1. Constant Bearing Geometry

The rotation rate of the LOS is found from

$$r\dot{\psi} = -V_t \sin A + V_m \sin L \qquad \text{(IV.B-2)}$$

where $V_t \sin A$ and $V_m \sin L$ are the velocity components normal to LOS. For a constant bearing course, ψ = constant and $\dot{\psi} = 0$. The proper missile lead angle L is found from Eq. (IV.B-2)

$$\sin L = \frac{V_t}{V_m} \sin A \qquad \text{(IV.B-3)}$$

2. Classical Proportional Navigation Guidance Law

A classical proportional navigation course is defined as a course in which the rate of change of missile heading is directly proportional to the rate of rotation of the line-of-sight from the missile to the target. The purpose of such a course is to counter the tendency for the line-of-sight to rotate and therefore approximate a constant bearing course. To permit a tractable analytical treatment, the missile and target speeds are assumed constant. Mathematically, the classical proportional navigation equation can be expressed as

$$\dot{\gamma}_m = N\dot{\psi} \qquad \text{(IV.B-4)}$$

where

$\dot{\gamma}_m$ is the rate of change of the missile heading (velocity vector)

$\dot{\psi}$ is the rate of change of the line-of-sight, and

N is the navigation ratio.

The direction of the missile velocity vector cannot be controlled directly; therefore, proportional navigation is implemented by controlling the missile acceleration, a_{mn}, which equals $V_m\dot{\gamma}_m$, where V_m is the missile velocity. Implementation of proportional navigation results in the following guidance law:

$$a_{mn} = N\ V_m\ \dot{\psi} \qquad \text{(IV.B-5)}$$

or

$$a_{mn} = \frac{\eta\ V_c}{\cos\ L}\ \dot{\psi} \qquad \text{(IV.B-6)}$$

where η is the effective navigation ratio, V_c equals $-\dot{r}$, the relative closing velocity along the line-of-sight, and L is the angle between the line-of-sight and the missile velocity vector. The above two equations are equivalent. The effective navigation ratio η is a critical parameter that characterizes the missile system response, and typical values of η between 3 and 6 are normally employed, as it will be shown by the following-on study cases.

The above equations are somewhat idealized because they do not account for any time constants in the system. A space stabilized sensor is used onboard the missile to measure $\dot{\psi}$. Implementation of this sensor usually results in a single time constant transfer function. Implementation of a means for commanding missile acceleration proportional to the measured $\dot{\psi}$ also results in at least one additional time

constant. These time constants must be small relative to the missile flight time in order to minimize the miss-distance.

Guidance law equations are classically written as perturbations in missile and target position relative to a constant bearing course. These equations are linear differential equations which are valid provided the commanded missile acceleration does not exceed the lateral acceleration capability of the missile. If acceleration saturation does not occur, the missile system is linear and superposition can be used if several errors occur simultaneously.

Classical treatment of proportional navigation generally assumes that the missile and target are flying a constant bearing course and that the missile and target velocities are constant. Errors relative to a constant bearing course are then introduced into the differential equation which give the perturbation in position. Conditions that cause deviations from a constant bearing course are:

Initial missile heading error

Target maneuver

Control system acceleration bias

Initial tracker error

Wind.

If the system remains linear and the flight time is long, relative to the missile system time constant, the miss-distance will be small. For a given effective navigation

ratio η, factors that degrade missile system performance and increase the miss-distance are:

Missile system acceleration saturation

(Acceleration limiting)

Missile system time constants

Instability at short range

Scintillation

Angular glint, and

Seeker/sensor internal noise sources.

Acceleration saturation and missile time constant effects are described in following sections.

C. GENERAL DIFFERENTIAL EQUATION OF P.N. FOR KINEMATIC ANALYSIS

In the analysis of proportional navigation in this section the constant-bearing course is employed as a basic coordinate reference, and motions or perturbations of both target and missile are examined relative to their respective collision courses. Each interception problem may be broken down into various component geometric considerations such as a target maneuver and an initial heading error. Superposition can then be used to find the total solution, providing the system remains linear, i.e., acceleration limiting does not occur.

Figure (IV.C-1) shows the geometry of a missile target interception based upon a constant-bearing course. At a given time, t_1, the missile would be at position 1 if a

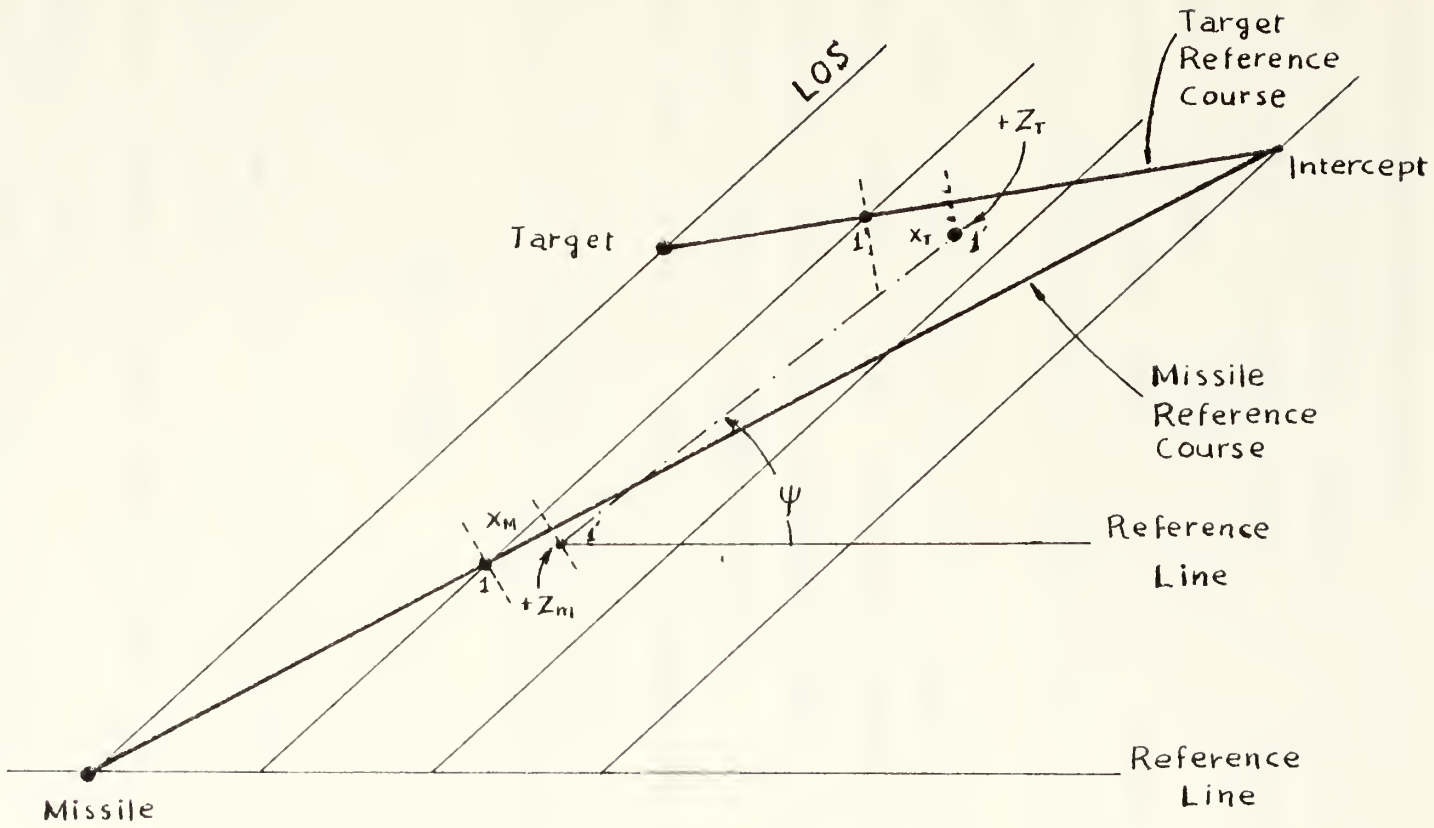

Fig. IV.C-1. Missile and Target Perturbation Geometry

constant-bearing course were flown, but the missile is actually at point 1'. The perturbation in position is X_m units along the missile reference course and is $+Z_m$ units normal to the missile reference course. The target at time t_1 would be at position 1 shown in figure (IV.C-1) if a constant-bearing course were flown but is actually at position 1'. The target perturbation is X_t units measured along the target reference course and is Z_t units measured normal to the target reference course.

The missile velocity vector is at an angle γ_m relative to the arbitrary reference line. The angle between the line-of-sight vector and the arbitrary reference line is defined as ψ. The latter is shown in figure (IV.C-1).

Proportional navigation requires that the angular rate of the missile flight path (missile turning rate) be proportional to the angular rate of change of the line-of-sight or

$$\frac{d\gamma_m}{dt} = N \frac{d\psi}{dt} \qquad \text{(IV.C-1)}$$

where:

γ_m = angle between missile velocity vector and a fixed reference line;

$\frac{d\psi}{dt}$ = rate of change of the line-of-sight; and

N = navigation ratio.

One form of mechanizing proportional navigation is to use a target tracker to measure $d\psi/dt$. Figure (IV.C-2) shows a

missile system containing a tracker. The LOS is shown at the angle ψ, the missile axis is shown at an angle θ, and the missile velocity vector is shown at an angle γ_m. The angle of attack α is the angle between the missile axis and the missile velocity vector. The tracking antenna boresight is at an angle D and the tracking error which is the LOS angle minus the boresight is shown as ε.

A typical implementation for a homing angle tracker is shown in figure (IV.C-3) as a type 1 servo. The input to the tracker is target position ψ and the output from the tracker is ε. The antenna motor is shown as part of the feedback loop included in the K_2/s term. The antenna motor acts as an integrator because the antenna turning rate is proportional to the input voltage or current. The tracker transfer function is

$$\varepsilon = \dot{\psi} \frac{\tau}{\tau s + 1} \qquad \text{(IV.C-2)}$$

The denominator acts as a low pass filter with a time constant of τ, and the output ε, is $\tau\dot{\psi}$ in the steady state. The tracker output, ε, is a direct measure of the sight line rate. The tracker must be space stabilized to prevent missile motion from influencing the ψ measurement.

The direction of the missile velocity cannot be controlled directly, but the tracker output is amplified by a factor K and is used to command the missile acceleration. Thus,

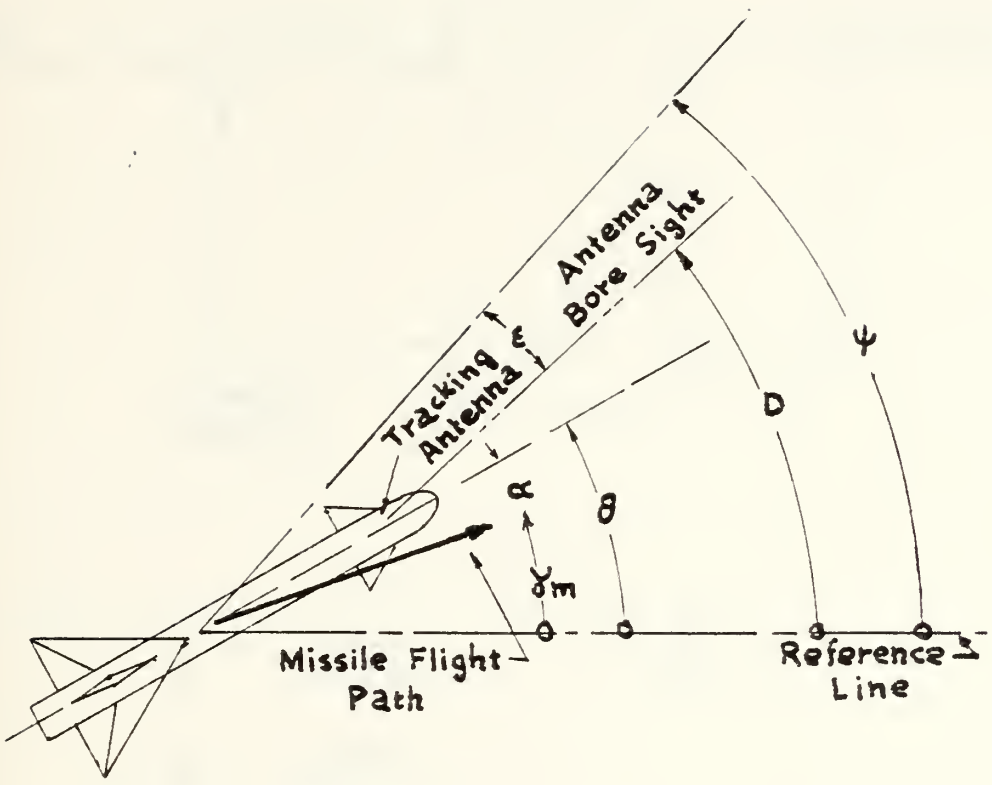

Fig. IV.C-2. Missile and Tracking System

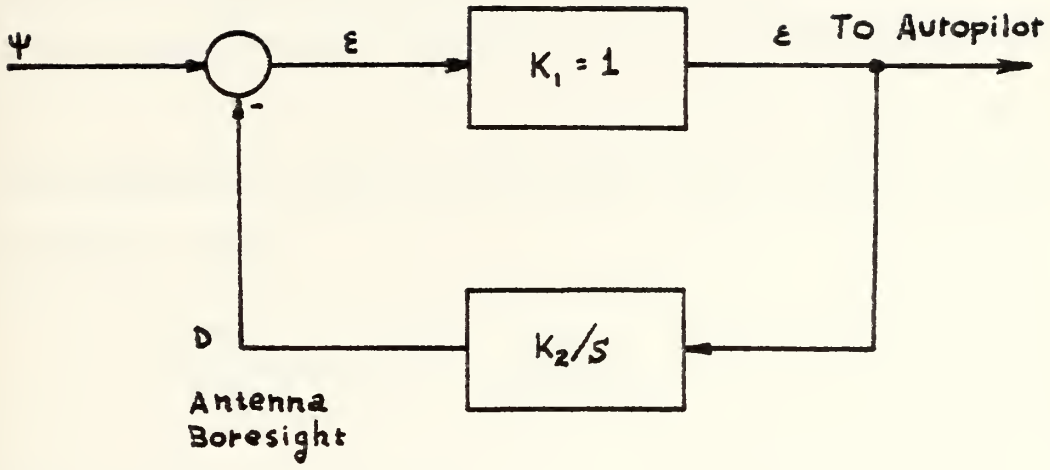

$$\frac{D}{\Psi} = \frac{1}{\tau s + 1} \qquad \tau = \frac{1}{K_2}$$

$$\frac{\varepsilon}{\Psi} = \frac{\tau s}{\tau s + 1}$$

$$\frac{\varepsilon}{\dot{\Psi}} = \frac{\tau}{\tau s + 1}$$

Fig. IV.C-3. Typical Homing Angle Tracker

$$n_m = \frac{a_{mn}}{32.2} = Ke = \frac{K\tau}{\tau s + 1}\,\dot{\psi} \quad \text{in g's} \qquad \text{(IV.C-3)}$$

where n_m is the missile lateral acceleration in g's and a_{mn} is the missile lateral acceleration in ft/sec^2. The above equation is a linear first order differential equation relating the commanded acceleration, (n_m), to the sight line rate $\dot{\psi}$.

The commanded missile acceleration from figure (IV.C-1) is d^2Z_m/dt^2 so that:

$$\frac{d^2Z_m}{dt^2} = -n_m g = -\frac{gK\tau}{\tau s + 1}\,\dot{\psi} \qquad \text{(IV.C-4)}$$

The above equation reduces to

$$\tau\frac{d^2Z_m}{dt^2} + \frac{dZ_m}{dt} = -gK\tau\psi + \tau\left(\frac{d^2Z_m}{dt^2}\right)_{t=0} + \left(\frac{dZ_m}{dt}\right)_{t=0} + gK\tau(\psi)_{t=0} \qquad \text{(IV.C-5)}$$

where:

τ = tracker time constant,

$\frac{d^2Z_m}{dt^2}$ = missile acceleration normal to the missile constant bearing course,

$\frac{dZ_m}{dt}$ = missile velocity normal to the missile constant bearing course,

ψ = line-of-sight angle,

$\left(\frac{d^2Z_m}{dt^2}\right)_{t=0}$ = initial missile lateral acceleration at t = 0,

$\left(\frac{dZ_m}{dt}\right)_{t=0}$ = initial missile lateral velocity at t = 0, and

$(\psi)_{t=0}$ = initial LOS error angle at t = 0.

Since the above equation is a perturbation type equation, ψ is the actual LOS angle minus the constant bearing LOS angle. The perturbation in ψ is

$$\psi = \tan \psi = \frac{X_m \sin L + Z_m \cos L - X_t \sin A - Z_t \cos A}{r} \qquad \text{(IV.C-6)}$$

where r is the missile to target range which is

$$r = V_c(T - t)$$

where:

V_c is the missile to target closing velocity along the LOS

T is the total homing flight time and

t is the elapsed homing time.

Substituting the equation for r and the equation for ψ into the differential equation for missile position results in a basic trajectory equation given below:

$$\tau \frac{d^2 Z_m}{dt^2} + \frac{dZ_m}{dt} + n \frac{Z_m}{T-t} = -\frac{n}{T-t} X_m \tan L - X_t \frac{\sin A}{\cos L} - Z_t \frac{\cos A}{\cos L} + \tau \left(\frac{d^2 Z_m}{dt^2}\right)_{t=0} + \left(\frac{dZ_m}{dt}\right)_{t=0} + gK\tau(\psi)_{t=0} \qquad \text{(IV.C-7)}$$

where:

$n = \frac{gK\tau \cos L}{V_c} = \frac{N V_m}{V_c} \cos L$ is the effective navigation ratio.

In the above equation X_m and X_t are zero if the missile and target velocities are constant.

The above general differential equation is applied to specific problems in the following subsections of this section which provide general curves showing the required missile acceleration for initial heading errors, target maneuvers, control system acceleration bias and an initial tracking error. Curves are given for a system with and without a time constant.

Missile acceleration curves are important because they show the missile response to the initial conditions as well as the maximum missile acceleration required to intercept a target under the conditions imposed.

Assumptions contained in the derivation of the General Differential Equation for P.N. are:

(1) Equation is written as a perturbation about a constant bearing course;

(2) Missile and target velocities are constant;

(3) Linear system operation (no acceleration saturation);

(4) A single system time constant exists due to the tracker.

The above equation is used to derive the differential equation of motion for various imput conditions.

1. Proportional Navigation with Initial Heading Error and No Time Constant

For this problem the missile has an initial heading error of a_0 when compared to the heading required for a

constant bearing course. The initial missile velocity, $(dZ_m/dt)_{t=0}$, is $-V_m a_0$ for relatively small heading errors.

For no time constant and constant target and missile velocities, the general differential equation for the perturbation normal to the constant bearing course, reduces to the following:

$$\frac{dZ_m}{dt} + n \frac{Z_m}{T - t} = V_m \, a_0 \qquad \text{(IV.C-8)}$$

where:

Z_m is normal to the constant bearing flight path;

n is the effective navigation ratio;

T is the total missile flight time;

V_m is the missile velocity; and

a_0 is the initial missile heading error in radians.

This equation is directly integrable and results in a missile acceleration of

$$n_m = - \frac{V_m \, a_0}{g \, T} \, n \left(\frac{T - t}{T} \right)^{n - 2} \qquad \text{(IV.C-9)}$$

and a missile displacement normal to the constant bearing course given by:

$$Zm = \begin{cases} \dfrac{V_m a_0 \, T \, 1 - \frac{t}{T} \, \cos B}{n - 1} \left[1 - \left(1 - \frac{t}{T} \right)^{n - 1} \right] & \text{, for } n \neq 1 \\ V_m \, a_0 \, T \left(1 - \frac{t}{T} \right) \cos B \, \ln \left(1 - \frac{t}{T} \right) & \text{for } n = 1 \end{cases} \qquad \text{(IV.C-10)}$$

Equation (IV.C-9) is plotted in figure IV.C-4 for values of n between 2 and 6. The horizontal scale is the normalized missile flight time t/T. t = 0 corresponds to initiation of proportional navigation, and t = T corresponds to intercept. The vertical axis is the missile acceleration a_{mn}, normalized (divided) by an equivalent acceleration disturbance equal to the initial normal velocity divided by the total flight time, $V_m a_0/T$.

Examination of the curves of figure IV.C-4 shows that for n = 2 a constant acceleration is required throughout the flight. For higher values of n, a larger acceleration is required early in flight and a lower acceleration is required near the end of flight. It is desirable to correct the heading error early in flight so that the missile system has full maneuvering capability near the end of flight. Values of n between 3 and 6 are desirable for the case of an initial heading error in order to reduce the acceleration requirements at intercept.

Equation (IV.C-10) is plotted in figure IV.C-5 for values of $6 \geq n \geq 2$. The horizontal scale is the normalized missile flight time t/T. t = 0 corresponds to initiation of proportional navigation and t = T corresponds to intercept. The vertical axis is the missile's displacement normal to the constant bearing course, normalized by (divided) $V_m a_0 \cos B$.

Examination of the curves of figure IV.C-5 shows that as n increases the lateral missile displacement decreases.

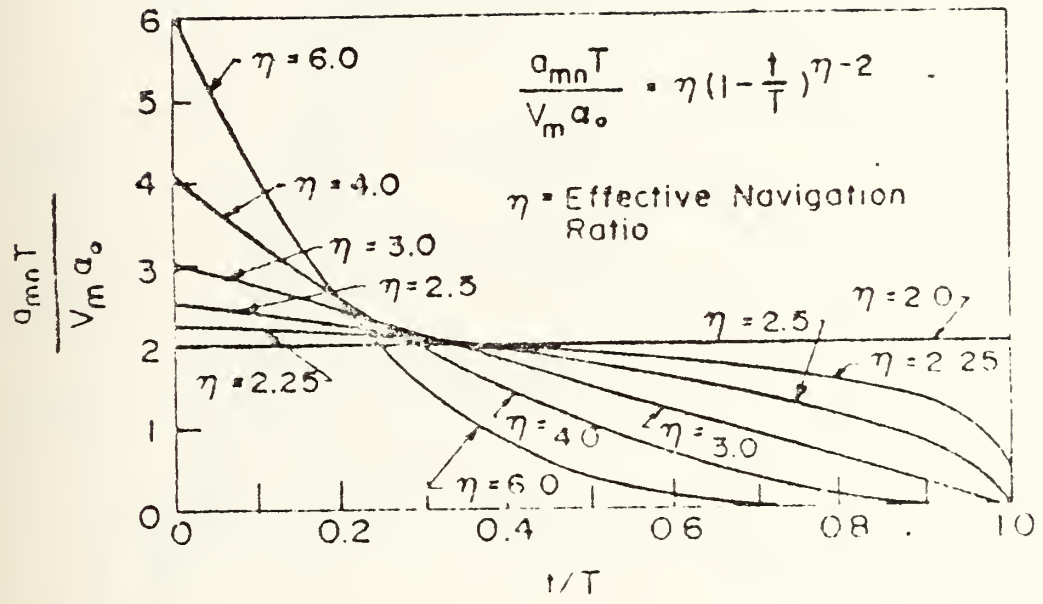

Fig. IV.C-4. Missile Acceleration Required to Eliminate an Initial Heading Error (see equation (IV.C-9) Unlimited System, NO Time Lags, Constant Target Velocity

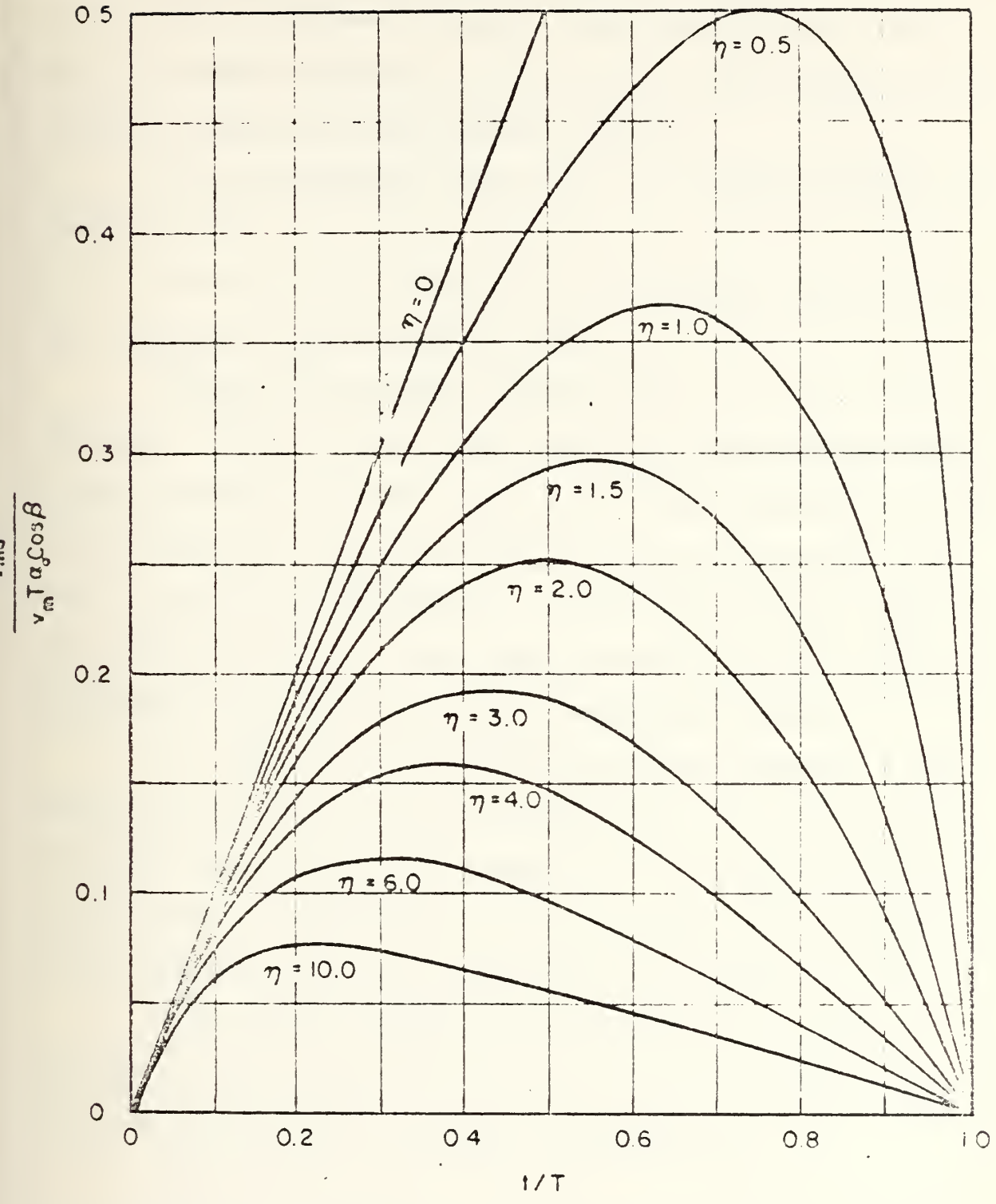

Fig. IV.C-5. Relative Missile Trajectory Caused by Aiming Error (see equation IV.C-10) Unlimited System, NO Time Lags, Constant Velocity Target

Also as n increases, the maximum displacement occurs earlier in the total engagement flight. This was expected, because as it is shown in figure IV.C-4, we get larger accelerations early in flight and lower during the end.

It is noticeable that for n = 2, maximum displacement occurs at T/2.

Finally, it is observed that no matter how much the η is, the final miss-distance is zero.

Given the numerical values of V_m, a_0, T, B, the normalizing factors for the acceleration n_m and the displacement Z_m can be derived. Then, multiplying these factors with the values obtained through figures (IV.C-4) and (IV.C-5), the real n_m and Z_m are determined. If the acceleration limits of the missile are known, then these curves can also be used to determine if missile acceleration saturation occurs.

In summary an initial heading error requires a high missile acceleration early in flight and a low missile acceleration near the end of flight for $\eta \geq 3$. The magnitude of the missile acceleration and displacement are proportional to the heading error a_0. The final miss distance is zero.

The computer program which was used to implement equations (IV.C-9) and (IV.C-10), in order to obtain figures (IV.C-4) and (IV.C-5), is given in appendix A.

2. Proportional Navigation with a Maneuvering Target and No Time Constant, No Initial Aiming Error

In this case, it is assumed that the target and missile are flying a collision course and at t = 0 the target initiates a lateral acceleration of a_t ft/sec^2, normal to the target collision course flight path. Then, the general differential equation for P.N. (IV.C-7) turns into:

$$\frac{dZ_m}{dt} + \frac{Z_m}{T-t} = -\frac{n}{T-t}\left(\frac{\cos A}{\cos L}\right)\frac{1}{2}\,a_t\,t^2 \qquad \text{(IV.C-11)}$$

Equation (IV.C-11) is directly integrable and results in a missile acceleration of:

$$\eta_m = \left(\frac{n}{n-2}\right)\left(\frac{\cos A}{\cos L}\right)\left[1 - \left(\frac{T-t}{T}\right)^{n-2}\right]\eta_t \qquad \text{(IV.C-12)}$$

and a missile lateral displacement normal to constant bearing course flight path given by:

$$Z_m = -V_t\,T^2\,\Delta\dot{\phi}\cos\phi_0\left[\frac{\left(1-\frac{t}{T}\right)}{n-1} - \frac{\left(1-\frac{t}{T}\right)^2}{n-2} + \frac{\left(1-\frac{t}{T}\right)^n}{(n-1)(n-2)}\right] \qquad \text{(IV.C-13)}$$

where:

η_m is the missile acceleration in g's

η_t is the target acceleration in g's

V_t is target speed

$\Delta\dot{\phi}$ is target turning rate

ϕ_0 is the target velocity vector angle with respect to the constant bearing course when it initiates the maneuver.

Figure IV.C-6 is the plotting of equation (IV.C-12). The horizontal axis is the normalized time of flight t/T, and the vertical axis is the missile acceleration n_m divided by $(n_t \cos A)/\cos L$. The vertical axis can also be interpreted as the component of missile acceleration normal to the LOS divided by the component of target acceleration normal to the LOS. The initial requirement on n_m is zero, but n_m increases as the flight time increases. For values of n less than 3, the required missile acceleration at intercept is very high. For n between 3 and 6, the final missile acceleration is between 3 n_t and 1.5 n_t.

Figure (IV.C-7) is the plotting of equation (IV.C-13). The horizontal axis is the normalized time of flight t/T, and the vertical axis is the missile lateral displacement off the constant bearing course flight path, normalized (divided) by $V_t T^2 \Delta\dot{\phi} \cos \phi_0$. It is noticeable that in this subcase also, the final miss-distance is also zero. Again, the more n the less miss-distance occurs rather at the end of the later part of the engagement.

The computer program which was used to implement equations (IV.C-12) and (IV.C-13), in order to obtain figures (IV.C-6) and (IV.C-7), is given in appendix B.

3. Proportional Navigation with an Initial Heading Error and a Single Time Constant

In this case, it is assumed that the missile is launched with an initial heading error of a_0 when compared to

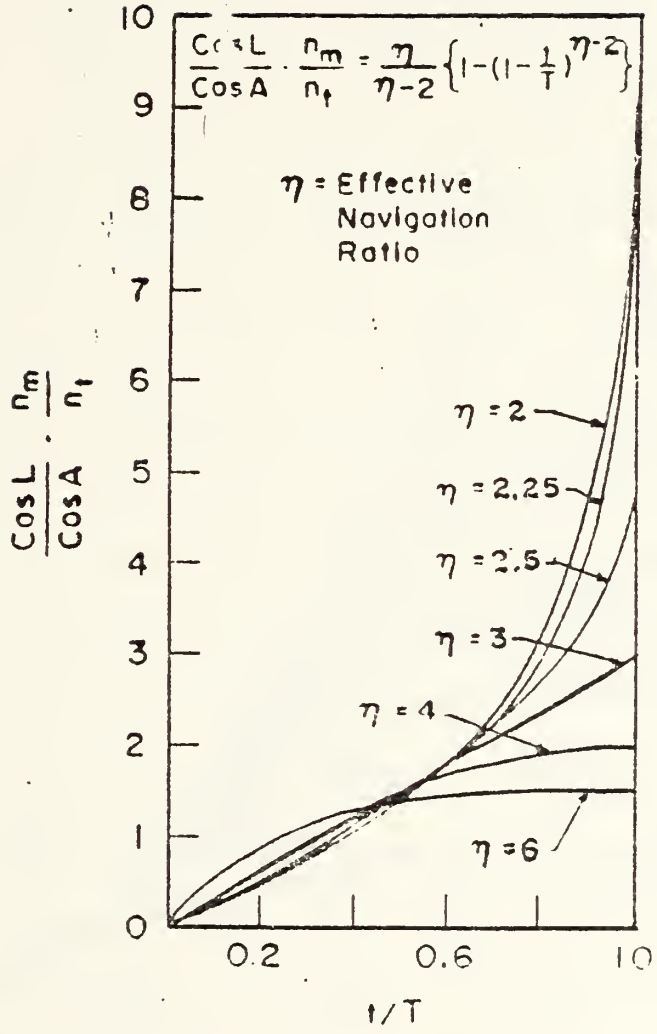

Fig. IV.C-6. Missile Acceleration Required for Maneuvering Target (see equation IV.C-12) Unlimited Missile, NO Time Lags

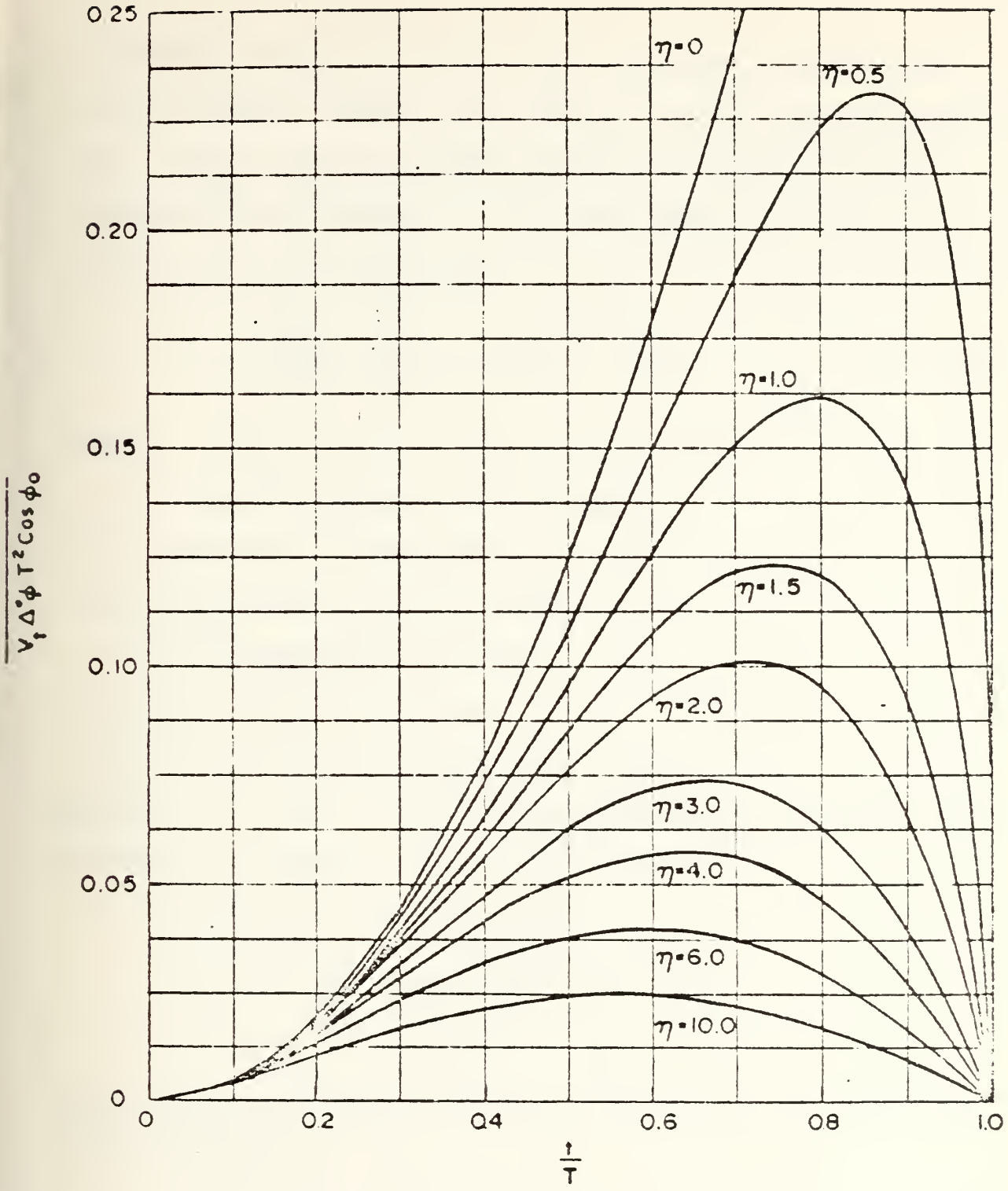

Fig. IV.C-7. Relative Missile Trajectory Caused by Target Maneuver, (see equation IV.C-13) Unlimited Missile, NO Time Lags

the heading required for a constant bearing course. The initial missile velocity $(dZ_m/dt)_{t=0}$ is $V_m\ a_0$ for relatively small heading errors and the missile is provided with a seeker of time constant τ. Then the general differential equation (IV.C-7) turns into:

$$\tau \frac{d^2 Z_m}{dt^2} + \frac{dZ_m}{dt} + \eta \frac{Z_m}{T - t} = -V_m\ a_0 \qquad \text{(IV.C-14)}$$

where:

τ is the time constant of the seeker

T is the time of engagement

a_0 is the initial heading error

η is the navigation constant

V_m is the missile velocity

Z_m is the vertical displacement error.

Equation (IV.C-14) is not directly integrable in closed form and must be solved by numerical integration.

Defining $t' = t/T$ follows:

$$dt' = dt/T \quad \text{and} \quad dt = T\ dt'$$

$$(dt')^2 = (dt/T)^2 \qquad dt^2 = T^2\ dt'^2$$

Substituting into equation (IV.C-14) and after minor manipulations it gives:

$$\frac{d^2(Z_m/T)}{(T/\tau)dt'^2} + \frac{d(Z_m/T)}{dt'} + \frac{\eta}{(1 - t')}\left(\frac{Z_m}{T}\right) = -V_m\ a_0 \qquad \text{(IV.C-15)}$$

Dividing through by $V_m a_0$ and multiplying by T/τ, equation (IV.C-15) turns into:

$$\frac{d^2(Z_m/TV_m a_0)}{dt'^2} + \left(\frac{T}{\tau}\right)\frac{d(Z_m/TV_m a_0)}{dt'} + \left(\frac{T}{\tau}\right)\frac{\eta}{1-t'}\frac{Z_m}{TV_m a_0} = -\frac{T}{\tau} \qquad \text{(IV.C-16)}$$

Defining $Q = Z_m/TV_m a_0$, $K = T/\tau$ and substituting, equation (IV.C-16) turns into:

$$\frac{d^2Q}{dt'^2} + K\frac{dQ}{dt'} + K\frac{\dot{\eta}}{1-t'}Q = -K \qquad \text{(IV.C-17)}$$

Then, by numerical computational approximations, figure (IV.C-8), figure (IV.C-9) and figure (IV.C-10) were obtained.

Figure (IV.C-8) is the plotting of missile acceleration for $\eta = 3$. The horizontal axis is the normalized time of flight t/T, and the vertical axis is missile acceleration a_{mn} divided by $V_m a_0/T$. For T/τ equal to 15 or greater, the missile acceleration is close to the $T/\tau = \infty$ case (case of no time constant).

Figure (IV.C-9) is the plotting of missile acceleration for $\eta = 4$. Again for $T/\tau = 15$ the deviation from $T/\tau = \infty$ case is not serious, and that at values less than 15, larger differences occur.

Figure (IV.C-10) is the plotting of missile acceleration for $\eta = 5$. Again, the same results as for the case of $\eta = 4$ are noticed.

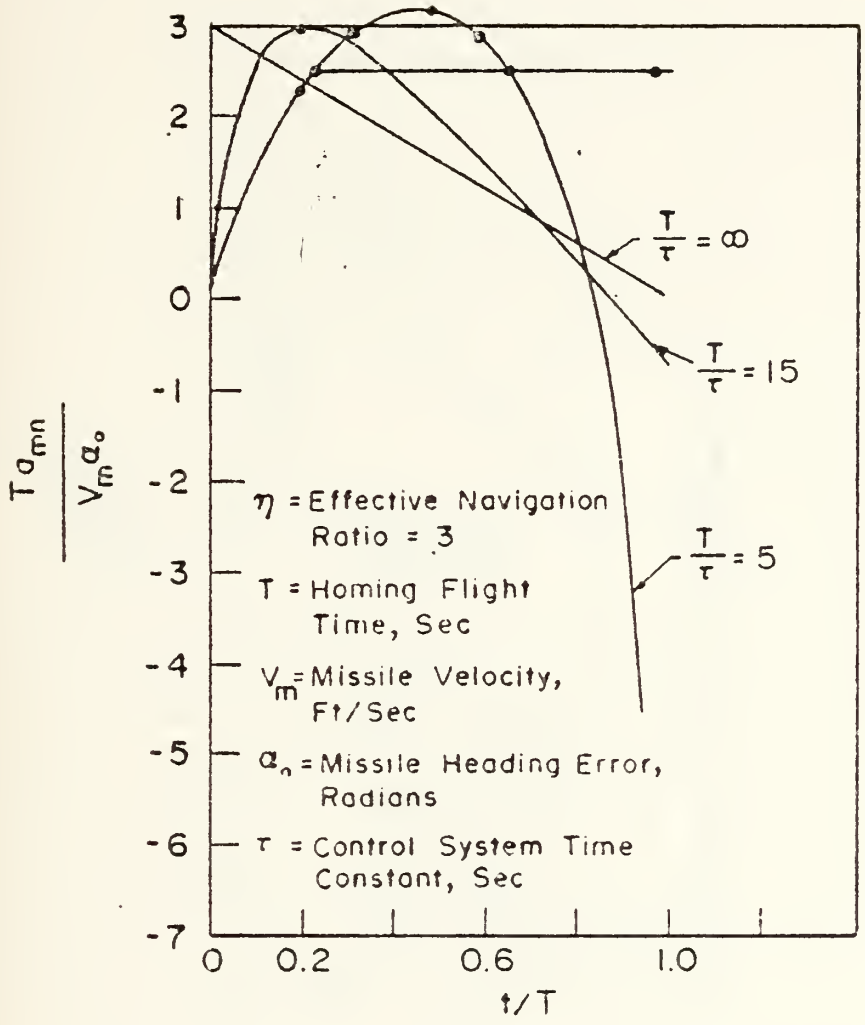

Fig. IV.C-8. Missile Acceleration Required for an Initial Heading Error and a Single Time Constant

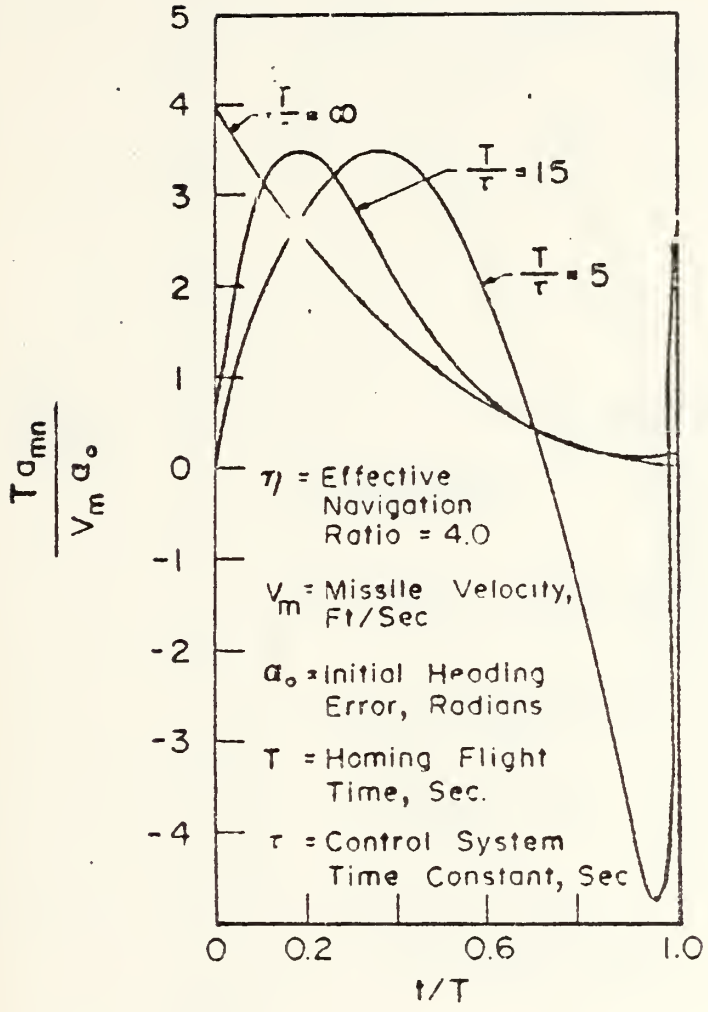

Fig. IV.C-9. Missile Acceleration Required for Maneuvering Target

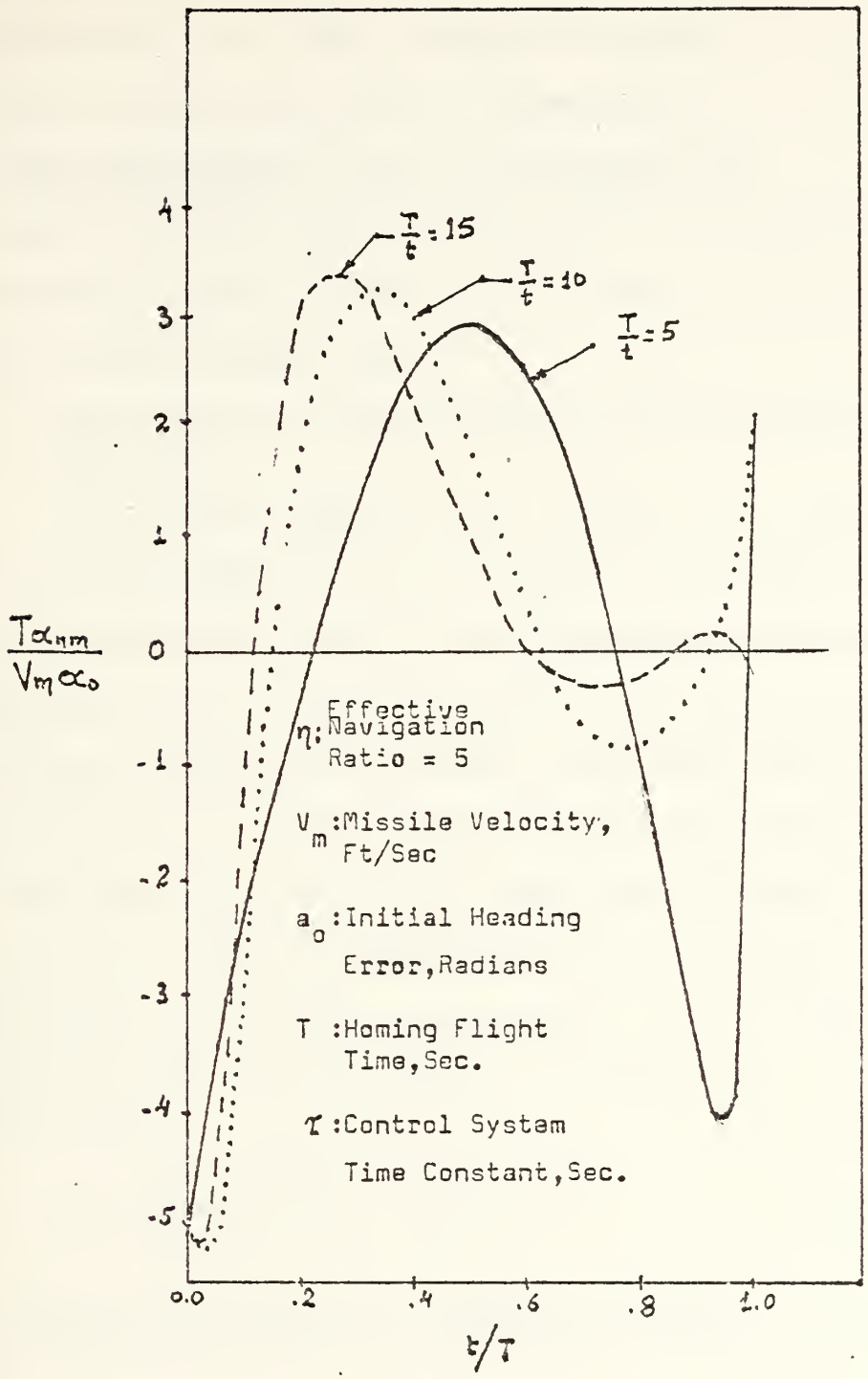

Fig. IV.C-10. Missile Acceleration Required for Maneuvering Target

The computer program which was used to implement equation (IV.C-17), in order to obtain figures (IV.C-8), (IV.C-9) and (IV.C-10), is given in appendix C.

4. Other Sub-cases of the P.N. Guidance Law

Continuing the study of the general Differential Equation for P.N. (see equation IV.C-7), the following sub-cases can be distinguished also:

a. P.N. with No Time Constant and Acceleration Limiting

In previous section IV.C.2 about "P.N. with maneuvering target and no initial heading error and no time constant" it was shown that the required missile acceleration increases with the time of flight (see figure (IV.C-6)). If the required acceleration exceeds that which the missile system can provide, acceleration saturation or limiting will occur. The time t_L at which this occurs can be found using figure (IV.C-6). The missile system will be acceleration limiting from $t = t_L$ through intercept at $t = T$. Then, the miss-distance Y_m at intercept time T is given by:

$$Y_m = \frac{g\, n_t \cos A}{2} \left(\frac{T - t_L}{T}\right)^n T^2 \qquad \text{(IV.C-18)}$$

where Y_m is the target-missile separation normal to the L.O.S. at $t = T$.

Miss-distance due to an initial heading error should be zero even if acceleration limiting occurs, provided

the flight time is long. In figure (IV.C-4), the required acceleration for an initial heading error is shown. The highest acceleration is required early in flight, so that the missile system will be into acceleration limiting between 0 and t_s seconds, after which linear operation will occur. The trajectory errors caused by the initial heading error and saturation will result in a new heading error at $t = t_s$. The remaining portion of the flight is linear and the resulting miss-distance is zero.

b. P.N. with Control System Acceleration Bias and No Time Constant

If the control system contains an inadvertent bias which demands a fixed acceleration, in addition to that called for by the tracking signal, the missile acceleration is

$$n_m = n_b + K\tau\dot{\psi} \qquad \text{(IV.C-19)}$$

where n_b = acceleration bias in g's.

The differential equation for the missile perturbation becomes

$$\frac{dZ_m}{dt} + n\,\frac{Z_m}{T - t} = -g\,n_b\,t \qquad \text{(IV.C-20)}$$

The differential equation is directly integrable resulting in a solution of

$$\frac{n_m}{n_b} = \frac{n}{n - 2}\left(1 - \frac{t}{T}\right)^{n-2} - \frac{2}{n - 2} \qquad \text{(IV.C-21)}$$

This equation is plotted in figure (IV.C-11). The horizontal axis is the normalized time of flight and the vertical axis is $-n_m/n_b$. To keep the missile acceleration low near the end of flight, values for n between 3 and 6 are required.

The overall effect of an acceleration bias is to force a missile acceleration over the entire flight time. This acceleration would use up some part of the available acceleration dynamic range of the missile.

c. P.N. with a Control System Acceleration Bias and Single Time Constant

For a single time constant the differential equation of motion is

$$\tau \frac{d^2 Z_m}{dt^2} + \frac{dZ_m}{dt} + \eta \frac{Z_m}{T - t} = -g\, n_b\, t + \tau \left(\frac{d^2 Z_m}{dt^2} \right)_{t=0} \qquad \text{(IV.C-22)}$$

Using the initial condition that $\left(d^2 Z_m/dt^2\right)_{t=0}$ is $-g\ n_b$, the differential equation becomes

$$\tau \frac{d^2 Z_m}{dt^2} + \frac{dZ_m}{dt} + \eta \frac{Z_m}{T - t} = -g\, n_b\, (t + \tau) \qquad \text{(IV.C-23)}$$

The above equation is not directly integrable in closed form.

Utilizing numerical integration, required normalized missile acceleration for a system bias n_b versus normalized time of flight t/T for several effective navigation ratios n can be derived.

In figure (IV.C-12) curves of n_m/n_b versus t/T are drawn for values of n = 3 and T/t = 5, 10, 15 and ∞. It

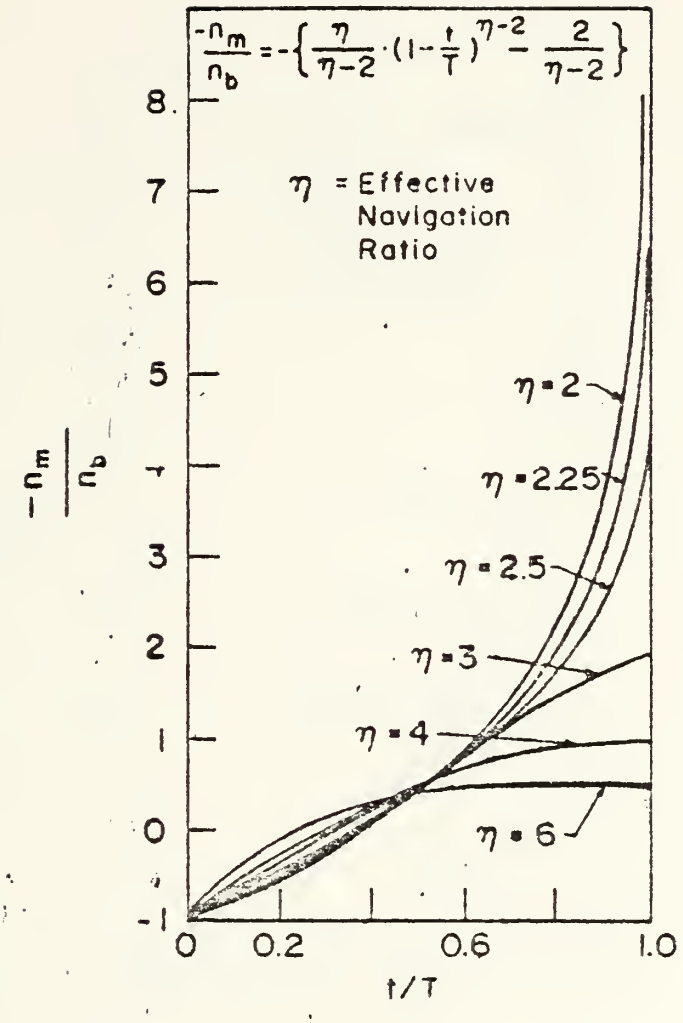

Fig. IV.C-11. Missile Acceleration Required for a System Acceleration Bias, n_b.

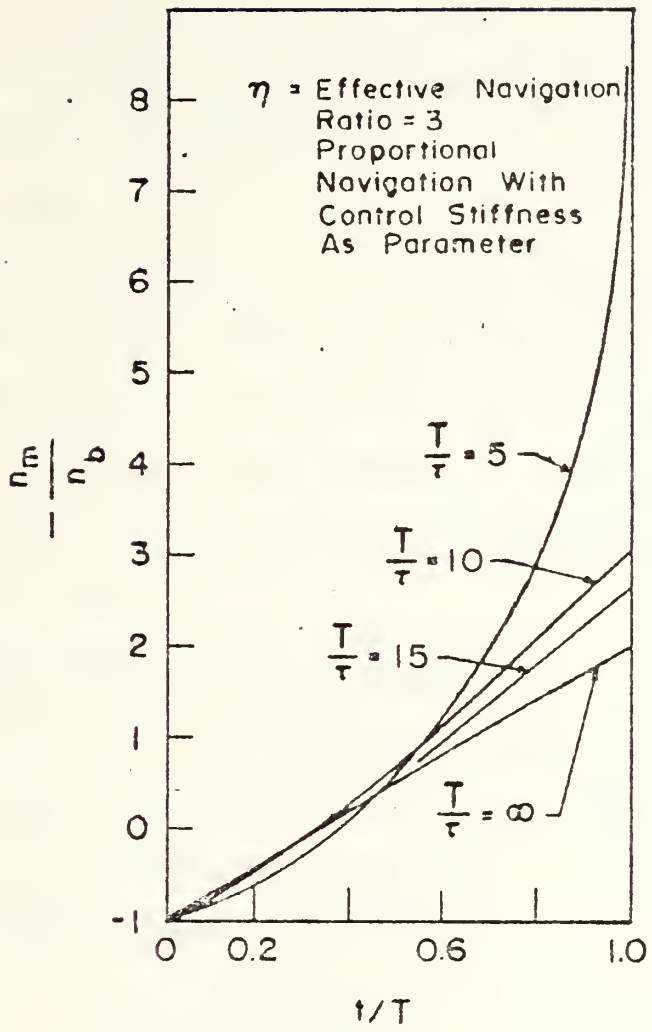

Fig. IV.C-12. Missile Acceleration Required for a System Bias, n_b

is observed that for reasonable demands on the missile acceleration, T/t should be 10 or greater, which means that the missile flight time should be 10 tracking loop time constants or longer.

In figure (IV.C-13), curves of $-n_m/n_b$ versus t/T are drawn for values of n = 4. From these plots it appears that the flight time should be 15 tracking loop time constants or longer.

The effect of a bias error is to require a missile acceleration over the entire flight time. The effect of a time constant and an acceleration bias in the navigation equation is to place higher demands on the missile acceleration and to require that the missile flight time be about 15 time constants long.

5. Augment Proportional Navigation

In section IV.B.2 it was derived that the required missile acceleration, normal to the flight path of the missile in case of constant bearing flight, is given by equation IV.B-5 or equation IV.B-6 which is:

$$a_{mn} = n V_c \dot{\psi}/\cos L \qquad \text{(IV.B-6)}$$

From figure IV.B-1 it is derived that:

$$n_c = a_{mn} \cos L \qquad \text{(IV.C-24)}$$

where n_c: missile acceleration perpendicular to the L.O.S. Upon substituting equation (IV.C-24) into equation (IV.B-6) it is derived

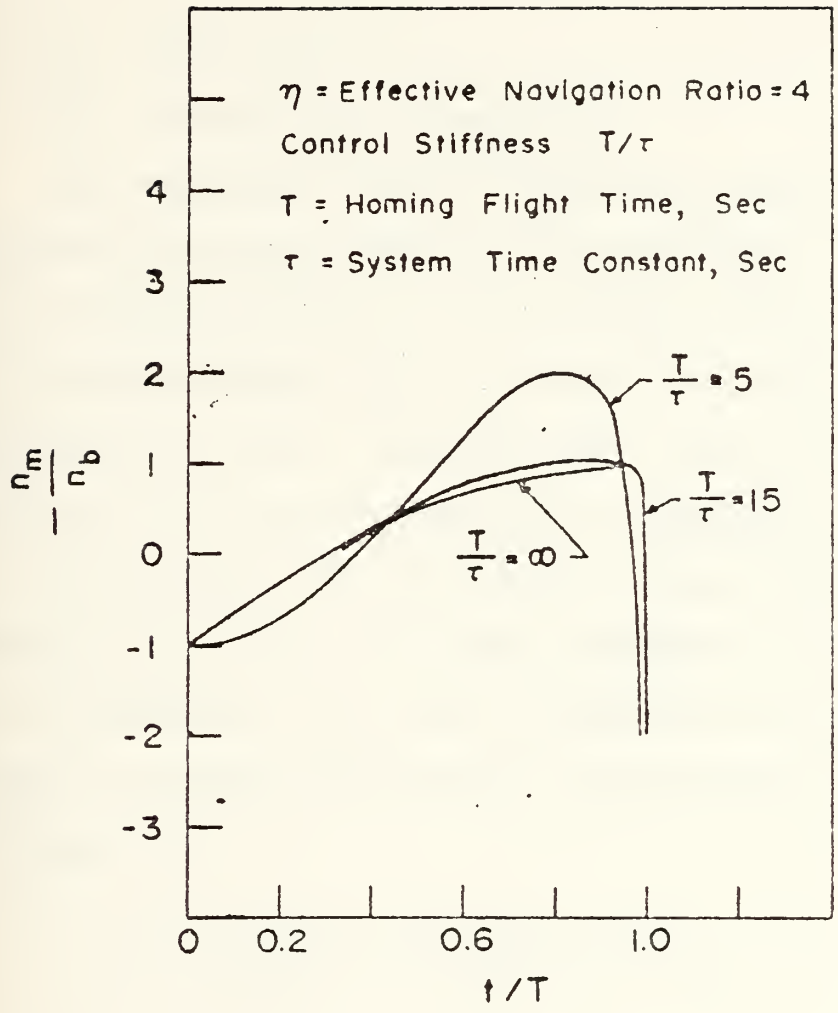

Fig. IV.C-13. Missile Acceleration Required for a System Bias, n_b

$$n_c = n V_c \dot{\psi} \qquad \text{(IV.C-25)}$$

or

$$n_c = n V_c \frac{d}{dt}\left(\frac{y}{V_c t_{go}}\right) = \frac{n}{t^2_{go}}[y + \dot{y} t_{go}] \qquad \text{(IV.C-26)}$$

where t_{go}: time to go

y: differential displacement

The expression in the brackets of equation (IV.C-26) represents the miss-distance that would result (in the absence of target maneuver) if the missile made no further corrective accelerations, and is referred to as the zero effort miss-distance (Z.E.M). Therefore, P.N. can be thought of as a guidance law in which acceleration commands are issued inversely proportional to the square of time-to-go and directly proportional to Z.E.M. If target maneuver, of n_T acceleration, is considered, the Z.E.M. changes and a new guidance law known as augment proportional navigation, APN, results as follows:

$$n_c = \frac{n}{t^2_{go}}\left[y + \dot{y} t_{go}\right] + \frac{1}{2} n_T t^2_{go} \qquad \text{(IV.C-27)}$$

This law is compared later on with the P.N. and modern guidance implemented in the same guidance system.

6. Conclusions

The classical definition of proportional navigation is:

$$\dot{\gamma}_m = N\dot{\psi}$$

where N is the navigation ratio.

Since the angle of the velocity vector cannot be controlled directly the missile commanded acceleration is made proportional to $\dot{\psi}$. This results in a guidance equation of

$$a_{mn} = N V_m \frac{\dot{\psi}}{\tau S + 1}$$

or

$$a_{mn} = \frac{nV_c}{\cos L} \frac{\dot{\psi}}{\tau S + 1}$$

A differential equation is derived that gives the missile response (perturbations) relative to a constant bearing course with the assumption of constant target and missile velocity, linear missile operation and a single system time constant due to the tracker.

An initial missile velocity vector pointing error results in a high missile acceleration early in flight and a low acceleration near the end of flight ($3 \leq n \leq 6$). The effect of a time constant is to increase the missile acceleration and values of T/τ of 15 are needed to prevent excessive missile acceleration.

A target maneuver results in a low missile acceleration early in flight and a higher acceleration near the end of flight. Values for the effective navigation ratio between 3 and 6 keeps the missile acceleration demands relatively low. A missile flight time of about 15 time constants or more is needed to minimize the missile acceleration requirements.

In almost all cases $3 \leq n \leq 6$ is required to minimize the missile acceleration near the end of flight. In almost all cases, the flight time should be equal to or greater than 15 tracker time constants to minimize the missile acceleration.

All the used computer programs of simulation are enclosed in appendices A, B and C.

V. MODERN CONTROL MISSILE GUIDANCE LAWS

A. GENERAL

As was mentioned in part III, there have been developed many guidance laws, which have been categorized in two major subsets, the "classical" and the "modern" guidance laws.

In part III and IV, the "classical" missile guidance laws were studied. This part intends to outline the basic principles and theory which deal with the "modern control" guidance laws

All the guidance laws which are characterized as "modern" have been categorized in two major subsystems, the "modern control guidance laws based on optimal control theory" and the "modern control guidance laws based on differential games."

The basic difference in philosophy between missile guidance laws based on optimal control theory and those based on differential game theory is in the assumptions made by the guidance laws on the target's future trajectory and maneuvering capabilities.

"Optimal control" theory assumes that the target's future maneuver strategy is completely defined, either in open-loop or closed-loop form. The feedback nature of missile guidance laws allows the missile to correct for inaccurate predictions of target maneuvers.

In contrast, the "Differential Game" approach makes no assumption on future target maneuvers, but instead takes into consideration the target's maneuver capabilities. The guidance law then guides the missile so as to minimize the potential effects of the target's intelligent use of his maneuver capabilities.

Optimal control theory has been used to derive a variety of deterministic guidance laws for intercept missiles. These laws are all based on the application of linear-quadratic optimal control theory to a linear constant coefficient missile model with various assumptions on availability of target acceleration information, enforcement of zero final miss distance, and the model used for the airframe/autopilot response of the missile. In all cases the resulting optimal guidance law is a modified form of Proportional Navigation.

In contrast, the application of zero sum perfect information differential game theory to the derivation of intercept missile guidance laws has been less extensive. Due to the complexity and difficulty that arises in the implementation of differential game theory into actual missile guidance it currently does not appear often in the scene.

From theoretical studies and computer simulations it turns out that the major advantage of differential game guidance laws compared with optimal control theory is that the differential game laws are less sensitive to errors in estimates of target acceleration. This results from the fact

that the differential game guidance laws are based only on the maneuver capabilities of the target and not a projected future acceleration history as is required for the optimal control laws. Therefore, the use of differential game methods in the design of guidance laws for intercept missiles appears to result in better missile performance against highly maneuverable targets than does the use of optimal control theory.

B. MODERN CONTROL GUIDANCE LAWS BASED ON OPTIMAL CONTROL THEORY

The optimal control theory was developed mainly during the late 1950's and early 1960's. Up to this time the missile guidance designers used to base the missile guidance control system on the principles of the "classical" control theory. But during the late 1960's and early 1970's, a few missile designers did take a cursory look at applying the modern control theory to the tactical missiles. Basically, such an approach would replace the low pass filter with an optimal estimator such as the Kalman filter. In theory, this would allow one to "optimally" separate the signal from the noise by using information about the missile dynamics and noise covariances rather than filtering based only on frequency content. In addition, missile/target states other than line-of-sight rate could be estimated, even if not measured, provided they were mathematically observable. This, in turn, would allow one to design more advanced guidance

laws based upon optimal control theory, because such theory usually requires complete information concerning the missile states.

Figure V-1 provides in a block diagram form a functional comparison between "classical" and "modern" control approaches. It is seen that the two methods differ in filtering theory, in guidance law and in feedback states (channels).

The recent years' evolution of science in electronics domain, numerical techniques for solving complex equations and the birth of microcomputer and microprocessor, allow the performance of more calculations, more often, more accurate, at less cost, and in a smaller volume than anyone would have imagined a few years ago. Thus, the resulting guidance laws, due to the application of optimal control theory, can be easily implemented in real life.

The study of the modern control theory has not been completed yet. Extensive research programs are conducted to investigate and improve furthermore these modern control and estimation techniques that have potential application, especially, for improving short range air-to-air missile performance.

Subjects of further investigation for future applications of optimal control theory are:

a. In guidance and control theory: Linear and Nonlinear Quadratic Theory, Linear Quadratic Gaussian, Adaptive Control, Reachable Set Theory, Parameter Insensitive and Differential Games.

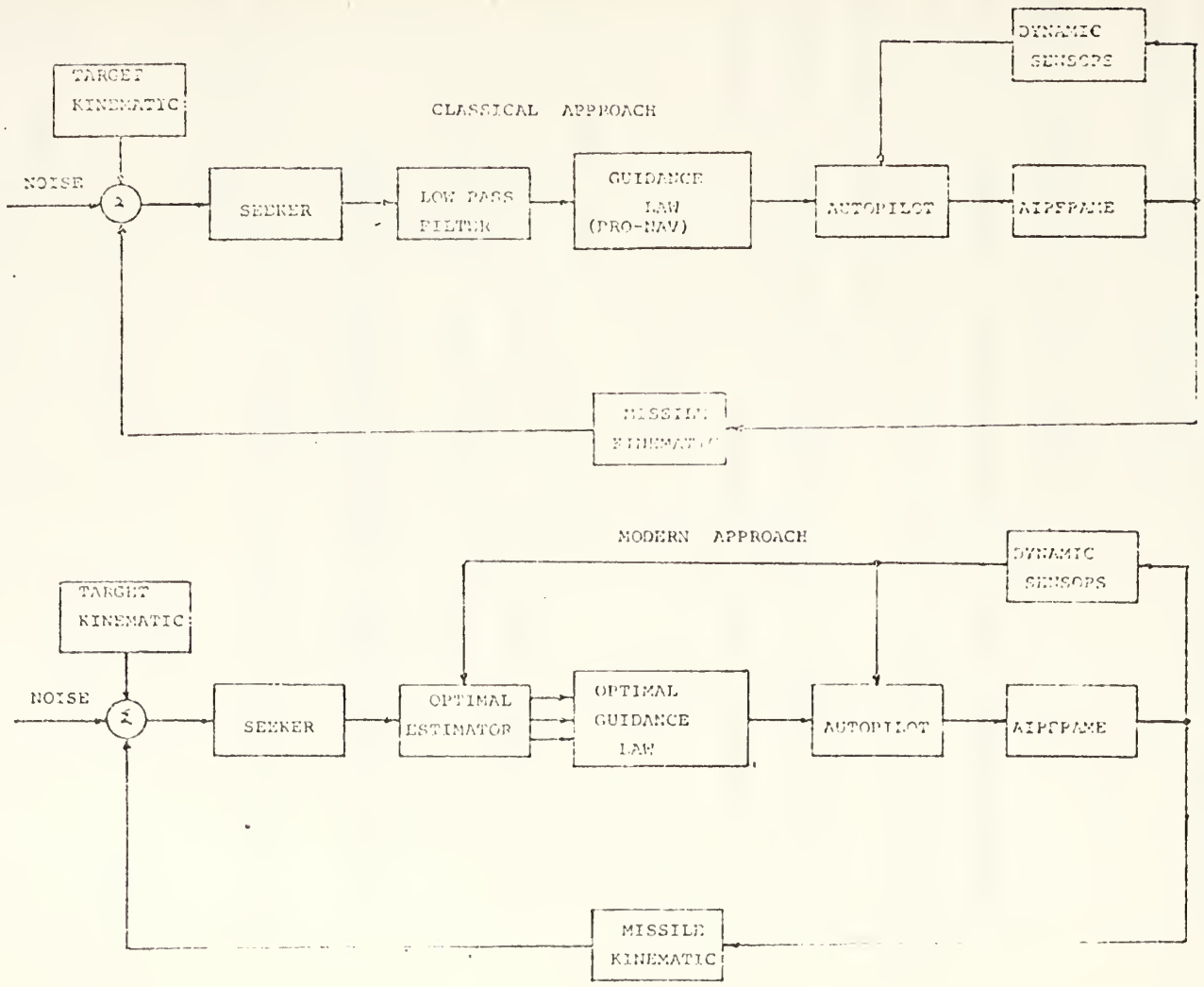

Figure V-1. Functional Comparison between Classical and Modern Guidance and Control.

b. In Estimation Theory: Extended Kalman Filtering, Observers, Adaptive Filters, Nonlinear Filters, Splines and Polynomial Techniques.

The early studies on modern control theory applicability into missile guidance and control design, pointed out that a simplistic and straightforward application of "modern" control theory results in very little performance improvement over "classical" design techniques.

C. GENERAL OPTIMAL CONTROL THEORY

This part intends to review some of the more salient features of the "optimal control theory" and to highlight its usefulness and its limitations.

In general, any dynamic system can be represented by a set of nonlinear differential equations as follows:

$$\dot{\underline{X}} = \underline{f}(\underline{x},\underline{u},t) \qquad \text{(V.C-1)}$$

where: $\underline{X}$: State vector of the system

$\dot{\underline{X}}$: The time derivative of the state vector

$\underline{u}$: The system control vector input

$\underline{f}(.)$: A vector function whose components are nonlinear functions of the state and control vector components and of time.

Such a system may also be subject to terminal equality constraints of the form:

$$\underline{\psi}(t_i,t_f,x_i,x_f) = 0 \qquad \text{(V.C-2)}$$

where: t_i = the initial time

t_f = the final time

x_i = the initial state

x_f = the final state

$\psi(.)$ = a vector function whose components are nonlinear functions of the initial and final state vector components and the initial and final times.

The theory can also handle inequality constraints on both the control vector and state vector, but this generality will be omitted here for the sake of brevity and space limitations, even though it is an important consideration in practical applications.

The optimal control problem can be stated as follows: Select a control vector $\underline{u}(t)$, for $t_i \leq t \leq t_f$ such that to minimize some performance index (P.I) (or sometimes referred to as a cost function), of the form:

$$P.I = g(t_i, t_f, \underline{x}_i, \underline{x}_f) + \int_{t_i}^{t_f} L(t, \underline{x}, \underline{u}) dt \qquad \text{(V.C-3)}$$

where: $g(.)$: a scalar function of the initial and terminal times and states.

$L(.)$: a scalar time-varying function of the state and control vectors form $t_i \leq t \leq t_f$.

The so far formulated general optimal control problem, highlights the following properties:

(1) It includes any system that can be represented by a set of nonlinear time-varying differential equations.

(2) The system and controls can be subject to a large class of equality or inequality constraints.

(3) The performance index includes both initial and final conditions, plus the time history of the control and state vectors.

Although the above stated formulation of the general optimal control problem has tremendous generality, the practical disadvantages become evident when the solution is examined. There are many representations of the solution, all of which of course give the same answer. Perhaps the most popular representation is in terms of the Hamiltonian. Define the following quantities:

$$H(t,\underline{x},\underline{u},\underline{\lambda}) \triangleq L(t,\underline{x},\underline{u}) + \underline{\lambda}\,\underline{f}(t,\underline{x},\underline{u})$$

where H is called the Hamiltonian and $\underline{\lambda}$ is the vector of Lagrangian multipliers so often used in the calculus of variations;

$$G(t_i,t_f,\underline{x}_i,\underline{x}_f,\underline{\nu}) = g(t_i,t_f,\underline{x}_i,\underline{x}_f) + \underline{\nu}^T\underline{\psi}(t_i,t_f,\underline{x}_i,\underline{x}_f)$$

where $\underline{\nu}$ is also a vector of Lagrangian multipliers.

It has been proved that the solution to the problem stated in (V.C-1) through (V.C-3) is given by:

$$\dot{\underline{\lambda}} = -\frac{\partial H}{\partial \underline{x}} \qquad \text{(V.C-4)}$$

$$\dot{x} = \frac{\partial H}{\partial \underline{\lambda}} \qquad \text{(V.C-5)}$$

$$\frac{\partial H}{\partial \underline{u}} = 0 \qquad \text{(V.C-6)}$$

$$\frac{\partial G}{\partial \underline{x}_i} = -\underline{\lambda}/t_i \qquad \text{(V.C-7)}$$

$$\frac{\partial G}{\partial \underline{x}_f} = -\lambda/t_f \qquad \text{(V.C-8)}$$

$$\frac{\partial G}{\partial t_i} = H/t_i \qquad \text{(V.C-9)}$$

$$\frac{\partial G}{\partial t_f} = H/t_f \qquad \text{(V.C-10)}$$

A typical solution procedure is based upon the following steps

Step 1: Solve equation (V.C-6) for u(t).

Step 2: Solve equation (V.C-5) for $\underline{\lambda}(t)$. Note that, in general, this involves the solution of nonlinear differential equations, which may or may not have an analytical closed-form solution. Also note that this differential equation may be coupled with equation (V.C-4).

Step 3: Substitute the solution for $\underline{\lambda}(t)$ from step 2 into the solution for $\underline{u}(t)$ in step 1. Then substitute this form of $\underline{u}(t)$ into (V.C-5).

Step 4: Solve equation (V.C-5) for $\underline{x}(t)$. This is also a nonlinear differential equation which might be coupled to equation (V.C-4).

Step 5: Note that the solution to $\underline{x}(t)$ and $\underline{\lambda}(t)$ involves 2n unknown constants where n is the dimension of the state vector. Use all given initial and final conditions for $\underline{x}(t)$ along with the solutions to equation (V.C-7) through (V.C-10). This should result in 2n equations in 2n unknown constants, which in theory can be solved completely.

It should be obvious that there are very few conditions under which closed form solutions for $\underline{u}(t)$ exist. In general, complex numerical techniques must be employed, involving a large amount of data and numerous calculations. There are two other disadvantages to this formulation which should be

noted. First, the solution is initial and/or final condition dependent. Hence, for each launch condition and target maneuver in an air-to-air missile engagement, the solution must be completely recalculated. Also note that, in general, the solution for the optimal control depends only on time. This is what is referred to as an open-loop solution since it does not depend directly upon the missile state $\underline{x}(t)$. If it did, then it is referred to as a closed-loop or a feedback solution. This fact has severe consequences in practical solutions, since the actual state trajectory will in general diverge from the optimal one if there is any error in the dynamic model (equation V.C-1).

Although the solution of the general nonlinear time varying optimal control problem requires a tremendous amount of effort, recent studies proved that, when advanced numerical techniques are used in combination with the computational power of modern microprocessors, reasonable solutions can be obtained for somewhat simplified nonlinear formulations. In addition, a feedback solution can be approximated by re-solving the problem at appropriate time intervals in real-time on-board the missile. Although such a solution would not be the optimal one from launch to fuzing, it does offer significant advantages over classical proportional navigation and may be the only approach when the system involves significant non-linearities. The disadvantages of the general non-linear theory led researchers to search for less general

but more tractable formulations of the optimal control problem. The result was Linear Quadratic Theory.

D. LINEAR QUADRATIC THEORY

Linear Quadratic Theory is a subset of the general nonlinear optimal control theory. The key elements in the formulation are the same: a dynamical system model, a performance index (or cost functional) and appropriate constraints. The difference in formulation lies in the fact that the dynamical system model must be linear, the cost functional must be quadratic in nature, and only a limited set of constraints are allowed. The linearity assumption is the most severe for air-to-air missiles. Nonlinear aerodynamics, nonlinear equations of motion and nonlinear kinematics are prevalent in air-to-air missile engagements.

The limited nature of the allowable constraints are somewhat less of a problem. Two of the more important constraints (terminal state $\underline{x}_f = \underline{0}$ and $\underline{u}(t) \leq \underline{u}_{max}$) are still allowable. The problem of allowing only quadratic cost functionals is usually workable. This is primarily because it is still allowed to use a time varying weighting matrix and most intuitively reasonable costs are of a quadratic (or positive definite) nature.

There are several techniques available for applying this linear theory to nonlinear systems. Some of the most common ones are:

(a) Ignore the nonlinearities by postulating what seems to be a reasonable linear model of the nonlinear system and hope that this will not significantly decrease the overall optimality of the solution.

(b) Compute some optimal nominal trajectory using nonlinear theory. Then linearize the nonlinear system equations about this nominal trajectory, using small perturbation theory. Apply the optimal linear theory to the linear perturbation equations. This will result in two control functions, one for the nominal trajectory ($\underline{u}_N(t)$) and one for the perturbation trajectory ($\underline{u}_L(t)$). One disadvantage of this approach is that it forces the missile trajectory to follow the optimal nonlinear trajectory of the "model" and this trajectory may be far from the true optimal trajectory for the actual missile. Another drawback is that the optimal nominal trajectory is a function of initial conditions. Hence, one either has to compute a new optimal nominal trajectory for each launch condition (using the complex solution process outlined in section V.C) or contend that the differences in optimal nominal trajectories for various launch conditions are unimportant in the overall optimality of the solution.

(c) Linearize the nonlinear equations about the current value of the state vector and re-solve the linear problem on-line at various points along the trajectory. This technique will usually cause the solution to "forgive mistakes" made in the past due to invalid linearity assumptions.

There are two major deficiencies associated with all these methods. First, there is no a priori analytical global method of determining how much is sacrificed in optimal performance (i.e., how much does the performance index increase) when these approximations are used. The only real way to evaluate this is through extensive computer simulations. Second and more important, there are not even analytical methods available to ascertain whether or not the solutions remain stable. (This is not exactly true. There are a few special types of nonlinearities for which analytical methods have been developed to ascertain stability.) Although the Linear Quadratic theory has all these drawbacks, it is used extensively due to its properties and relative ease of implementation.

Let the dynamical system be represented by the following linear nonhomogeneous differential equation:

$$\dot{\underline{X}}(t) = \underline{F}(t)\underline{X}(t) + \underline{G}(t)\underline{U}(t) + \underline{C}(t) \qquad \text{(V.D-1)}$$

where $\underline{X}(t)$: State vector

$\underline{U}(t)$: Control vector

$\underline{C}(t)$: Column vector of the same dimensions as $\underline{x}$

$\underline{X}_0$: Given initial conditions.

The quadratic performance index (Q.P.I.) may have the following general form:

$$2J = (x^T S_f x)_{t_f} + \int_{t_0}^{t_f} (x^T A x + u^T B u)\,dt \qquad \text{(V.D-2)}$$

The necessary conditions for an optimal trajectory become:

$$\underline{\dot{\lambda}}^T = -\partial H/\partial \underline{x} = -\underline{A}\underline{x} - \underline{F}\underline{\lambda} \qquad \text{(V.D-3)}$$

$$\text{with} \quad \underline{\lambda}(t_f) = \underline{S}_f \, \underline{x}(t_f)$$

$$\partial H/\partial \underline{u} = 0 = \underline{B}\underline{u} + \underline{G}^T\underline{\lambda} \qquad \text{(V.D-4)}$$

where H, the Hamiltonian equation, is defined as:

$$H = \tfrac{1}{2}(x^T A x + U^T B U) + \lambda^T(Fx + Gu + C) \qquad \text{(V.D-5)}$$

The explicit solution of equation (V.D-4) gives:

$$U(t) = -B^{-1} \, G^T \, \lambda$$

Equations (V.D-1) and (V.D-3) can be combined into a matrix notation:

$$\begin{vmatrix} X \\ \dot{\lambda} \end{vmatrix} = \begin{vmatrix} F & -G\,B^{-1}\,G^T \\ -A & -F^T \end{vmatrix} \begin{vmatrix} X \\ \lambda \end{vmatrix} + \begin{vmatrix} C \\ 0 \end{vmatrix} \qquad \text{(V.D-7)}$$

where $X(t_0)$ is given and $\lambda(t_f) = P_f \, X(t_f)$.

Assume a solution, for the linear inhomogeneous equations (V.D-7) of the form:

$$\lambda(t) = P(t)X(t) + K(t) \qquad \text{(V.D-8)}$$

The differentiation of equation (V.D-8) gives

$$\dot{\lambda} = \dot{P}X + P\dot{X} + \dot{K} \qquad \text{(V.D-9)}$$

while the substitution of equation (V.D-8) into (V.D-7) gives

$$\dot{\lambda} = -AX - F^T(PX + K) \qquad \text{(V.D-10)}$$

Equating equation (V.D-9) and (V.D-10), replacing $\dot{X}$ with its equivalent from equation (V.D-1) and upon collecting terms, it turns out:

$$\left[\dot{P} + PF + F^T P - PGB^{-1}G^T P + A\right]X + \left[\dot{K} + (F^T - PGB^{-1}G^T)K + PC\right] = 0 \qquad \text{(V.D-11)}$$

The introduction of the arbitrary n component vector K(t) introduces the freedom of specifying n arbitrary conditions consistent with the boundary conditions given. Vector K(t) can be selected properly so that the second bracket in equation (V.D-11) can be vanished. This means that K(t) must satisfy a differential equation

$$\dot{K} + (F^T - PGB^{-1}G^T)K + PC = 0 \qquad \text{(V.D-12)}$$

with the boundary condition $K(t_f) = 0$.

The first bracket in equation (V.D-11) must vanish independently and as $\underline{X}$ is an arbitrary vector, the necessary condition for this implies the usual matrix RICCATI equation.

$$\dot{P} + PF + F^T P - PGB^{-1}G^T P + A = 0 \qquad \text{(V.D-13)}$$

with the boundary condition $P_f = P_{(t_f)}$. The solution P(t) of equation (V.D-13) is used in equation (V.D-12), which must hold for all values of P(t). Knowing K(t), in turn, gives the desired control law which from equation (V.C-6) and (V.C-8) is seen to be:

$$U = -B^{-1}G^T PX - B^{-1}G^T K \qquad \text{(V.C-14)}$$

The solution for u(t) in equation (V.C-14) has several attractive properties. The most important ones for the usual applications are as follows:

(a) Note that the solution for $\underline{u}(t,\underline{x})$ and P(t) are independent of $\underline{x}_i$ or $\underline{x}_f$. This is extremely important because it means that the problem need be solved only once (off-line) and this solution will be valid for all initial and final conditions. This was not the case for the nonlinear theory.

(b) $\underline{u}(t,\underline{x})$ is a function of the system state $\underline{x}(t)$. The fact that $\underline{u}(t,\underline{x})$ is a feedback control law means that it is less sensitive to noise, external disturbances, and modeling errors. Such a property is called robustness in the literature.

(c) K(t) is called the control gain. All the information needed to determine K(t) can be computed off-line and stored in a missile computer. Furthermore, if F, G, A and B are constant and $t_f \to \infty$, K becomes a constant. However as the true missile system is not linear, if the on-line linearization technique is used, a new K must be computed for each new value of F, G, A and B.

Besides the general disadvantages already noted at the beginning of this section for linear theory, there are two others which deserve mentioning. First the solution depends on a good choice for t_f. At first one might argue that t_f is a "free" parameter, subject to the designer's selection. In theory this is true, but in practice t_f really determines how good the solution is. A review of equation (V.D-2) reveals

that the choice of t_f not only affects the minimum value of PI but also drives the optimal trajectory solution and the final state $\underline{x}_f$. In the air-to-air missile problem, selecting a given value of t_f in effect determines the terminal miss distance for a given launch condition. If the true objective is to minimize terminal miss distance, then the problem now becomes one of selecting the "optimal" t_f which results in the minimum miss distance. In effect, there is a freedom in selecting the missile time of flight from launch to intercept. The problem now becomes one of selecting both the $\underline{u}(t,\underline{x})$ and the t_f which will result in the smallest value of PI.

The other disadvantage of the linear theory is the requirement for a real-time knowledge of $\underline{x}(t)$, the relative target/missile state. Since the missile model is only a crude linear approximation and since there is no definite knowledge of future target maneuvers, $\underline{x}(t)$ must be determined on-board the missile. Current sensors provide an estimate of only a few missile states. To increase the quantity and quality of the missile sensor would also add significant cost.

An alternative approach is to use optimal estimation theory to extract the mathematically observable states from the limited measurement data.

E. MISSILE AND TARGET STATE ESTIMATION

In the proceeding parts, two potential drawbacks associated with the application of the optimal control theory to the tactical missiles were discussed. One drawback was the need to have an accurate and current knowledge of the system models. This is true whether linear or nonlinear theory is used. Secondly, the linear quadratic theory results in a feedback solution for $\underline{U}(t,\underline{x})$, requiring a complete knowledge of all the states of the system model. Additional assumptions and approximations could reduce this requirement, but the statement is true in general.

Completely accurate system models are never possible, even if nonlinear theory is used. The aerodynamic properties of a missile can only be approximated, even if extensive wind tunnel and free flight testing results are provided.

Many of the missile subsystems include unknown nonlinearities and noise characteristics, which at best can only be modelled by stochastic processes. Even the six-degrees-of-freedom equations of motion often include simplifications made for practical considerations. If it is chosen to linearize the system model in order to apply the linear theory, the model becomes even more inaccurate and could require periodic updating throughout the missile trajectory.

In a small low cost tactical missile, few of the relative target/missile states which are required for a feedback guidance law are directly measurable. Typical sensors on-board

such missiles consist of two rate gyros (pitch and yaw), two normal accelerometers, and a roll gyro. Sometimes pitch and yaw attitude gyros and a roll rate gyro are also included, either as additions or replacements for the other sensors. All of these sensors have been used in the past for autopilot rather than guidance law implementation. They also require their own models, including appropriate stochastic models for noise.

Additional state information, of course, is provided by the seeker. This sensor has been the principle source for guidance law information in the past. The primary quantity measured by the seeker is inertial line-of-sight rate; a radar seeker could also provide range rate and range. The seeker is also a dynamical system, and it must be deterministically and stochastically modelled in the same manner as the other sensors. The seeker gimbal angles (angles between the seeker axes and the missile axes) can also usually be measured for little additional cost, but they have seldom been used in the past for guidance law or autopilot implementation. The current research has shown that these angles contain much valuable information, since they provide an approximation of the missile/target boresight angle. Recent studies have also indicated that including the target inertial acceleration in the model can also significantly increase performance, but currently there are no missile sensors which can directly measure this quantity.

Clearly the gap between required state information and measured state information creates a significant problem if the modern control theory is applied to develop advanced guidance laws. The additional requirement that the models be accurate for both linear and nonlinear formulations and in the presence of stochastic processes presents additional challenges. The objective is to provide accurate estimates of all states and model parameters required for the advanced guidance law without significantly increasing the sensor requirements (and therefore cost) for future tactical missiles. The computational requirements for such algorithms are similar to those for the optimal control algorithms. However, the one important difference is that the estimation algorithms always require repeated solution on-board the missile in real time. This is primarily due to the fact that they are continually processing measurement data to update the estimates for the constantly changing states and model parameters.

F. INFORMATION PROCESSING BY OPTIMAL ESTIMATION THEORY

Information processing represents a substantial link between the information needs of the guidance law and the possible information offer of the feasible sensor equipment of a guided missile system. Especially the considerations about extended guidance law design are influenced by two features: on one hand information can be obtained from noisy measurements only; on the other hand direct information sensing

cannot be performed for each signal by physical and/or economical reasons.

Filtering theory provides for tools of information processing on noisy measurements. It is based on the reasonable idea to separate the measurement signals in time-correlated signals and time-uncorrelated disturbances. The latter do not possess any information about the past which may be useful in the future; they are purely random. Therefore filtering techniques aim at estimation of the complete time-correlated information.

The correlated portion of measurement signals includes the information signals as well as time-correlated disturbances, i.e. colored noise. To describe their dynamical behavior mathematically, differential equations can be used. From the physical point of view, uncorrelated disturbances represent noise with negligible time correlation relative to the correlated signals. Mathematically they can be modelled by "white" noise. Restricting the review to the linear, Gaussian case, filtering theory is based on the following mathematical (real world) model:

(1) Measurement model:

$$\underline{Z} = \underline{H}\underline{x} + \underline{v} \qquad \text{(V.F-1)}$$

where: $\underline{Z}(t)$: m-dimensional measurement vector,

$\underline{x}(t)$: n-dimensional state vector for correlated signal modelling,

$\underline{v}(t)$: m-dimensional measurement noise vector with white Gaussian noise, $v(t) \rightarrow N(0,R(t))$.

(2) State space model:

$$\dot{\underline{X}} = \underline{F}\underline{x} + \underline{G}\,\underline{u} + \underline{C}\underline{w} \quad ; \quad x(t_0) \sim N(x_0, P_0) \qquad \text{(V.F-2)}$$

where: $\underline{U}(t)$: r-dimensional deterministic input vector

$\underline{w}(t)$: s-dimensional input noise vector with white, Gaussian noise.

The matrices F(t), C(t), G(t) and H(t) are of appropriate dimensions. Since the state vector $\underline{x}(t)$ contains all useful information, the design aim of filtering theory consists of developing algorithms to produce a state estimate $\hat{\underline{x}}(t)$ using the available measurements $Z(T)$, $t_0 \leq \tau \leq t$. In the case of high quality demands on the estimation performance, it is advantageous to formulate the estimation problem as an optimal filtering problem with regard to the estimation-error variances as performance measure:

Given measurements $\underline{Z}(T)$, $t_0 \leq \tau \leq t$ based on a state vector model (see equations V.F-1,2), find a state estimate $\underline{x}(t)$ of the actual state $\hat{\underline{x}}(t)$ such that a quadratic performance criterion J on the error-covariance matrix $P_{(t)} = E\{\tilde{\underline{X}}(t)\ \tilde{\underline{X}}^T(t)\}$ with the estimation error vector $\tilde{\underline{X}}(t) = \underline{X}(t) - \hat{\underline{X}}(t)$ is minimized:

$$J = \text{trace } P(t) \rightarrow \min \qquad \text{(V.F-3)}$$

There are many different optimal estimation techniques currently undergoing research. One of the most popular optimal estimation techniques is the well known KALMAN-BUCY filter, which consists of:

(1) A linear vector differential equation for the state estimate $\hat{\underline{X}}(t)$:

$$\dot{\hat{\underline{X}}} = \underline{F}\hat{\underline{X}} + \underline{K}_f(\underline{Z} - \underline{H}\hat{\underline{X}}) + \underline{G}\underline{U} \; ; \quad \hat{\underline{X}}(t_0) = \underline{X}_0 \qquad \text{(V.F-4)}$$

(2) A non-linear matrix differential equation (the well known Riccati equation), for the error-covariance matrix $\underline{P}(t)$ to be integrated forward in time:

$$\dot{\underline{P}} = FP + PF^T - PH^TR^{-1}HP + CQC^T \; ; \quad \underline{P}_{(t_0)} = \underline{P}_0 \qquad \text{(V.F-5)}$$

(3) A computational rule for the filter feedback matrix $K_f(t)$:

$$K_f = PH^TR^{-1} \qquad \text{(V.F-6)}$$

The solution of the filtering problem by the time domain approach of the Kalman-Bucy filtering offers essential advantages as against the frequency domain approach of Wiener filtering. These advantages are:

- The cases of multi-noise inputs and multi-sensors configuration can be treated within this framework.
- The real world model (see equations V.F-1,2) is formulated to include time-varying system coefficients and statistic parameters.
- There are numerically efficient algorithms to solve the matrix Riccati equation by means of a digital computer.
- If real world and real world model coincide, the estimation accuracy of information processing can directly be obtained from the diagonal elements of the error-covariance matrix P(t). Otherwise it has to be determined by sensitivity analysis or simulation.

But despite the theoretical optimality and the above outlined advantages, there are difficulties to be overcome in the application to practical problems. These include divergence, degradation of control performance and large computational requirements.

Divergence can occur due to:

- Inaccuracies in the system model (including unaccounted for nonlinearities or simple error in the selection of coefficients for the system matrices).
- Inaccuracies (including state dependence) in the statistical models of the system and observation noise processes.
- Simple computational truncation and round-off errors. Computational inaccuracies may even result in calculated covariances which are not positive semidefinite with disastrous consequences.

It has been shown that an optimal state-feedback control law (based on LQ theory), with a Kalman Bucy filter estimate of the state substituted for a direct measurement of the state, will always have degraded performance, even if the models are perfect. However, it has also been shown that this is the optimal solution to the combined linear control/estimation problem if the optimization criteria is to minimize J = E(PI). But in the non-linear case, the estimation and control problems are not in general separable. This means that a controller which would be optimal if perfect state information were available may no longer be the best controller if only estimates of the state can be used.

The computational requirements of a Kalman Bucy filter can become very large, especially if the number of measurements or number of states is large. For real-time processing, this may force a simplification of the filter algorithm or system model, and will at least require the use of very efficient algorithms and programs. This will of course be true of any filter selected for this problem.

Techniques have been devised to permit consideration of non-white and cross-correlated measurement and system noise. These essentially amount to ways to restructure the system model to permit direct application of the Kalman-Bucy filter, which remains optimal and conceptionally unmodified.

Of more present concern are problems which force a modification of the filter. These problems include:

1) Nonlinear state and/or measurement equations;
2) State-dependent noise processes;
3) Uncertainty in the system model;
4) Uncertainty in the statistical properties of the noise processes.

The missile problem suffers from all of these difficulties, although it may be possible or advisable (if established by more specific analysis) to gloss over or ignore some of them without excessive penalty.

VI. MAJOR MISSILE SUBSYSTEMS

A. GENERAL

Each missile has its own configuration and carries certain subsystems depending upon many factors, due to the particular design specifications and criteria. But it is possible to generically describe the subsystems and their interrelationships with the aid of figure IV.A-1, which is a functional diagram of the major subsystems. A brief description of each subsystem follows.

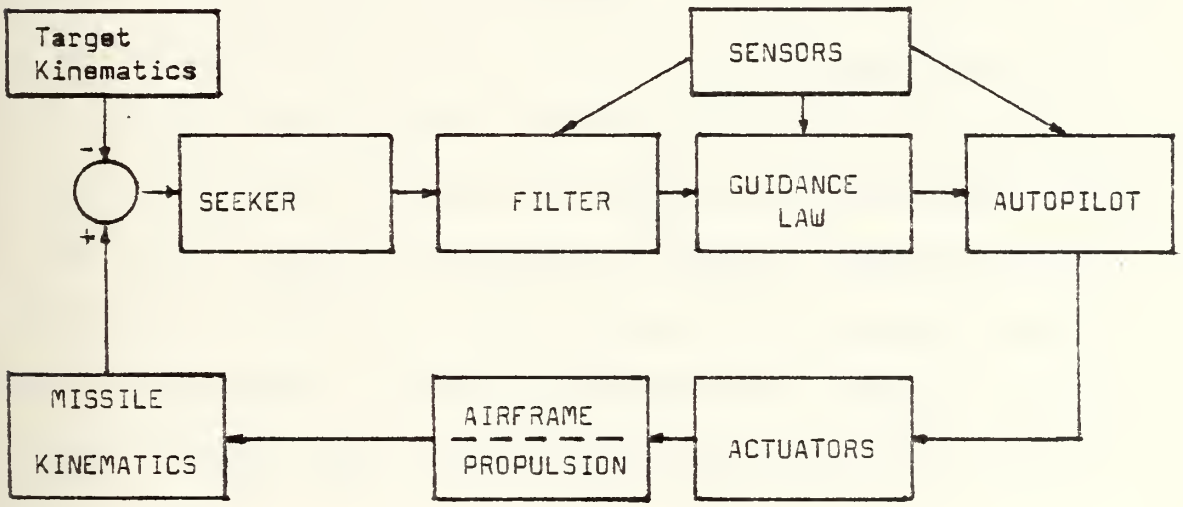

Fig. VI.A-1. Major Missile Subsystems

1. Airframe

The airframe serves two purposes. First it is the container for all the other subsystems (including the pay

load). Secondly, by proper design and in partnership with the propulsion, it can be used effectively to produce the required lift and drag forces for accomplishing the mission objectives.

2. Missile-Target Kinematics

By virtue of Newton's second law and all its ramifications, these net forces determine the kinematic variables of the missile, such as position, velocity and acceleration. These variables, in combination with those produced by the target, result in something new for the seeker to see.

3. Seeker

The seeker can be thought of as the "eyes" of the missile. Its purpose is to detect, acquire and track a target by sensing some unique characteristic associated with it. This unique characteristic usually consists of the radiation or reflection by the target of energy in a specified region of the electromagnetic spectrum. Typical regions include ultraviolet, infrared, laser, visible, millimeter wave and radar frequencies. Some missiles may have seekers which can operate in more than one region at the same time or at different times.

a. Detection

Detection is the process whereby the seeker senses a certain amount of energy (in some region of the electromagnetic spectrum) above that normally expected from background or internal seeker noise.

b. Acquisition

Acquisition is the process whereby the seeker, after experiencing one or more incidents of detection, decides (according to some pre-established criteria or algorithm) that a valid target has been located.

c. Tracking

Tracking is the process whereby the seeker continually specifies the angular location of the target relative to some fixed coordinate system.

4. Filter

The filter operates on the seeker data to produce a clearer "image" of the target behavior by extracting the pertinent kinematic variables.

5. Guidance Law

The guidance law decides the best trajectory (physical action) for the missile based upon its knowledge of the missile capability, target capability and desired objectives. Thus, an appropriate acceleration command to intercept the target is produced which is then sent to the autopilot.

6. Autopilot

An autopilot is a closed loop system and it is a minor loop inside the main guidance loop. Broadly speaking, autopilots either control the motion in the pitch and yaw planes, in which case they are called lateral autopilots, or they control the motion about the fore and aft axis in which case they are called roll autopilots. The function of an

autopilot is to determine what "muscle" control (actuator position) is required to best execute the command issued via guidance law.

7. Actuator

The purpose of the actuator is to alter the external geometry of the missile such that the net forces which result will approximate the guidance law command. This alteration may take the form of a wing deflection, tail deflection, canard deflection, thrust control, or some combination of these. The first three alterations change the aerodynamic properties in such a manner that the proper moments and forces are achieved.

Filter, guidance law and autopilot are three major subsystems of a missile which can be thought of as the "brain" of the missile. The make-up of this "brain triad" depends heavily on the nature of the other subsystems too. A brief survey of the evolution of flight control design practices over the past twenty years shows the following trends:

a. Flight control systems require more sensors that measure dynamic motions of the missile, resulting in an increased number of feedback paths.

b. Filter or compensation networks as command augmentation are introduced to modify and improve command inputs to the servos that drive the aerodynamic surfaces.

c. Filters, compensation networks and washout networks are being added in abundance to the flight control system.

d. "Inner loops" in the form of feedback are being proposed to improve the performance and stability.

These developments taken individually may be justified for individual airframes and flight tasks but the tendency is to build in gradually upon previous designs by cascading, resulting in increased complexity and a very high order system. Such a development is demonstrated in a primitive mode later on.

B. SEEKER

Homing missiles use a seeker to detect, acquire and track the target motion. The type of seeker to be used is crucial to the missile design as well as to flight control system design.

There are several methods available for tracking a target, depending on whether the seeker has a wide or narrow field-of-view, or whether the seeker is gimballed or fixed to the air frame. The instantaneous field-of-view is the angular region (usually conical) about the seeker centerline which is capable of receiving useful energy. The portion of the electromagnetic spectrum which will be sensed by the seeker is also crucial to the design. For instance, the high frequency of an infrared seeker allows a reasonable angular field of view even with a small diameter seeker, but requires a hemispherical Infra Red (IR) dome to avoid image quality degradation. But the hemispherical dome causes appreciable drag on the missile. On the other hand, radar-guided anti-aircraft missiles, due to their longer wavelength,

typically require a larger missile diameter, but the lower frequency allows a tapered dome, which improves aerodynamic efficiency at the expense of increased dome refraction slopes.

If the seeker has a large field-of-view, it is possible to fix the angular orientation of its centerline relative to the airframe centerline (strapdown seeker). The type of tracking information available in such case is an indication of the angle between the line-of-sight (straight line from missile to target) and the missile centerline.

If the seeker has a narrow field-of-view, it is usually mounted on a gimballed platform. The seeker maintains the target within the narrow field-of-view by rotating the platform. If the platform is inertially stabilized, the rotation is accomplished by applying torques which are proportional to the target displacement from the field-of-view center. The tracking information provided by this type of seeker is an indication of the inertial rotational rate of the line-of-sight (L.O.S.).

The primary quantity measured by the seeker is inertial L.O.S. rate. Other information which the seeker might be capable of providing to a guidance law is missile-to-target range and/or range rate. Radar seekers are the only ones which currently provide such information. (Active radar seekers can provide both, semi-active radar seekers can provide range rate, and passive radar seekers can provide neither). Techniques involving modern estimation theory

are being studied which might provide this same capability for passive seekers and/or other frequency spectrums. The seeker is also a dynamical system and it must be deterministically and stochastically modelled in the same manner as the other sensors.

1. Seeker Modelling and Error Sources

The dynamics of a seeker depending upon the complexity of its design, can be represented by a transfer function of first, second, or even higher order.

The modelling of a seeker and used sensor hardware allows one to evaluate the effect of these components on the derived L.O.S. rate. Seekers and inertial sensors do cause errors in the computed L.O.S. rate, and these errors in turn can produce system instability effective navigation gain errors, and degradation of accuracy. The method of generating the inertial L.O.S. rate also affects, to some degree, the sensitivity to each error source. The component errors to be considered fall in three broad classes:

a. Linearity or gain errors (radome, receiver/detector, phase shifter, gyro and seeker/gyro dynamics)

b. Time-varying random errors (thermal noise, glint or apparent target motion, gyro noise)

c. Offsets (seeker boresight errors, gyro offsets and drift).

Other error sources such as cross-coupling, sampling, rate, break-lock or blind range, winds, target motion, body-bending, vibrations and launch offsets, have been proved, via numerous studies, to be of secondary importance.

The mentioned component errors cause corresponding errors in the derived inertial LOS rate. Gain errors cause components of the missile body rate to appear in the derived LOS rate, which can cause stability problems and errors. Random errors in the seeker and rate gyro cause random errors in the LOS rate with a corresponding loss of accuracy. Finally, offsets can cause anomalies in the derived LOS rate depending on their location with respect to the derivative network. Offsets in the LOS rate also result in degradation of miss distance and some increase in required maneuverability.

Seeker noise can also be a problem at low signal-to-noise ratios, particularly since the seeker output must be differentiated. Reducing the derivative network bandwidth minimizes these effects, but stability problems then come into play as discussed previously. Seeker boresight errors and attitude gyro offsets have no effect on the LOS rate since the d.c. gain of the derivative network is zero. However, drifts in the gyro will appear in the output of the derivative network as a LOS rate. In most cases these effects will be insignificant.

For practical computer simulation study purposes, two simplified transfer functions of seeker dynamics are outlined as follows.

a. First Order Seeker

An inertially stabilized seeker may have a block diagram as in figure (VI.B-1) is shown, where:

ψ: actual line of sight angle

D: boresight angle of tracking antenna

$\dot{D}$: rate of boresight angle

e: angular error of $\dot{\psi}$ minus D

T: time constant of the seeker

y: present zero effort miss distance (Z,E,M)

R_{TM}: relative target to missile distance

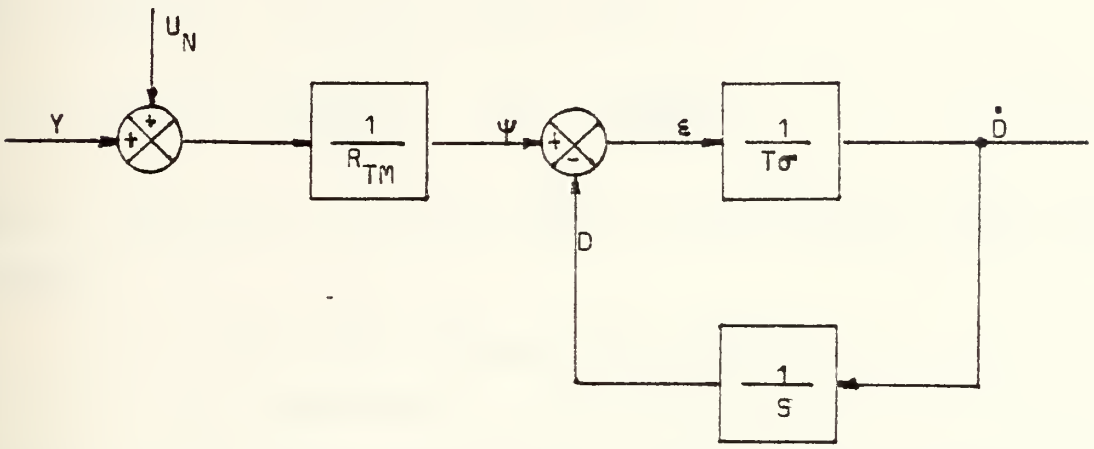

Fig. VI.B-1. First Order Seeker Block Diagram

The close loop transfer function of this first order seeker is:

$$\frac{\dot{D}}{\psi} = \frac{1/T_\sigma}{1 + \frac{1}{S}T_\sigma}$$

or

$$\frac{\dot{D}}{\psi} = \frac{S}{1 + ST_\sigma} \qquad \text{(VI.B-1)}$$

or

$$S\dot{D} = \frac{1}{T_\sigma}(S\psi - \dot{D}) \qquad \text{(VI.B-1a)}$$

where

$$\psi = \frac{Y + U_N}{R_{TM}}$$

Equation (VI.B-1a) can be expressed in state form as follows:

Let $Y = X5$, $\dot{Y} = \dot{X}5 = X6$

$\dot{D} = \hat{\psi} = X8$, $\ddot{D} = \dot{\hat{\psi}} = \dot{X}8$

Then, equation (VI.B-1a) turns into:

$$\dot{X}8 = \frac{1}{T\sigma}\frac{1}{R_{TM}}X6 - X8 + \frac{1}{T\sigma R_{TM}}U_N \qquad \text{(VI.B-1b)}$$

NOTE: States X5, X6, X8 are used to confirm with later on studies.

b. First Order Seeker with Observer

An improvement in the performance of a guidance system can be achieved utilizing a seeker with an observer. Such a combination may have a block diagram as in figure VI.B-2.

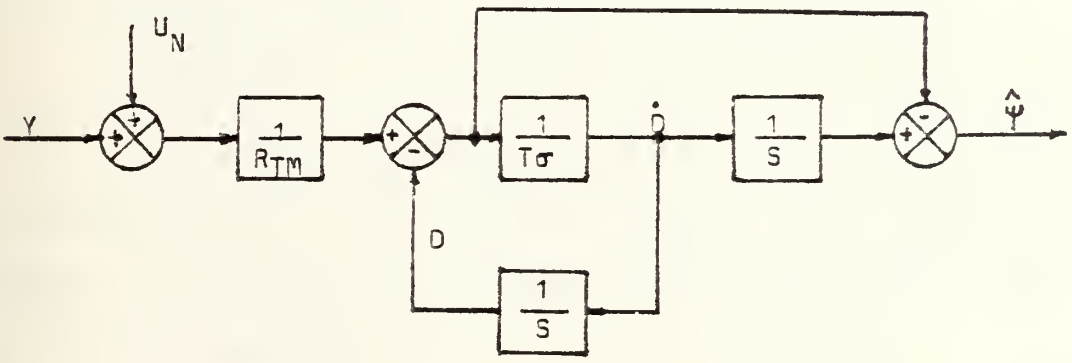

Fig. VI.B-2. First Order Seeker with an Observer

In this case, the application of Mason's rule gives:

$$\frac{\hat{\psi}}{\psi} = \frac{1 - ST\sigma}{1 + ST\sigma} \qquad \text{(VI.B-2)}$$

or

$$S\hat{\psi} = \frac{1}{T\sigma}(\psi - S\psi T\sigma - \hat{\psi}) \qquad \text{(VI.B-2a)}$$

Equation (VI.B-2a) can be expressed in state form as follows:

$$\text{Let } Y = X5 \ , \quad \dot{Y} = \dot{X}5 = \dot{X}6$$

$$\hat{\psi} = X8 \qquad \dot{\hat{\psi}} = \dot{X}8$$

and upon substituting and after minor manipulations, equation (VI.B-2a) turns into:

$$\dot{X}8 = \frac{1}{R_{TM}T\sigma}X5 - \frac{1}{R_{TM}}X6 - \frac{1}{T\sigma}X8 + \frac{U_N}{T\sigma R_{TM}} - \frac{\dot{U}_N}{T\sigma R_{TM}} \qquad \text{(VI.B-2b)}$$

In equation (VI.B-2b) the glint noise U_N is exponentially correlated while in equation (VI.B-1b) it is white noise normally distributed. The probabilistic properties of the glint noise are one of the major parameters influencing the performance of the system.

2. Tracker Modelling

a. A Second Order Close Loop Tracker with Position Servo

Consider an antenna centered along the fuselage of a missile and pointing toward a target. For simplicity reasons it is assumed that target and missile motion take place on the same plane.

Let θ_m and θ_t be the angular position of the missile antenna and target respectively with respect to some reference direction. It is desired to have: $\theta_m(t) \cong \theta_t(t)$, for all $t \geq t_0$.

The "plant" will consist of the antenna and the electric motor as in figure VI.B-3. In this plant, it is denoted:

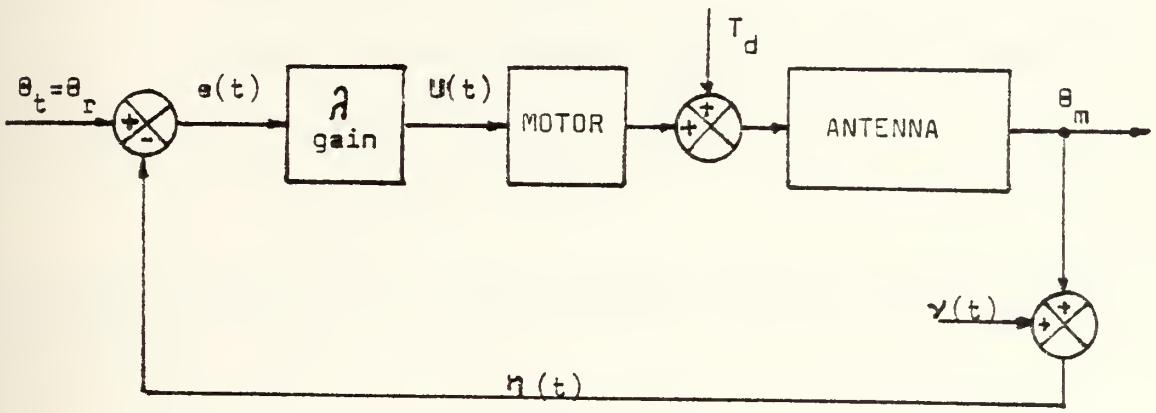

Fig. VI.B-3. Functional Block Diagram of a Tracker

$\theta_t(t)$: Angular direction of the target (it is considered as the reference variable)

$\theta_m(t)$: Angular position of the missile antenna. This is the variable to be controlled

$\nu(t)$: Measured noise

$\eta(t)$: The observed variable

$e(t)$: Angular position error between target and missile antenna

λ: Gain of the motor

T_d: Disturbance torque acting on the antenna and the motor.

The motion of the antenna can be described by a differential equation as follows:

$$J\ddot{\theta}_m(t) + B\dot{\theta}_m(t) = T_m(t) + T_d(t) \qquad \text{(VI.B-3)}$$

where J: The moment of inertia of all rotating parts of the tracker including the antenna

B: The viscous friction coefficient

$T_m(t)$: The torque applied by the motor

$T_d(t)$: The disturbing torque.

Assume that the motor torque $T_m(t)$ is proportional to the applied input current; then

$$T_m(t) = KU(t) \qquad \text{(VI.B-4)}$$

and substituting $T_m(t)$ into equation (VI.B-3) the latter turns into:

$$J\ddot{\theta}_m(t) + B\dot{\theta}_m(t) = KU(t) + T_d(t) \qquad \text{(VI.B-5)}$$

let: $a = B/J$ $\qquad K = k/J$ $\qquad \gamma = 1/J$

$\theta_m = X1$ $\qquad \dot{\theta}_m = \dot{X}1 = X2$ $\qquad \ddot{\theta}_m = \dot{X}2$

and upon substitution into equation (VI.B-3) the following state variable system follows:

$$\begin{bmatrix} \dot{X}1 \\ \dot{X}2 \end{bmatrix} = \begin{bmatrix} 0 & 1 \\ 0 & -a \end{bmatrix} \begin{bmatrix} X1 \\ X2 \end{bmatrix} + \begin{bmatrix} 0 \\ K \end{bmatrix} U(t) + \begin{bmatrix} 0 \\ \gamma \end{bmatrix} T_a(t) \qquad \text{(VI.B-6)}$$

From the functional block diagram of figure VI.B-3 it is obtained that

$$U(t) = \lambda\left[\theta_t(t) - \theta_m(t) - \nu(t)\right] \qquad \text{(VI.B-7)}$$

and upon substitution into equation (VI.B-4) and after minor manipulations it turns into:

$$\begin{bmatrix}\dot{X}1\\ \dot{X}2\end{bmatrix} = \begin{bmatrix}0 & 1\\ -\lambda k & -a\end{bmatrix}\begin{bmatrix}X1\\ X2\end{bmatrix} + \begin{bmatrix}0\\ \lambda k\end{bmatrix}\theta_t(t) - \begin{bmatrix}0\\ \lambda k\end{bmatrix}\nu(t) + \begin{bmatrix}0\\ \gamma\end{bmatrix}T_a(t) \qquad \text{(VI.B-8)}$$

To simplify the study at this stage, it is assumed that:

$$\nu(t) = T_d(t) = 0$$

at all t. Then equation (VI.B-8) turns into:

$$\begin{bmatrix}\dot{X}1\\ \dot{X}2\end{bmatrix} = \begin{bmatrix}0 & 1\\ -\lambda k & -a\end{bmatrix}\begin{bmatrix}X1\\ X2\end{bmatrix} + \begin{bmatrix}0\\ \lambda k\end{bmatrix}\theta_t(t) \qquad \text{(VI.B-8a)}$$

The characteristic equation of this second-order system is given by:

$$C(s) = (sI - A) = s\begin{bmatrix}1 & 0\\ 0 & 1\end{bmatrix} - \begin{bmatrix}0 & 1\\ -\lambda k & -a\end{bmatrix}$$

$$= \begin{bmatrix}s & -1\\ \lambda k & s+a\end{bmatrix}$$

$$= s^2 + aS + \lambda k = 0 \qquad \text{(VI.B-9)}$$

Recalling from classical Control theory that the characteristic equation of a second order system is of the form

$$S^2 + 2J\omega_n S + \omega_n^2 = 0$$

and comparing it with equation (VI.B-9) it comes out that:

$$\omega_n = \sqrt{\lambda k} \qquad \text{(VI.B-10a)}$$

$$J = \frac{a}{2\sqrt{\lambda k}} \qquad \text{(VI.B-10b)}$$

From the characteristic equation (VI.B-9), the tracker can be modeled as follows:

It is known that the characteristic equation of a closed loop control system is given by:

$$C(s) = 1 + G(s)H(s) = 0$$

$$\text{or} \quad -1 = G(s)H(s) \qquad \text{(VI.B-11)}$$

From equation (VI.B-7) it is easily obtained that:

$$-1 = \frac{\lambda k}{S(S+a)} \qquad \text{(VI.B-12)}$$

In figure VI.B-3 it is shown that there is not any scalar factor for the observed variable, which means that $H(s) = 1$; thus:

$$G(s) = \frac{\lambda k}{S(S+a)} = \lambda \cdot \frac{k}{(S+a)} \cdot \frac{1}{S} \qquad \text{(VI.B-14)}$$

Equation (VI.B-14) can be represented in a block diagram form as follows:

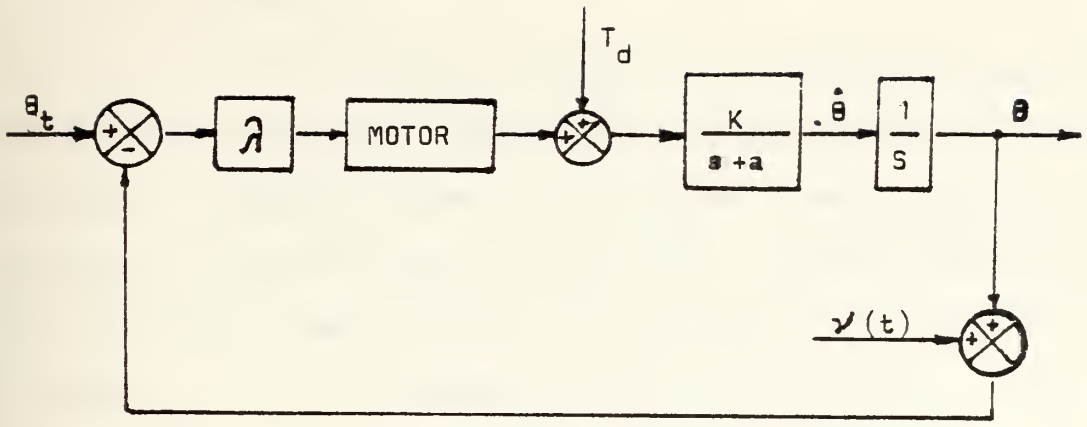

Fig. VI.B-4. Block Diagram of a 2nd Order Tracker

Figure (VI.B-5) shows the root locus of this second-order tracker, derived from equation (VI.B-12):

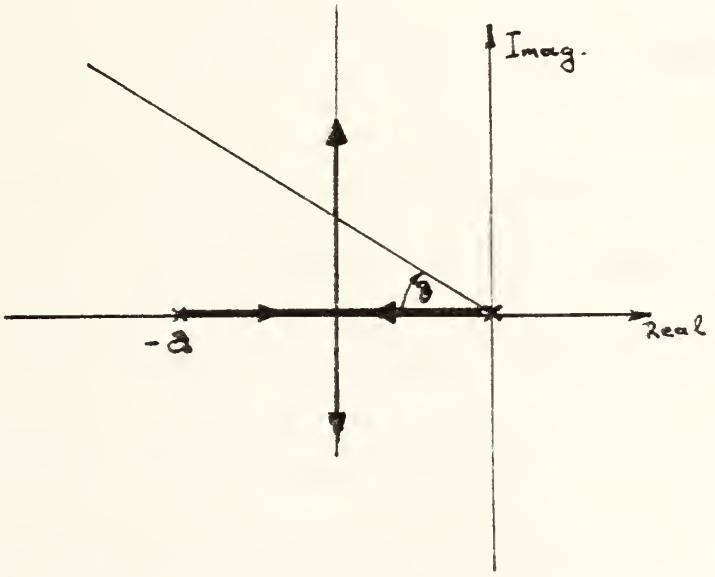

Fig. VI.B-5. Root Locus Diagram of a 2nd Order Tracker

From this root loci it is seen that this second-order control system is an ideal tracker and it is always stable no matter the gain parameters, while $\theta = \cos \xi = \cos^{-}(a/2\sqrt{\lambda k})$.

b. A Third-Order Close Loop Tracker with Position Servo

The derivation of the so far described second order tracker was based upon many assumptions and a lot of important parameters were not included. Among these was the electrical time constant of the motor. Taking into account the electrical time constant of the motor, the block diagram of figure (VI.B-4) becomes as in figure (VI.B-6):

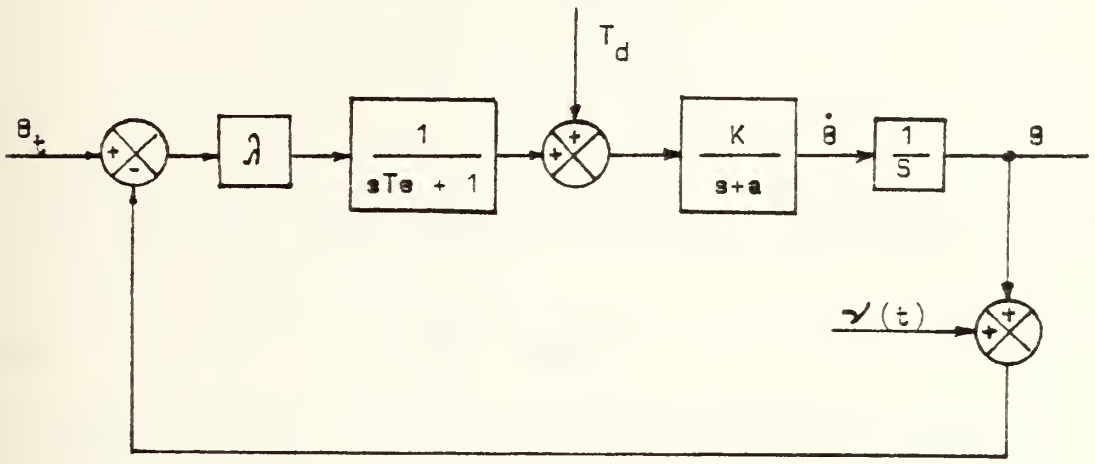

Fig. VI.B-6. Block Diagram of a 3rd Order Tracker

Then the transfer function of this close loop system becomes:

$$T(s) = \frac{\lambda k}{S(s+a)(sTe+1) + \lambda k} \qquad \text{(VI.B-15)}$$

Then, the characteristic equation is given by:

$$C(s) = S(s+a)\left(s+\frac{1}{Te}\right) + \frac{\lambda k}{Te} = 0 \qquad \text{(VI.B-16)}$$

It is obvious that the so derived characteristic equation belongs to a third-order control system. The root locus of

such a third-order system would look like that in figure (VI.B-6a):

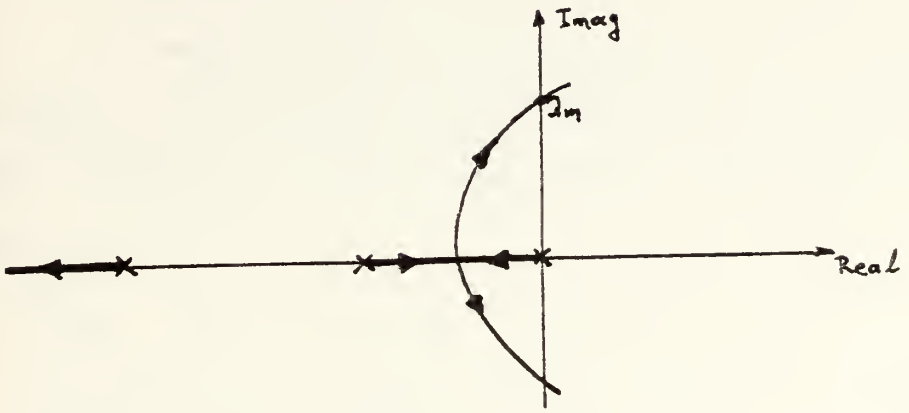

Fig. VI.B-6a. Root Locus Diagram of a 3rd Order Tracker

where $$\lambda_m = \frac{a}{k}\left(a + \frac{1}{Te}\right) \qquad \text{(VI.B-17)}$$

For values of $\lambda \geq \lambda_m$ the closed loop system is unstable.

The performance of the so far obtained trackers will depend upon the values of the several parameters which are involved in the problem. Utilizing adapting control methods, such as inner close loop sensing the angular velocity, etc., better performance characteristics can be obtained. But the purpose of this part and study is to outline some instructive methods for future work and not to examine thoroughly every possible aspect of this particular problem. Thus, abandoning the further development of the tracker, the next part deals with a somehow general way of studying the

required input signal to a tracker and the resulting error, from a stochastic process standpoint of view.

c. Stochastic Analysis of a Tracker with Position Servo

In part VI.B.2.a, it was found that a second-order tracker with position servo and having no disturbance and noise influence, is given by equation (VI.B-8a) which is rewritten:

$$\begin{bmatrix} \dot{X}1 \\ \dot{X}2 \end{bmatrix} = \begin{bmatrix} 0 & 1 \\ -\lambda k & -a \end{bmatrix} \begin{bmatrix} X1 \\ X2 \end{bmatrix} + \begin{bmatrix} 0 \\ \lambda k \end{bmatrix} \theta_t(t) \qquad \text{(VI.B-8a)}$$

It is known also that the target position signal is exponentially correlated to white noise and that it is expressed by the following radar glint equation:

$$\dot{\theta}_t(t) = -\frac{1}{T_r}\,\theta_t(t) + W(t) \qquad \text{(VI.B-18)}$$

where T_r: Radar time constant depending upon the system parameters

$W(t)$: White noise with intensity $v = 2\sigma^2/T_r$

Defining $\theta_t(t) = X3$ $\qquad$ $\dot{\theta}_t(t) = \dot{X}3$

and combining equation (VI.B-8a) with equation (VI.B-18) it comes out:

$$\begin{bmatrix} \dot{X}1 \\ \dot{X}2 \\ \dot{X}3 \end{bmatrix} = \begin{bmatrix} 0 & 1 & 0 \\ -\lambda k & -a & \lambda k \\ 0 & 0 & -1/T_r \end{bmatrix} \begin{bmatrix} X1 \\ X2 \\ X3 \end{bmatrix} + \begin{bmatrix} 0 \\ 0 \\ 1 \end{bmatrix} W(t) \qquad \text{(VI.B-19)}$$

Equation (VI.B-19) is of the form:

$$\dot{\underset{\sim}{x}}(t) = \underset{\sim}{A}\underset{\sim}{x}(t) + \underset{\sim}{B}\underset{\sim}{W}(t)$$

where $\underset{\sim}{A}$ and $\underset{\sim}{B}$ are constant matrices (matrix A is also asymptotically stable)

W(t) is white noise with intensity V.

It is known that in such a case, as the above, the variance matrix of $\underset{\sim}{x}(t)$ tends to a constant nonnegative matrix which is defined by:

$$\underset{\sim}{\Sigma} = \int_0^{\infty} e^{At} B V B^T d^{A^T t} dt \qquad \text{(VI.B-20)}$$

Furthermore, it is known that matrix $\underset{\sim}{\Sigma}$ is the solution of the Liapunov equation which states that:

$$\dot{\underset{\sim}{\Sigma}}(t) = \underset{\sim}{A}\underset{\sim}{\Sigma}(t) + \underset{\sim}{\Sigma}(t)\underset{\sim}{A}^T + \underset{\sim}{B}V\underset{\sim}{B}^T \qquad \text{(VI.B-21)}$$

Each control designer is interested to obtain:

$$\dot{\underset{\sim}{\Sigma}} = [0]$$

Utilizing Liapunov's equation (VI.B-21) for the case of equation (VI.B-19) and desiring to obtain $\dot{\underset{\sim}{\Sigma}} = [0]$, it comes out after direct substitutions and minor manipulations that:

$$\underset{\sim}{\Sigma}(\Sigma_{ij}, k, \lambda, a, T_r) = -\frac{2\sigma^2}{T_r}\begin{vmatrix} 0 & 0 & 0 \\ 0 & 0 & 0 \\ 0 & 0 & 1 \end{vmatrix} \qquad \text{(VI.B-22)}$$

where i,j = 1,2,3

But matrix $\underset{\sim}{\Sigma}$ is a symmetric one, that is:

$$\underset{\sim}{\Sigma}(t) = \begin{vmatrix} \Sigma_{11} & \Sigma_{12} & \Sigma_{13} \\ \Sigma_{21} & \Sigma_{22} & \Sigma_{23} \\ \Sigma_{31} & \Sigma_{32} & \Sigma_{33} \end{vmatrix} \qquad \text{where: } \Sigma_{12} = \Sigma_{21},\ \Sigma_{13} = \Sigma_{31},\ \Sigma_{23} = \Sigma_{32}$$

Equalizing terms in equation (VI.B-22) and solving for the Σ_{ij}'s, it comes out the STEADY-STATE VARIANCE MATRIX as follows:

$$\underset{\sim}{\Sigma} = \frac{k\lambda\sigma^2}{a + \frac{1}{T_r} + k\lambda T_r} \begin{vmatrix} \left(\frac{1}{a} + T_r\right) & 0 & T_r \\ 0 & \lambda k/a & 1 \\ T_r & 1 & \frac{a + \frac{1}{T_r} + \lambda k T_r}{\lambda k} \end{vmatrix} \qquad \text{(VI.B-23)}$$

At this point, it is necessary to introduce two important factors which characterize the quality and the expected performance of a control system (and for the present study, of the tracker). These are:

a) Mean Square Error (m.s.e.), Ce(t): it is defined as:

$$Ce(t) = E\left\{e^T(t)\ We(t)\ e(t)\right\}\ ,\quad t \geq t_0 \qquad \text{(VI.B-24)}$$

where e(t): Tracking Error given by

$$e(t) = \theta_m(t) - \theta_r(t)\ ,\quad t \geq t_0$$

We(t): a non-negative definite symmetric weighting matrix.

When We(t) is diagonal, as it is usually, Ce(t) is the weighted sum of the mean square errors of the components of the controlled variable. When the error e(t) is a scalar variable and We = 1, then $\sqrt{Ce(t)}$ is the Root Mean Square (r.m.s.) tracking error.

b) Mean Square Input (m.s.i.), Cu(t): it is defined as:

$$Cu(t) = E\{U^T(t)\ Wu(t)\ U(t)\} \quad , \quad t \geq t_0 \qquad \text{(VI.B-25)}$$

where U(t): control signal, input to the motor given by

$$U(t) = \lambda(\theta_m(t) - \theta_t(t))$$

Wu(t): non-negative definite symmetric weighting matrix When the input U(t) is scalar and Wu(t) = 1, then $\sqrt{Cu(t)}$ is the Root Mean Square (r.m.s.) input.

The aim of every control system designer is to reduce the mean square tracking error Ce(t) as much as possible; but decreasing Ce(t) it usually implies incrementation of the mean square input Cu(t). Since the maximally permissible value of the mean square input is determined by the capacity of the plant (electrical characteristics of motor and antenna), a compromise must be found between the requirement of a small mean square tracking error and the need to keep the mean square input down to a reasonable level.

Thus, a basic design objective can be stated as follows: "In the design of a control system, the lowest possible mean square tracking error should be achieved without

letting the mean square input exceed its maximally permissible value."

Assume that for the present study, it is given

$$We(t) = Wu(t) = I.$$

Then, equation (VI.B-24) becomes:

$$Ce(t) = E\left\{e^T(t)\, We(t)\, e(t)\right\} = E\left\{e^T(t)\, e(t)\right\}$$

or

$$\underset{t\to\infty}{Ce(t)} = \underset{t\to\infty}{Lim}\, E\left\{e^2(t)\right\} = \underset{t\to\infty}{Lim}\, E\left\{(X1 - X3)^2\right\}$$

$$= \underset{t\to\infty}{Lim}\left\{E\, X1^2 + X3^3 - 2X1X3\right\} = \Sigma_{11} + \Sigma_{33} - 2\Sigma_1\Sigma_3 \qquad \text{(VI.B-26)}$$

Note: the subscript of each steady state variable determines the coefficient to be taken from the variance matrix.

Substituting into equation (VI.B-26) the equivalents from equation (VI.B-23) it comes out that: the steady state mean square tracking error is given by:

$$\underset{t\to\infty}{Ce(t)} = \frac{a + \frac{1}{T_r} + \frac{\lambda k}{a}}{a + \frac{1}{T_r} + \lambda k T_r}\,\sigma^2 \qquad \text{(VI.B-26a)}$$

Equation (VI.B-25), due to $Wu(t) = 1$, becomes:

$$Cu(t) = E\left\{U^T(t)\, Wu(t)\, U(t)\right\} = E\left\{U^T(t)\, U(t)\right\}$$

or

$$\underset{t\to\infty}{Cu(t)} = \underset{t\to\infty}{Lim}\, E\left\{U^2(t)\right\} = \underset{t\to\infty}{Lim}\, E\left\{\left[\lambda\left(\theta_m(t) - \theta_t(t)\right)\right]^2\right\}$$

$$\underset{t\to\infty}{Lim}\, E\left\{\lambda^2[X1 - X3]^2\right\} = \lambda^2 \underset{t\to\infty}{Lim}\, E\left\{(X1 - X3)^2\right\} = \lambda^2 \underset{t\to\infty}{Ce}$$

Thus, for the case of $We(t) = Wu(t) = I$

$$\underset{t\to\infty}{Cu(t)} = \lambda^2 \underset{t\to\infty}{Ce(t)} \qquad \text{(VI.B-27)}$$

Finally, from equations (VI.B-26a) and (VI.B-27) are easily obtained the:

$\sqrt{\underset{t\to\infty}{Ce(t)}}$: r.m.s. tracking error steady-state

$\sqrt{\underset{t\to\infty}{Cu(t)}}$: r.m.s. input signal steady-state

Depending upon the numerical values of this system, plottings similar to the following are easily derived.

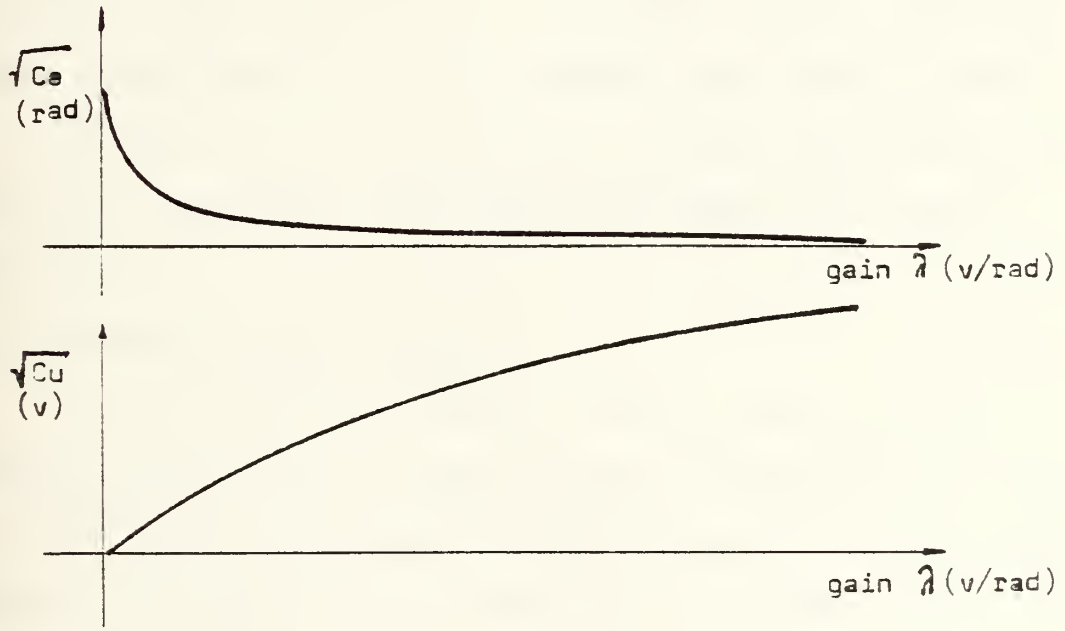

Fig. VI.B-7. rms Tracking Error and rms Input Voltage as Functions of the Gain for a Tracker with Position Servo

Figure VI.B-7 shows that, according to what one would intuitively feel, the rms input keeps increasing with the gain λ. Comparing the behavior of the rms tracking error and the rms

input voltage confirms the opinion that there is very little point in increasing the gain beyond a certain point, since the increase in rms input voltage does not result in any appreciable reduction in the rms tracking error. Depending upon the desired control system specifications the derived steady-state values will indicate whether the design was sufficient or not. In case that the system is rejectable, other adaptive schemes must be researched.

C. FILTER

The purpose of a filter is to estimate as accurately as possible the real value of all the system states, given inaccurate measurements of a few (perhaps only one) of them. The two outmost popular theories for filter calculations and construction are these established by Wiener and Kalman respectively.

1. Wiener Optimal Filter

In the case of an optimal Wiener Filter, the disturbances entering the guidance system are considered to be white glint noise with spectral density Φ_N and random target maneuver. The Wiener filter formulation is based upon the determination of a transfer function H_0 which will minimize the integral of the mean square signal, that is,

$$\text{minimize} \int_0^\infty e^2 \, dt \qquad \text{(VI.C-1)}$$

The optimal transfer function H_o can be found from the explicit solution of the Wiener-Hopf integral equation

$$H_o = \frac{1}{(W_s + W_N)^+}\left[\frac{W_s}{(W_s + W_N)^-}\right]^+ \qquad \text{(VI.C-2)}$$

where W_s and W_N are the spectral densities of the signal and noise, $(W_s + W_N)^+$ represents that part which has all its poles and zeros in the left half-plane, while $(W_s + W_N)^-$ represents that part which has all its poles and zeros in the right half-plane. The expression $[\cdot]^+$ is the component of $[\cdot]$ which has all its poles in the left half-plane. (To obtain $[\cdot]^+$, expand $[\cdot]$ in partial fractions and throw away all the terms corresponding to poles in the right half-plane). The output spectral densities of the signal and noise, W_s and W_N, can be expressed in terms of the spectral densities, Φ_s and Φ_N, and the used shaping network transfer function.

2. Kalman Optimal Filter

The Wiener optimal filter theory is a design technique of an optimal stochastic control system based on the minimization of a Performance Index (PI) when the future values of the variables are not well defined but are random functions of time. In order to be possible that some progress could be made, the study was restricted to stationary random signals and assumed that their power spectra were available. In the case of the Kalman optimal filter, the

mathematical modeling of the following concept is attempted. "If a physical model, equivalent to an actual system, could be constructed on some form of simulator then, in principle at least, it would be possible to use the values of the state variables given by the simulator model without any further reference to the original system. Provided the simulator model is started with the correct initial conditions it will continue to mimic the behavior of the actual system, thus eliminating the need for measurements on that system."

Unfortunately such an ideal situation cannot be obtained. Even if the actual system model structure, parameter values and initial conditions are known exactly, the input W (where W represents zero mean white noise, contaminating the target motion, of power per unit bandwidth q^2 such that $\Phi_T = \frac{q^2}{1 + W^2\tau^2}$), being a random function of time, cannot be reproduced in the simulator model.

Effectively W represents the uncertainty in our knowledge of the actual system. Of course, in practice some measurements will be made on the system. These measurements will not be perfect since there are always errors associated with any measurement process. It is usually the case to obtain as measurement not the actual target and missile states separately but only the difference between them. This situation is depicted in figure VI.C-1 in a more general notation, where Z represents the measurement and ν the measurement noise.

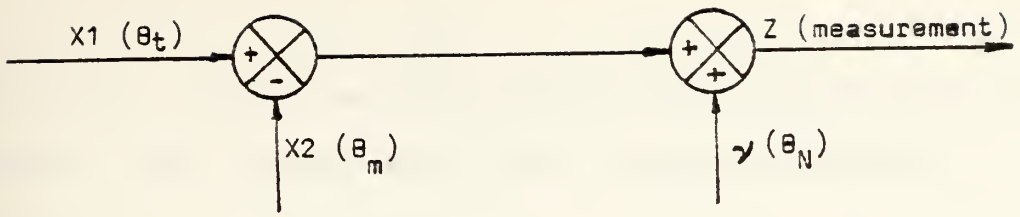

Fig. VI.C-1. Measurement Z contaminated by noise ν

The aim of any one designer is to obtain best estimates, in some sense, of the states X_1 and X_2 given the measurement Z, a knowledge of the structure of the system and its parameter values, and the statistical characteristics of the noise sources w and ν. The assumed system model, which is equivalent to the previously proposed simulator model, is identical to the actual system model except for the zero mean white noise source w. Since the best guess of w at any instant is zero, it is omitted entirely and thus represents the uncertainty in the assumed system model.

In the Kalman filter formulation, the measurement process and system model outputs are treated as two independent estimates of the state of the actual system. It combines these outputs together to form a best estimate (in the sense of having minimum variance). The mathematical formulation of a Kalman optimal filter has as follows:

Given an actual system

$$\dot{\underset{\sim}{x}} = \underset{\sim\sim}{A}\underset{\sim}{x} + \underset{\sim\sim}{B}\underset{\sim}{u} + \underset{\sim}{w} \qquad \text{(VI.C-3)}$$

and a measurement

$$\underset{\sim}{Z} = \underset{\sim\sim}{H}\underset{\sim}{x} + \underset{\sim}{\nu} \qquad \text{(VI.C-4)}$$

where $\underset{\sim}{w}$ and $\underset{\sim}{\nu}$ are white noise vectors with spectral density matrices Q and R respectively then the best estimate $\hat{\underset{\sim}{X}}$ of $\underset{\sim}{X}$ is given by:

$$\dot{\hat{\underset{\sim}{X}}} = \underset{\sim\sim}{A}\hat{\underset{\sim}{x}} + \underset{\sim\sim}{B}\underset{\sim}{u} + K(\underset{\sim}{Z} - \underset{\sim\sim}{H}\hat{\underset{\sim}{x}}) \qquad \text{(VI.C-5)}$$

where

$$K = P\,H^T\,R^{-1} \qquad \text{(VI.C-6)}$$

and P is derived from the solution of Riccati equation

$$P = AP + PA^T + Q - PH^TR^{-1}HP \qquad \text{(VI.C-7)}$$

For the Q and R matrices, the elements on the main diagonal are the spectral densities of the individual system and measurement noise sources. Elements off the main diagonal indicate correlation between noise sources in terms of a cross spectral density but in many problems the noise sources are independent and hence these elements will be zero. However, this is not the case for the P matrix. Here the off diagonal terms are covariances which indicate how one best estimate is related to another and these, in general, will not be zero. For this reason it is usual to refer to P as the covariance matrix even though the terms on the main diagonal still correspond to the variances of the individual best estimates.

In this estimation case, the boundary conditions are defined at the start of the engagement and represent initial

guesses at the entries in the covariance matrix P. Provided the system is time invariant and the noise sources stationary, then the elements of P should tend to steady values as the estimation process proceeds and these values can be found by integrating the Riccati equations forward in time.

a. A Third-Order Kalman Filter Estimator

As the most important disturbances entering a guidance control system are considered to be white glint noise with spectral density Φ_N and random target maneuver, the target maneuver can be considered as a step function whose initiation time is uniformly distributed over the flight time. It can be shown [Ref. 12] that integrated white noise has the same autocorrelation function as this maneuver process. Thus the input process can be considered as having spectral density Φ_S. A Kalman filter formulation may be like that shown in figure VI.C-2.

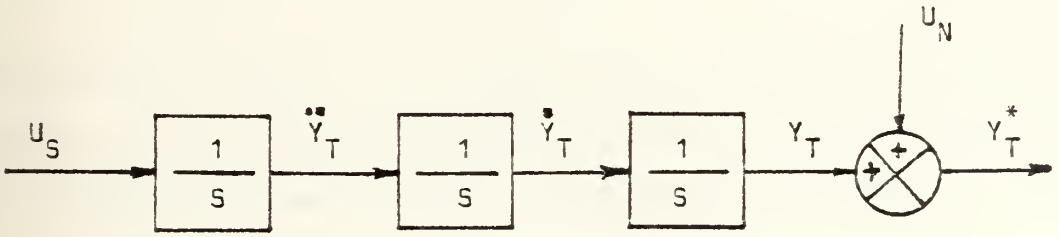

Figure VI.C-2. Kalman Filter Formulation

The state equations are:

$$\begin{vmatrix} \dot{Y}_T \\ \ddot{Y}_T \\ \dddot{Y}_T \end{vmatrix} = \begin{vmatrix} 0 & 1 & 0 \\ 0 & 0 & 1 \\ 0 & 0 & 0 \end{vmatrix} \begin{vmatrix} Y_T \\ \dot{Y}_T \\ \ddot{Y}_T \end{vmatrix} + \begin{vmatrix} 0 \\ 0 \\ U_S \end{vmatrix} \qquad \text{(VI.C-8)}$$

which is of the form of equation (VI.C-3)

$$\dot{\underset{\sim}{x}} = \underset{\sim\sim}{A}\underset{\sim}{x} + \underset{\sim}{w} \qquad \text{(VI.C-3a)}$$

The measurement equation is

$$\underset{\sim}{Z} = \underset{\sim\sim}{A}\underset{\sim}{X} + \underset{\sim}{\nu} \qquad \text{(VI.C-4)}$$

and for this case

$$Y_T^* = [1 \quad 0 \quad 0] \begin{bmatrix} Y_T \\ \dot{Y}_T \\ \ddot{Y}_T \end{bmatrix} + U_N \qquad \text{(VI.C-9)}$$

The Kalman filter equation is given by equation (VI.C-5) via equations (VI.C-6) and VI.C-7) where

$$Q = \begin{vmatrix} 0 & 0 & 0 \\ 0 & 0 & 0 \\ 0 & 0 & \Phi_S \end{vmatrix}, \quad \underset{\sim}{R} = \Phi_N$$

Recognizing that the covariance matrix $\underset{\sim}{P}$ is symmetric, the scalar equations representing the steady state solution ($\dot{P} = 0$) can be derived from equation (VI.C-7) as follows:

$$P_{11}^2 = 2P_{11}\Phi_N \qquad \text{(VI.C-10a)}$$

$$P_{12}^2 = 2P_{23}\Phi_N \qquad \text{(VI.C-10b)}$$

$$P_{13}^2 = \Phi_S\Phi_N \qquad \text{(VI.C-10c)}$$

$$P_{11}P_{12} = \Phi_N(P_{22} + P_{13}) \qquad \text{(VI.C-10d)}$$

$$P_{11}P_{13} = P_{23}\Phi_N \qquad \text{(VI.C-10e)}$$

$$P_{12}P_{13} = P_{33}\Phi_N \qquad \text{(VI.C-10f)}$$

The solution of equation (VI.C-10) yields the following steady state Kalman filter gains:

$$\underset{\sim}{K} = \begin{vmatrix} K_1 \\ K_2 \\ K_3 \end{vmatrix} = \begin{vmatrix} 2(\Phi_S/\Phi_N)^{1/6} \\ 2(\Phi_S/\Phi_N)^{1/3} \\ (\Phi_S/\Phi_N)^{1/2} \end{vmatrix} \qquad \text{(VI.C-11)}$$

Defining:

$$w_o = (\Phi_S/\Phi_N)^{1/6}$$

the gain matrix (equation VI.C-11) becomes:

$$\underset{\sim}{K} = \begin{vmatrix} 2w_o \\ 2w_o^2 \\ w_o^3 \end{vmatrix} \qquad \text{(VI.C-11a)}$$

Now, substituting equation (VI.C-11a) into equation (VI.C-5) the filter equations are obtained:

$$\begin{vmatrix} \dot{\hat{Y}}_T \\ \ddot{\hat{Y}}_T \\ \dddot{\hat{Y}}_T \end{vmatrix} = \begin{vmatrix} 0 & 1 & 0 \\ 0 & 0 & 1 \\ 0 & 0 & 0 \end{vmatrix} \begin{vmatrix} \hat{Y}_T \\ \dot{\hat{Y}}_T \\ \ddot{\hat{Y}}_T \end{vmatrix} + \begin{vmatrix} 2w_o \\ 2w_o^2 \\ w_o^3 \end{vmatrix} \left| Y^* - \hat{Y}_T \right| \qquad \text{(VI.C-12)}$$

The transfer function between the position estimate output and the position measurement input can easily be obtained via equation (VI.C-12):

$$\frac{Y_T}{Y_T^*} = \frac{1 + 2S/w_o + 2S^2/w_o^2}{1 + 2S/w_o + 2S^2/w_o^2 + S^3/w_o^3} \qquad \text{(VI.C-13)}$$

D. AUTOPILOTS

An autopilot is a closed loop system and it is a minor loop inside the main guidance loop; not all missile systems require an autopilot. A missile will maneuver up-down or left-right in an apparently satisfactory manner if a control surface is moved or the direction of thrust altered. If the missile carries accelerometers and/or gyros to provide additional feedback into the missile servos to modify the missile motion, then the missile control system is usually called an autopilot, but this definition is not universally accepted. Broadly speaking, autopilots either control the motion in the pitch and yaw planes, in which case they are called lateral autopilots, or they control the motion about the fore and aft axis in which case they are called roll autopilots. For a symmetrical cruciform missile, as in this present study, pitch and yaw autopilots are identical.

The reliance on classical control techniques in autopilot design usually results in an autopilot with three independent channels for yaw, pitch and roll. These three motions are assumed uncoupled because classical control techniques are in

general limited to single input, single output linear systems (their extension to multi-input, multi-output systems is quite complex). In flight, inherent aerodynamic interactions comprise coupling modes between steering and roll motions. Therefore, the channels of the autopilot are not independent and this leads to stability problems. The cross-coupling stability problem gets worse with increasing angle-of-attack. To partially decouple the roll and steering control systems, autopilot designers limit the steering response speed so that the roll system bandwidth is two to four times the steering system bandwidth. Also, the designers limit the missile angle-of-attack as much as possible.

The autopilot gains in each of the channels are often variable. This variation is required to produce the optimum performance for different Mach numbers, dynamic pressures and control effectiveness as the missile response depends on the semi non-dimensional form of the aerodynamic derivatives, and thus it follows that all the aspects of the missile response will vary as the mass and inertia vary with bandwidth. Thus a satisfactory guidance loop cannot be engineered if very large tolerances exist inside the loop. To simplify the further discussion on this present study, it will be assumed that the guidance law and autopilot are designed independently. Not only is the assumption not necessary, but better guidance laws can be designed if the autopilot characteristics are included in the guidance law derivation. To do so,

however, makes the design too vehicle dependent which in turn further dilutes generality. In addition, autopilot design and mechanization techniques are now available which result in very good guidance law command execution, regardless of the airframe or guidance law characteristics.

There have been developed several special purpose autopilots. These can be classified as in figure VI.D-1 is shown. Autopilot design can be attempted either by classical or by optimal control theories.

1. Autopilot Design by Classical Control Method

In part II.E the longitudinal and lateral decoupled and linearized sets of missile motion equations were derived. Also, it has been essentially identified the missile motion in the xz plane as the "pitch motion," the motion in the xy plane as the "yaw" motion, while the motion in the zy plane as the "roll" motion.

The longitudinal equations set was found to be:

$$\begin{bmatrix} \dot{u} \\ \dot{w} \\ \dot{q} \\ \dot{\theta} \end{bmatrix} = \begin{bmatrix} X_u & X_w & 0 & -g \\ Z_u & Z_w & U_o & 0 \\ (M_u+M_{\dot{w}}Z_u) & (M_w+M_{\dot{w}}Z_w) & (M_q+M_{\dot{w}}U_o) & 0 \\ 0 & 0 & 1 & 0 \end{bmatrix} \begin{bmatrix} u \\ w \\ q \\ \theta \end{bmatrix} + \begin{bmatrix} X_\delta \\ Z_\delta \\ (M_\delta+M_{\dot{w}}Z_\delta) \\ 0 \end{bmatrix} \delta \qquad \text{(VI.D-2)}$$

In the case of a missile with 90° rotational symmetry, the relations shown in table II.E-1 will hold where $q = -r$, $v = w$, etc. Then, neglecting the gravity force and assuming

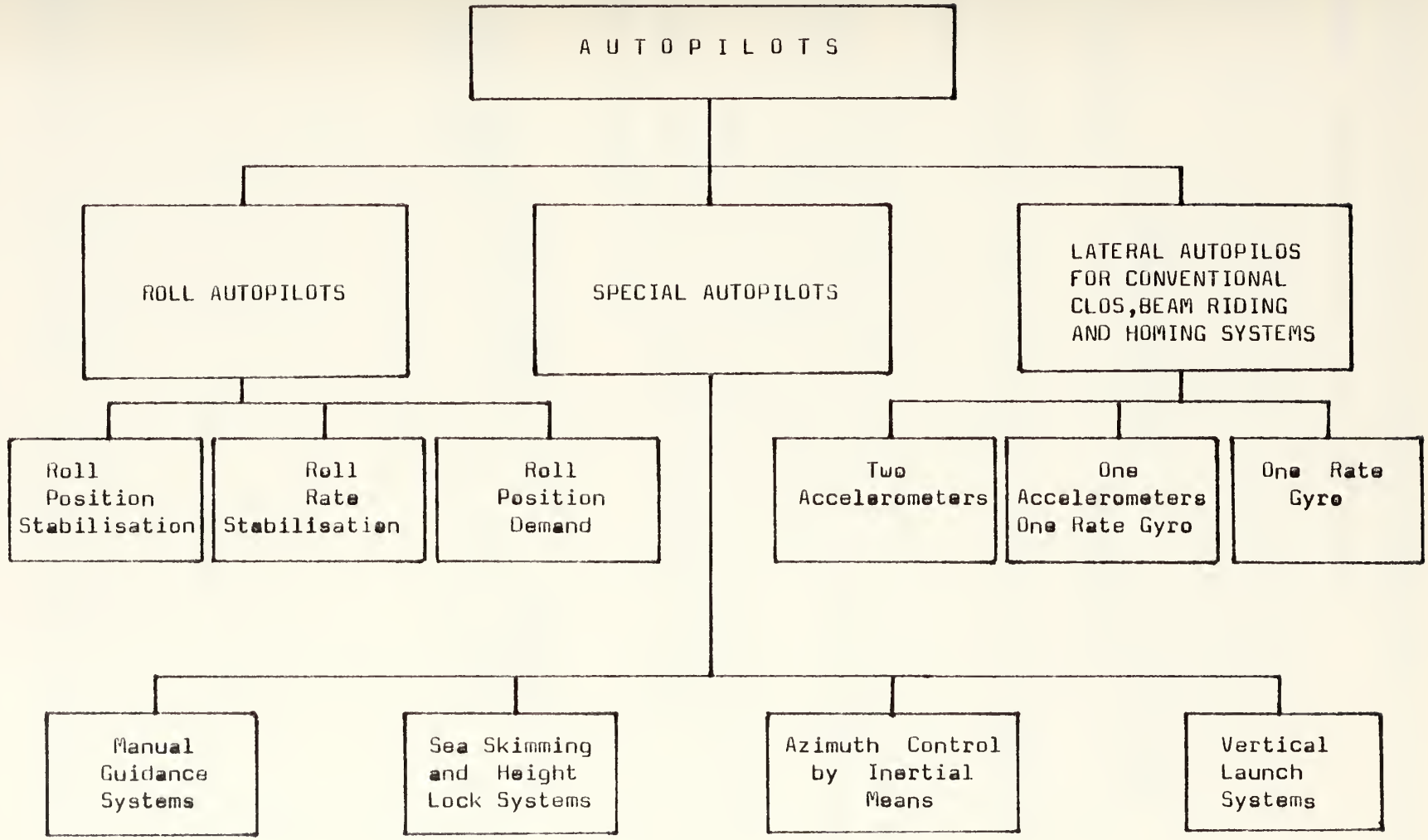

Figure VI.D-1 Classification Tree of Special Purpose Autopilots

negligible the forward velocity perturbation, it is easily obtained the yaw motion set of equations:

$$\begin{bmatrix} \dot{v} \\ \dot{w} \\ \dot{q} \\ \dot{r} \end{bmatrix} = \begin{bmatrix} Y_v & 0 & 0 & -U_o \\ 0 & Z_w & U_o & 0 \\ 0 & (M_w + M_{\dot{w}} Z_w) & (M_q + M_{\dot{w}} U_o) & 0 \\ (N_v + N_{\dot{v}} Y_v) & 0 & 0 & (N_r + N_{\dot{v}} U_o) \end{bmatrix} \begin{bmatrix} v \\ w \\ q \\ r \end{bmatrix} + \begin{bmatrix} 0 \\ 0 \\ M_u + M_{\dot{w}} Z_u \\ 0 \end{bmatrix} U \qquad \text{(VI.D-2)}$$

Due to symmetry, the u component would be the same for each equation.

This analysis shows that under conditions where p = 0 (no roll), both "pitch" and "yawing" reactions are the same as long as gravity force is neglected.

Generically, an autopilot would have the structure of a closed loop control system with unity feedback as it is shown in figure VI.D-2.

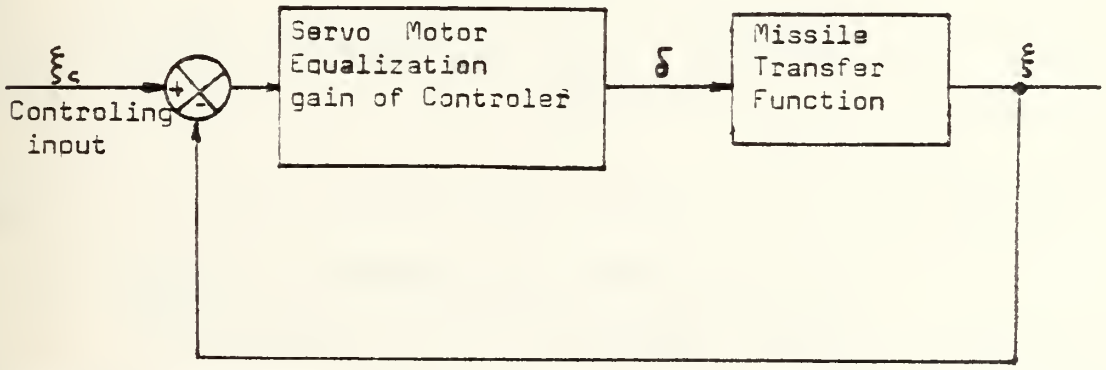

Fig. VI.D-2. General Block Diagram of an Autopilot

The missile transfer function can be easily obtained from the set of the lateral or longitudinal equations

accordingly, by applying Cramer's rule. The so derived transfer function would look like

$$\frac{\xi(S)}{\delta(S)} = \frac{A(S + a_1)(S + a_2)}{S^2 + \left(2\zeta_p w_p S + w_p^2\right)\left(S^2 + 2\zeta_{sp} w_{sp} S + w^2_{sp}\right)} \qquad \text{(VI.D-3)}$$

In the case of "pitch" or "yaw" autopilot study, the expression $\left(S^2 + 2\zeta_p w_p S + w_p^2\right)$ in the denominator of equation (VI.D-3) characterizes the "phugoid" motion of the missile while the expression $\left(S^2 + 2\zeta_{sp} w_{sp} S + w^2_{sp}\right)$ characterizes the "short period" motion. A very sufficient approximation of the system behavior can be obtained by analyzing it, based only on the characteristic equation of the "short period" motion. In this case, in order to derive the "short period" transfer function, the first row and first column of equation (VI.D-1) is deleted. Then:

$$\begin{vmatrix} \dot{w} \\ \dot{q} \\ \dot{\theta} \end{vmatrix} = \begin{vmatrix} Z_w & U_o & 0 \\ (M_w + M_{\dot{w}} Z_w) & (M_q + M_{\dot{w}} U_o) & 0 \\ 0 & 1 & 0 \end{vmatrix} \begin{vmatrix} w \\ q \\ \theta \end{vmatrix} + \begin{vmatrix} Z_\delta \\ M + M_{\dot{w}} Z_\delta \\ 0 \end{vmatrix} \qquad \text{(VI.D-4)}$$

Equation (VI.D-4) is the "short period longitudinal set."

2. Stability Augmentation System (S.A.S.)

The implementation of a missile lateral or longitudinal set of equations into an open loop autopilot, utilizing the corresponding aerodynamic derivatives, is probably not acceptable for highly maneuverable missiles which have very small static margins, especially those which do not operate

at a constant height and speed. In order to obtain a stable control system, some kind of a feedback must be introduced. A usual method is to select a feedback such as to artificially augment certain key aerodynamic derivatives. This artificial augmentation usually improves the missile performance. Such an augmented closed loop system is called "Stability Augmentation System" (S.A.S.) and actually it is an interior loop of an autopilot which in turn is an interior loop of a guidance system (see figure (VI.D-3)).

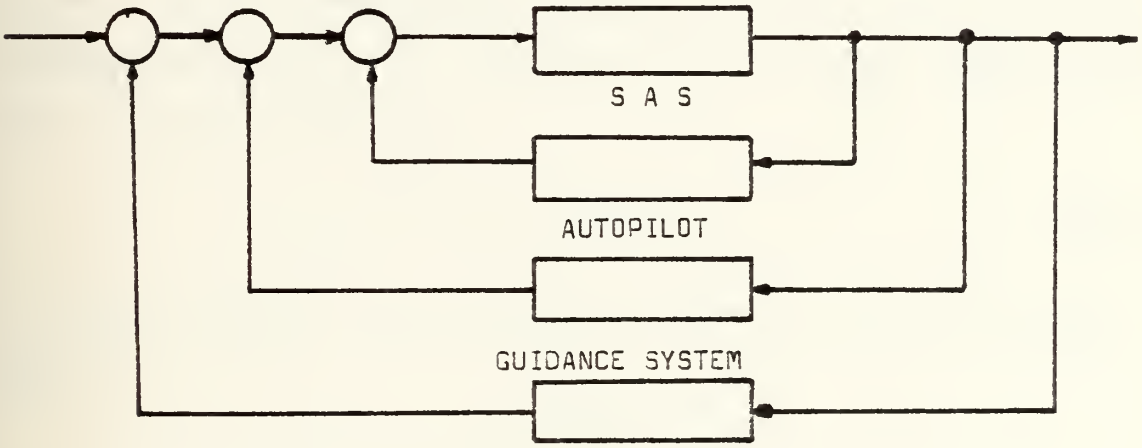

Figure VI.D-3. General Idea of a Guidance System

A S.A.S. effects favorably not only the damping characteristics of a missile but also its frequency behavior. Thus, one can have a so called M_a or "stiffness" S.A.S.; this also applies to the N_β or "weather cock" stability.

By augmenting L_p a roll damper is derived; by augmenting M_q a pitch damper is derived, while by augmenting N_r a yaw

damper is derived. In consequence the derivation of such dampers is outlined.

a. Roll Damper

In part II.E the linearized decoupled lateral equations were derived; in that set of equations the "roll" was found to be given by:

$$\dot{p} = L'_{\beta}\beta + L'_{p}p + L'_{r}r + L'_{\delta}\delta \qquad \text{(VI.D-5)}$$

But this equation is a three degree of freedom equation, while an equation of one degree of freedom is required. This is achieved by neglecting the β and r motions, considering that $L'_{\beta}\beta << L'_{p}p$ and $L'_{r}r << L'_{p}p$. Thus, equation (VI.D-5) reduces to:

$$\dot{p} = L'_{p}p + L'_{\beta}\beta \qquad \text{(VI.D-6)}$$

Utilizing Laplace transformation, equation (VI.D-6) turns into:

$$(S - L'_{p})p(S) = L'_{\beta}\beta(S)$$

or

$$\frac{p(S)}{\delta(S)} = \frac{L'_{\delta}}{S - L'_{p}} \qquad \text{(VI.D-7)}$$

Equation (VI.D-7) is an open loop transfer function.

Introducing a feedback loop as in figure VI.D-4 is shown, $\delta(S)$ becomes:

$$\delta(S) \equiv \delta_{a}(S) = \delta_{c}(S) - k_{p}p \qquad \text{(VI.D-8)}$$

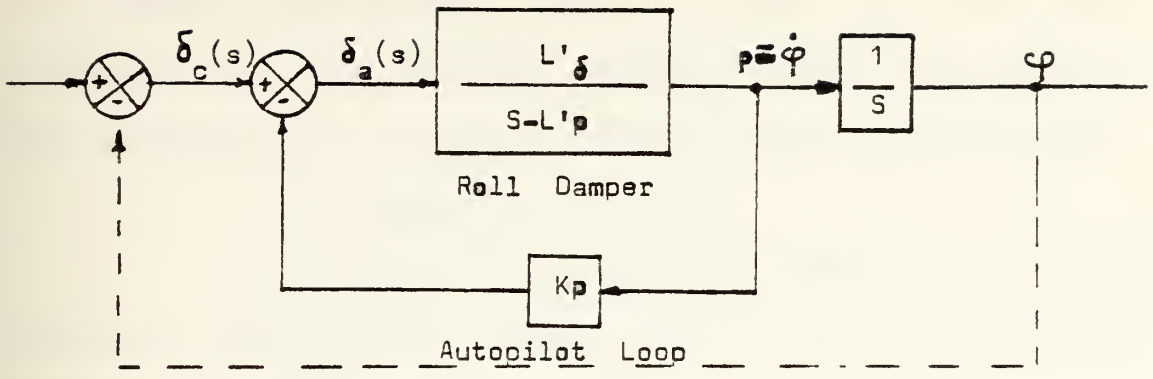

Fig. VI.D-4. Block Diagram of a Roll Damper

where $\delta_c(S)$ is the "commanded" deflection

$\delta_a(S)$ is the aeleron deflection

and upon substituting equation (VI.D-8) into equation (VI.D-7) the last turns into:

$$\frac{p(S)}{\delta_c(S)} = \frac{L'_\delta}{S - (L'_p - L'_\delta k_p)} \qquad \text{(VI.D-9)}$$

Equation (VI.D-9) is the transfer function of a roll damper, where the term $(L'_p - L'_\delta k_p)$ represents the augment aerodynamic derivative. From equation (VI.D-9) the augment "roll" lateral equation can be easily derived and it is:

$$\dot{p} = L'_\beta \beta + (L'_p - L'_\delta k_p)p + L'_r r + L'_\delta \delta \qquad \text{(VI.D-10)}$$

The direct effect of the introduced feedback of rolling angle rate ($p = \dot{\phi}$) (see figure VI.D-4) is an increase in the subsidence frequency of the roll. Equation (VI.D-9) can be rewritten as:

$$\frac{p(S)}{\delta_c(S)} = L'_\delta \frac{1}{S - L'_{p_{augment}}} = L'_\delta \frac{1/L'_{p_{aug}}}{S/L'_{p_{aug}} - 1} = L' \frac{Tr}{S\,Tr - 1} \qquad \text{(VI.D-9a)}$$

The achieved augmentation permits a tighter roll attitude of the autopilot. The utilized feedback can be combined with a lead compensator in order to fulfill given specifications.

b. Pitch Damper

In part II.E the linearized decoupled longitudinal equations were derived; in that set of equations, the pitch motion was found to be given by:

$$\dot{q} = (M_u + M_{\dot{w}} Z_u)U + (M_w + M_{\dot{w}} Z_w)w + (M_q + M_{\dot{w}} U_o)q + (M_\delta + M_{\dot{w}} Z_\delta)\delta \qquad \text{(VI.D-11)}$$

For a preliminary design, a very good approximation is obtained by assuming M_u, M_w, $M_{\dot{w}}$, M_δ as negligible quantities and omitting them; equation (VI.D-11) turns into:

$$\dot{q} = M_q q$$

the solution of which is:

$$q = e^{M_q t} \qquad \text{(VI.D-11a)}$$

Note: M_q is a negative quantity.

After getting an idea from the above approximation, the next step is to obtain a better approximation. Assuming $M_{\dot{w}}$ as a negligible quantity, that is $M_{\dot{w}} = 0$, equation (VI.D-11) turns into:

$$\dot{q} = M_u u + M_w w + M_q q + M_\delta \delta \qquad \text{(VI.D-12)}$$

Utilizing Laplace transformation and after minor manipulations, equation (VI.D-12) turns into a transfer function of the type:

$$\frac{S\theta(S)}{S(S)} = \frac{q(S)}{\delta(S)} = \frac{AS + B}{S^2 + CS + D} \qquad \text{(VI.D-12a)}$$

where $A = M_\delta + Z_\delta M_{\dot{w}}$

$B = Z_\delta M_w - M_\delta Z_w$

$C = 2\zeta_{sp} w_{u_{sp}} = -(U_o M_{\dot{w}} + Z_w + M_q) = -(Z_w + M_q + M_{\dot{a}})$

$D = w^2_{u_{sp}} = M_q Z_w - U_o M_w = M_q Z_w - M_a$

Note: Recall that $Z_w = \frac{1}{m}\frac{\partial Z}{\partial w}$ and $Z_a = \frac{\partial Z}{\partial a}$ due to $a = w/U_o$ which also implies that $Z_a = U_o Z_w$, $M_a = U_o M_w$.

Equation (VI.D-12a) is the transfer function of a pitch autopilot open loop. The denominator is the characteristic equation of the "short period" pitch motion approximation. Noticeable also is that $w_{n_{sp}} \cong \sqrt{-M_a}$ where M_a is a negative quantity.

Next step is to augment the most important aerodynamic derivative which is the M_q.

Introducing a negative feedback as it is shown in figure (VI.D-5), it is obtained:

$$\delta(S) \equiv \delta_e(S) = \delta_c(S) - k_q q$$

and upon substituting into equation (VI.D-12) the last turns into:

$$\dot{q} = M_u u + M_w w + (M_q - M_{\delta_e} k_q) q + M_{\delta_e} \delta_e \qquad \text{(VI.D-13)}$$

where $(M_q - M_{\delta_e} k_q) = M_{q_{augment}}$.

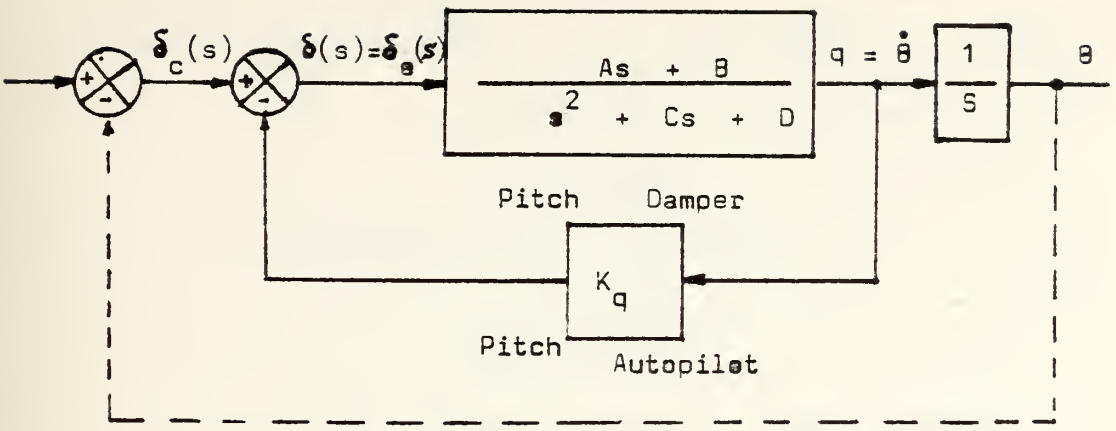

Fig. VI.D-5. Block Diagram of a Pitch Damper

c. Yaw Damper

In part II.E the linearized decoupled lateral equations were derived; in that set of equations, the "yaw" motion was found to be given by:

$$\dot{r} = N'_{\beta}\beta + N'_{p}p + N'_{r}r + N'_{\delta_r}\delta_r \qquad \text{(VI.D-14)}$$

Note: Recall that in case of a 90° rotational symmetry, as it is in the present study, $I_{xz} = I_{xy} = I_{yz} = 0$ and thus equation (VI.D-14) is written as:

$$\dot{r} = N_{\beta}\beta + N_{p}p + N_{r}r + N_{\delta_r}\delta_r \qquad \text{(VI.D-14a)}$$

Making use of arguments similar to that used in the derivation of previous dampers, the utilization of a negative feedback, as it is shown in figure (VI.D-6), will augment the main aerodynamic derivative N_r as follows:

$$\delta(S) \equiv \delta_r(S) = \delta_c(S) - k_r r(S)$$

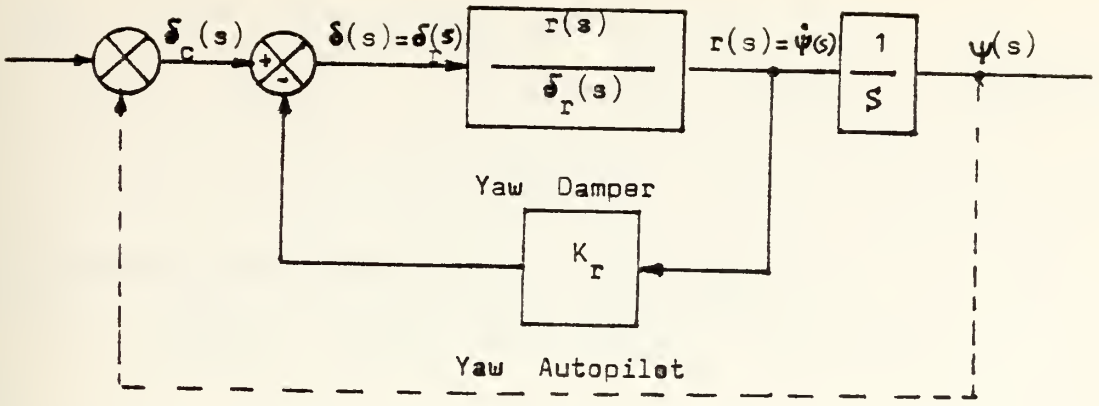

Fig. VI.D-6. Block Diagram of a Yaw Damper

and upon substituting into equation (VI.D-14a) and after minor rearrangements, the following "yaw" equation is derived:

$$\dot{r} = N_\beta \beta + N_p p + (N_r - k_r N_{\delta_r}) r + N_{\delta_r} \delta_r \qquad \text{(VI.D-15)}$$

where $N_r - k_r N_{\delta_r} = N_{r\ \text{augment}}$ (augment aerodynamic derivative) (VI.D-15a)

It is known that for a missile with 90° rotational symmetry, $N_r = -M_q$ which means that there exist damping in yaw. For relatively small L_β which usually is the case of missiles with small dihedral effect, the lateral motion can be approximated by "β: sideslipping" and "ψ: yawing". This is equivalent to eliminating the roll equation from the set of the lateral equations. Considering that $Y_r \neq 0$, knowing that $r = \dot{\psi}$, deleting 2nd and 4th row and column from the set of the lateral equations and utilizing Laplace transformation, it is easily obtained:

$$\begin{vmatrix} (SU_o - Y_\beta) & S(U_o - Y_r) \\ -N_\beta & S(S - N_r) \end{vmatrix} \begin{vmatrix} \beta(s) \\ \psi(s) \end{vmatrix} = \begin{vmatrix} Y_\delta \\ N_\delta \end{vmatrix} \delta(s) \qquad \text{(VI.D-16)}$$

The characteristic equation for this case is:

$$S(SU_o - Y_\beta)(S - N_r) + SN_\beta(U_o - Y_r) = 0$$

or

$$S\left[S^2 - (N_r + Y_\beta/U_o)S + (Y_\beta - N_\beta U_o - N_\beta Y_r)/U_o\right] = 0 \qquad \text{(VI.D-17)}$$

For S = 0 a "neutral" heading stability results. The overall performance in yawing motion is adequately described by the second order equation into the brackets of equation (VI.D-17), that is:

$$S^2 - S(N_r + Y_\beta U_o) + (Y_\beta + N_\beta U_o - N_\beta Y_r)/U_o = 0 \qquad \text{(VI.D-17a)}$$

Comparing to the well known second order equation

$$S^2 + 2\zeta\omega_n S + \omega_n{}^2 = 0$$

it comes out that:

$$\omega_n = \left[(Y_\beta N_r + N_\beta U_o - N_\beta Y_r)/U_o\right]^{1/2} \qquad \text{(VI.D-17b)}$$

and in case of very small Y_β and Y_r it comes out that:

approximately, $\omega_n \cong \sqrt{N_\beta}$ (VI.D-17b.1)

while $\zeta = -(N_r + Y_\beta/U_o)/2\omega_n$ (VI.D-17c)

Looking back to equation (VI.D-15a), it is obvious that the augmentation of the aerodynamic derivative N_r increases directly the damping.

After the above treatment, a functioning block diagram of a yaw damper would be like that in figure (VI.D-7). In this schematic representation, it is emphasized that the yaw velocity is sensed by a rate gyro. The block "Missile Dynamics" could be either the approximated transfer function of the system that results in via equation (VI.D-16), or the full transfer function from the rudder (δ_r) to r, which is given by

$$\frac{r(S)}{\delta_r(S)} = \frac{A_r S^3 + B_r S^2 + C_r S + D_r}{\Delta_{lat}}$$

where $A_r = N'_\delta$

$$B_r = Y^*_\delta N'_\beta + L'_\delta N'_p - N'_\delta (Y_r + L'_p)$$

$$C_r = Y^*_\delta (L'_\beta N'_p - N'_\beta L'_p) - L'_\delta Y_r N'_p + N'_\delta Y_r L'_p$$

$$D_r = g(L'_\delta N'_\beta - N'_\delta L'_\beta)/U_o$$

$$\Delta_{lat} = AS'' + BS^3 + CS^2 + DS + E$$

$$A = 1 - I^2_{xx}/I_x I_y$$

$$B = -Y_r(1-I^2_{xx}/I_x I_y) - L_p - N_r - N_p I_{xz}/I_x - L_r I_{xz}/I_z$$

$$C = N_\beta + L_p(Y_r+N_r) + N_p(Y_r I_{xz}/I_x - L_r) + Y_r(L_r I_{xz}/I_z + N_r) + L_\beta I_{xz}/I_z$$

$$D = -N_\beta L_p + Y_r(N_p L_r - L_p N_r) + N_p L_\beta - (L_\beta + I_{xz} N_\beta/I_x) g/U_o$$

$$E = (L_\beta N_r - N_\beta L_r) g/U_o$$

The discussion so far pointed out the physical significance of the aerodynamic derivatives and also methods for

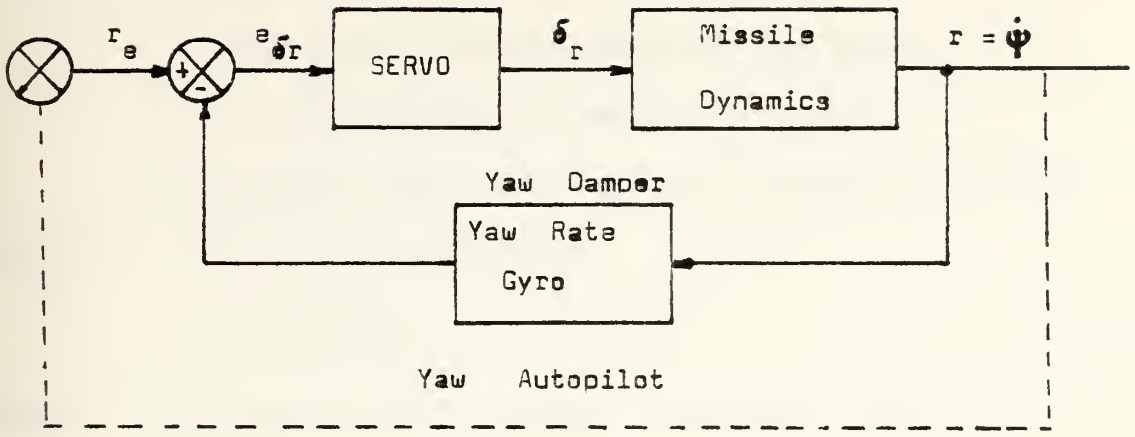

Fig. VI.D-7. Functional Block Diagram of a Yaw Damper

preliminary design studies concerning the development of dampers and further more autopilots.

3. Autopilot Design by Modern Control Method

There have been developed several modern theories tending to achieve optimal control. Such a reasonably straightforward method is the so called "linear quadratic." This modern theory method can be summarized as follows:

Given a time-varying linear control system,

$$\dot{\underset{\sim}{x}}(t) = \underset{\sim}{A}(t)\underset{\sim}{x}(t) + \underset{\sim}{B}(t)\ \underset{\sim}{U}(t) \qquad \text{(VI.D-19)}$$

where $\underset{\sim}{x}(t_o) = \underset{\sim}{x}_o$, having a control variable $Z(t)$ such that:

$$\underset{\sim}{Z}(t) = \underset{\sim}{H}(t)\underset{\sim}{X}(t)$$

try to determine the values of the input variable $\underset{\sim}{U}(t)$ for $t_o \leq t \leq t_1$ for which the following "Performance Index" is minimized.

$$2J = \underset{\sim}{X}^T(t_1)\underset{\sim\sim}{P}\underset{\sim}{X}(t_1) + \int_{t_o}^{t_1} \left[\underset{\sim}{Z}^T(t)\underset{\sim}{Q}\underset{\sim}{Z}(t) + \underset{\sim}{U}^T(t)\underset{\sim\sim}{R}\underset{\sim}{U}(t)\right] dt \qquad \text{(VI.D-20)}$$

where: $\underset{\sim}{F}$: error covariance positive semidefinite matrix

$\underset{\sim}{Q}$: weighting positive semidefinite matrix

$\underset{\sim}{B}$: weighting positive definite matrix

The optimal input variable $\underset{\sim}{U}^*(t)$ which minimizes equation (VI.D-20) is given by:

$$\underset{\sim}{U}^*(t) = -\underset{\sim}{F}(t)\underset{\sim}{X}(t) \qquad \text{(VI.D-21)}$$

where: $\underset{\sim}{F}(t)$ is the state variable feedback given by:

$$\underset{\sim}{F}(t) = \underset{\sim}{R}^{-1}(t)\underset{\sim}{B}^T(t)\underset{\sim}{P}(t) \qquad \text{(VI.D-22)}$$

and where $\underset{\sim}{P}(t)$ is derived by solving the Riccati equation:

$$-\dot{P} = Q - PBR^{-1}B^TP + PA + A^TP \qquad \text{(VI.D-23)}$$

Note:

1. For steady state condition, it is desirable to have $\dot{P}(t) = 0$
2. For notational simplicity, the time dependence of the vectorial variables sometimes are suppressed.

Some illustrative examples of implementing the outlined method in the design of autopilots are following.

a. Roll Attitude Regulation Autopilot

Sometimes the demand arises for introducing a control system in order to maintain the roll attitude of a missile close to zero while remaining within the specified aileron deflection (δ) and aileron deflection rate ($\dot{\delta}$).

Note: To avoid nomenclature confusion, ω will be used to represent roll angular velocity instead of the normally used "p", which is also used permanently in the "Riccati" equation.

The equations for such a system are:

$$\dot{\delta} = U \qquad \text{(VI.D-21a)}$$

$$\dot{\omega} = -\frac{1}{\tau}\omega + \frac{Q}{\tau}\delta \qquad \text{(VI.D-21b)}$$

$$\dot{\phi} = \omega \qquad \text{(VI.D-21c)}$$

where: τ: roll time constant

Q: aileron effectiveness

U: commanded aileron rate

ω: roll angular velocity

$-1/\tau$: L_p

Q/τ: L_δ

A selected Performance Index may be as follows:

$$2J = \int_0^\infty (\phi^2 + \delta^2 + U^2)dt \qquad \text{(VI.D-22)}$$

which implies with reference to equation (VI.D-20) that:

$$Q = \begin{vmatrix} 1 & 0 & 0 \\ 0 & 0 & 0 \\ 0 & 0 & 1 \end{vmatrix}, \quad R = 1$$

Assuming complete controlability for the system of equation (VI.D-21), it can be written in state form as follows:

$$\begin{vmatrix} \dot{\delta} \\ \dot{\omega} \\ \dot{\phi} \end{vmatrix} = \begin{vmatrix} 0 & 0 & 0 \\ Q/\tau & -1/\tau & 0 \\ 0 & 1 & 0 \end{vmatrix} \begin{vmatrix} \delta \\ \omega \\ \phi \end{vmatrix} + \begin{vmatrix} 1 \\ 0 \\ 0 \end{vmatrix} U \qquad \text{(VI.D-23)}$$

The steady state Riccati equation is then given by:

$$Q - PBR^{-1}B^TP + PA + A^TP = 0 \qquad \text{(VI.D-24)}$$

because $\dot{P} = 0$. The solution of equation (VI.D-24) after equalization of terms leads to the following set of equations:

$$2\frac{Q}{\tau}P_{12} - P_{11}^2 + 1 = 0 \qquad \text{(VI.D-24a)}$$

$$\frac{Q}{\tau}P_{22} - \frac{1}{\tau}P_{12} + P_{13} - P_{11}P_{12} = 0 \qquad \text{(VI.D-24b)}$$

$$\frac{Q}{\tau}P_{23} - P_{11}P_{13} = 0 \qquad \text{(VI.D-24c)}$$

$$-\frac{2}{\tau}P_{22} + 2P_{23} - P_{12}^2 = 0 \qquad \text{(VI.D-24d)}$$

$$-P_{23} + \tau P_{33} - \tau P_{12}P_{13} = 0 \qquad \text{(VI.D-24e)}$$

$$1 - P_{13}^2 = 0 \qquad \text{(VI.D-24f)}$$

From equation (VI.D-24f) it follows that $P_{13} = 1$ and while from equation (VI.D-24c) it follows that $P_{23} = \frac{\tau}{Q}P_{11}$. Then the set of equation (VI.D-24) can be easily reduced to:

$$2\frac{Q}{\tau}P_{12} - P_{11}^2 + 1 = 0 \qquad \text{(VI.D-25a)}$$

$$\frac{Q}{\tau}P_{22} - \frac{1}{\tau}P_{12} + 1 - P_{11}P_{12} = 0 \qquad \text{(VI.D-25b)}$$

$$-\frac{2}{\tau}P_{22} + \frac{2\tau}{Q}P_{11} - P_{12}^2 = 0 \qquad \text{(VI.D-25c)}$$

$$-\frac{P_{11}}{Q} + P_{33} - P_{12} = 0 \qquad \text{(VI.D-25d)}$$

After some algebraic manipulations, it can be derived:

$$P_{11}^4 + \frac{4}{\tau}P_{11}^3 + \left(\frac{4}{\tau^2} - 2\right)P_{11}^2 - \frac{4}{\tau}(2Q+1)P_{11} + 1 - \frac{4}{\tau^2} - \frac{8Q}{\tau^2} = 0 \qquad \text{(VI.D-26)}$$

Depending on the settled specification values for τ and Q, equation (VI.D-26) is solved and the positive real roots are

accepted. Then, proceeding backwards and accordingly, the values of the rest P_{ij}'s can be derived. Finally, the optimal control input variable will be given by:

$$\begin{aligned} U^* &= -\underset{\sim}{F}\underset{\sim}{X} \\ &= -R^{-1}\underset{\sim}{B}^T\underset{\sim}{P}\underset{\sim}{X} \\ &= -\begin{bmatrix} P_{11} & P_{12} & P_{13} \end{bmatrix} \begin{bmatrix} \delta \\ \omega \\ \phi \end{bmatrix} \end{aligned} \qquad \text{(VI.D-27)}$$

b. g-Bias Autopilot

Suppose a missile in a horizontal cruise mode. It is desired to design an autopilot which will maintain a small vertical acceleration (g-bias). In this case, the longitudinal short period equations are given by:

$$\begin{vmatrix} \dot{a} \\ \dot{q} \end{vmatrix} = \begin{vmatrix} \frac{Z_a}{U_o} & 1 \\ M_a & M_q \end{vmatrix} \begin{vmatrix} a \\ q \end{vmatrix} + \begin{vmatrix} \frac{Z_\delta}{U_o} \\ M_\delta \end{vmatrix} \delta \qquad \text{(VI.D-28)}$$

where a: angle of attack

q: pitching rate

But normally, $Z_\delta << Z_a$ and $M_q << M_a$, thus equation (VI.D-28) can be reduced to:

$$\begin{vmatrix} \dot{a} \\ \dot{q} \end{vmatrix} = \begin{vmatrix} \frac{Z_a}{U_o} & 1 \\ M_a & 0 \end{vmatrix} \begin{vmatrix} a \\ q \end{vmatrix} + \begin{vmatrix} 0 \\ M_\delta \end{vmatrix} \delta \qquad \text{(VI.D-28a)}$$

A selected Performance Index for this case may be:

$$2J = \int_{t_o}^{t_f} \left(\frac{\delta^2}{\delta_o^2} + \frac{a^2}{a_o^2} + \frac{q^2}{q_o^2} \right) dt \qquad \text{(VI.D-29)}$$

where δ_o, a_o and q_o are maximum permitted values for the aileron deflection angle of attack and pitching rate and which implies, with reference to equation (VI.D-20), that:

$$Q = \begin{vmatrix} 1/a_o^2 & 0 \\ 0 & 1/q_o^2 \end{vmatrix}, \quad R = \frac{1}{\delta_o^2}$$

Then, by arguments similar to the previous example and by utilizing the Ricatti equation, the optimum control input variable can be determined. Noticeable is that in some cases the aileron deflection can be defined as:

$$\delta = C_1 a + C_2 q$$

The coefficients C_1 and C_2 can be determined by utilizing similar procedures as above.

Note: The full expansion of such a derivation is beyond the scope of this presentation and thus omitted.

VII. MATHEMATICAL MODELLING OF A MISSILE GUIDANCE CONTROL SYSTEM

A. THE MATHEMATICAL MODEL

There is a formidable difficulty in arriving at a general solution of the equations describing the behavior of any homing system. The guided missile, while operating in the real world, is subject to disturbing conditions, e.g. limited and noisy information, missiles and sensor dynamics, constraints on missile acceleration, etc. Since real world effects cannot be comprehended completely and described perfectly, the real world guidance problem is a fuzzy problem. It has to be solved by a progressive iterative step-by-step procedure in order to find an "optimal" solution in the sense of keeping the missile motion "sufficiently close" to the nominal course of kinematic guidance with regard to essential real world effects such as dynamic delays and noisy measurements. Hence real world affects the design of the feedback portion of the guidance law and necessitates information processing.

The step-by-step procedure is characterized by the analysis of essential effects and their influence on the system performance, by the synthesis of suitable information processing and guidance law algorithms and by the simulation of the guidance loop, in order to evaluate the system performance.

One can start up with linear model for the homing head and autopilot and linearity of the kinematics can be obtained by assuming that the effect of target maneuver, noise, or a heading error of the missile from the ideal direction which would lead to a constant bearing collision course, as a small perturbation from that collision course. Such assumptions permit to make small angle approximations. If the study is focused at the closing stages of the engagement, such assumptions could be argued that result in fair approximations as the missile is usually on a near-constant bearing trajectory just before impact. If the target makes large evasive maneuvers during the last stages period (as it is expected to be done with modern weapons), these assumptions lead to less valid models.

Design considerations using frequency domain control techniques usually involve parameter determination in the kinematic guidance laws and in noise suppressing filters.

The Wiener filter approach is limited to single-input-single-output systems with time independent system parameters and noise statistics, assumptions which are in general violated in missile guidance.

To include real world properties more systematically in the solution of the missile guidance problem modern, "time domain," control techniques offer attractive advantages in this case of a multi-input-multi-output system with time-varying system and noise parameters. Optimal (non linear or

linear) filtering techniques provide for noise suppression and additional information processing about guidance loop stages from the noisy measurements. Optimal control law design techniques lead to extended feedback control structures and parameter determination algorithms to compensate the disturbing influence of missile and sensor dynamics.

The following examples aim to demonstrate the design process and the benefit of applying modern guidance control theory versus classical proportional navigation and augment proportional navigation.

B. INSTRUCTIVE DESIGN DEVELOPMENT OF A GUIDANCE CONTROL SYSTEM

In part II, the motion equations were derived. After some reasonable assumptions, these equations were linearized and decoupled in order to simplify the study and in parallel to try to stay close to the reality in an acceptable mode.

The decouplization of the motion equations into two independent sets, permits the study of the missile either in a longitudinal plane or in a lateral plane. The design techniques are similar, thus no distinction concerning the used plane is done.

Before going on, an interception geometry review is considered necessary. This is shown in figure (VII.B-1).

The target is flying at an angle ϕ_o to the original line of sight M_oT_o which is regarded as a reference direction, while the missile is flying a small deviation angle ψ_ε to the

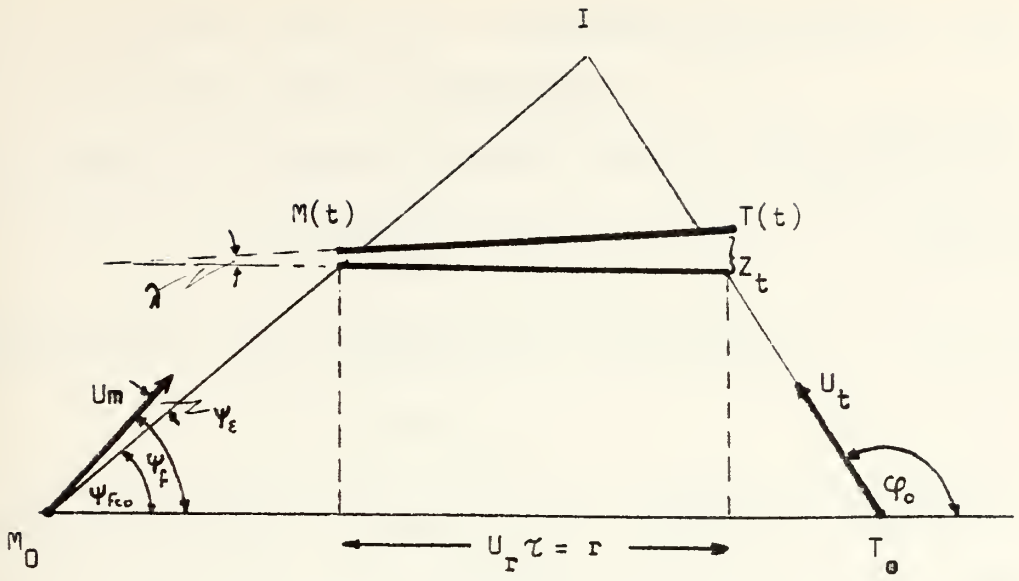

Fig. VII.B-1. Interception Geometry

correct flight path to obtain a collision at I. The correct flight path angle ψ_{fco} is given by:

$$U_m \sin \psi_{fco} = U_t \sin \phi_o \qquad \text{(VII.B-1)}$$

There is in fact an imaginary line which runs up the considered engagement plane parallel to M_oT_o at a velocity of $U_m \sin \psi_{fco}$. Any perturbation of the missile and target perpendicular to this line is denoted by Z_m and Z_t respectively. The below relationship follows:

$$\tan \lambda = (Z_t - Z_m)/r = (Z_t - Z_m)/U_r\tau \qquad \text{(VII.B-2)}$$

and for small angles where $\lambda \cong \tan \lambda$

$$\lambda \cong (Z_t - Z_m)/U_r\tau \qquad \text{(VII.B-2a)}$$

where: λ: sight line angle

U_r: relative or closing velocity = $U_m \cos \psi_f - U_t \cos \phi_o$

τ: time to go = T - t considered zero when r = 0

T: total time of engagement

If ψ_ε is small, it can be regarded that $\psi_f \cong \psi_{fco}$ because

$$\psi_f = \psi_{fco} \pm \psi_\varepsilon \qquad \text{(VII.B-3)}$$

and $\cos\psi_f = \cos(\psi_{fco} \pm \psi_\varepsilon) = \cos\psi_{fco}\cos\psi_\varepsilon \pm \sin\psi_{fco}\sin\psi_\varepsilon$ (VII.B-4)

$$\cong \cos\psi_{fco}$$

As miss distance in one plane is considered the difference $Z_t - Z_m$ at r = 0. Of course this is not the true vector miss distance but it can be shown that this is very nearly so provided that the concept of small perturbations still holds.

The miss distance can be determined utilizing a functional block diagram as follows:

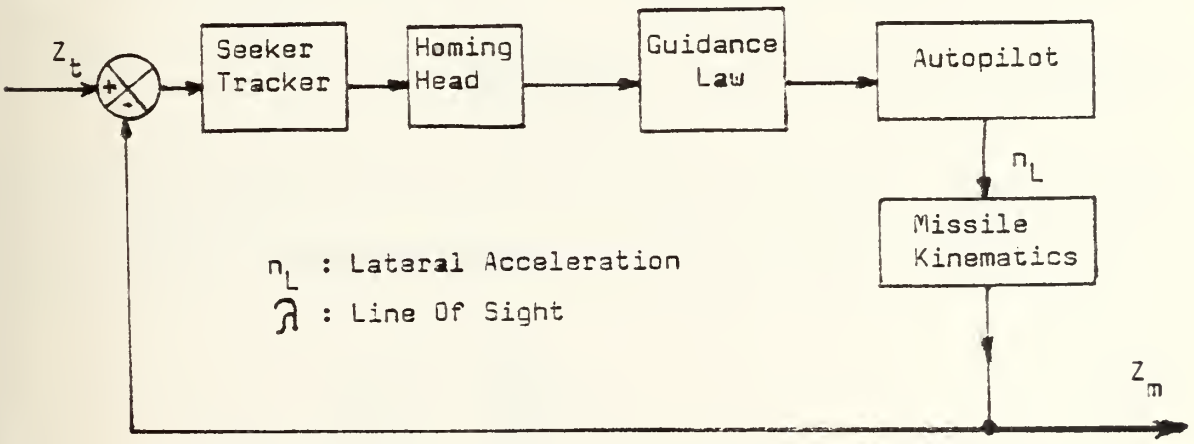

Fig. VII.B-2. Functional Representation of Homing System

Each block may be as complex as desired. The seeker or tracker provides the sight line angle (for small perturbations,

$\lambda = 1/r = 1/U_r\tau = 1/U_r(T - t)$. Homing head, autopilot and missile dynamics can be represented with a transfer function of any appreciable polynomial order. Therefore, their individual gains can be considered as the product of all the others and thus to be taken into manipulations as: $K = K_1K_2K_3$. Since the time to go $\tau = T - t$, where T is the time to go from the initial positioning M_oT_o to the interception point, is common to all systems and engagements, all systems will, for the same dynamic lags, be identical if:

$$\frac{K}{U_r} \cos \psi_{fco} = \text{a constant} \qquad \text{(VII.B-5)}$$

This constant has no dimensions and is usually known as the kinematic stiffness (for more details refer to part IV). Recall that if an optimum value for "a" exists, then it follows that one should adopt a navigation constant such that:

$$K = \frac{U_r a}{\cos \psi_{fco}} \qquad \text{(VII.B-6)}$$

The homing head can be modeled dynamically as a second order lag, having a transfer function of the form:

$$\frac{S}{\frac{S^2}{\omega^2_{nh}} + \frac{2\mu_h S}{\omega_{nh}} + 1} \qquad \text{(VII.B-7)}$$

where: ω_{nh}: homing head natural frequency

μ_h: homing head damping

The autopilot can be modelled adequately as a second order lag system too; having a transfer function of the form:

$$\frac{1}{\frac{S^2}{\omega_{na}^2} + \frac{2\mu_a S}{\omega_{na}} + 1} \qquad \text{(VII.B-8)}$$

where: ω_{na}: autopilot natural frequency

μ_a: autopilot damping

Finally, the missile dynamics can be modelled in a simplified form as $1/S^2$.

Based upon the above considerations the step-by-step progressive design development can start now.

1. Lag Free System

Assuming that the natural frequencies of the homing head and the autopilot are infinitely large, the system of figure (VII.B-2) turns into that shown in figure (VII.B-3). (The derivation is very simple, thus omitted.)

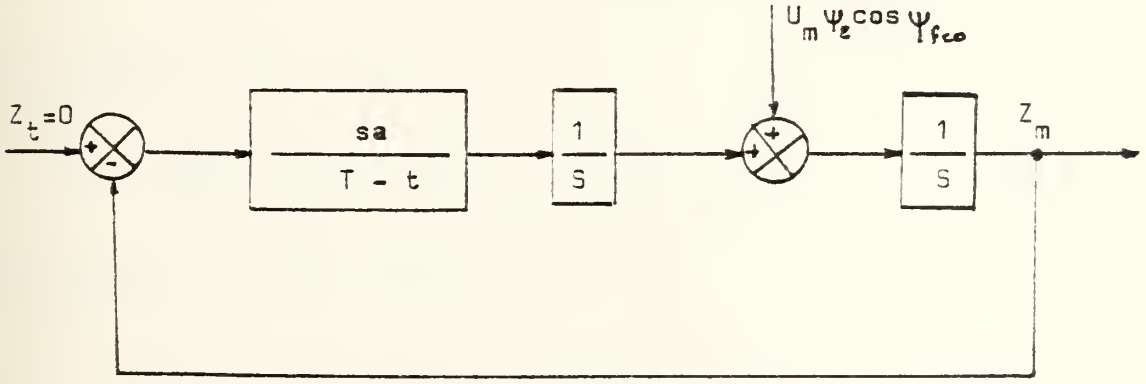

Fig. VII.B-3. Lag-free System with Step Velocity Input

In this case, a small initial aiming error is assumed. The initial missile velocity perpendicular to the

collision course is $U_m \psi_\varepsilon$ and the component perpendicular to the initial sight line $M_o T_o$ (see figure VII.B-1) is $U_m \psi_\varepsilon \cos \psi_{fco}$. This component can be regarded as an input to the system; in fact the system would detect no difference in the situation if the initial heading was correct and at $t = 0 + \varepsilon$ the target instantaneously changed its course to produce a velocity perpendicular to the original sight line $M_o T_o$ equal in magnitude to $U_m \psi_\varepsilon \cos \psi_{fco}$. For this reason a heading error is often referred to as a step velocity input.

By inspection, the output Z_m due to the input can be written:

$$Z_m = \frac{1}{S} U_m \psi_\varepsilon \cos \psi_{fco} - Z_m \frac{a}{S(T - t)} \qquad \text{(VII.B-9)}$$

or after term rearrangement and minor manipulations:

$$\frac{Z_m}{U_m \psi_\varepsilon \cos \psi_{fco}} = \frac{1}{S + \frac{a}{T - t}} \qquad \text{(VII.B-9a)}$$

or in differential form:

$$\frac{dZ_m}{dt} + \frac{a}{T-t} Z_m = U_m \psi_\varepsilon \cos \psi_{fco} \qquad \text{(VII.B-9b)}$$

and in state variable form:

$$\dot{x}_1 = - \frac{a}{T-t} X1 + U_m \psi_\varepsilon \cos \psi_{fco} \qquad \text{(VII.B-9c)}$$

which is of the general linear time-varying form of:

$$\dot{\underset{\sim}{x}}(t) = \underset{\sim}{A}(t)\underset{\sim}{x}(t) + \underset{\sim}{B}(t)\underset{\sim}{u}(t)$$

2. Single Quadratic Lag

Assuming that the natural frequency of the homing head is infinitely large, while the autopilot has a reasonable natural frequency, the central system has a block diagram representation as in following figure (VII.B-4). Then, by inspection, it will be:

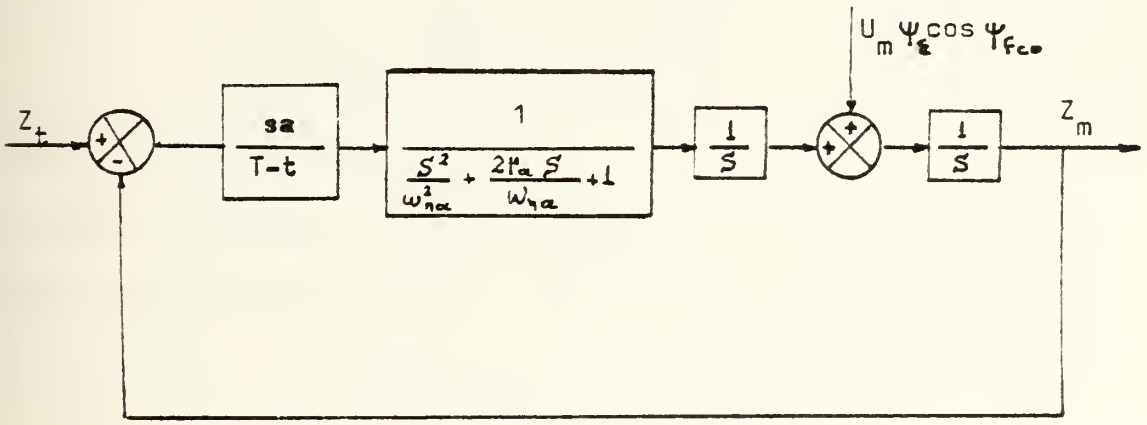

Fig. VII.B-4. Single Quadratic Lag System with Step Velocity Input

$$Z_m = \frac{1}{S} U_m \psi_\varepsilon \cos \psi_{fco} - Z_m \frac{1}{S} \frac{a}{T-t} \frac{1}{\frac{S^2}{\omega_{na}^2} + \frac{2\mu_a S}{\omega_{na}} + 1}$$

or

$$Z_m \left[1 + \left(\frac{a}{S(T-t)} \frac{1}{\frac{S^2}{\omega_{na}^2} \frac{2\mu_a}{\omega_{na}} S + 1}\right)\right] = \frac{1}{S} U_m \psi_\varepsilon \cos \psi_{fco}$$

After minor manipulations and rearrangements, it turns in the following transfer function, which can be studied by any one of the known methods.

$$\frac{Z_m}{U_m \psi_\varepsilon \cos \psi_{fco}} = \frac{S^2 + 2\mu_a \omega_{na} S + \omega_{na}^2}{S^3 + 2\mu_a \omega_{na} S^2 + \omega_{na}^2 S + \frac{a\omega_{na}^2}{T-t}} \qquad \text{(VII.B-10)}$$

Expanding equation (VII.B-10) it follows:

$$\frac{d^3 Z_m}{dt^3} + 2\mu_a \omega_{na} \frac{d^2 Z_m}{dt^2} + \omega_{na}^2 \frac{dZ_m}{dt} + \frac{a\omega_{na}^2}{T-t} Z_m = \frac{d^2 U'_t}{dt^2}$$

$$+ 2\mu_a \omega_{na} \frac{dU'_t}{dt} + \omega_{na}^2 U'_t \qquad \text{(VII.B-10a)}$$

where $U'_t = U_m \psi_\varepsilon \cos \psi_{fco}$

In case of constant velocity input (U'_t = constant), the right hand side of equation (VII.B-10a) is simplified to:

$$\omega_{na}^2 U_m \psi_\varepsilon \cos \psi_{fco}$$

Applying state variable format techniques, and denoting,

$Z_m = X_1$

$dZ_m/dt = \dot{X}1 = X2$

$d^2Z/dt^2 = \dot{X}2 = X3$

equation (VII.B-10a) is now written in matrix format as follows:

$$\begin{vmatrix} \dot{X}1 \\ \dot{X}2 \\ \dot{X}3 \end{vmatrix} = \begin{vmatrix} 0 & 1 & 0 \\ 0 & 0 & 1 \\ -\frac{a\omega_{na}^2}{T-t} & -\omega_{na}^2 & -2\mu_a \omega_{na} \end{vmatrix} \begin{vmatrix} X1 \\ X2 \\ X3 \end{vmatrix} + \begin{vmatrix} 0 \\ 0 \\ 1 \end{vmatrix} \omega_{na}^2 U_m \psi_\varepsilon \cos \psi_{fco} \qquad \text{(VII.B-10b)}$$

3. Double Quadratic Lag

The previous systems were not realistic by any means. A more realistic system occurs by assuming that both homing head and autopilot are reasonably fast, that means both have natural frequency ω_{nh} and ω_{na} respectively. Thus a double quadratic lag system occurs which has a block diagram representation as in following figure (VII.B-5).

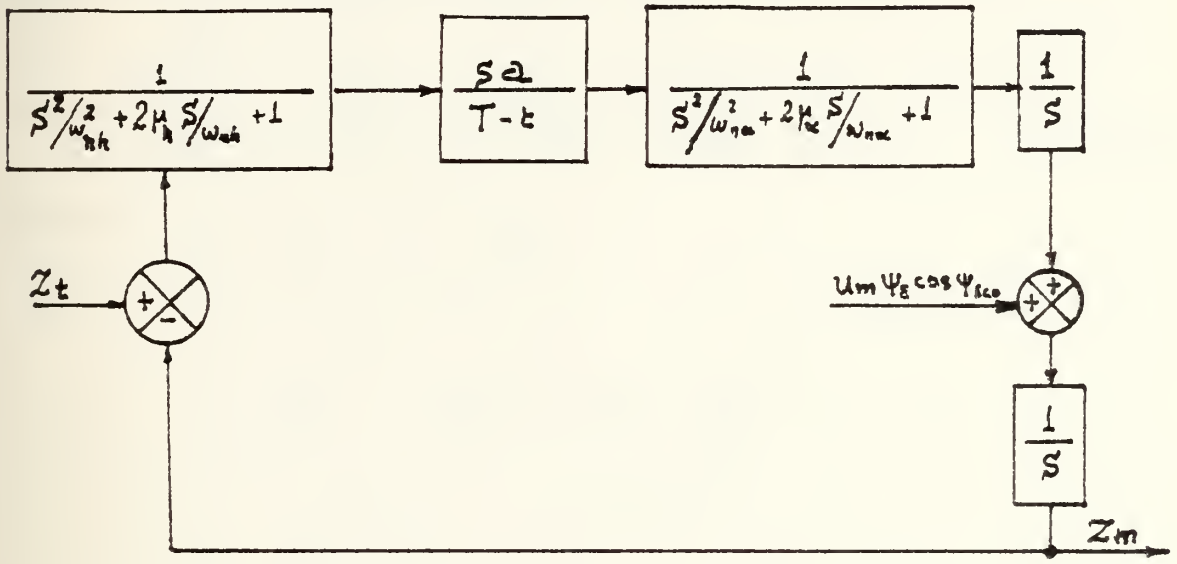

Fig. VII.B-5. Double Quadratic Lag System with Step Velocity Input

By inspection it is:

$$Z_m = \frac{1}{S} U_m \psi_\varepsilon \cos \psi_{fco} - \frac{Z_m}{S}\left(\frac{a}{T-t}\right)\left(\frac{1}{\frac{S^2}{\omega_{nh}^2} + \frac{2\mu_h S}{\omega_{nh}} + 1}\right)\left(\frac{1}{\frac{S^2}{\omega_{na}^2} + \frac{2\mu_a S}{\omega_{na}} + 1}\right)$$

or, after minor manipulations and rearrangements, it turn in:

$$\frac{Z_m}{U_m \psi_\varepsilon \cos \psi_{fco}} = \frac{\left(S^2 + 2\mu_h \omega_{nh} S + \omega_{nh}^2\right)\left(S^2 + 2\mu_a \omega_{na} S + \omega_{na}^2\right)}{S\left(S^2+2\mu_h \omega_{nh} S+\omega_{nh}^2\right)\left(S^2+2\mu_a \omega_{na} S+\omega_{na}^2\right) + \left(\frac{a\omega_{na}^2 \omega_{nh}^2}{T - t}\right)} \qquad \text{(VII.B-11)}$$

Expanding equation (VII.B-11) it follows:

$$\frac{d^5 Z_m}{dt^5} + A\frac{d^4 Z_m}{dt^4} + B\frac{d^3 Z_m}{dt^3} + C\frac{d^2 Z_m}{dt^2} + D\frac{dZ_m}{dt} + \frac{a\omega_{nh}^2 \omega_{na}^2}{T - t} Z_m$$

$$= \frac{d^4 U'_t}{dt^4} + A\frac{d^3 U'_t}{dt^3} + B\frac{d^2 U'_t}{dt^2} + C\frac{dU'_t}{dt} + DU'_t \qquad \text{(VII.B-12)}$$

where: $U'_t = U_m \psi_\varepsilon \cos \psi_{fco}$

$A = 2\mu_h \omega_{nh} + 2\mu_a \omega_{na}$

$B = \omega_{nh}^2 + 4\mu_a \mu_h \omega_{na} \omega_{nh} + \omega_{na}^2$

$C = 2\mu_a \omega_{na} \omega_{nh}^2 + 2\mu_h \omega_{nh} \omega_{na}^2$

$D = \omega_{nh}^2 \omega_{na}^2$

In case of constant velocity input (U'_t = constant), the right hand side of equation (VII.B-12) is simplified to $\omega_{nh}^2 \omega_{na}^2 U'_t$. Applying state variable format techniques and denoting:

$Z_m = X_1$

$dZ_m/dt = \dot{X}1 = X2$

$d^2 Z_m/dt^2 = \dot{X}2 = X3$

$d^3 Z_m/dt^3 = \dot{X}3 = X4$

$d^4 Z_m/dt^4 = \dot{X}4 = X5$

Equation (VII.B-12) is now written in matrix format as follows:

$$\begin{vmatrix} \dot{X}1 \\ \dot{X}2 \\ \dot{X}3 \\ \dot{X}4 \\ \dot{X}5 \end{vmatrix} = \begin{vmatrix} 0 & 1 & 0 & 0 & 0 \\ 0 & 0 & 1 & 0 & 0 \\ 0 & 0 & 0 & 1 & 0 \\ 0 & 0 & 0 & 0 & 1 \\ \frac{-a\omega_{na}^{2}\omega_{nh}^{2}}{T-t} & -D & -C & -B & -A \end{vmatrix} \begin{vmatrix} X1 \\ X2 \\ X3 \\ X4 \\ X5 \end{vmatrix} + \begin{vmatrix} 0 \\ 0 \\ 0 \\ 0 \\ 1 \end{vmatrix} \omega_{na}^{2}\omega_{nh}^{2}U't \qquad \text{(VII.B-12a)}$$

4. Computational Comparison

The three so far discussed systems can be easily implemented into a computer program in order to investigate and study the expected response of each system under various conditions and parameter values. It is assumed that the homing head is the main lag in the system and that both homing head and autopilot can be represented by second order lags. If this is accepted, then all systems must lie between the two extremes of:

(a) $\omega_{na} = \omega_{nh}$ (autopilot and homing head lags equal)

(b) $\omega_{na} = \infty$ (autopilot infinitely faster than homing head and therefore effectively only one quadratic lag in the system)

For comparison, the above three systems were implemented into one program, as is shown in appendix D. The program was run for a badly and a well damped homing head for practical values of navigation constant "a" of 2.5 and 4.5 (these being on the low and high sides respectively and for relatively "short" and

"long" engagements defined by $\omega_{nh}T = 10$ and 30 respectively. From the above runs, the required missile lateral acceleration vs. normalized time was derived, as is shown in figures (VII.B-6) through (VII.B-16). From these plottings it is seen that for short engagements, inadequate damping and high values of "a" result in oscillatory responses. (The autopilot damping ratio has been set to 0.5 in all cases.) If the open loop gain is high, the system is possible to become unstable at a short range to go. In the absence of noise (not any real system is ever entirely free from noise), a long engagement results in the transient decaying before instability sets in and the effect is not apparent. If the engagement is very short, oscillations do not have enough time to build up. Consider figures (VII.B-14) to (VII.B-16) which have been computed for $\omega_{nh}T = 20$ and an underdamped homing head; this engagement is neither "short" nor "long". Any response of a real system which diverges, from the response of the ideal lag-free system, can be regarded as unstable as the time passes. It is not possible to discern instability for a = 2.5, but for a = 3.5 a system represented by a single quadratic lag could be argued to be unstable later than $t/T = 0.75$ say. For a = 4.5 instability sets in at about $t/T = 0.6$.

Nevertheless, the discussion so far is rather an instructive guidance method than a complete and detailed study.

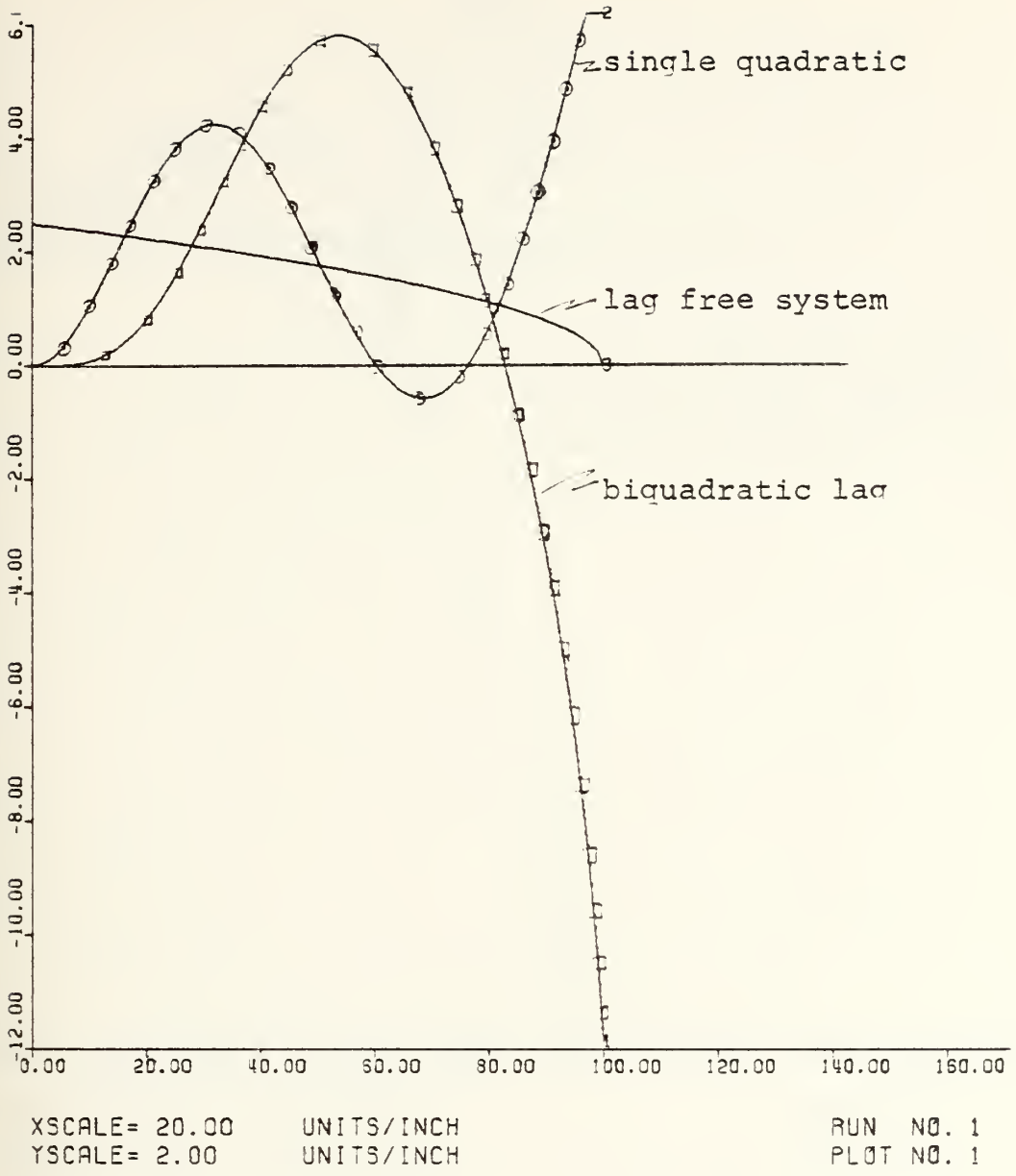

Fig. VII.B-6. Required missile lateral acceleration in case of an initial heading error.
Utilized parameters: Nav. Constant = 2.5

$W_{seeker} = 10.0 = W_{autop}$

$\mu_{seeker} = 0.25$

$\mu_{autopil} = 0.5$

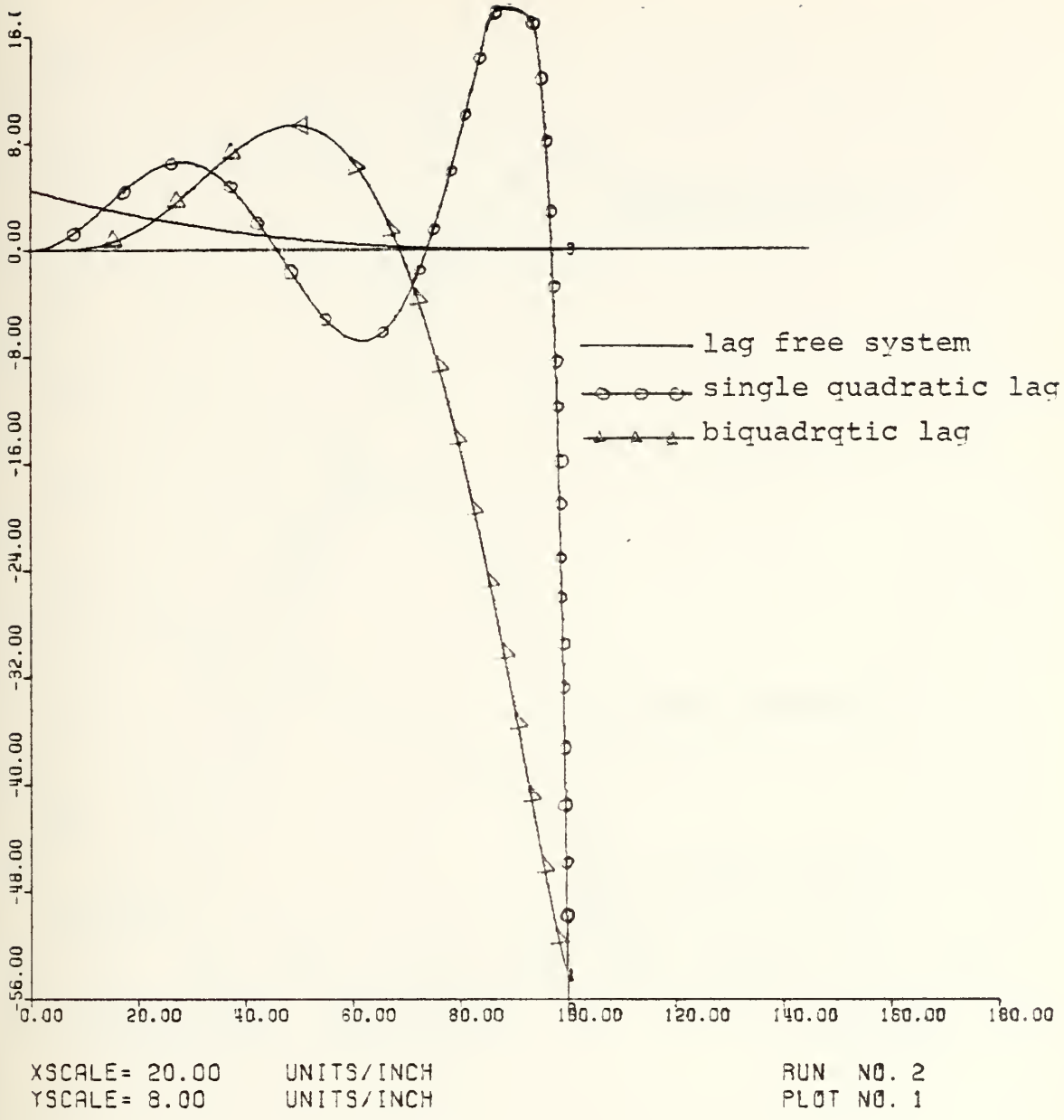

Fig. VII.B-7. Required missile lateral acceleration in case of an initial heading error.
Utilized parameters: Nav. Constant = 4.5

$W_{seeker} = 10.0 = W_{ap}$

$\zeta_{seeker} = 0.25$

$\zeta_{autop.} = 0.5$

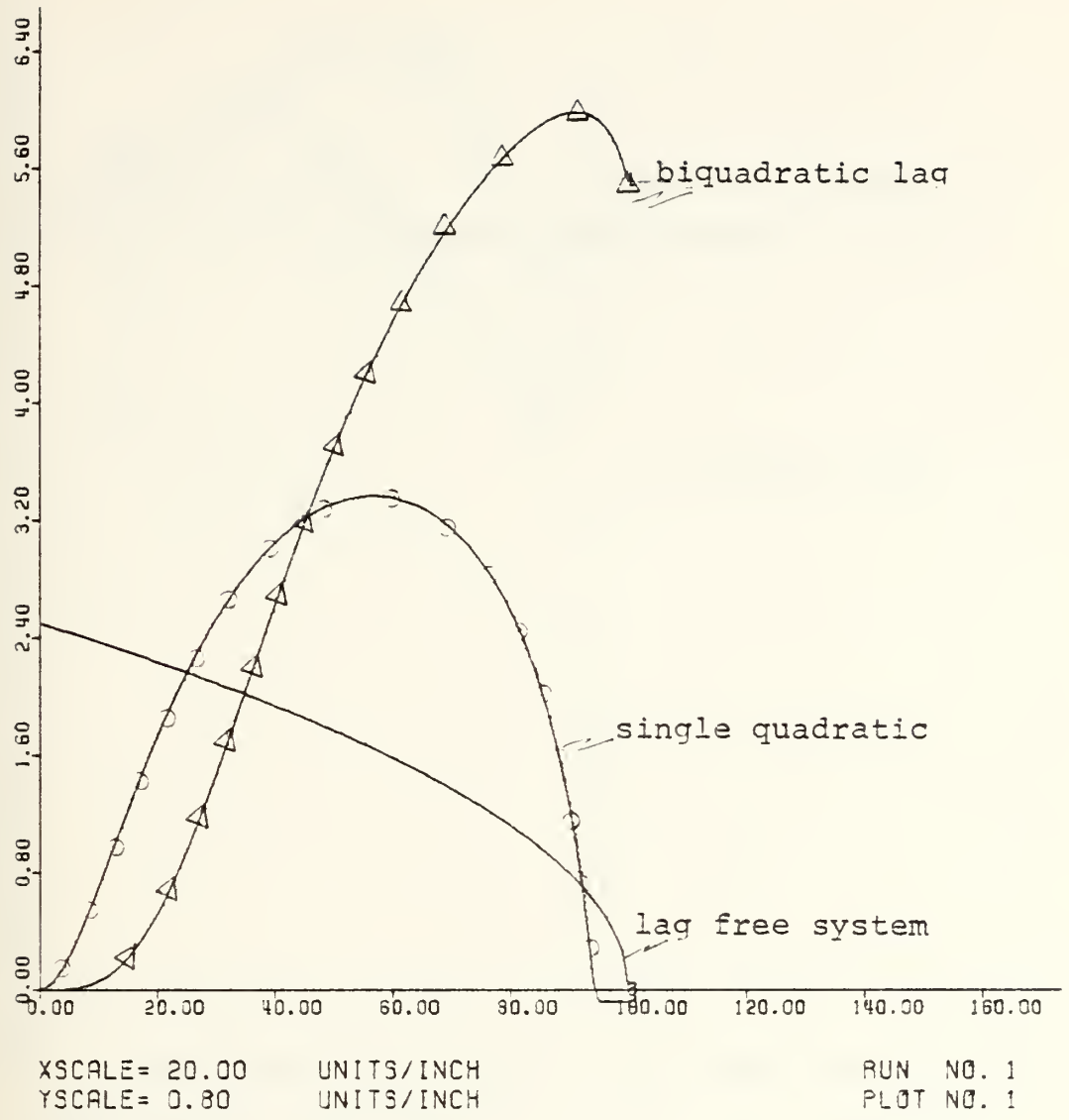

Fig. VII.B-8. Required missile lateral acceleration in case of an initial heading error. Utilized parameters: Nav. Constant = 2.5

$W_{seeker} = 10 = W_{autop}$

$\mu_{seeker} = 1.0$

$\mu_{autop} = 0.5$

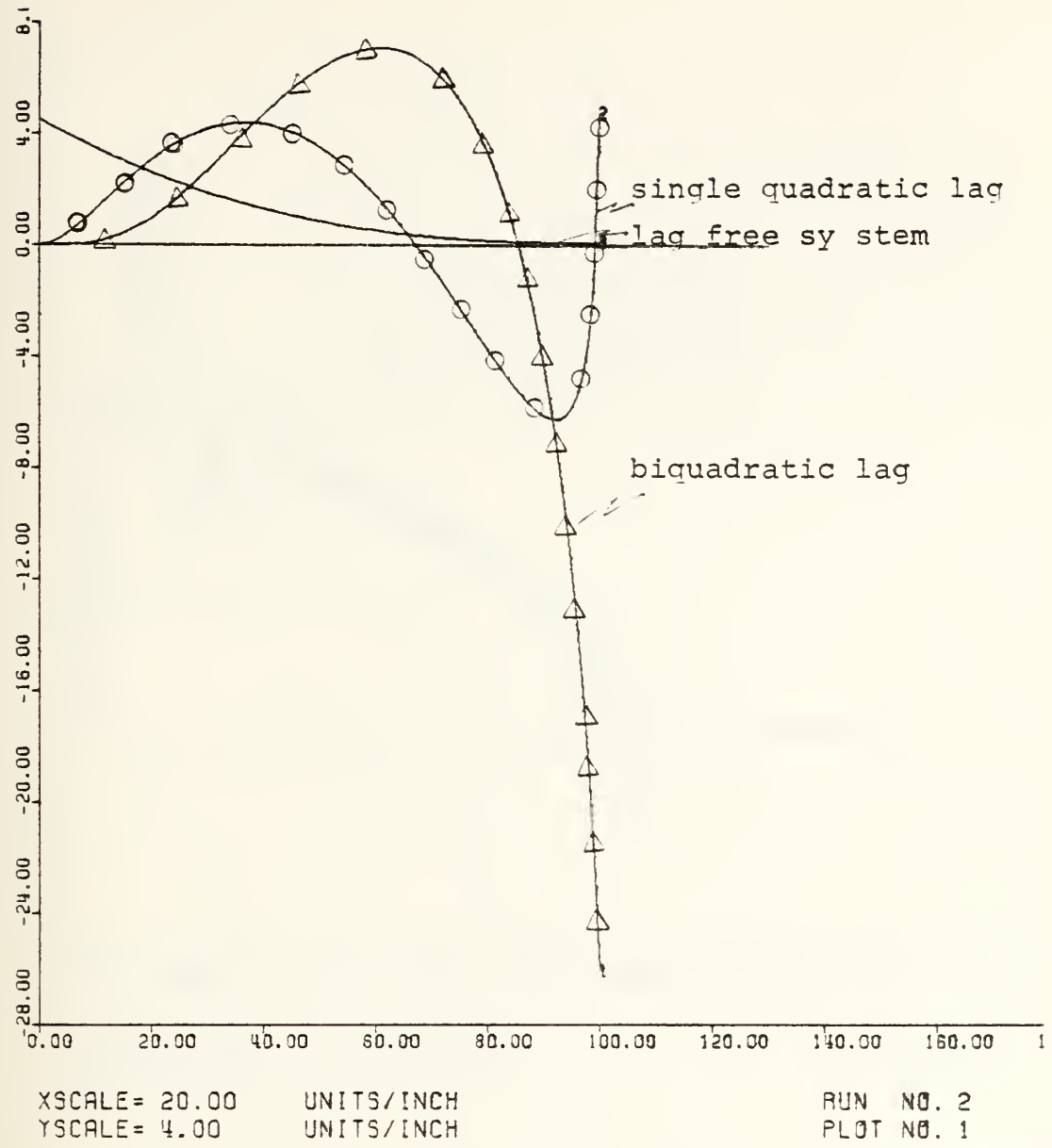

Fig. VII.B-9. Required missile lateral acceleration in case of an initial heading error.
Utilized parameters: Nav. Constant = 4.5

$W_{seeker} = 10. = W_{autop}$

$\zeta_{seeker} = 1.0$

$\zeta_{autopil} = 0.5$

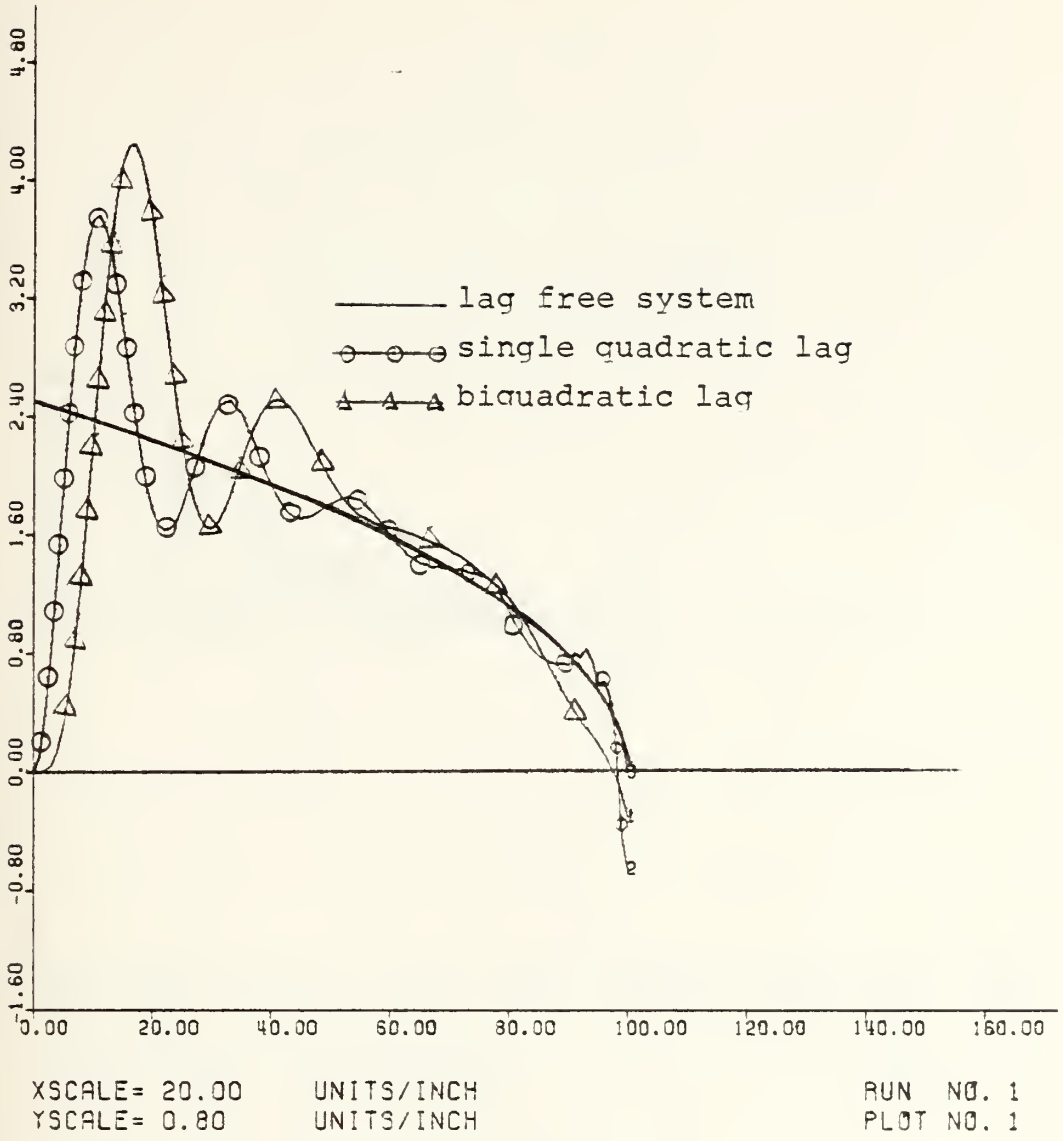

Fig. VII.B-10. Required missile lateral acceleration in case of an initial heading error.
Utilized parameters: Nav. Constant = 2.5

$W_{seeker} = 30.0 = W_{autop}$

$\mu_{seeker} = 0.25$

$\mu_{autop.} = 0.5$

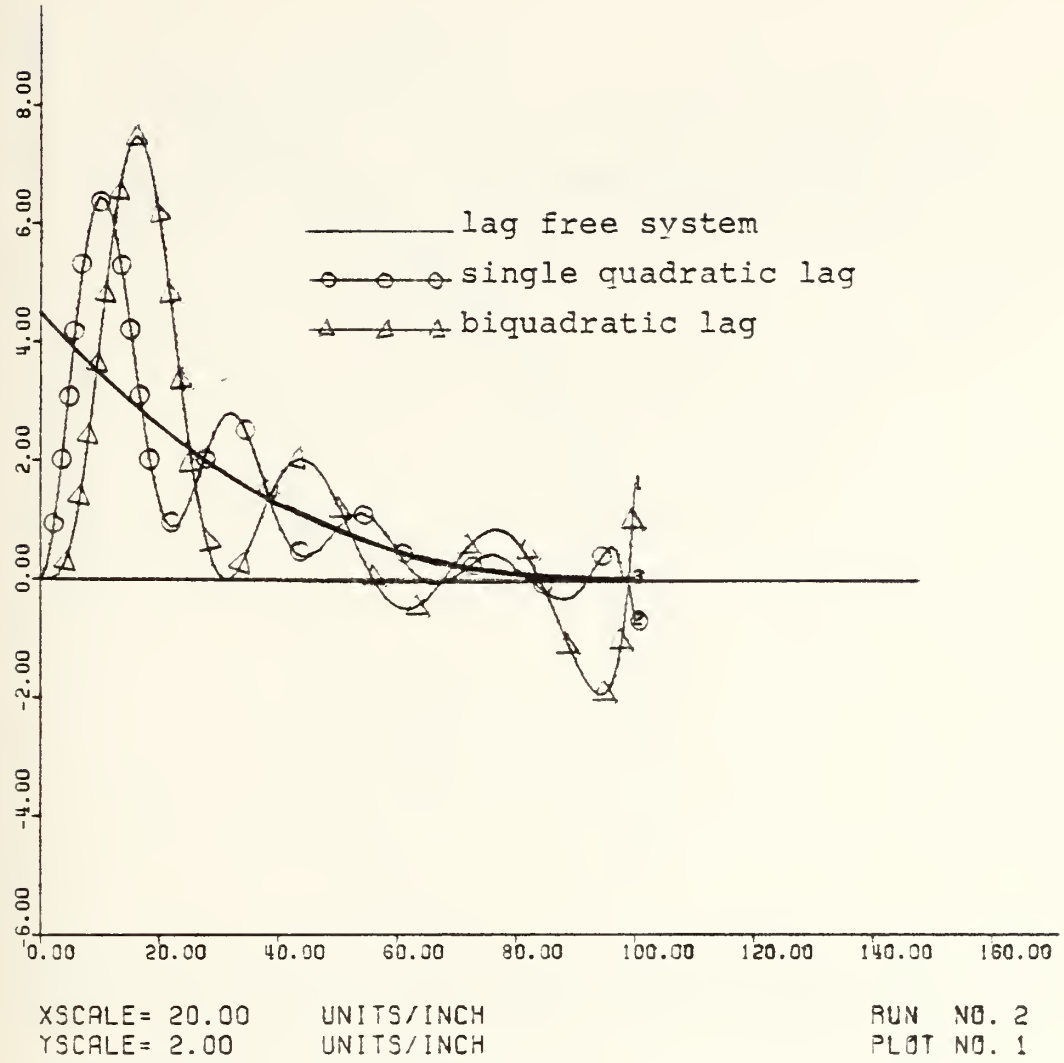

Fig. VII.B-11. Required missile lateral acceleration in case of an initial heading error.
Utilized parameters: Nav. Constant = 4.5

$W_{seeker} = 30.0 = W_{autop}$

$\mu_{seeker} = 0.25$

$\mu_{autopil} = 0.50$

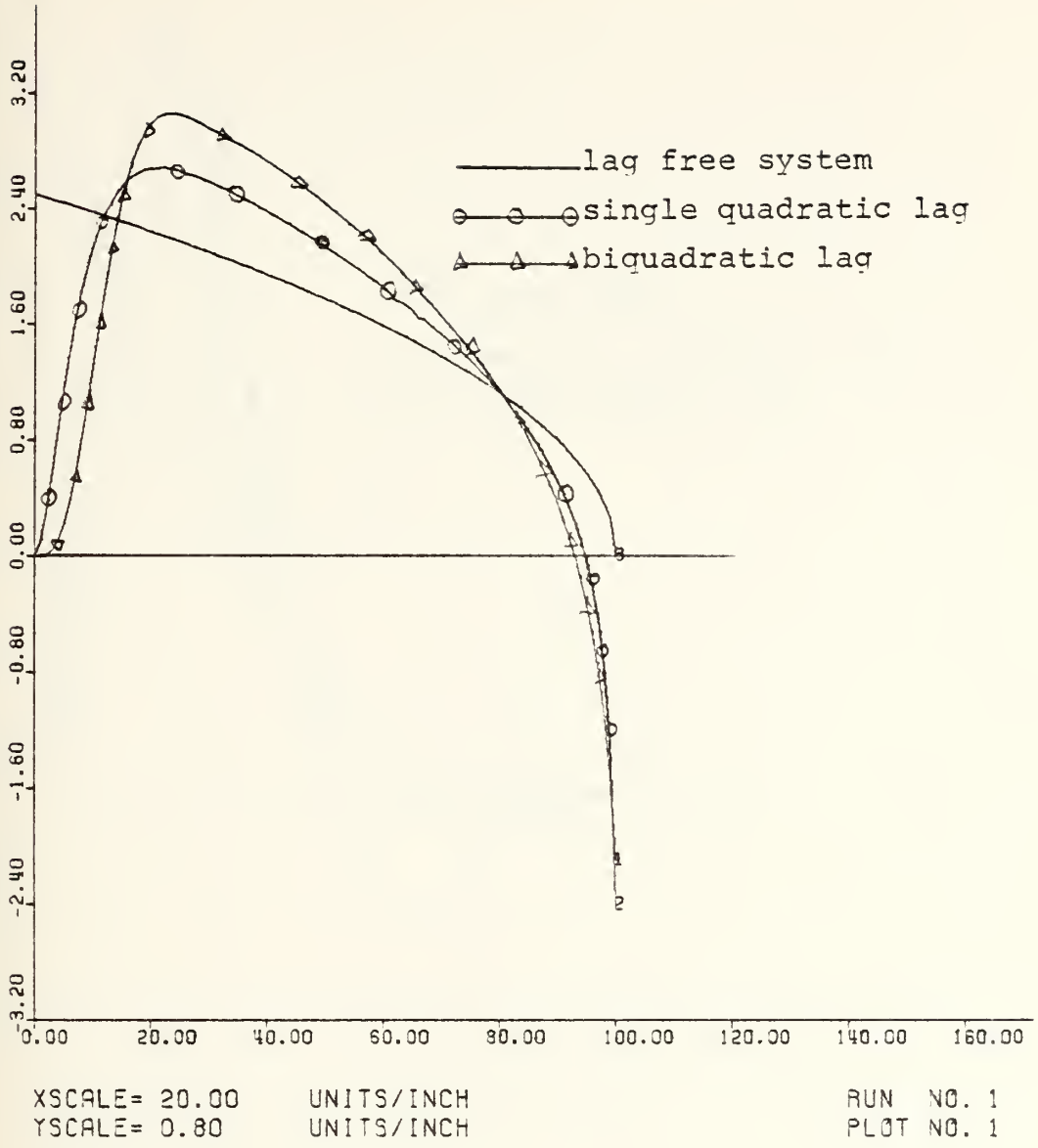

Fig. VII.B-12. Required missile lateral acceleration in case of an initial heading error. Utilized parameters: Nav. Constant = 2.5

$W_{seeker} = 30 = W_{autop}$

$\mu_{seeker} = 1.0$

$\mu_{autopil} = 0.5$

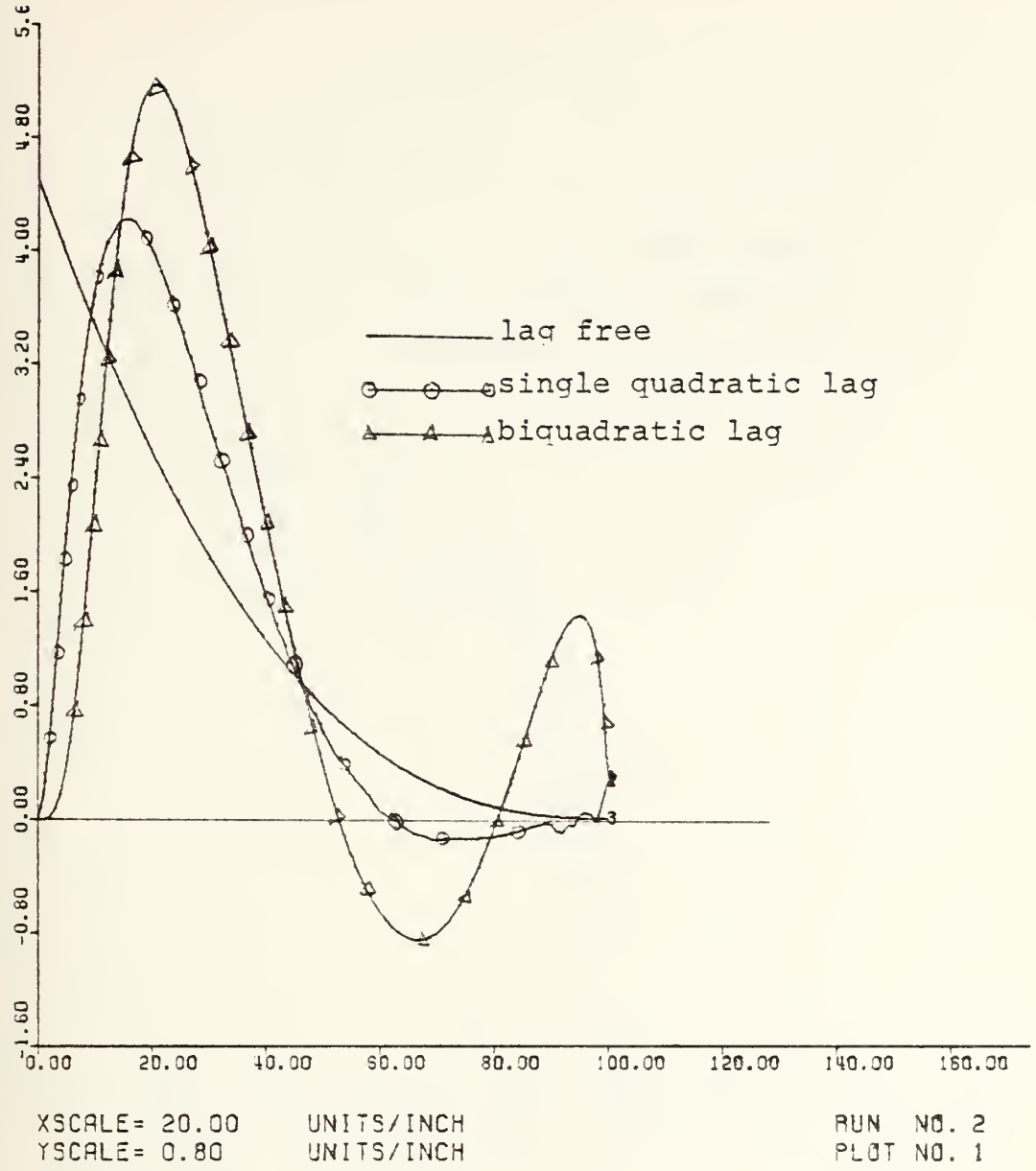

Fig. VII.B-13. Required missile lateral acceleration in case of an initial heading error.
Utilized parameters: Nav. Constant = 4.5

$W_{seeker} = 30.0 = W_{autop}$

$\mu_{seeker} = 1.0$

$\mu_{autop} = 0.5$

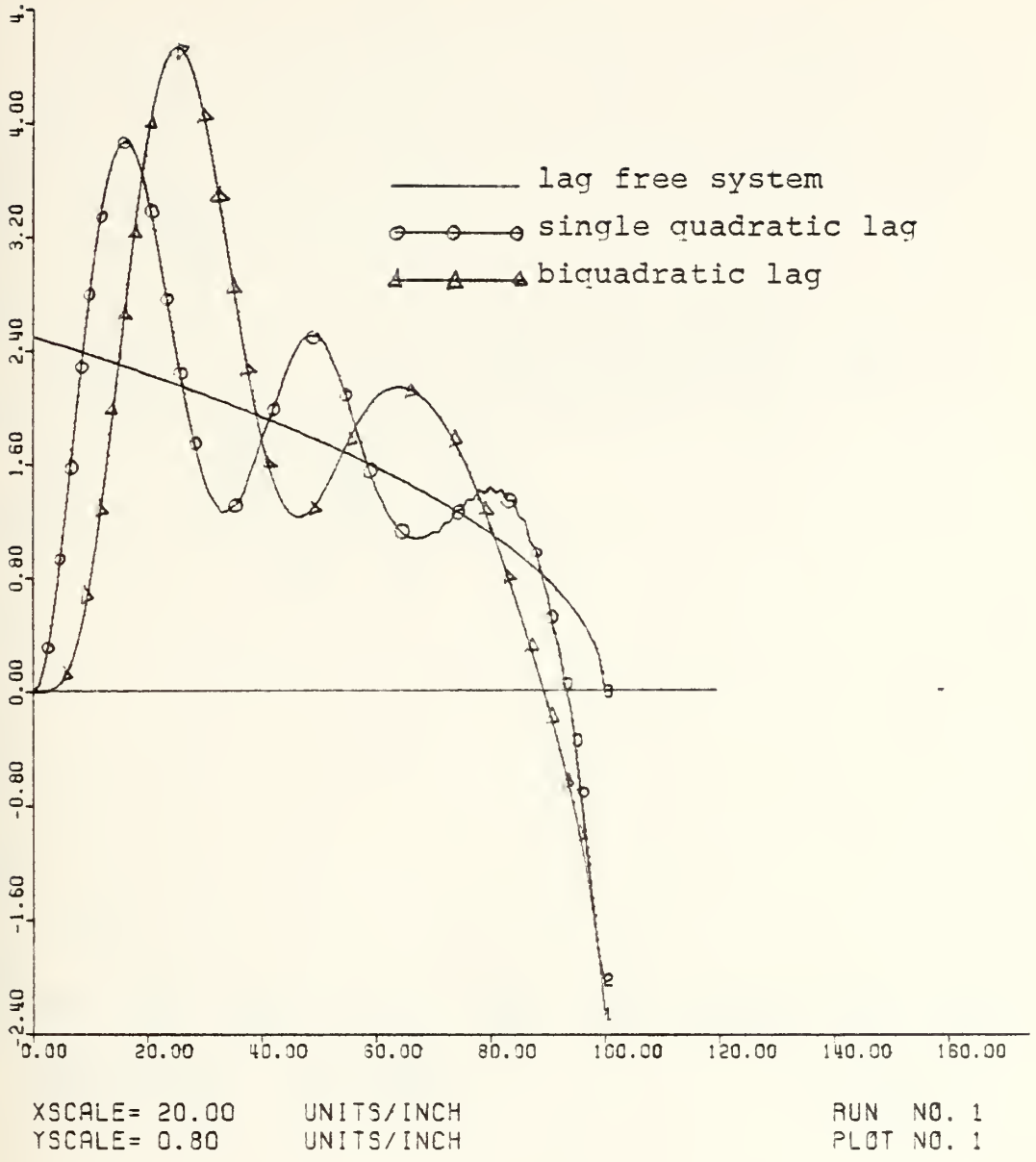

Fig. VII.B-14. Required missile lateral acceleration in case of an initial heading error.
Utilized parameters: Nav. Constant = 2.5

$W_{seeker} = 20.0 = W_{autop}$

$\mu_{seeker} = 0.25$

$\mu_{autop} = 0.50$

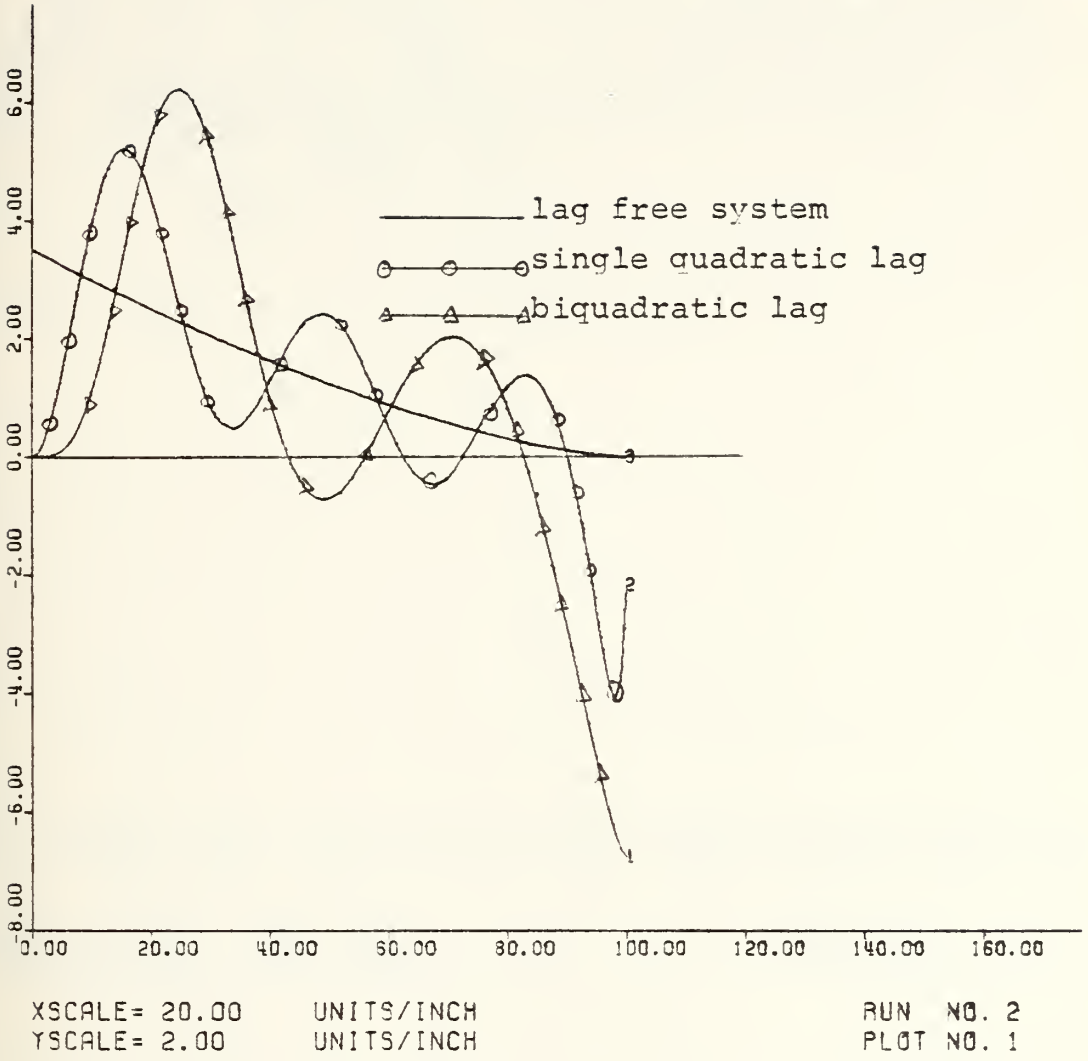

Fig. VII.B-15. Required missile lateral acceleration in case of an initial heading error.
Utilized parameters: Nav. Constant = 3.5

$W_{seeker} = 20.0 = W_{autop}$

$\mu_{seeker} = 0.25$

$\mu_{autop} = 0.25$

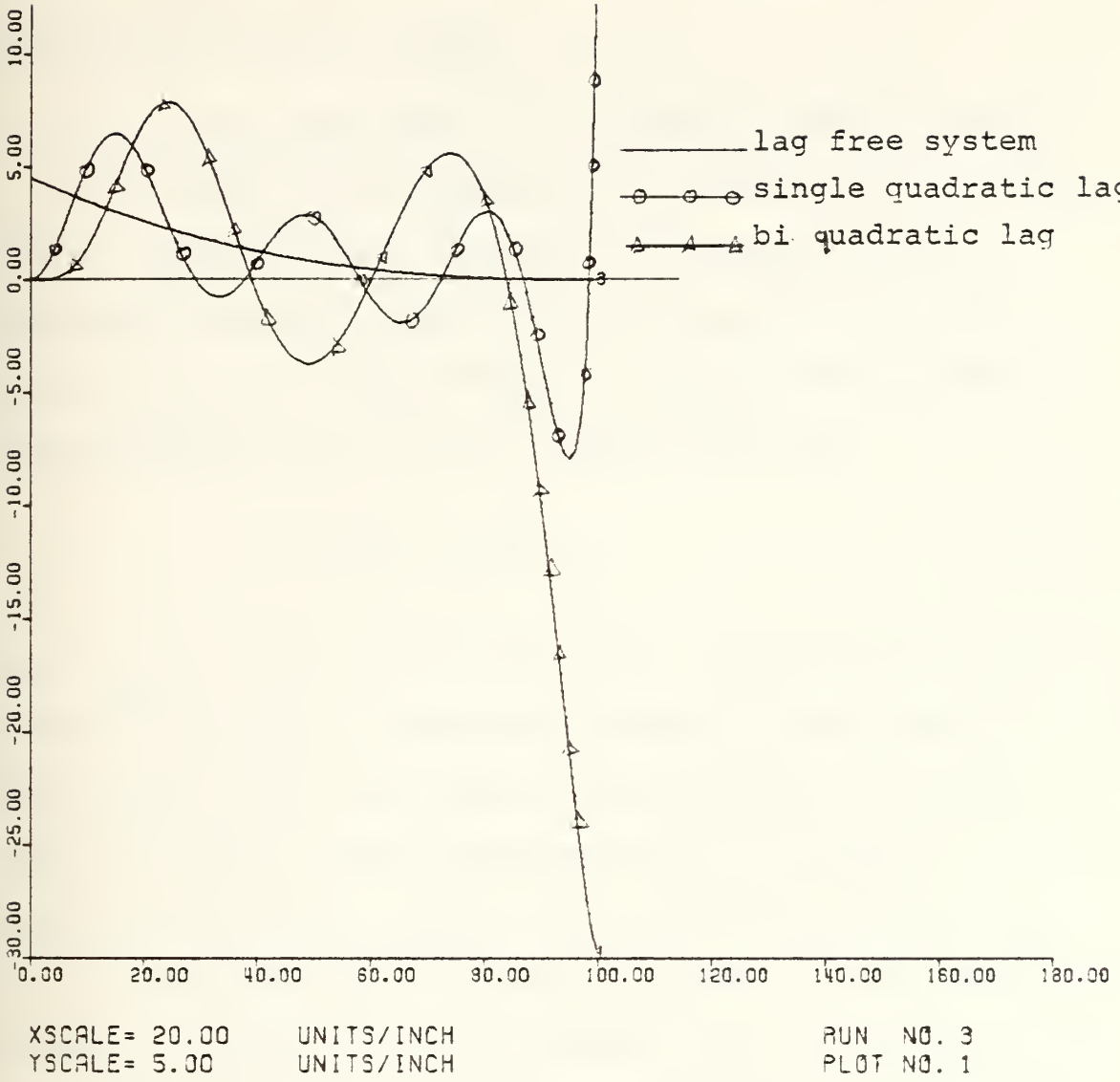

Fig. VII.B-16. Required missile lateral acceleration in case of an initial heading error.
Utilized parameters: Nav. Constant = 4.5

$W_{seeker} = 20.0 = W_{autop}$

$\mu_{seeker} = 0.25$

$\mu_{autop} = 0.50$

It pointed out how to proceed for the development of a more sophisticated control system.

C. AN ADVANCED DEVELOPMENT OF A GUIDANCE CONTROL SYSTEM

In this part it is attempted to integrate into a control system sensors, filter, kinematics and noise. Thus, a linearized kinematic homing loop is assumed as is shown in figure (VII.C-1). Here autopilot dynamics was decided to be represented by a first order transfer function

$$\frac{n_L}{n_c} = \frac{1}{1 + S/\omega_{ap}} \qquad \text{(VII.C-1)}$$

where ω_{ap} is the autopilot bandwidth. Here also are considered the two most important stochastic error sources, namely glint noise and random target maneuver. A relative target to missile range measurement R_{TM} is assumed. The complexity of the filter depends upon the used guidance law. So, in case of PN usage, a simple law pass filter may be sufficient. In case of modern guidance law, a more complex filter is required (as it will be outlined later on) because in a modern guidance system the Zero Effort Mis-distance (ZEM) is modified to take into account target maneuver and missile guidance system dynamics. In the case that the guidance system dynamics are represented by a first order transfer function, with bandwidth ω, the usage of either modern control theory [Ref. 6] or Schwartz Inequality [Ref. 16] results in

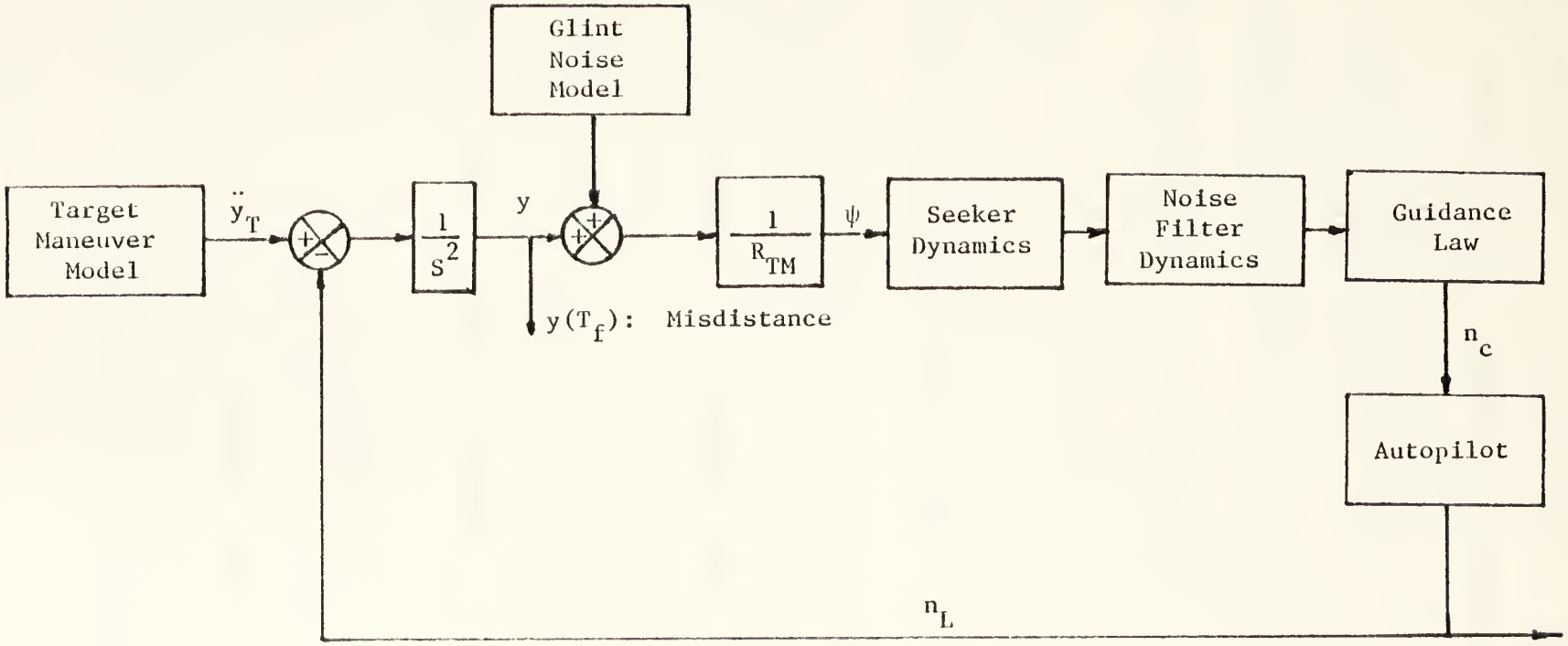

Fig. VII.C-1. Kinematic Homing Loop

a guidance law which drives the misdistance to zero while minimizing the integral of the square of the acceleration:

$$y(t_f) = 0 \quad \text{subject to minimizing} \int_0^{t_f} n_c^2 dt \qquad \text{(VII.C-2)}$$

This modern guidance law can be written as:

$$n_c = \frac{N'}{t_{go}^2}\left[y + \dot{y}t_{go} + \tfrac{1}{2}n_T t_{go}^2 - n_L \frac{(e^{-T} - 1 + T)}{\omega^2}\right] \qquad \text{(VII.C-3)}$$

where: $T = \omega t_{go}$ (VII.C-3a)

$$N' = \frac{6T^2(e^{-T} - 1 + T)}{2T^3 + 3 + 6T - 6T^2 - 12Te^{-T} - 3e^{-2T}} \qquad \text{(VII.C-3b)}$$

The expression within the brackets of equation (VII.C-3) is the ZEM and equation (VII.C-3b) shows that the effective navigation ratio is a form of APN (recall part IV.C.5 equation IV.C-27), with an extra term to account for guidance system dynamics and a time-varying navigation ratio. This guidance law, unlike PN, requires information concerning time-to-go (t_{go}), guidance system bandwidth (ω), and achieved missile acceleration (n_L).

The states required for the implementation of this guidance law ($y, \dot{y}, n_T$) must be estimated via a Kalman filter estimator. In part (VI.C.2.a) such a simple third order Kalman filter estimator was derived (see equation VI.C-12), which will be used here. This Kalman filter is stationary and it

is represented by a transfer function of equation (VI.C-13) which is rewritten:

$$\frac{\hat{y}}{y^*} = \frac{1 + 2S/\omega_o + 2S^2/\omega_o{}^2}{1 + 2S/\omega_o + 2S^2/\omega_o{}^2 + S^3/\omega_o{}^3} \qquad \text{(VI.C-13)}$$

with characteristic frequency ω_o, given by

$$\omega_o = \left(\Phi_S/\Phi_N\right)^{1/6} \qquad \text{(VI.C-13a)}$$

where Φ_S and Φ_N are estimates of the spectral density levels of the target maneuver process noise and glint measurement noise respectively. It is obvious that the characteristic frequency of the filter increases with increasing process noise and decreases with increasing measurement noise.

Here also, a first order seeker with an observer will be used, as this was developed in part VI.B-1.b. Due to this seeker, the line of sight angle is reconstructed from a measurement of the boresight error and by integrating the rate gyro measurement of the seeker dish rate. This angle can be then converted to relative target-missile position, y*, by the multiplication of the range measurement. This signal is then sent through the Kalman filter in order to obtain estimates of the necessary states for the implementation of the modern guidance law. These states are multiplied by control gains, which are functions of the estimated time to go and atuopilot bandwidth, in order to generate an acceleration command. This command is applied to an acceleration autopilot

in order to develop the commanded acceleration. All the above process is presented in a block diagram form in figure (VII.C-2). Next, the mathematical model of this system is derived.

1. Mathematical Model

In the previous work, it was seen that the guidance navigation law for PN, APN and MGC was respectively:

a. For PN: $n_c = \frac{N'}{t_{go}^2}(y + \dot{y}t_{go})$

b. For APN: $n_c = \frac{N'}{t_{go}^2}\left(y + yt_{go} + \tfrac{1}{2}n_T t_{go}^2\right)$

c. For MGC: $n_c = \frac{N'}{t_{go}^2}\left(y + yt_{go} + \tfrac{1}{2}n_T t_{go}^2 - n_L \frac{e^{-T} - 1 + T}{\omega^2}\right)$

This shows that equation (VII.C-3) (which is the guidance law for MGC) includes PN and APN accordingly.

Thus, it is possible to derive the mathematical model of the previously proposed control scheme, which will be possible to be simulated with the above three guidance laws, in order to obtain performance comparison of their implementation. Of course, it is realized that the instrumentation requirements for each of the above cases is different.

Considering that:

The plant equations are

$$\begin{vmatrix} \dot{Y}_T \\ \ddot{Y}_T \\ \dddot{Y}_T \end{vmatrix} = \begin{vmatrix} 0 & 1 & 0 \\ 0 & 0 & 1 \\ 0 & 0 & 0 \end{vmatrix} \begin{vmatrix} Y_T \\ \dot{Y}_T \\ \ddot{Y}_T \end{vmatrix} + \begin{vmatrix} 0 \\ 0 \\ U_s \end{vmatrix} \qquad \text{(VII.C-14)}$$

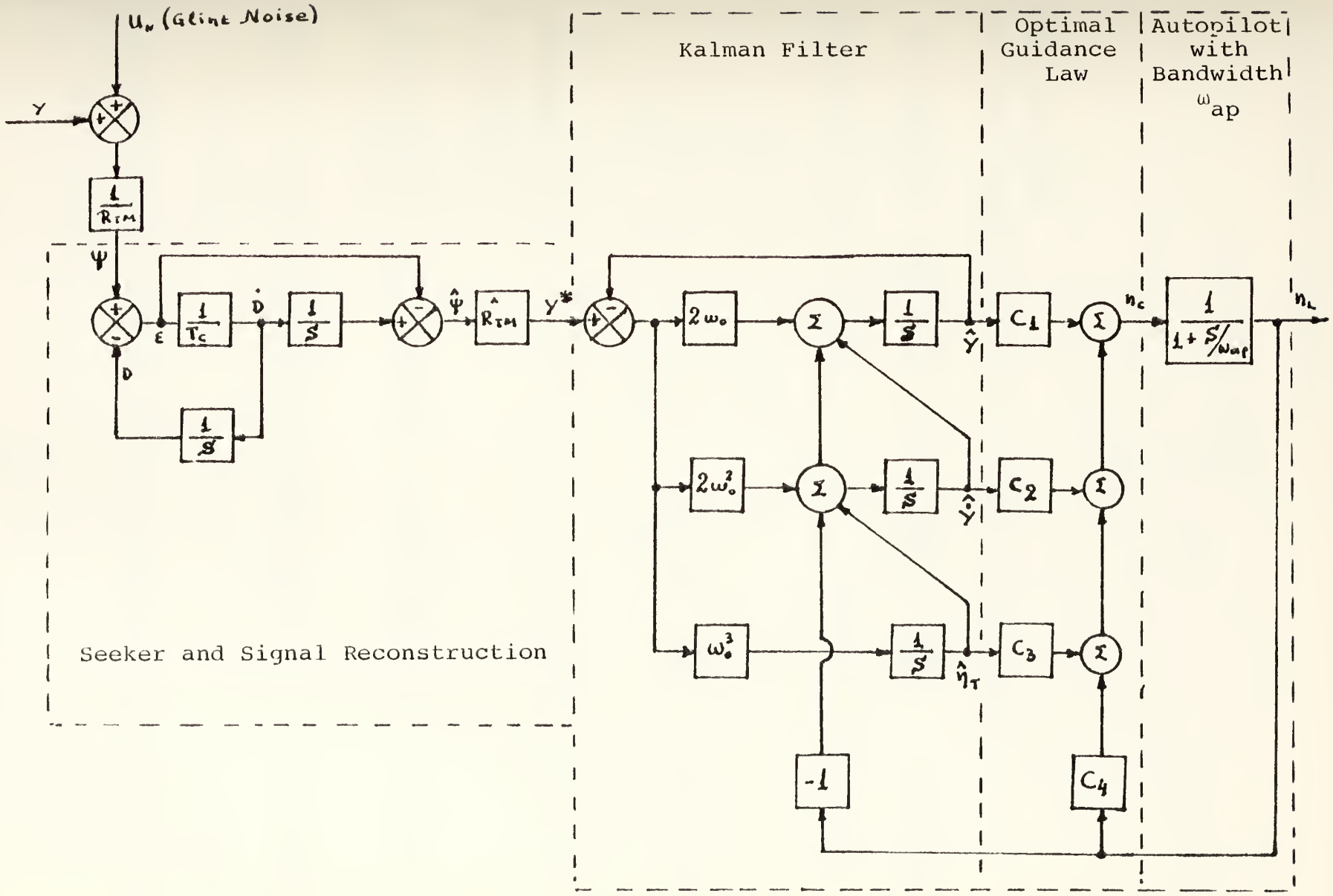

Fig. VII.C-2. Advanced Development of a Terminal Guidance Control System

the measurement equation is:

$$Y_T^* = [1 \quad 0 \quad 0] \begin{bmatrix} Y_T \\ \dot{Y}_T \\ \ddot{Y}_T \end{bmatrix} + U_N \qquad \text{(VII.C-14)}$$

and recalling:

the seeker equation (VI.B-2b), which is rewritten:

$$\dot{X}B = \frac{1}{T_\sigma R_{TM}} X5 - \frac{1}{R_{TM}} X6 - \frac{1}{T_\sigma} X8 + \frac{U_N}{T_\sigma R_{TM}} - \frac{\dot{U}_N}{T_\sigma R_{TM}} \qquad \text{(VI.B-2b)}$$

the Kalman filter equations (VI.C-12), which are rewritten:

$$\begin{vmatrix} \dot{\hat{Y}}_T \\ \ddot{\hat{Y}}_T \\ \dddot{\hat{Y}}_T \end{vmatrix} = \begin{vmatrix} 0 & 1 & 0 \\ 0 & 0 & 1 \\ 0 & 0 & 0 \end{vmatrix} \begin{vmatrix} \hat{Y}_T \\ \dot{\hat{Y}}_T \\ \ddot{\hat{Y}}_T \end{vmatrix} + \begin{vmatrix} 2\omega_o \\ 2\omega_o^2 \\ \omega_o^3 \end{vmatrix} \left| Y^* - \hat{Y}_T \right| \qquad \text{(VI.C-12)}$$

the modern Guidance Control Law of equation (VII.C-3), which is rewritten:

$$n_c = \frac{N'}{t_{go}^2} \left[y + \dot{y} t_{go} + \tfrac{1}{2} n_T t_{go}^2 - n_L \frac{e^{-T} - 1 + T}{\omega^2} \right] \qquad \text{(VI.C-3)}$$

where $$N' = \frac{6T^2 (e^{-T} - 1 + T)}{2T^3 + 3 + 6T - 6T^2 - 12Te^{-T} - 3e^{-2T}} \qquad \text{(VI.C-3b)}$$

$$T = \omega t_{go}$$

the acceleration autopilot transfer function equation (VII.C-1) which is rewritten:

$$\frac{n_L}{n_c} = \frac{1}{1 + S/\omega_{ap}} \qquad \text{(VII.C-1)}$$

and denoting:

$$X1 \equiv \hat{Y}_T \,, \quad X2 \equiv \hat{\dot{Y}}_T \,, \quad X3 \equiv \hat{\ddot{Y}}_T \,, \quad X4 \equiv n_L$$

$$X5 \equiv Y_T \,, \quad X6 \equiv \dot{Y}_T \,, \quad X7 \equiv \ddot{Y}_T \,, \quad X8 \equiv \psi$$

$$C_1 = N'/T_{go}^{\,2} \qquad C_2 = N'/t_{go}$$

$$C_3 = N'n_T/2 \qquad C_4 = N'(1-T-e^{-T})/t_{go}^{\,2}$$

After substitution and minor manipulations the mathematical model of the proposed guidance control scheme is derived in state variable form as is shown in figure VII.C-3. In figure VII.C-4, the block diagram of this advanced guidance system is shown. For simulation purposes, this system was implemented, utilizing DSL, into a computer program as is seen in appendix E. In this program, the characteristic frequency of the Kalman filter "ω_0" was derived utilizing a "random noise generation function named NORMAL" with random "seeds", "means" and standard deviations. From equation (VI.C-13a) which is rewritten:

$$\omega_o = \left(\Phi_S/\Phi_N\right)^{1/6} \qquad \text{(VI.C-13a)}$$

it follows that:

$$\omega_o = \left(\Phi_S/\Phi_N\right)^{1/6} = \left(\sigma_S^{\,2}/\sigma_N^{\,2}\right)^{1/6} = \left(\sigma_S/\sigma_N\right)^{1/3} \qquad \text{(VI.C-13b)}$$

$$
\begin{vmatrix} \dot{X}1 \\ \dot{X}2 \\ \dot{X}3 \\ \dot{X}4 \\ \dot{X}5 \\ \dot{X}6 \\ \dot{X}7 \\ \dot{X}8 \end{vmatrix} =
\begin{vmatrix}
-2\omega_o & 1 & 0 & 0 & 0 & 0 & 0 & 2\omega_o R_{TM} \\
-2\omega_o^2 & 0 & 1 & -1 & 0 & 0 & 0 & 2\omega_o^2 R_{TM} \\
-\omega_o^3 & 0 & 0 & 0 & 0 & 0 & 0 & \omega_o^3 R_{TM} \\
\omega_{ap}C_1 & \omega_{ap}C_2 & \omega_{ap}C_3 & \omega_{ap}(C_4 - 1) & 0 & 0 & 0 & 0 \\
0 & 0 & 0 & 0 & 0 & 1 & 0 & 0 \\
0 & 0 & 0 & -1 & 0 & 0 & 1 & 0 \\
0 & 0 & 0 & 0 & 0 & 0 & 0 & 0 \\
0 & 0 & 0 & 0 & \frac{1}{T_\sigma R_{TM}} & \frac{1}{R_{TM}} & 0 & -\frac{1}{T_\sigma}
\end{vmatrix}
\begin{vmatrix} X1 \\ X2 \\ X3 \\ X4 \\ X5 \\ X6 \\ X7 \\ X8 \end{vmatrix} +
\begin{vmatrix} 0 \\ 0 \\ 0 \\ 0 \\ 0 \\ n_T \\ U_s \\ \frac{U_N}{T_\sigma R_{TM}} \end{vmatrix}
$$

where $R_{TM} = V_{CLOSING}(\hat{T} - \text{time})$

$\hat{T} = AT + B$

Fig. VII.C-3. State Variable Form of Mathematical Model

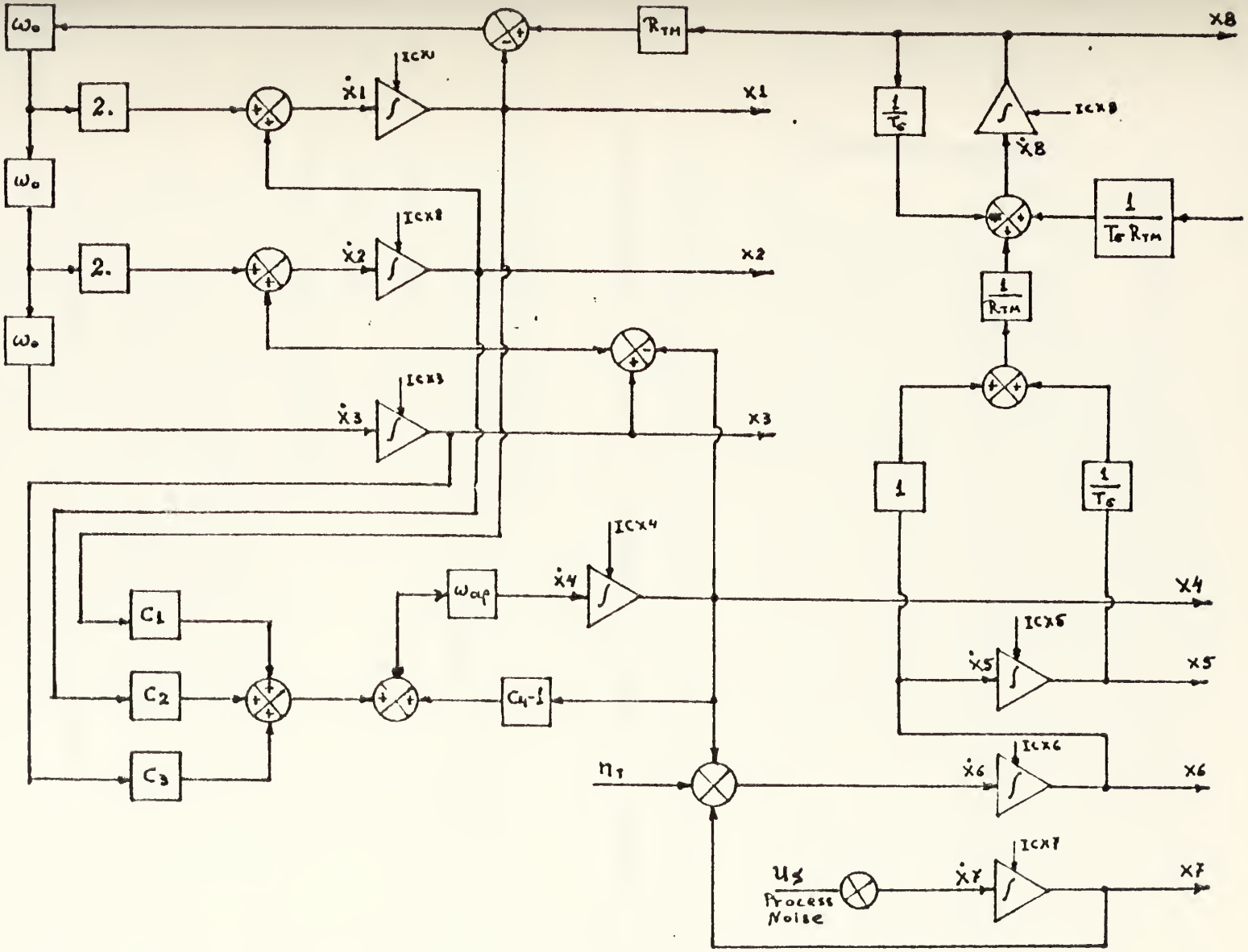

Fig. VII.C-4. Block Diagram of Advanced Terminal Guidance Control System with First Order Acceleration Autopilot

The used standard deviation combinations were derived from table (VI.C-1).

Table VII.C-1. Correlation of ω_o and σ_S, σ_N

ω_o	σ_S	σ_N	σ_S	σ_N	σ_S	σ_N	σ_S	σ_N
.8	.1	.195	.2	.390	.3	.586	.4	.781
1.0		.100	.200	.300		.400		.400
1.2		.058	.116	.174		.231		.231
1.4		.036	.073	.109		.146		.146

ω_o =

σ_S: corresponds to SP3 in computer program of appendix E

σ_N: corresponds to NP3 in computer program of appendix E

2. Performance Comparison

The main parameters that influence the performance of the proposed system are:

U_N: Glint Noise

U_s: Target Random Maneuver

$\hat{t}_{go}$: $At_{go} + B$. The estimated time to go is considered to be a simple linear function of t_{go}.

$\hat{W}_{ap} = CW_{ap}$. The estimated acceleration of autopilot bandwidth may be a simple function of ω_{ap}.

The influence of all the above parameters can be investigated.

Utilizing the computer program which is included in appendix E, and assuming:

(a) $\hat{t}_{go} = At_{go} + B$ where B = zero

and A: several values between 0.4 and 1.8

(b) $\hat{\omega}_{ap} = C_{ap}$ where C = 1

and making use of several combinations of ω_{ap}, ω_o, T_σ, A, T, some data concerning the resulting misdistance due to utilization of PN, APN and MCG laws, were obtained. These data have been tabulated in tables VII.C-2 through VII.C-5. The study of these tables leads to the following comments:

On first sight, the advantage of APN over PN is seen, as utilizing APN the resulting misdistances are almost always less than those where PN law is used.

It is seen that in the case of PN law, the misdistance variation with respect to $\hat{t}_{go}$ keeps a positive slope and varies between 40 ft and 80 ft with slight influence of the ω_{ap} or $\hat{\omega}_{ap}$ values variation. It is noticeable that as the filter characteristic frequency ω_o increases, which means that as the system noise decreases, better performance is obtained.

In case of APN law utilization, figure VII.C-5 shows the plotted domain of misdistance variation with respect to $\hat{t}_{to}$, ($\hat{t}_{go} = At_{to} + B$), for several values of the filter characteristic frequency ω_o (ω_o = 0.8, 1.0, 1.2). From this plotting it is seen that in case of ω_o = 0.8 and ω_o = 1.0,

Table VII.C-2. Resulting Misdistances in Case of a 1st Order Autopilot (of Bandwidth W_{ap}) and a Kalman Filter of Characteristic Frequency W_o = 0.8

Total Time of Engagement: T = 1.

Seeker Time Constant: T_σ = 0.01

$\hat{t}_{go} = At_{go} + B$, where A: several values, B: zero

ω_{ap}	A	PN	APN	MCG	ω_{ap}	PN	APN	MCG	ω_{ap}	PN	APN	MCG	ω_{ap}	PN	APN	MCG
8.	.4	57.[illegible]	[illegible].10	57.91	10.	[illegible].13	57.[illegible]6	57.92	12.	58.69	57.91	57.87	14.	58.05	57.87	57.78
	.6	[illegible].11	[illegible].17	[illegible].[illegible]		59.13	[illegible].[illegible]9	[illegible].[illegible]5		59.25	[illegible].[illegible]	58.[illegible]8		58.[illegible]4	58.[illegible]7	58.15
	.8	51.1	50.20	51.86		60.52	51.28	51.85		60.55	52.31	52.61		59.82	52.32	52.49
	1.0	[illegible].1[illegible]	[illegible].[illegible]9	[illegible].[illegible]3		67.[illegible]	47.65	48.78		65.16	51.03	50.01		65.62	50.54	51.08
	1.2	77.17	56.13	5[illegible].56		75.86	54.84	5[illegible].43		75.13	54.14	54.73		74.47	54.32	54.84
	1.4	78.09	43.51	4[illegible].51		76.58	43.69	44.63		75.9	42.6	43.7		75.15	43.14	44.[illegible]
	1.6	79.12	25.01	27.01		77.84	25.43	27.37		76.97	26.55	28.2		76.45	26.93	28.37
	1.8	82.77	33.6	34.5		81.83	32.91	34.14		81.09	32.94	34.2		80.41	33.06	34.27
16.	.4	57.[illegible]	57.81	57.71	18.	57.90	57.72	57.63	20.	57.8	57.63	57.56	22.	57.57	57.49	57.44
	.6	58.[illegible]	58.[illegible]2	58.02		58.73	58.09	58.03		59.02	57.97	57.92		59.01	57.92	57.89
	.8	59.62	52.5[illegible]	52.66		59.52	52.66	52.72		58.86	53.27	53.26		59.30	52.82	53.[illegible]6
	1.0	65.50	49.6	49.98		65.12	51.37	51.65		64.92	51.62	51.[illegible]3		64.84	51.7	51.86
	1.2	73.51	5[illegible].[illegible]2	5[illegible].8		73.40	54.08	55.16		73.05	54.89	5[illegible].20		73.82	54.97	55.24
	1.4	74.[illegible]3	44.4	45.22		74.28	43.74	44.4		73.93	44.05	44.63		73.59	44.38	44.88
	1.6	75.63	27.88	29.14		75.48	28.04	29.11		75.10	28.57	29.51		74.82	29.32	30.13
	1.8	79.96	41.92	42.8		79.51	41.9	42.73		79.12	41.97	42.74		78.66	36.68	37.46
24.	.4	57.58	[illegible].[illegible]3	57.36	26.	57.54	57.33	57.32	28.	57.52	57.32	57.31	30	57.51	57.3	57.3
	.6	[illegible].96	[illegible].[illegible]	57.86		59.05	58.13	58.11		50.04	58.1	58.08		59.01	57.[illegible]	57.[illegible]
	.8	59.25	52.[illegible]	52.88		[illegible].69	54.02	54.0		59.65	54.03	53.0		59.04	52.9[illegible]	52.98
	1.0	64.56	[illegible].35	[illegible].48		65.86	54.38	51.5		64.53	52.0	52.08		64.37	50.92	50.98
	1.2	72.[illegible]	[illegible].[illegible]	55.31		71.66	55.4	55.57		72.53	54.72	54.78		72.1	55.4	5[illegible].58
	1.4	73.3	44.[illegible]	45.07		73.53	44.07	44.47		72.88	45.26	45.60		72.96	44.85	45.17
	1.6	74.06	30.81	31.72		73.99	36.24	30.[illegible]2		73.76	36.52	37.04		74.06	31.29	31.81
	1.8	78.23	36.72	37.43		78.41	35.85	30.50		78.13	36.1	31.68		77.7	34.36	34.93

Table VII.C-3. Resulting Misdistances in Case of a 1st Order Autopilot (of Bandwidth W_{ap}) and a Kalman Filter of Characteristic Frequency $W_o = 1.$

Total Time of Engagement: $T = 1.$

Seeker Time Constant: $T_\sigma = 0.01$

$\hat{t}_{go} = At_{go} + B$, where A: several values, B: zero

ω_{ap}	A	PN	APN	MCG		PN	APN	MCG		PN	APN	MCG		PN	APN	MCG
8.	0.4	5 . 3	5 .48	49,95	10.	50.11	49.81	49.76	12.	50.12	49.72	49.69	14.	50.13	49.66	49.62
	0.6	51.23	5 .61	50.59		51.31	50.68	50.36		51.87	49.9	49.65		51.74	49.83	49.62
	0.8	55.67	36.54	38.77		54.82	38.94	40.12		54.36	40.32	40.95		54.07	41.11	41.45
	1.0	62.34	24.7	28.11		61.37	26.78	29.12		60.45	29.13	30.71		59.84	30.69	31.78
	1.2	70.48	23.49	25.99		69.50	23.59	25.72		68.27	25.12	26.82		66.48	28.27	29.67
	1.4	73.09	7.63	10.56		71.69	8.39	11.31		71.74	8.46	11.12		70.10	9.52	11.52
	1.6	75.79	16.24	12.76		73.8	13.35	9.83		73.06	13.12	10.05		72.35	12.1	9.45
	1.8	78.89	2.66	12.8		77.88	13.61	10.87		77.0	13.9	11.2		76.18	13.5	10.98
16.	0.4	49.9	49.64	49.59	18.	50.05	49.54	49.49	20.	49.78	49.4	49.36	22.	49.74	49.35	49.33
	0.6	51.72	49.66	49.50		51.7	49.53	49.4		51.31	49.74	49.64		51.32	49.63	49.56
	0.8	53.85	41.67	49.84		53.67	42.06	42.14		53.54	42.30	42.33		53.50	42.47	42.47
	1.0	59.16	33.37	34.13		58.12	33.52	34.09		58.22	35.77	36.15		58.59	34.77	35.08
	1.2	66.71	27.53	28.66		66.15	28.55	29.45		65.75	29.26	30.00		66.20	27.68	28.32
	1.4	68.88	11.18	12.85		68.36	12.24	13.64		67.93	13.15	14.33		67.51	14.54	15.53
	1.6	71.91	11.46	9.21		71.38	10.32	8.37		71.66	9.88	8.18		70.73	7.62	6.15
	1.8	75.5	12.2	9.94		75.12	12.1	10.17		74.85	11.84	10.03		73.79	9.59	8.
24.	0.4	49.75	49.33	49.32	26.	49.81	49.35	49.34	28.	49.68	49.29	49.29	30.	49.69	49.29	49.29
	0.6	51.34	49.54	49.49		51.35	49.48	49.44		51.21	49.55	49.52		51.29	49.47	49.45
	0.8	53.35	42.59	42.58		53.29	42.67	42.64		53.25	42.68	42.65		53.27	42.71	42.68
	1.0	58.50	33.72	33.97		58.64	33.78	33.97		58.42	33.85	34.0		57.97	35.27	35.34
	1.2	69.18	30.29	30.79		64.65	30.92	31.34		64.84	30.88	31.25		64.81	30.74	31.06
	1.4	67.22	15.16	16.01		68.13	12.68	12.87		17.97	12.98	13.67		66.58	17.2	17.75
	1.6	70.42	6.89	5.6		70.19	6.39	5.24		69.92	5.67	4.64		69.79	5.44	4.51
	1.8	73.50	9.14	7.7		73.38	9.2	7.9		73.14	8.74	7.55		72.85	8.02	6.94

Table VII.C-4. Resulting Misdistances in Case of a 1st Order Autopilot (of Bandwidth W_{ap}) and a Kalman Filter of Characteristic Frequency W_o = 1.2

Total Time of Engagement: T = 1.

Seeker Time Constant: T_σ = 0.01

$\hat{t}_{go} = At_{go} + B$, where A: several values, B: zero

Wap	A	PN	APN	IGG	Wap	PN	APN	IGG	Wap	PN	APN	IGG	Wap	PN	APN	IGG
8.	.4	43.12	42.[illegible]	42.[illegible]	10.	43.06	42.28	42.24	12.	43.0	42.17	42.16	14.	42.92	42.13	42.14
	.6	45.[illegible]7	41.72	41.[illegible]		45.01	42.38	42.0		45.0	42.30	41.88		44.94	42.18	41.[illegible]
	.8	5[illegible].24	24.73	28.27		50.01	26.53	26.46		49.51	28.73	29.75		49.17	29.99	30.54
	1.0	57.65	6.47	7.06		56.47	8.30	10.13		51.69	9.34	11.97		50.11	11.72	13.56
	1.2	[illegible]...	[illegible].32	[illegible].13		62.75	23.65	1[illegible].65		61.64	20.39	16.66		[illegible].44	15.96	13.00
	1.4	[illegible]..[illegible]	44.97	[illegible].74		65.45	42.39	37.09		65.54	40.99	36.61		64.73	38.51	34.90
	1.6	76.[illegible]3	60.5	5[illegible].61		70.48	57.48	52.37		69.88	58.73	54.2		68.91	56.67	52.68
	1.8	76.05	71.35	67.80		73.94	70.0	65.35		73.20	71.64	67.28		71.85	68.56	64.38
16.	.4	4[illegible].4	42.14	42.14	18.	42.91	42.13	42.14	20.	42.89	42.12	42.15	22.	42.9	42.13	42.16
	.6	44.71	42.58	42.29		44.74	42.27	42060		44.78	41.99	41.82		44.48	42.40	42.28
	.8	49.21	31.15	31.45		45.12	31.58	31.74		48.90	32.27	32.33		48.76	32.6	32.61
	1.0	55.20	12.36	13.69		54.32	15.76	15.69		54.56	14.80	16.53		53.71	18.0	17.5
	1.2	5[illegible].2[illegible]	11.47	9.21		56.86	9.89	8.1		58.45	8.26	6.82		58.5	8.68	7.49
	1.4	64.4	41.27	38.18		63.4	37.38	34.79		63.25	37.02	34.84		62.97	35.95	34.09
	1.6	66.55	61.99	58.47		67.98	60.37	57.31		67.38	57.90	55.28		67.0	56.6	54.3
	1.8	71.32	78.21	74.23		70.74	76.86	73.32		70.29	75.8	72.65		69.89	74.71	71.89
24.	.4	42.9	42.15	42.17	26.	42.86	42.11	42.13	28.	42.92	42.19	42.21	30.	43.01	42.27	42.29
	.6	44.83	41.62	41.52		44.82	41.53	41.45		44.82	41.45	41.38		44.69	41.53	41.49
	.8	48.70	32.73	32.74		48.6	34.71	34.65		47.97	34.71	34.65		48.39	33.29	33.23
	1.0	54.19	16.13	17.27		53.92	17.12	17.45		53.81	17.48	17.75		53.29	19.18	19.26
	1.2	58.4	8.44	7.44		58.68	7.0	6.169		57.92	6.47	5.77		57.23	3.76	3.43
	1.4	62.48	33.7	32.2		62.50	34.01	32.64		61.05	26.5	25.41		61.44	29.52	28.85
	1.6	66.66	55.42	53.04		66.37	54.38	52.58		65.04	47.65	46.07		64.19	44.43	43.49
	1.8	69.35	73.7	71.17		69.32	73.19	70.9		69.03	72.17	70.09		67.74	66.56	65.51

Table VII.C-5. Resulting Misdistances in Case of a 1st Order Autopilot (of Bandwidth W_{ap}) and a Kalman Filter of Characteristic Frequency W_o = 1.4

Total Time of Engagement: T = 1.

Seeker Time Constant: T_σ = 0.01

$\hat{t}_{go} = At_{go} + B$, where A: several values, B: zero

W_{ap}	A	PN	APN	MCG	W_{ap}	PN	APN	MCG	W_{ap}	PN	APN	MCG	W_{ap}	PN	APN	MCG
8.	.4	36.84	36.94	35.85	10.	36.79	35.44	35.6	12.	36.89	35.42	35.65	14.	36.75	35.76	35.87
	.6	37.05	36.85	36.73		38.80	34.16	33.78		38.57	35.72	34.79		38.32	36.12	35.5
	.8	45.0	6.17	12.05		44.41	11.25	14.31		43.95	14.8	16.39		43.48	17.81	18.60
	1.0	53.38	40.17	31.12		51.91	32.75	26.55		50.87	26.36	22.66		49.66	18.76	16.66
	1.2	59.68	75.8	86.08		56.97	67.0	59.4		55.76	61.58	55.57		54.76	56.12	51.50
	1.4	64.71	110.6	102.0		62.22	102.6	94.0		61.33	100.0	94.0		60.69	99.55	93.97
	1.6	69.15	140.0	133.0		67.14	138.0	130.0		65.6	131.0	124.0		64.63	131.0	125.0
	1.8	72.44	162.0	155.0		70.98	165.0	157.0		69.0	164.0	157.0		68.5	161.0	154.0
16.	.4	36.79	35.65	35.8	18.	36.83	35.8	35.87	20.	36.86	35.86	35.86	22.	36.85	35.87	35.88
	.6	38.34	35.65	35.17		38.36	35.27	35.27		38.71	33.76	33.48		38.28	34.94	34.73
	.8	43.22	19.39	19.78		43.06	20.25	20.42		43.04	20.30	20.36		43.07	20.07	20.07
	1.0	49.75	12.47	17.28		47.96	8.77	7.34		48.18	9.98	8.87		47.93	8.55	7.72
	1.2	54.22	53.16	49.55		53.73	50.32	47.77		53.38	48.35	46.65		53.27	47.86	45.97
	1.4	58.87	88.67	84.6		59.35	93.0	89.0		57.54	81.6	78.35		57.42	81.36	78.57
	1.6	63.8	129.0	123.0		63.4	127.0	122.0		62.86	125.0	121.0		62.37	123.0	119.0
	1.8	67.8	160.0	154.0		67.3	159.0	154.0		66.7	157.0	152.0		66.08	153.0	149.0
24.	.4	36.91	35.82	35.83	26.	36.91	35.83	35.84	28.	37.0	35.58	35.6	30.	36.83	36.07	36.07
	.6	38.21	34.88	34.69		38.22	34.68	34.53		38.77	32.9	32.78		36.48	33.63	33.53
	.8	42.56	22.57	22.48		42.56	22.4	22.3		42.33	23.4	23.27		42.41	22.92	22.8
	1.0	47.83	7.95	7.3		47.72	7.38	6.88		47.35	5.24	4.88		47.63	7.09	6.79
	1.2	52.95	45.9	44.36		52.66	44.1	42.87		52.46	42.95	41.86		51.4	36.0	35.24
	1.4	57.04	79.0	76.8		56.91	78.8	76.69		56.74	77.8	76.0		56.76	78.0	77.0
	1.6	61.99	120.0	117.0		61.75	120.0	117.0		61.5	118.0	116.0		61.25	117.0	115.0
	1.8	65.69	151.0	147.0		65.37	150.0	146.0		65.0	149.0	145.0		64.85	148.0	145.0

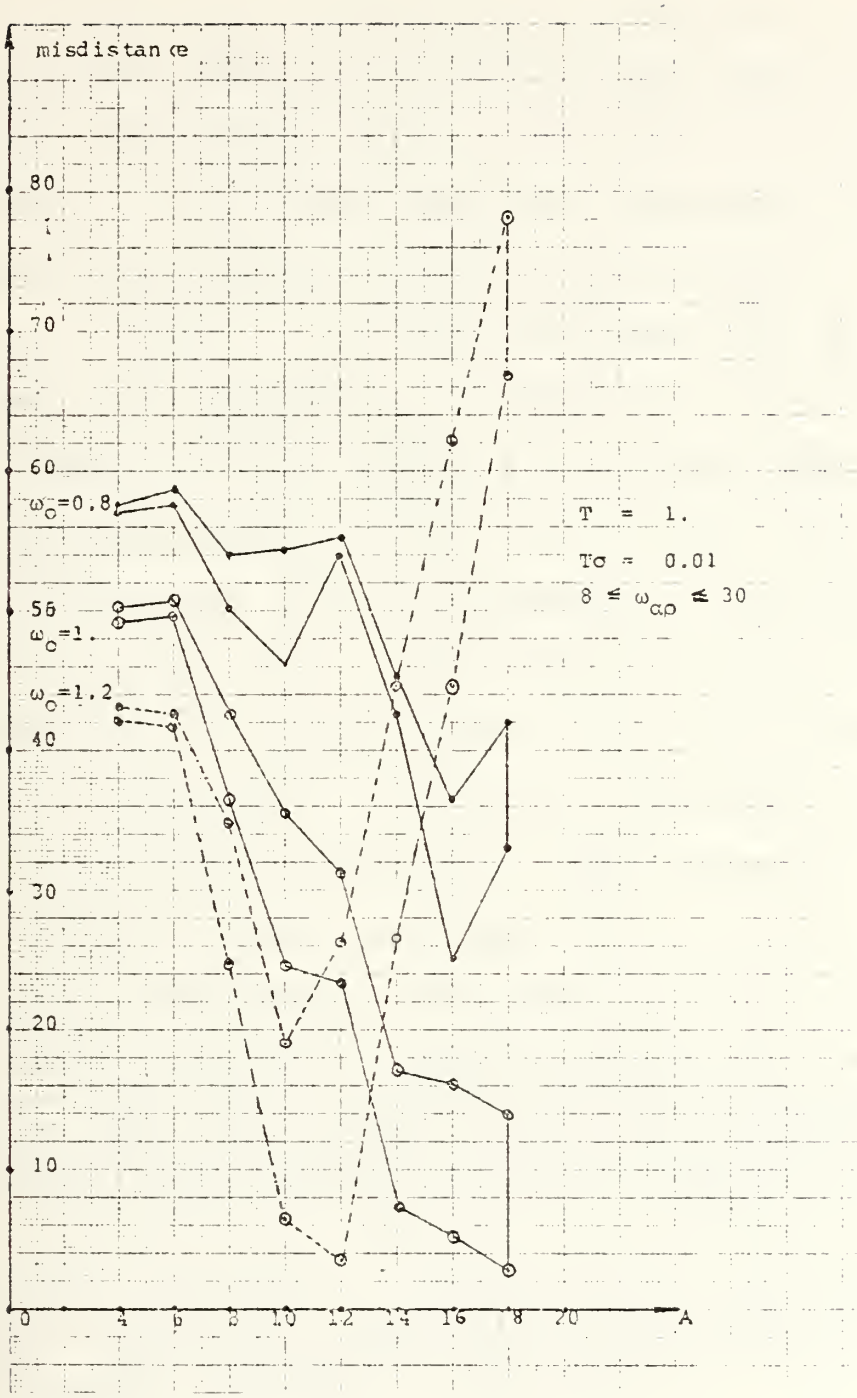

Fig. VII.C-5. APN Law Utilization. Domain of misdistance variations vs. $\hat{t}_{go}$ ($A = \hat{t}_{go}/t_{go}$). Case of 1st order autopilot.

the misdistance variation generally follows a negative slope. In case of $\omega_o = 1.2$, the misdistance variation follows a parabolic shape degradation with the curvature pointing downwards. From figure VII.C-5 also and from tables VII.C-2 to VII.C-5, it can be seen that the misdistance variation is slightly influenced by the ω_{ap} or $\hat{\omega}_{ap}$ variation for the same values of ω_o and A. It is also noticeable that as the filter characteristic frequency ω_o increases, for $\omega_o = 0.8$ to $\omega_o = 1.0$ for all values of A and for $\omega_o = 1.2$ in the range of $0.4 \leq A \leq 1.3$, the misdistance is reduced, which means that as the system noise decreases, better performance is obtained.

In figure VII.C-6, the resulting misdistance vs. ω_{ap} is plotted due to the utilization of PN and APN respectively in case of no time to go inaccuracy (that means for A = 1), T = 1, $T_\sigma = 0.01$ and for various values of ω_o ($\omega_o = 0.8, 1.0, 1.2$). From this figure it is seen that:

- APN gives much better performance than PN.
- For the same value of autopilot characteristic frequency ω_{ap} as the filter characteristic frequency ω_o increases (which means that as the system noise decreases), the resulting misdistance is drastically reduced in case of APN law, while it is sufficiently reduced in case of PN.
- In case of PN law utilization, for constant filter characteristic frequency ω_o, the misdistance variation with respect to autopilot bandwidth ω_{ap} has a very slight negative slope. (For instance, in the range $14 \leq \omega_{ap} \leq 30$, the misdistance variation is about 2 ft.)
- In case of APN law utilization, the resulting misdistance vs. the acceleration autopilot bandwidth ω_{ap}, has an almost always positive slope. As the filter characteristic frequency ω_o increases the slope increases, so that the misdistance variation becomes bigger.

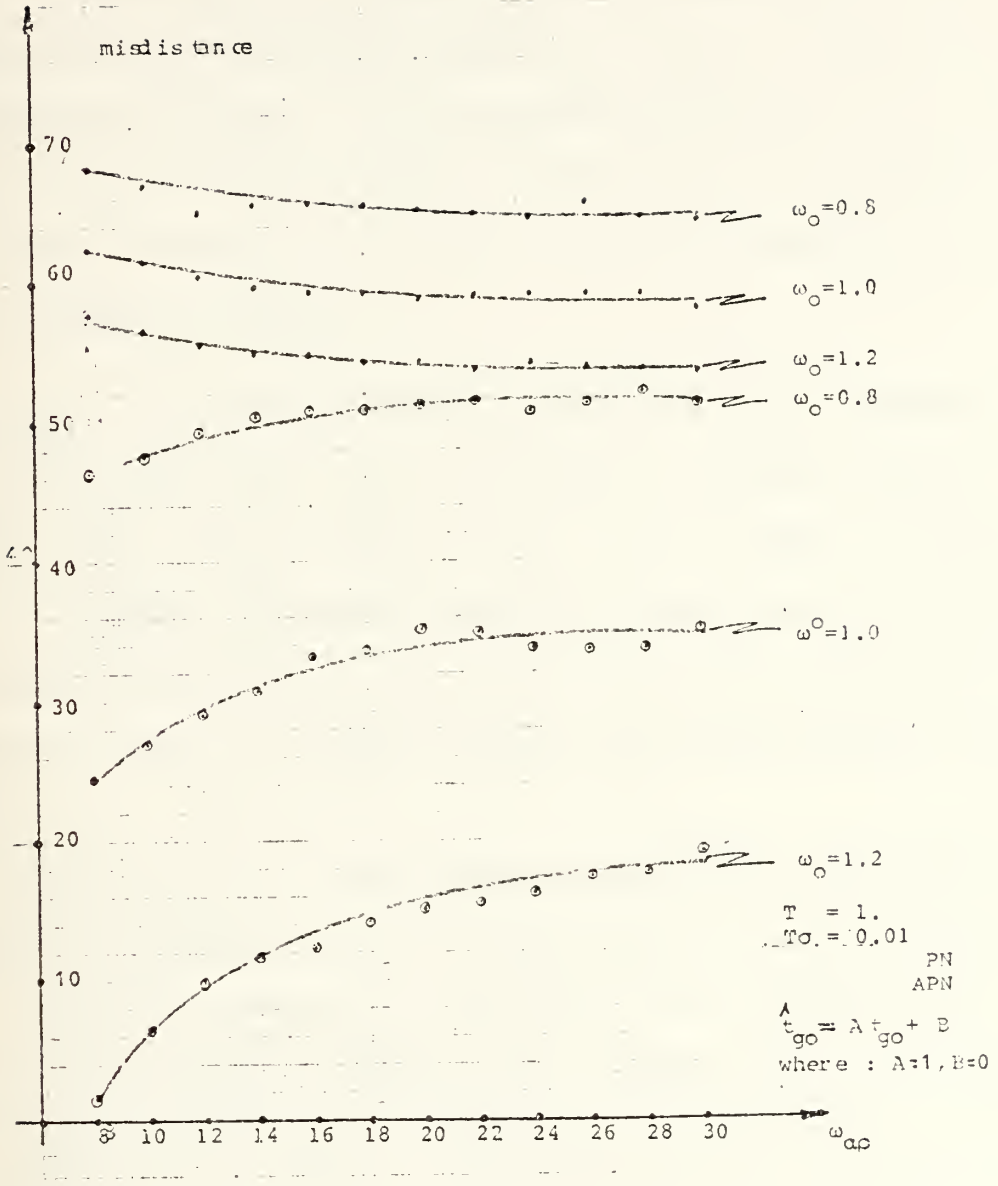

Fig. VII.C-6. Misdistance vs. ω_{ap} (bandwidth of acceleration autopilot). Comparison between PN and APN law for various values of ω_o (ω_o = 0.8, 1.0, 192). Case of 1st order autopilot.

In case of MCG law usage, almost the same arguments as for the case of APN hold.

Comparing the resulting misdistances due to the usage of APN and MCG, it is seen that both laws are competitive. In appendix E, there are given some typical plots of misdistance and achieved lateral acceleration vs. elapsed time for several combinations of the involved parameters as is shown on each of them.

D. FURTHER DEVELOPMENT OF AN ADVANCED GUIDANCE CONTROL SYSTEM

In previous part VII.C, a kinematic homing loop was suggested. The block diagram of this loop is seen in figure VII.C-1. Also, it was mentioned that each block represents an interdiscipline mechanism, which can be as complex as the designer wishes or as much as the cost-effectiveness criteria permit.

In part VII.C.1, a mathematical model of the suggested system was derived, based on components of relative simplicity. Then this model was simulated via a computer DSL program and the obtained results (see tables VII.C-2 to VII.C-5) were studied sufficiently (see part VII.C.2, "Performance Comparison"). In general, the resulting misdistances by utilizing APN law were much less than those where PN law was used (see figure VII.C-6).

On the contrary, APN and MCG laws were competitive as both resulted in similar misdistances.

Although the suggested system was not thoroughly investigated (due to lack of time only ω_{ap}, ω_o and A variation were studied, while keeping constant T, T_σ, B), in this part it is attempted to replace the previous 1st order autopilot with a second order autopilot and then run the system under the same conditions in order to investigate any improvement which may arise in the performance.

1. Mathematical Model

In the previous mathematical model (part VII.C.1, figure VII.C-3), the equation of the first order autopilot was replaced by an equation representing a second order acceleration autopilot, as this was derived in part VII.B-2. Such an autopilot may have an equation like:

$$\frac{n_L}{n_c} = \frac{\omega_{ap}^2}{S^2 + 2\mu_{ap}\omega_{ap}S + \omega_{ap}} \qquad \text{(VII.D-1)}$$

After minor manipulations, the derived mathematical model in state variable matrix form is as is shown in figure VII.D-1.

The derived mathematical model, as is seen in figure VII.D-1, can be easily implemented into a computer program for simulation purposes. Utilizing DSL, the written program is shown in appendix F. Assuming:

(a) $\hat{t}_{go} = At_{go} + B$ where $.4 \leq A \leq 1.8$
$B = 0$

(b) $\hat{\omega}_{ap} = C\omega_{ap}$ where $C = 1.$

$$
\begin{bmatrix} \dot{X}1 \\ \dot{X}2 \\ \dot{X}3 \\ \dot{X}4 \\ \dot{X}5 \\ \dot{X}6 \\ \dot{X}7 \\ \dot{X}8 \\ \dot{X}9 \end{bmatrix} =
\begin{bmatrix}
-2\omega_o & 1 & 0 & 0 & 0 & 0 & 0 & 0 & 2\omega_o R_{TM} \\
-2\omega_o^2 & 0 & 1 & -1 & 0 & 0 & 0 & 0 & 2\omega_o^2 R_{TM} \\
-\omega_o^3 & 0 & 0 & 0 & 0 & 0 & 0 & 0 & \omega_o^2 R_{TM} \\
0 & 0 & 0 & 0 & 1 & 0 & 0 & 0 & 0 \\
\omega_{ap}^2 C_1 & \omega_{ap}^2 C_2 & \omega_{ap}^2 C_3 & \omega_{ap}^2 (C_4 - 1) & -2\mu_{ap}\omega_{ap} & 0 & 0 & 0 & 0 \\
0 & 0 & 0 & 0 & 0 & 0 & 1 & 0 & 0 \\
0 & 0 & 0 & -1 & 0 & 0 & 0 & 1 & 0 \\
0 & 0 & 0 & 0 & 0 & 0 & 0 & 0 & 0 \\
0 & 0 & 0 & 0 & 0 & \frac{1}{T_\sigma R_{TM}} & 0 & 0 & \frac{-1}{T_\sigma}
\end{bmatrix}
\begin{bmatrix} X1 \\ X2 \\ X3 \\ X4 \\ X5 \\ X6 \\ X7 \\ X8 \\ X9 \end{bmatrix} +
\begin{bmatrix} 0 \\ 0 \\ 0 \\ 0 \\ 0 \\ 0 \\ n_T \\ U_S \\ \frac{U_N}{T_\sigma R_{TM}} \end{bmatrix}
$$

Fig. VII.D-1. State Variable Form of Mathematical Model

and making use of several combinations of ω_{ap}, ω_o, T_σ, A, T, some data, concerning the resulting misdistance due to utilization of PN, APN and MCG laws were obtained. These data have been tabulated in tables VII.D-1 through VII.D-3. In appendix F are also given some typical plots of misdistance and achieved lateral acceleration vs. elapsed time for several combinations of the involved parameters as is shown on each of them.

2. Performance Comparison

The study of resulting misdistances (tables VII.D-1 through VII.D-3) leads to the following comments, via several graphs and plots. On first sight at the tables the advantage of APN over PN is seen, as utilizing APN the resulting misdistances are almost always less than those where PN law is used. It is also seen that in case of PN law utilization, the resulting misdistance variation with respect to $\hat{t}_{go}$ ($\hat{t}_{go} = At_{go} + B$), keeps a positive slope and varies between 65 ft to 90 ft, with slight influence of the ω_{ap} or ω_{ap} values variation. It is noticeable also that, as the filter characteristic frequency ω_o increases, which means that as the system noise decreases, better performance is obtained.

Also, on first sight at the tables VII.D-1 through VII.D-3, the advantage of MCG over APN law in general is seen.

Next, the misdistances that occur by utilizing APN law and for several combinations of the involved parameters (as these are shown in tables VII.D-1 through VII.D-3) were

Table VII.D-1. Resulting Misdistances in Case of a 2nd Order Autopilot (of Bandwidth ω_{ap}) and a Kalman Filter of Characteristic Frequency $\omega_o = 0.8$

Total Time of Engagement: $T = 1$

Seeker Time Constant: $T_\sigma = 0.01$

$\hat{t}_{go} = At_{go} + B$, where A: several values, B: zero

					ω_{ap}				ω_{ap}				ω_{ap}			
8.	.4	86.15	72.0	50.27	10.	78.49	70.1	56.5	12.	76.87	67.65	56.16	14.	75.79	66.00	55.34
	.6	87.17	73.11	49.5		80.17	77.28	58.3		85.39	75.86	57.7		84.97	74.64	56.92
	.8	88.1	74.4	51.52		87.03	72.5	51.81		87.32	71.13	51.6		86.82	70.68	51.55
	1.0	91.62	75.65	46.85		90.43	74.10	48.5		90.0	72.92	49.46		89.73	72.04	49.59
	1.2	93. 5	79.39	51.0		92.73	78.12	51.48		92.47	77.18	52.0		92.34	76.53	51.65
	1.4	93.49	75.34	38.38		93.2	74.87	38.72		92.97	73.81	39.29		92.72	72.84	40.22
	1.6	93.86	77.77	28.83		93.62	76.2	28.64		93.38	75.02	29.98		93.2	74.14	30.44
	1.8	94.69	84.68	49.52		94.5	83.48	38.8		94.38	82.59	38.15		94.26	81.65	37.9
16.	.4	76.6	64.82	55.6	18.	74.34	63.64	55.66	20.	73.7	62.95	55.56	22.	73.18	62.23	55.49
	.6	84.15	73.83	56.59		83.75	73.22	56.59		83.32	72.59	56.5		83.05	72.10	56.47
	.8	86.39	69.96	51.47		86.04	68.59	51.33		85.74	68.0	51.2		85.47	67.58	51.17
	1.0	89.35	71.29	50.64		89.24	70.73	49.6		89.03	70.26	49.7		88.74	69.53	50.17
	1.2	92.1	75.93	52.64		91.94	75.46	53.0		91.8	75.07	53.2		91.70	74.77	53.25
	1.4	92.6	72.21	39.72		92.51	71.77	40.34		92.29	71.26	41.42		92.24	71.28	41.98
	1.6	93.06	73.24	30.78		93.94	72.66	31.09		92.87	71.9	29.81		92.8	71.61	30.64
	1.8	94.15	81.25	38.09		94.07	80.77	38.1		93.91	80.37	38.24		93.94	80.0	38.02
24.	.4	73.12	62.09	55.54	26.	72.44	61.23	55.38	28.	72.14	60.84	95.35	30.	71.92	60.55	55.34
	.6	82.75	71.66	56.46		82.56	71.35	56.46		82.31	71.0	56.43		82.2	70.95	56.47
	.8	85.24	67.2	51.1		85.0	66.87	51.02		84.87	66.58	50.95		84.71	66.34	50.89
	1.0	88.72	69.57	49.8		88.57	69.23	49.74		88.37	68.67	50.02		88.29	68.8	50.29
	1.2	91.62	74.69	53.53		91.64	74.53	53.11		91.55	74.38	53.26		91.37	73.9	53.4
	1.4	92.23	71.0	41.42		92.14	70.63	41.42		92.02	70.17	41.58		91.89	70.16	42.71
	1.6	92.71	71.17	30.58		92.63	70.92	31.15		92.59	70.74	31.34		92.45	70.24	32.26
	1.8	93.88	79.73	38.26		93.80	79.48	38.82		93.75	79.25	38.92		93.73	49.06	38.84

Table VII.D-2. Resulting Misdistances in Case of a 2nd Order Autopilot (of Bandwidth ω_{ap}) and a Kalman Filter of Characteristic Frequency $\omega_o = 1.0$

Total Time of Engagement: $T = 1$

Seeker Time Constant: $T_\sigma = 0.01$

$\hat{t}_{go} = At_{go} + B$, where A: several values , B: zero

ω_{ap}	A	PN	APN	MCG	ω_{ap}	PN	APN	MCG	ω_{ap}	PN	APN	MCG	ω_{ap}	PN	APN	MCG
8.	.4	74.57	57.34	36.07	10.	72.4	53.75	41.80	12.	70.8	51.23	41.44	14.	69.22	48.97	40.74
	.6	83.23	64.19	48.66		82.7	62.12	45.13		81.63	60.02	44.66		80.78	58.55	43.9
	.8	87.38	61.59	38.77		86.56	58.9	38.3		85.6	56.9	38.08		85.02	55.33	37.82
	1.0	90.56	63.14	24.36		89.29	60.59	27.45		88.78	58.7	28.99		88.4	57.29	29.45
	1.2	92.1	66.53	16.39		91.57	64.22	20.75		91.32	62.5	19.93		91.0	61.2	21.22
	1.4	92.8	65.84	1.05		92.45	61.34	0.9		92.16	59.56	2.6		91.9	57.99	3.04
	1.6	93.38	65.46	14.31		93.0	62.88	14.5		92.8	60.93	13.17		92.5	59.4	9.77
	1.8	94.0	70.8	2.96		93.8	74.68	5.67		93.7	67.4	10.95		93.5	65.6	9.73
16.	.4	68.33	47.63	41.13	18.	67.51	46.51	41.51	20.	66.84	45.62	41.68	22.	66.23	44.84	41.82
	.6	80.28	57.50	43.32		79.67	56.48	42.71		79.2	55.72	42.44		78.76	55.06	42.23
	.8	84.53	54.2	37.51		84.11	53.26	37.2		83.75	52.49	36.95		83.45	51.85	36.7
	1.0	88.06	56.12	29.78		87.79	55.2	29.92		87.53	54.53	30.53		87.32	53.92	30.69
	1.2	90.8	60.17	23.2		90.48	59.1	24.64		90.31	58.43	25.1		90.16	57.87	25.5
	1.4	91.62	56.87	6.78		91.44	55.97	7.68		91.34	55.22	6.94		91.28	55.0	7.866
	1.6	92.44	56.29	10.58		92.24	56.73	9.39		92.1	55.79	8.56		92.0	55.0	7.87
	1.8	93.35	64.9	8.6		93.25	64.07	8.15		93.18	63.26	8.63		93.9	62.64	7.97
24.	.4	65.8	44.3	41.91	26.	65.43	43.84	41.97	28.	65.1	43.45	42.0	30	65.0	43.27	41.98
	.6	78.26	54.55	42.14		77.97	54.0	42.09		77.8	53.63	42.0		77.7	53.45	41.96
	.8	83.13	51.32	36.49		82.95	50.87	36.3		82.75	50.48	36.0		82.56	50.14	35.93
	1.0	86.99	53.07	31.59		86.70	52.86	31.43		86.7	52.44	31.55		86.64	52.18	31.41
	1.2	90.0	57.38	25.6		89.92	56.97	25.82		89.8	56.61	26.0		89.66	56.43	27.22
	1.4	91.15	54.5	9.3		91.1	54.07	8.24		91.02	53.7	8.695		90.94	53.35	9.03
	1.6	91.95	54.25	9.63		91.87	53.75	9.18		91.74	53.4	8.08		91.67	53.1	7.35
	1.8	93.0	62.2	6.71		93.0	61.88	7.9		92.94	61.48	7.49		92.87	61.14	6.38

Table VII.D-3. Resulting Misdistances in Case of a 2nd Order Autopilot (of Bandwidth ω_{ap}) and a Kalman Filter of Characteristic Frequency $\omega_o = 1.2$

Total Time of Engagement: $T = 1.$

Seeker Time Constant: $T_\sigma = 0.01$

$\hat{t}_{go} = At_{go} + B$, where A: several values, B: zero

ω_{ap}	A	PN	APN	MCG	ω_{ap}	PN	APN	MCG	ω_{ap}	PN	APN	MCG	ω_{ap}	PN	APN	MCG
8.	.4	68.28	35.13	22.4	10.	66.02	31.2[illegible]	27.45	12.	64.24	28.6	26.6	14.	63.0	26.78	25.52
	.6	81.16	47.16	34.24		79.63	43.27	31.33		78.5	40.5	29.7		77.39	38.32	28.41
	.8	86.13	40.15	21.96		5.09	42.4	22.78		84.2	39.5	22.98		83.68	37.57	21.66
	1.0	90.18	55.54	1 .98		88.9	48.49	31.12		88.3	45.79	5.85		87.85	43.73	6.23
	1.2	90.96	47.61	31.6		90.42	44.05	26.39		90.6	41.25	24.6		89.62	39.0	21.71
	1.4	91.60	44.96	58.4		91.14	40.95	55.41		90.8	38.38	51.14		90.46	36.13	48.42
	1.6	92.63	45,98	69.6		92.27	42.02	65.04		91.96	39.06	66.74		91.72	36.8	65.64
	1.8	93.09	44.63	82.8		92.82	40.74	80.17		92.57	37.71	86.34		92.36	35.45	85.77
16.	.4	62.64	25.47	26.13	18.	61.13	24.3[illegible]	24.57	20.	60.44	23.6	26.88	22.	59.88	23.0	27.21
	.6	76.75	36.[illegible]3	28.63		75.77	35.42	27.37		75.26	34.43	26.86		75.13	33.8	26.46
	.8	83.05	35.95	21.28		82.59	34.79	21.71		82.3	33.73	21.0		81.98	32.9	20.57
	1.0	87.47	42.11	8.26		87.02	40.87	10.7		86.82	39.64	10.78		86.4	38.77	11.96
	1.2	89.31	37.33	19.2		89.0	36.0	16.46		88.66	34.8	17.66		88.67	33.83	16.63
	1.4	90.15	34.38	42.5		89.96	32.93	41.38		81.77	31.74	39.92		89.6	30.76	38.35
	1.6	91.5	35.o	62.05		91.35	33.58	61.67		91.2	32.39	60.29		91.07	31.4	59.17
	1.8	92.2	33.78	83.4		92.096	32.6	84.49		91.98	31.09	83.15		91.87	30.12	81.54
24.	.4	59.19	22.57	27.73	26.	58.56	22.08	28.1o	28.	58.23	21.8	28.24	30.	58.01	21.63	28.31
	.6	74.34	32.8	25.23		74.02	32.14	26.0		73.7	31.64	25.83		73.59	31.31	25.66
	.8	81.95	31.88	20.67		81.18	31.83	20.4		80.97	31.33	20.06		80.77	30.90	19.79
	1.0	86.17	38.0	12.12		85.99	37.34	12.09		85.81	36.85	12.07		85.65	36.38	12.06
	1.2	88.29	33.10	11.9		8 .13	32.43	11.26		88.22	31.81	15.14		87.87	31.35	10.69
	1.4	89.44	29.91	36.92		89.38	29.17	37.78		89.25	28.57	36.44		89.19	28.03	36.98
	1.6	90.96	30.56	58.02		90.86	29.84	57.04		9[illegible].77	29.21	56.16		90.69	28.66	55.47
	1.8	9 1.72	29.19	77.37		91.68	28.45	79.35		91.63	27.89	79.27		91.57	27.33	78.87

plotted. In figure VII.D-2, these misdistances are given vs. the $\hat{t}_{go}$ error variation ($A = \hat{t}_{go}/t_{go}$). In this figure are given the domains of misdistance variation for each value of the filter characteristic frequency ω_o ($\omega_o = 0.8, 1.0, 1.2$) for all the various values of ω_{ap} ($8 \leq \omega_{ap} \leq 30$). Here it is noticeable that as the filter characteristic frequency ω_o increases, the misdistance variation due to the ω_{ap} variation and for the same value of A ($A = \hat{t}_{go}/t_{go}$), is increased, which means that as the system noise decreases, the system becomes more sensitive to the autopilot bandwidth estimate. It is also noticeable that as the filter characteristic frequency ω_o increases, the misdistance is reduced, which means that as the system noise decreases, better performance is obtained.

The misdistances that occur by utilizing MCG law and for several combinations of the involved parameters (as these are shown in tables VII.D-1 through VII.D-3) were plotted in figures VII.D-3 through VII.D-6. In these figures is plotted the misdistance vs. $\hat{t}_{go}$ error variation ($A = \hat{t}_{go}/t_{go}$) for all the values of $8 \leq \omega_{ap} \leq 30$.

In figure VII.D-3 is plotted the domain of occurring misdistances in case of MCG law utilization and for filter characteristic frequency $\omega_o = 0.8$. It is observed that the misdistance variation follows in general a negative slope of degradation. Similar comments are derived by studying figure VII.D-4 which contains the domain of occurring misdistances

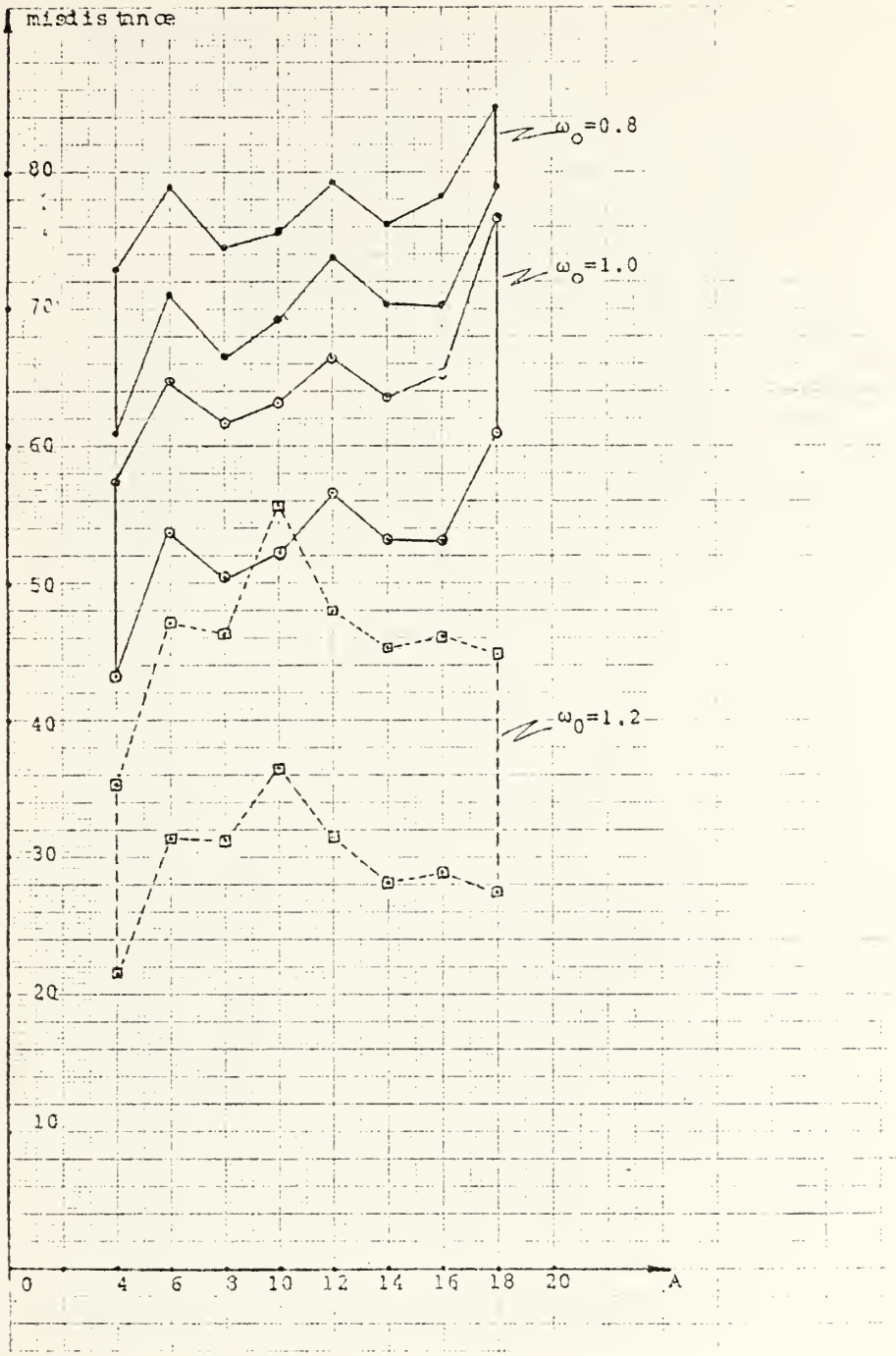

Fig. VII.D-2. APN Law Utilization. Domains of misdistance variation vs. $\hat{t}_{go}$ ($A = \hat{t}_{go}/t_{go}$) for the shown values of filter characterist frequency. Case of a 2nd order autopilot.

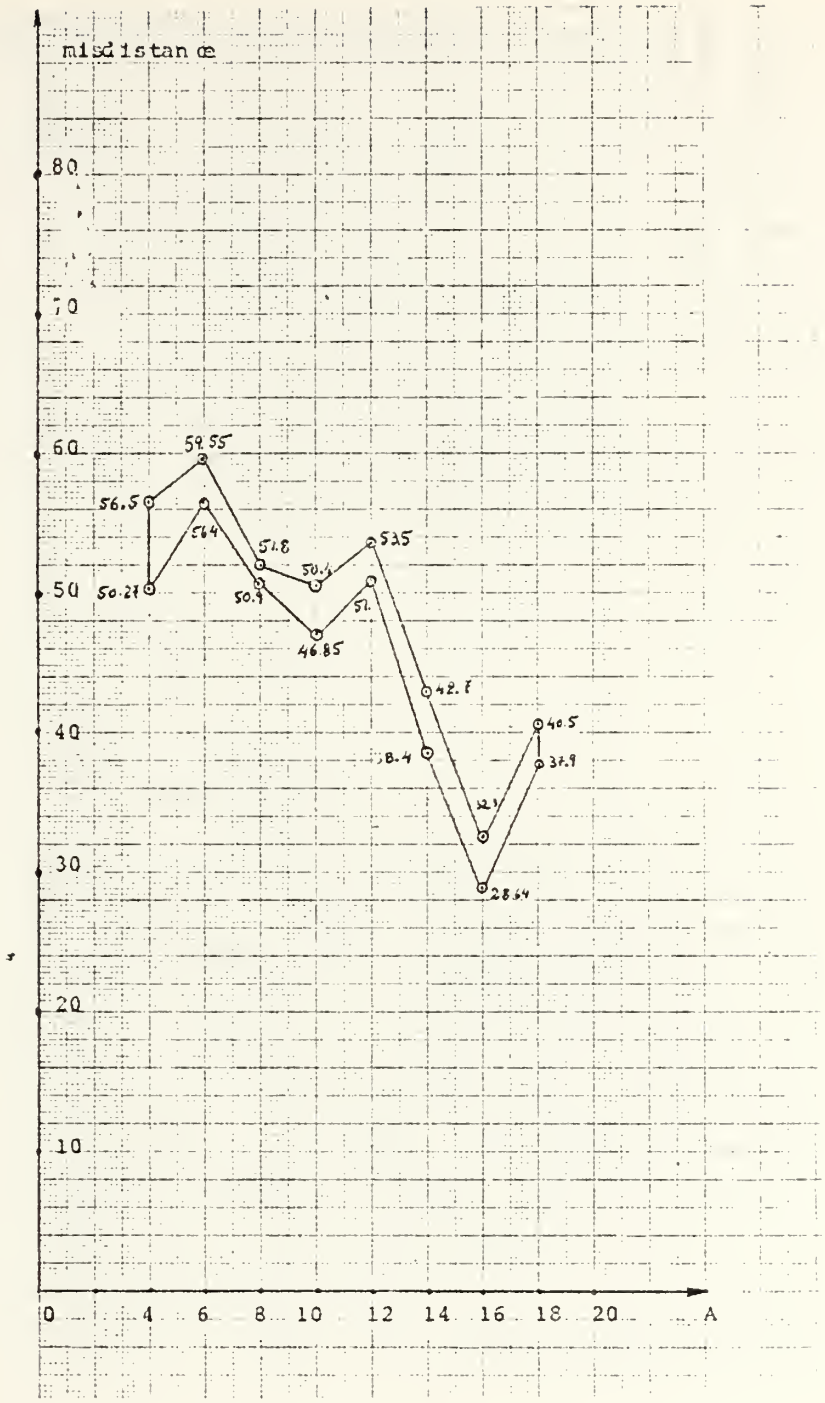

Fig. VII.D-3. MCG Law Utilization. Domain of misdistance variation vs. $\hat{t}_{go}$ ($A = \hat{t}_{go}/t_{go}$) and for filter characteristic frequency $\omega_o = 0.8$. Case of a 2nd order autopilot.

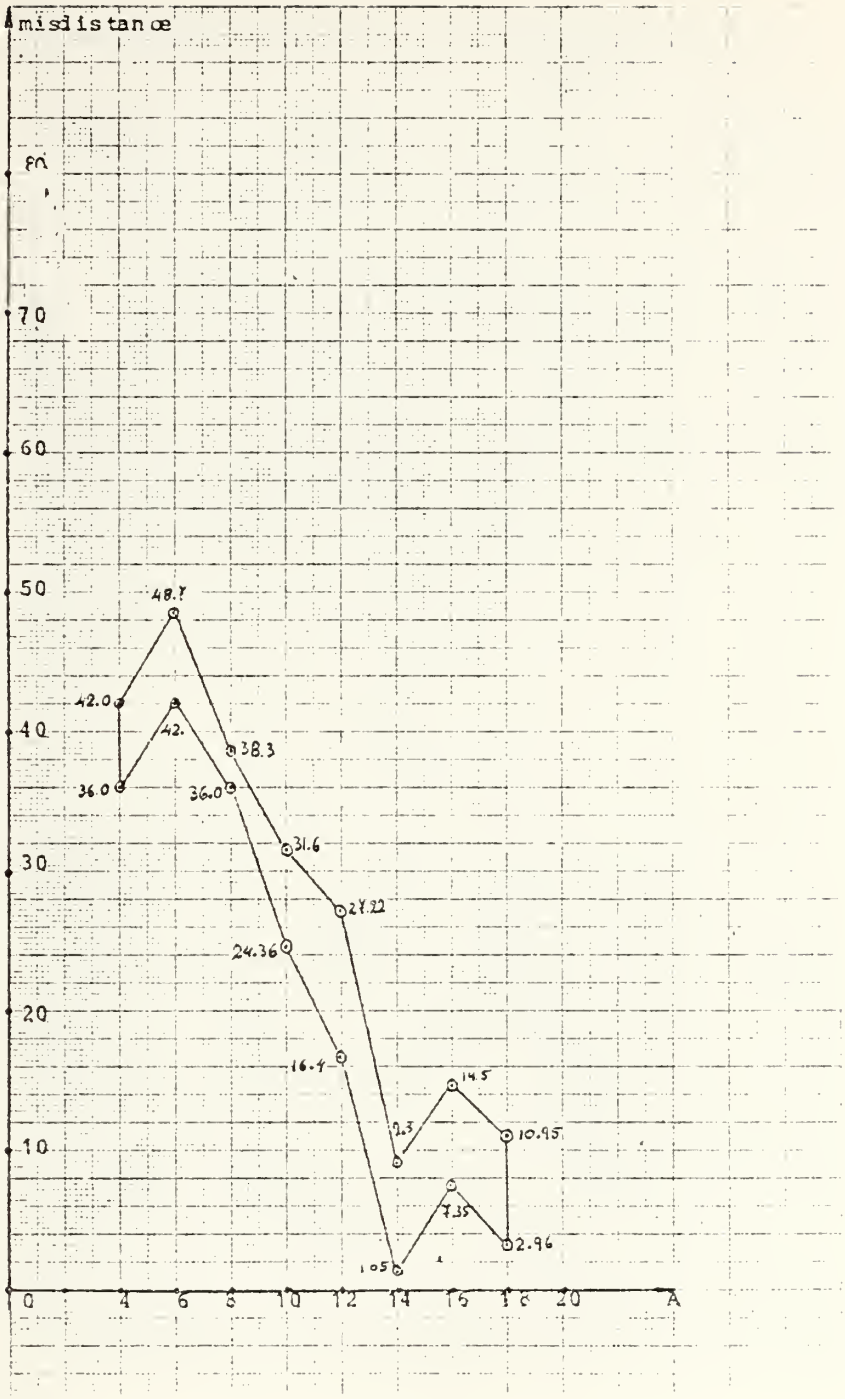

Fig. VII.D-4. MCG Law Utilization. Domain of misdistance variation vs. $\hat{t}_{go}$ ($A = \hat{t}_{go}/t_{go}$) and for filter characteristic frequency $\omega_o = 1.0$. Case of a 2nd order autopilot.

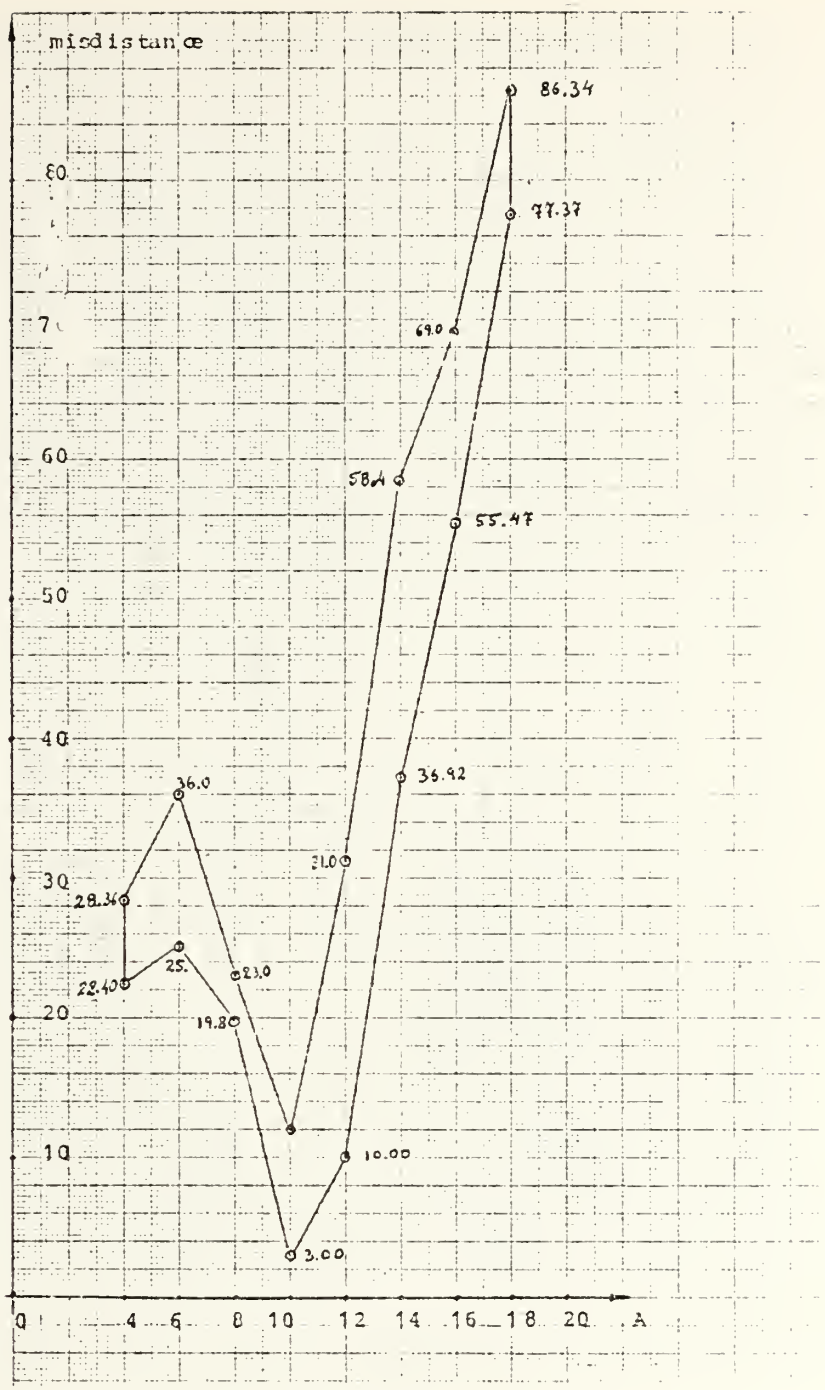

Fig. VII.D-5. MCG Law Utilization. Domain of misdistance variation vs. $\hat{t}_{go}$ and for filter characteristic frequency $\omega_o = 1.2$. Case of a 2nd order autopilot.

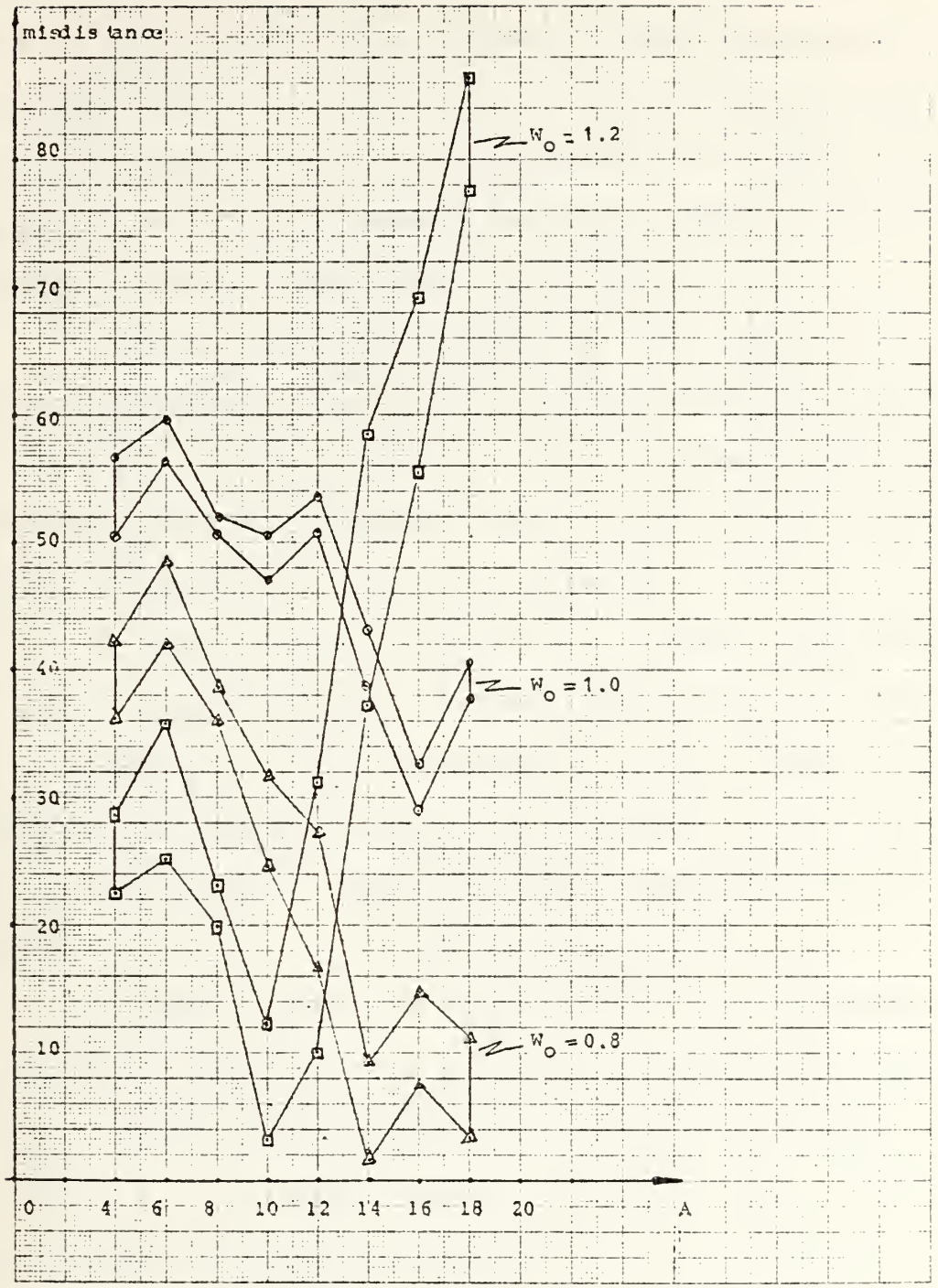

Fig. VII.D-6. MCG Law Utilization. Domains of misdistance variation vs. $\hat{t}_{go}$ ($A = \hat{t}_{go}/t_{go}$) for the shown values of filter characteristic frequency. Case of 2nd order autopilot.

in case of MCG law utilization and $\omega_o = 1$. In figure VII.D-5 is plotted the domain of occurring misdistances in case of MCG law utilization and with value of filter characteristic frequency $\omega_o = 1.2$. In general it is seen that the misdistance variation follows a parabolic shape of degradation, with minimum values occurring around A = 1.

In figure VII.D-6 are given all the above three domains of misdistances that occur in case of MCG law utilization and for $\omega_o = 0.8, 1.0, 1.2$. It is noticeable that the minimum values of misdistances occur at the following combinations of ω_o and A: at $\omega_o = 0.8$ and A = 1.6; at $\omega_o = 1.0$ and A = 1.4; and at $\omega_o = 1.2$ and A = 1. These combinations lead to the conclusion that as the filter characteristic frequency ω_o increases, which means that as the system noise decreases, the system becomes more sensitive to the $\hat{t}_{go}$, which in turn means it takes less to provide more accurate guidance.

In figures (VII.D-7) through (VII.D-9) are plotted, for comparison purposes, the resulting misdistances variation domains in case of APN or MCG law utilization and for $\omega_0 = 0.8, 1.0, 1.2$ respectively. In general the advantage of MCG law over the APN is shown.

In figure VII.D-10 is given a comparison view of resulting misdistances vs. autopilot bandwidth ω_{ap}, in case of utilizing PN, APN or MCG law and with no time to go estimate error ($A = \hat{t}_{go}/t_{go} = 0$). For the case of PN law

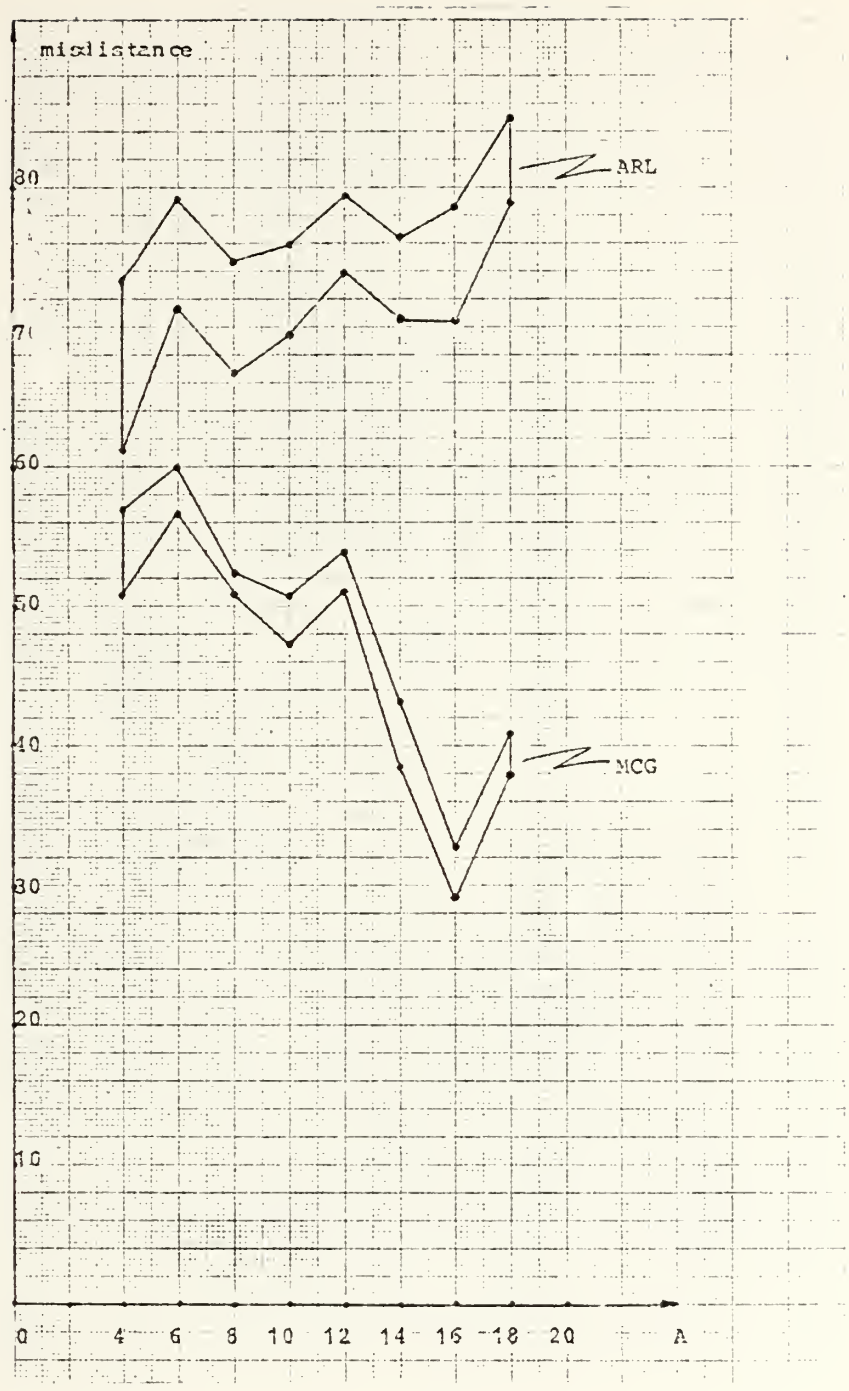

Fig. VII.D-7. Comparison of misdistance variation domain between APN and MCG law, vs. $\hat{t}_{go}$ ($A = \hat{t}_{go}/t_{go}$) and for $\omega_o = 0.8$.

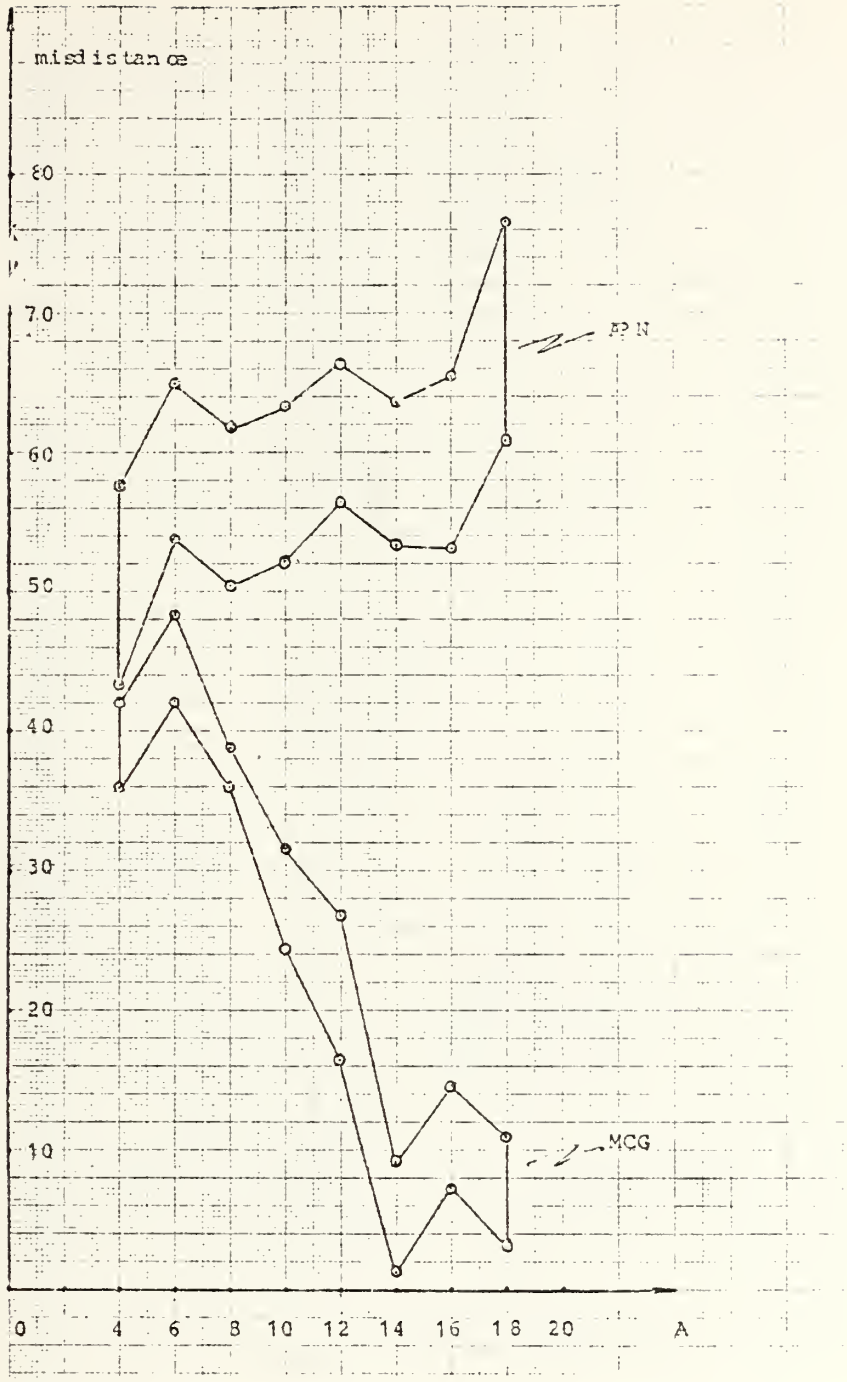

Fig. VII.D-8. Comparison of misdistance variation domain between APN and MCG law, vs. $\hat{t}_{go}$ ($A = \hat{t}_{go}/t_{go}$) and for $\omega_o = 1.0$.

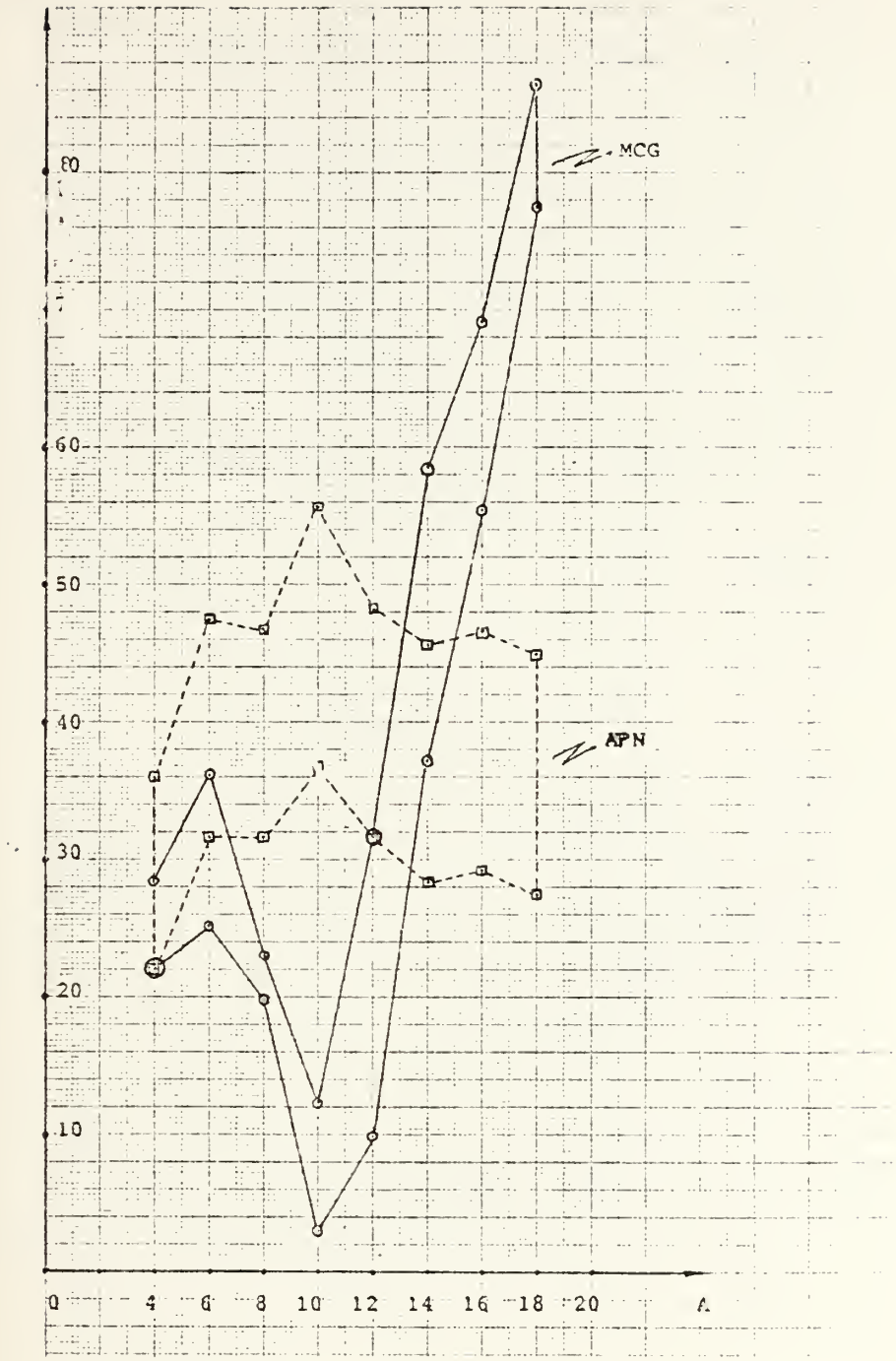

Fig. VII.D-9. Comparison of misdistance variation domain between APN and MCG law, vs. $\hat{t}_{go}$ ($A = \hat{t}_{go}/t_{go}$) and for $\omega_o = 1.2$.

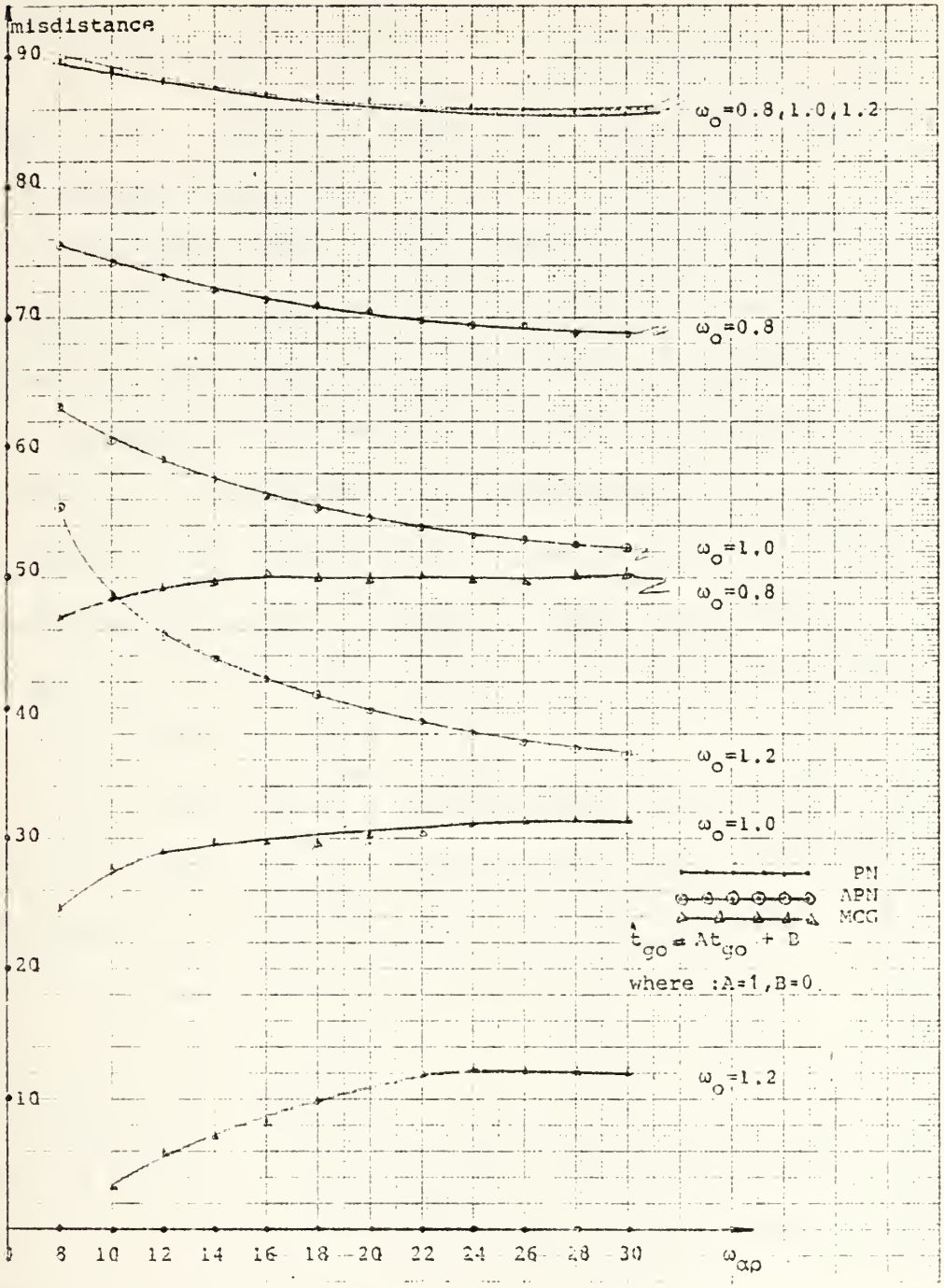

Fig. VII.D-10. Misdistance vs. ω_{ap} (autopilot bandwidth), comparison of PN, APN and MCG law for various values of ω_0 (= 0.8, 1.0, 1.2) and for no time to go estimate error ($A = \hat{t}_{go}/t_{go}$).

utilization, it is seen that there is a slight negative slope. In the range $12 \leq \omega_{ap} \leq 30$ the misdistance variation is about 2 ft. Also it is seen that the misdistance for this case is almost independent of the ω_o variation.

From the figure VII.D-10 and for the case of APN law utilization it is seen that the misdistance vs. ω_{ap} follows a sufficient negative slope; also, it is seen that as the filter characteristic frequency ω_o increases, which means as the system noise decreases, the misdistance vs. ω_{ap} curve moves drastically and parallelly downwards, which means better performance occurs. Finally, from figure VII.D-10 the advantage of MCG law over APN law is easily seen which in turn is advantageous over PN law.

In figure VII.D-11 are plotted the minimum misdistances that occur vs. ω_{ap} utilizing MCG law. These minimum misdistances occur at the following combinations:

(a) $\omega_o = 0.8$ $\quad A = 1.6$

(b) $\omega_o = 1.0$ $\quad A = 1.4$

(c) $\omega_o = 1.2$ $\quad A = 1.2$

From this figure, it is seen that best combination is $\omega_o = 1.0$ and $A = 1.4$. Also it is seen that the resulting misdistances by the utilization of combinations of cases (a) and (b) differ by almost 3 ft. Figure VII.D-11 also gives handle to the thought that the optimum combination must lie somewhere in the ranges $0.8 \leq \omega_o \leq 1.2$ and $1 \leq A \leq 1.6$ (lack of time did not permit this investigation).

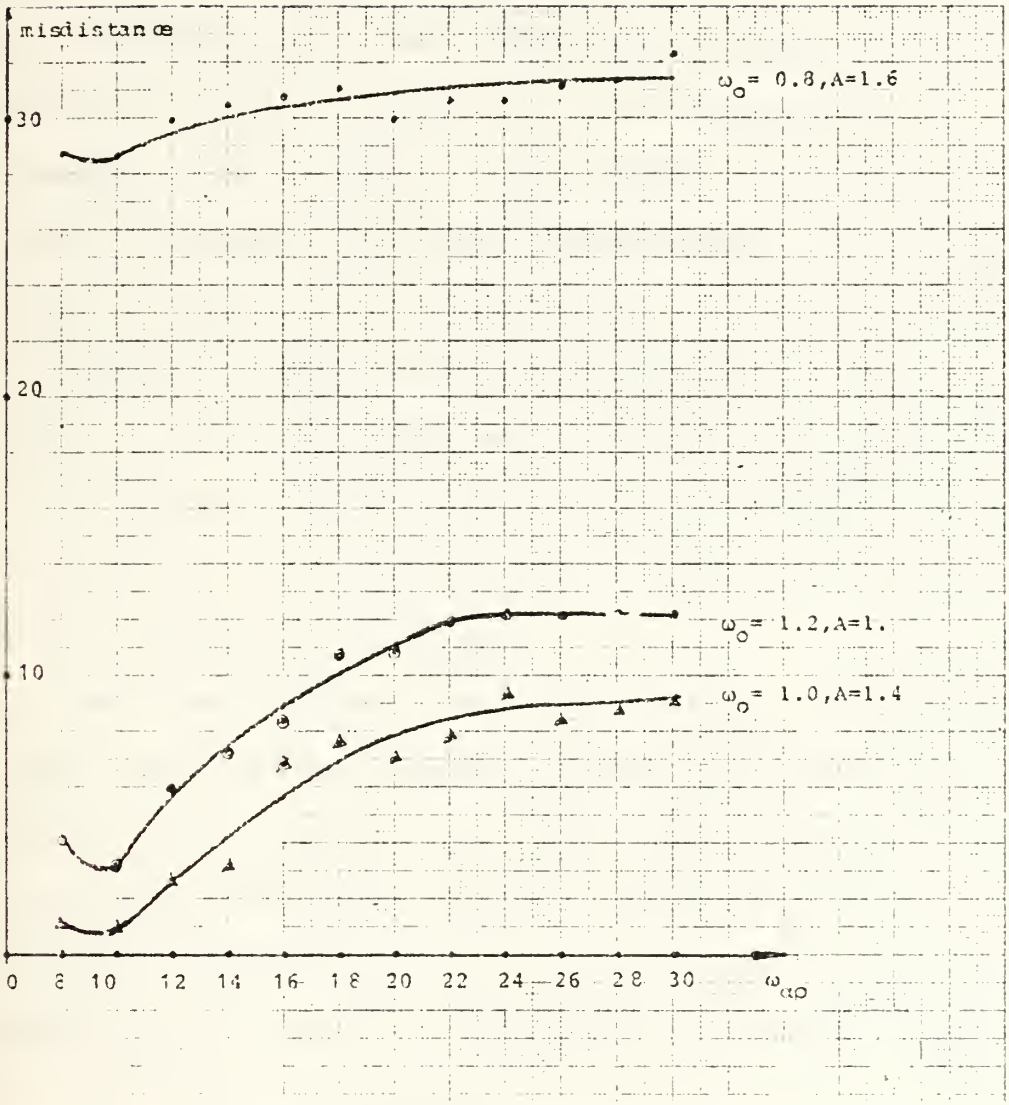

Fig. VII.D-11. MCG Law Utilization. Minimum misdistances vs. ω_{ap} for the shown combinations of ω_o and A.

E. COMMENTS--CONCLUSIONS--SUGGESTIONS

1. Over-all Performance Comparison--Conclusions

In this part, a performance comparison of the two investigated systems (in parts VII.C and VII.D) is attempted, based on the data which are tabulated in tables VII.C-2 through VII.C-5 and in tables VII.D-1 through VII.D-3. From these tables, table (VII.E-1) was formed. In table VII.E-1 are given the resulting minimum misdistances, utilizing MCG law with an autopilot of 1st order or 2nd order respectively and in case of no time to go estimate error ($A = \hat{t}_{go}/t_{go} = 1$). The data of this table have been plotted in figure VII.E-1 and the advantage of the system with a 2nd order autopilot over that with a 1st order autopilot are obvious for all the cases of ω_o and ω_{ap} variations.

Next table VII.E-2 was constructed. In this table are shown the absolute minimum misdistances that occur under the shown combinations of ω_o, ω_{ap}, A and autopilot. These data have been plotted in figure VII.E-2. From this figure it is shown that generally for a second order autopilot with bandwidth ω_{ap} less than 17 rad/sec, better performance occurs.

As a concluding remark it can be stated that the complexity of the used components may improve the overall performance of the suggested terminal guidance control system.

Table VII.E-1. Minimum Obtained Misdistances in Case of No $\hat{t}_{go}$ error (A = 1, B = 0) Utilizing MCG Law

Order of Autopilot	1st	2nd	1st	2nd	1st	2nd
w_o	0.8		1.0		1.2	
w_{ap} \ A	1.	1.	1.	1.	1.	1.
8.	47.93	46.85	28.11	24.36	7.06	18.98
10.	48.78	48.50	29.12	27.45	10.13	3.12
12.	50.01	49.46	30.71	28.99	11.97	5.85
14.	51.08	49.59	31.78	29.45	13.56	6.23
16.	49.98	50.40	34.13	29.78	13.69	8.26
18.	51.65	49.60	34.09	29.92	15.69	10.70
20.	51.83	49.70	36.15	30.53	16.53	10.98
22.	51.86	50.17	35.08	30.69	17.50	11.96
24.	50.48	49.80	33.97	31.59	17.27	12.12
26.	51.50	49.74	33.97	31.43	17.45	12.09
28.	52.08	50.02	34.00	31.55	17.75	12.07
30.	50.98	50.29	35.34	31.41	19.26	12.06

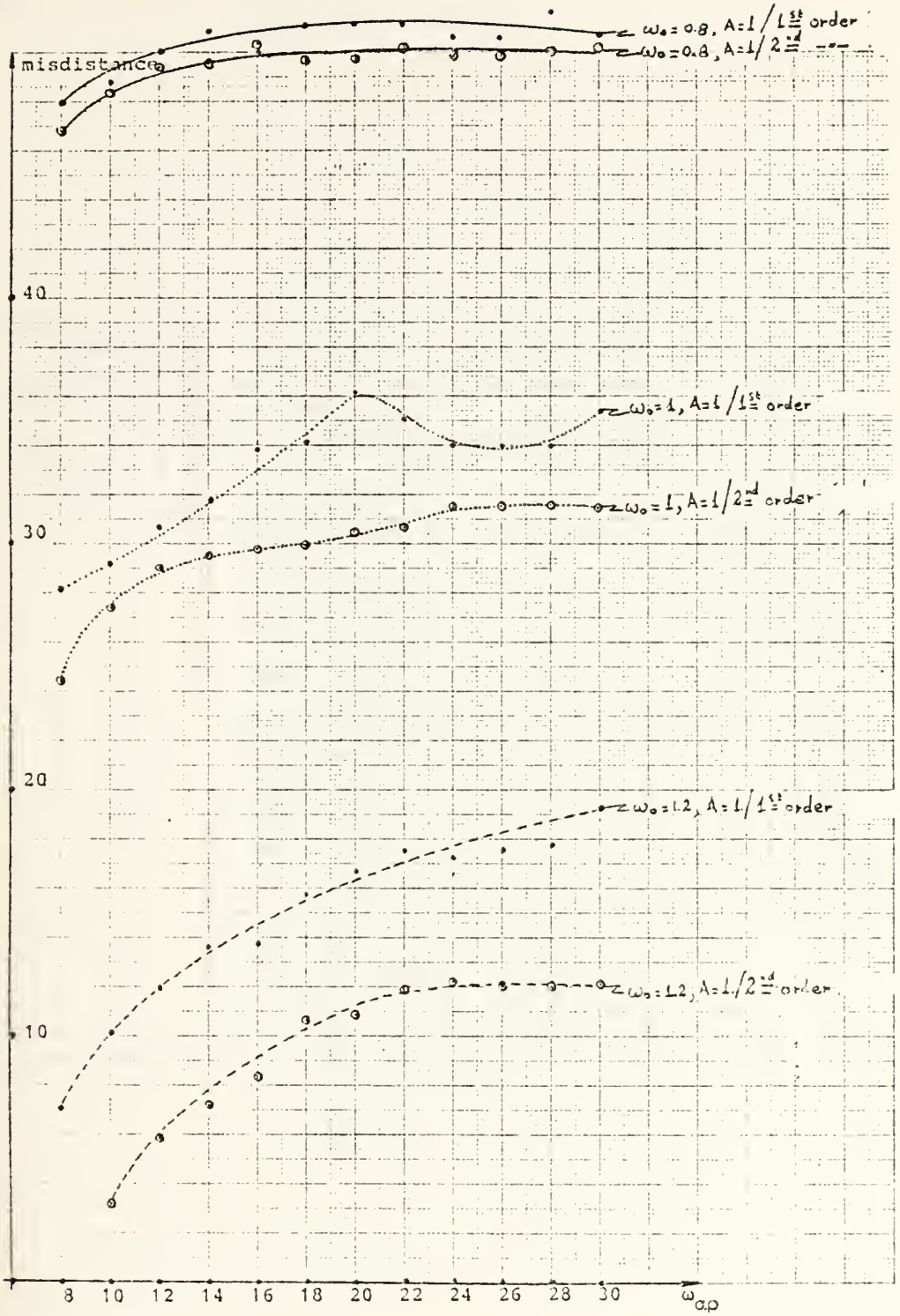

Fig. VII.E-1. MCG law utilization with an autopilot of 1st order respectively. Minimum misdistances vs. ω_{ap} for no time to go estimate error ($\hat{A} = \hat{t}_{go}/t_{go}$).

Table VII.E-2. Absolute Minimum Achieved Misdistances Utilizing MCG Law

Order of autopilot	1st	2nd	1st	2nd	1st	2nd
w_o	0.8		1.0		1.2	
w_{ap} \ A	1.6	1.6	1.6	1.4	1.2	1.0
8.	27.01	28.83	12.76	1.05	7.06*	18.98
10.	27.37	28.64	9.83	.90	10.13*	3.12
12.	28.20	29.98	10.05	2.60	11.97*	5.85
14.	28.37	30.44	9.45	3.04	6.82	6.23
16.	29.14	30.78	9.21	6.78	13.00	8.26
18.	29.11	31.09	8.37	7.68	9.21	10.70
20.	29.51	29.81	8.18	6.94	8.10	10.98
22.	30.13	30.64	6.15	7.80	7.49	11.96
24.	31.32	30.58	5.60	9.30	7.44	11.90*
26.	36.82	31.15	5.24	8.24	6.17	11.26*
28.	37.04*	31.34	4.64	7.49*	5.77	12.07
30.	31.81*	32.26	4.51	6.38*	3.43	10.69*

Note: Asterisk (*) means that the shown value was obtained by utilizing another combination of A.

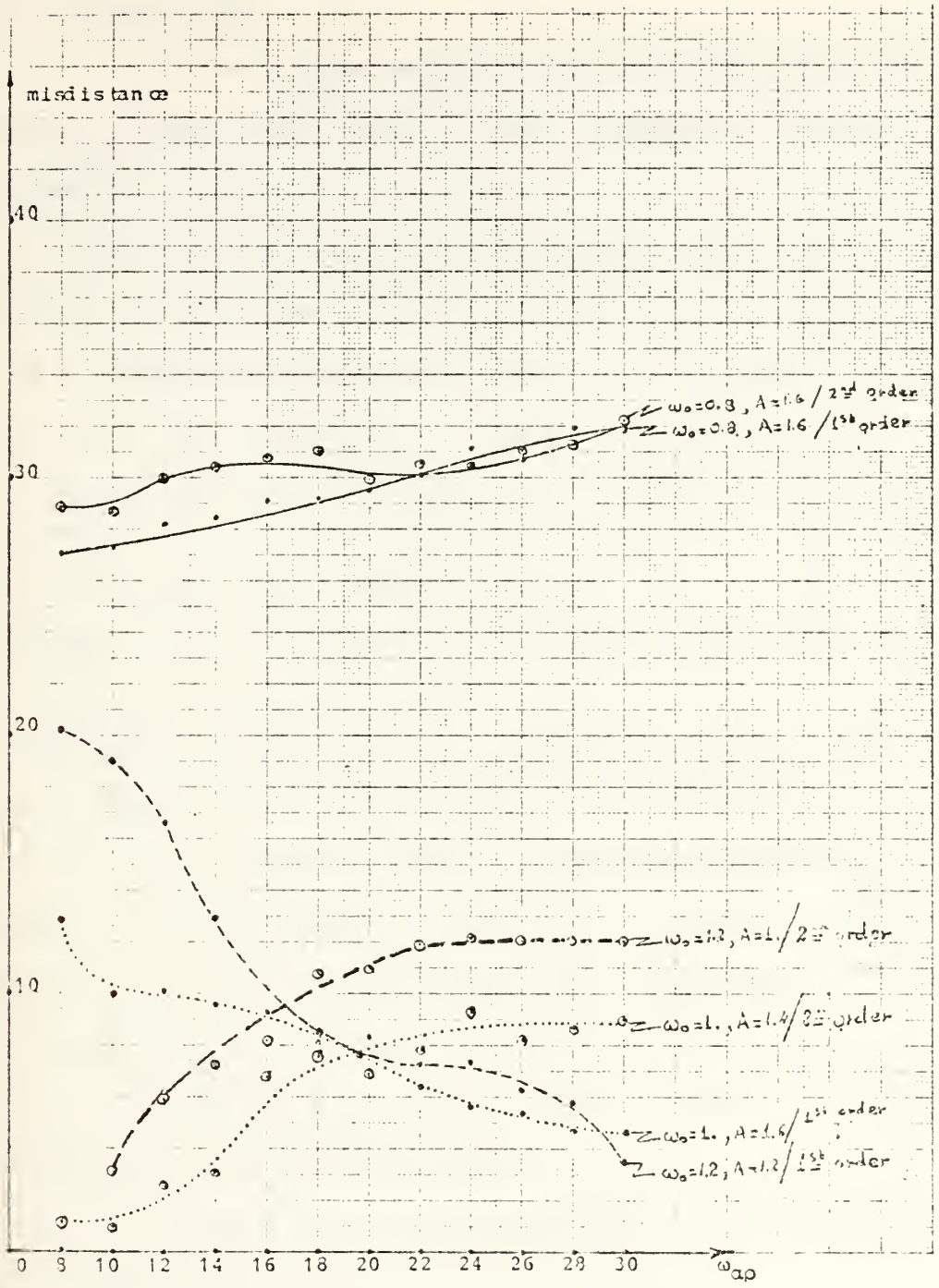

Fig. VII.E-2. MCG law utilization with an autopilot of 1st order respectively. Absolute minimum misdistances vs. ω_{ap} for the shown $\hat{t}_{go}$ errors ($A = \hat{t}_{go}/t_{go}$).

2. Suggestions

In this part some suggestions are given for future investigation and improvement of the suggested Terminal Guidance Control System.

a. Both computer programs, which are given in appendices E and F respectively and which are the implementation of mathematical models of parts VII.C.1 and VII.D.1 respectively, must be simulated varying:

(1) The total time of engagement, T (i.e. T = 2, 3, 4, 5 sec);

(2) The seeker time constant, T_σ;

(3) Time to go estimate by utilizing a bias error B ($\hat{t}_{go} = At_{go} + B$).

These suggested simulations, if (happened to be) done, will give a more thorough view of the overall performance.

b. The whole work was an instructive methodology for developing and improvement of Terminal Guidance Control System. Thus, several components can be replaced by more complex schemes, i.e. better seeker of filter, etc.

c. Limiters, analogous to the expected missile airframe strength, can be introduced.

d. Airframe and radome dynamics can be included if a specific missile is required to be studied.

e. The required acceleration in each case must also be studied in order to get a feeling of the extremes.

APPENDIX A

COMPUTER PROGRAM TO SIMULATE EQUATIONS (IV.C-9) AND (IV.C-10) WHICH GIVE THE REQUIRED MISSILE ACCELERATION AND DISPLACEMENT, UTILIZING THE CLASSICAL P.N. LAW, IN CASE OF INITIAL HEADING ERROR AND NO TIME CONSTANT

```
                    INPUT FOR DSL/360 TRANSLATOR (VERSION 1)


      TITLE * INITIAL HEADING ERROR. NO TIME CONSTANT *
      *     *    NORMALIZED DISPLACEMENT OFF-L.O.S    *
      *     *     NORMALIZED MISSILE ACCELERATION     *
      *
      INTGER NPLOT,K
      *
      CONST NPLOT=1,K=1
      *
      STORAG N(5)
      *
      TABLE N(1-5)=2,3,4,5,6
      *
      PREPAR ZHTAM,NORACC
      *      ZHTAM   NORMALIZED MISSILE'S DISPLACEMENT OFF-L.O.S
      *      NORACC  NORMALIZED MISSILE'S ACCELERATION
      *
      DYNAMIC
            ZHTAM =(1/(1-N(K)))*(1-TIME)*((1-TIME)**(N(K)-1)-1)
            NORACC=N(K)*(1.-TIME)**(N(K)-2)
      *
      SAMPLE
            CALL DRWG(1,K,TIME,ZHTAM)
            CALL DRWG(1,K,TIME,NORACC)
      *
      TERMINAL
            K=K+1
            IF  (K  .GT.  5)   CALL ENDRW(NPLOT)
            IF  (K  .LE.  5)   CALL RERUN
      *
      PRINT 0.1,ZHTAM,NORACC
      *
      CONTRL FINTIM=1.0,DELT=0.001,DELS=0.005
      *
      END

COMMON VARIABLE LIST
TIME     DELT     DELMIN   FINTIM   CLKTIM   DELMAX   NALARM   DELS     NPLOT    K
ZZ0002   ZHTAM    NORACC   ZZ0003   ZZ0004   ZZ0005   ZZ0006   ZZ0007   N

DSL SYSTEM TABLES UTILIZATION - MAX IN ()

  OUT VARS    IN VARS     PARAMS    INTEGS+MEM BLKS    FORTRAN
   9(500)     7(1500)     5(400)        0(300)        89(3390)
      STOP

SUMMARY OF ERRORS FOR THIS JOB    ERROR NUMBER    NUMBER OF ERRORS
                                      217               1
```

APPENDIX B

COMPUTER PROGRAM TO SIMULATE EQUATIONS (IV.C-12) AND (IV.C-13), WHICH GIVE THE REQUIRED MISSILE ACCELERATION AND DISPLACEMENT, UTILIZING THE CLASSICAL P.N. LAW, IN CASE OF A MANEUVERING TARGET, NO TIME CONSTANT AND NO INITIAL AIMING ERROR

```
                    INPUT FOR DSL/360 TRANSLATOR (VERSION 1)


      TITLE * INITIAL HEADING ERROR. NO TIME CONSTANT *
      *     *          BUT MANEUVERING TARGET*
      *     *    NORMALIZED DISPLACEMENT OFF-L.O.S     *
      *     *     NORMALIZED MISSILE ACCELERATION      *
      *
      INTGER NPLOT,K
      *
      CONST NPLOT=1,K=1
      *
      STORAG N(6)
      *
      TABLE N(1-6)=2.001,2.25,2.5,3,4,6
      *
      PREPAR ZHTAM,NORACC
      *      ZHTAM   NORMALIZED MISSILE'S DISPLACEMENT OFF-L.O.S
      *      NORACC  NORMALIZED MISSILE'S ACCELERATION
      *
      DYNAMIC
            ZHTAM=(1.-TIME)**2/(N(K)-2)-(1.-TIME)/(N(K)-1)-(1.-TIME)*N(K)/...
                  (N(K)-1)/(N(K)-2)
            NORACC=N(K)/(N(K)-2)*( 1.-(1.-TIME)**(N(K)-2) )
      *
      SAMPLE
            CALL DRWG(1,K,TIME,ZHTAM)
            CALL DRWG(1,K,TIME,NORACC)
      *
      TERMINAL
            K=K+1
            IF  (K  .GT.  6)   CALL ENDRW(NPLOT)
            IF  (K  .LE.  6)   CALL RERUN
      *
      PRINT 0.1,ZHTAM,NORACC
      *
      CONTRL FINTIM=1.0,DELT=0.001,DELS=0.005
      *
      END

COMMON VARIABLE LIST
TIME     DELT     DELMIN   FINTIM   CLKTIM   DELMAX   NALARM   DELS     NPLOT    K
ZZ0002   ZHTAM    NORACC   ZZ0003   ZZ0004   ZZ0005   ZZ0006   ZZ0007   N

DSL SYSTEM TABLES UTILIZATION - MAX IN ()

  OUT VARS    IN VARS     PARAMS    INTEGS+MEM BLKS   FORTRAN
   9(500)     7(1500)     5(400)        0(300)       96(3390)
      STOP

SUMMARY OF ERRORS FOR THIS JOB   ERROR NUMBER   NUMBER OF ERRORS
                                     217              1
```

* INITIAL HEADING ERROR. NO TIME CONSTANT *

TIME	ZHTAM	NORACC
0.0	-1.0005E 03	0.0
1.0000E-01	-9.9054E 02	2.1086E-01
2.0000E-01	-9.6053E 02	4.4643E-01
3.0000E-01	-9.1050E 02	7.1362E-01
4.0000E-01	-8.4046E 02	1.0219E 00
5.0000E-01	-7.5041E 02	1.3865E 00
6.0000E-01	-6.4035E 02	1.8326E 00
7.0000E-01	-5.1028E 02	2.4077E 00
8.0000E-01	-3.6020E 02	3.2179E 00
9.0000E-01	-1.9011E 02	4.6021E 00
1.0000E 00	-1.5506E-03	2.7958E 01

DSL/360 SIMULATION TIME= 0.25 SECONDS.

0.0	-4.0000E 00	0.0
1.0000E-01	-3.9600E 00	2.3397E-01
2.0000E-01	-3.8400E 00	4.8833E-01
3.0000E-01	-3.6400E 00	7.6778E-01
4.0000E-01	-3.3600E 00	1.0790E 00
5.0000E-01	-3.0000E 00	1.4319E 00
6.0000E-01	-2.5600E 00	1.8426E 00
7.0000E-01	-2.0400E 00	2.3393E 00
8.0000E-01	-1.4400E 00	2.9813E 00
9.0000E-01	-7.6001E-01	3.9389E 00
1.0000E 00	-6.1989E-06	8.7330E 00

DSL/360 SIMULATION TIME= 0.81 SECONDS.

0.0	-2.0000E 00	0.0
1.0000E-01	-1.9800E 00	2.5658E-01
2.0000E-01	-1.9200E 00	5.2786E-01
3.0000E-01	-1.8200E 00	8.1670E-01
4.0000E-01	-1.6800E 00	1.1270E 00
5.0000E-01	-1.5000E 00	1.4645E 00
6.0000E-01	-1.2800E 00	1.8377E 00
7.0000E-01	-1.0200E 00	2.2614E 00
8.0000E-01	-7.2000E-01	2.7639E 00
9.0000E-01	-3.8000E-01	3.4189E 00
1.0000E 00	-3.0994E-06	4.9956E 00

DSL/360 SIMULATION TIME= 0.16 SECONDS.

0.0	-1.0000E 00	0.0
1.0000E-01	-9.9000E-01	3.0000E-01
2.0000E-01	-9.6000E-01	6.0000E-01
3.0000E-01	-9.1000E-01	9.0000E-01
4.0000E-01	-8.4000E-01	1.2000E 00
5.0000E-01	-7.5000E-01	1.5000E 00
6.0000E-01	-6.4000E-01	1.8000E 00
7.0000E-01	-5.1000E-01	2.1000E 00
8.0000E-01	-3.6000E-01	2.4000E 00
9.0000E-01	-1.9000E-01	2.7000E 00
1.0000E 00	-1.5497E-06	3.0000E 00

DSL/360 SIMULATION TIME= 0.81 SECONDS.

TIME	ZHTAM	NORACC
0.0	-5.0000E-01	0.0
1.0000E-01	-4.9500E-01	3.8000E-01
2.0000E-01	-4.8000E-01	7.2000E-01
3.0000E-01	-4.5500E-01	1.0200E 00
4.0000E-01	-4.2000E-01	1.2800E 00
5.0000E-01	-3.7500E-01	1.5000E 00
6.0000E-01	-3.2000E-01	1.6800E 00
7.0000E-01	-2.5500E-01	1.8200E 00
8.0000E-01	-1.8000E-01	1.9200E 00
9.0000E-01	-9.5001E-02	1.9800E 00
1.0000E 00	-7.7486E-07	2.0000E 00

DSL/360 SIMULATION TIME= 0.15 SECONDS.

0.0	-2.5000E-01	0.0
1.0000E-01	-2.4750E-01	5.1585E-01
2.0000E-01	-2.4000E-01	8.8560E-01
3.0000E-01	-2.2750E-01	1.1398E 00
4.0000E-01	-2.1000E-01	1.3056E 00
5.0000E-01	-1.8750E-01	1.4062E 00
6.0000E-01	-1.6000E-01	1.4616E 00
7.0000E-01	-1.2750E-01	1.4878E 00
8.0000E-01	-9.0000E-02	1.4976E 00
9.0000E-01	-4.7500E-02	1.4998E 00
1.0000E 00	-3.8743E-07	1.5000E 00

DSL/360 SIMULATION TIME= 0.86 SECONDS.

NPLOT= 1

APPENDIX C

COMPUTER PROGRAM TO SIMULATE EQUATION (IV.C-17) WHICH GIVES THE REQUIRED MISSILE ACCELERATION, UTILIZING THE CLASSICAL P.N. LAW, IN CASE OF AN INITIAL HEADING ERROR AND A SINGLE TIME CONSTANT

INPUT FOR DSL/360 TRANSLATOR (VERSION 1)

```
        TITLE * INITIAL HEADING ERROR  +  TIME CONSTANT *
        *     *    NORMALIZED DISPLACEMENT OFF-L.O.S    *
        *     *     NORMALIZED MISSILE ACCELERATION     *
        *
        INTGER NPLOT,K
        *
        CONST NPLOT=1,K=1
        *
        INCON IC1=0.0,IC2=0.0
        *
        STORAG N(5)
        *
        TABLE N(1-5)=5,10,15,20,30
        *
        PARAM ETA=3
        *
        PREPAR Q,Q2DOT
        *      Q       NORMALIZED MISSILE'S DISPLACEMENT OFF-L.O.S
        *      Q2DOT   NORMALIZED MISSILE'S ACCELERATION
        *
        DERIVATIVE
              Q2DOT =-N(K)*(1.+QDOT+ETA*Q/(1.-TIME))
            . QDOT  = INTGRL(IC1,Q2DOT)
              Q     = INTGRL(IC2,QDOT)
        *
        SAMPLE
              CALL DRWG(1,K,TIME,Q   )
              CALL DRWG(1,K,TIME,Q2DOT)
        *
        TERMINAL
              K=K+1
              IF  (K  .GT.  5)   CALL ENDRW(NPLOT)
              IF  (K  .LE.  5)   CALL RERUN
        *
        PRINT 0.1,Q,QDOT,Q2DOT
        *
        CONTRL FINTIM=0.999,DELT=0.001,DELS=0.005
        *
        END
```

```
OUTPUT VARIABLE SEQUENCE
Q2DOT    QDOT     Q        ZZ0004   ZZ0005   ZZ0006   ZZ0007   ZZ0008   K

COMMON VARIABLE LIST
TIME     DELT     DELMIN   FINTIM   CLKTIM   DELMAX   NALARM   DELS     QDOT
Q2DOT    ZZ0011   ZZ0009   ZZ0010   NPLOT    K        IC1      IC2      ETA
ZZ0005   ZZ0006   ZZ0007   ZZ0008   N

DSL SYSTEM TABLES UTILIZATION - MAX IN ()

  OUT VARS    IN VARS     PARAMS    INTEGS+MEM BLKS    FORTRAN
   9(500)    10(1500)    8(400)        2(300)        89(3390)
        STOP

SUMMARY OF ERRORS FOR THIS JOB    ERROR NUMBER    NUMBER OF ERRORS
                                      217               1
```

```
        * INITIAL HEADING ERROR  +  TIME CONSTANT *
     TIME            C              QDOT           Q2DOT
 0.0              0.0              0.0          -5.0000E 00
 1.0000E-01 -2.1034E-02 -3.8294E-01 -2.7347E 00
 2.0000E-01 -6.9762E-02 -5.6085E-01 -8.8770E-01
 3.0000E-01 -1.2767E-01 -5.7249E-01  5.9816E-01
 4.0000E-01 -1.7986E-01 -4.5210E-01  1.7570E 00
 5.0000E-01 -2.1475E-01 -2.3159E-01  2.6003E 00
 6.0000E-01 -2.2390E-01  5.6945E-02  3.1116E 00
 7.0000E-01 -2.0227E-01  3.7761E-01  3.2255E 00
 8.0000E-01 -1.4886E-01  6.8283E-01  2.7504E 00
 9.0000E-01 -6.8963E-02  8.8555E-01  9.1665E-01

DSL/360 SIMULATION TIME=    0.23 SECONDS.

***  RKS      INTEGRATION USED ***
 0.0              0.0              0.0          -1.0000E 01
 1.0000E-01 -3.5887E-02 -5.9893E-01 -2.8144E 00
 2.0000E-01 -1.0291E-01 -6.8351E-01  6.9415E-01
 3.0000E-01 -1.6455E-01 -5.2314E-01  2.2837E 00
 4.0000E-01 -2.0422E-01 -2.6129E-01  2.8238E 00
 5.0000E-01 -2.1615E-01  2.1505E-02  2.7536E 00
 6.0000E-01 -2.0085E-01  2.7668E-01  2.2972E 00
 7.0000E-01 -1.6282E-01  4.7178E-01  1.5638E 00
 8.0000E-01 -1.0934E-01  5.8142E-01  5.8710E-01
 9.0000E-01 -5.0251E-02  5.7885E-01 -7.1333E-01

DSL/360 SIMULATION TIME=    0.51 SECONDS.

***  RKS      INTEGRATION USED ***
 0.0              0.0              0.0          -1.5000E 01
 1.0000E-01 -4.6517E-02 -7.1728E-01 -1.9150E 00
 2.0000E-01 -1.1940E-01 -6.7844E-01  1.8928E 00
 3.0000E-01 -1.7564E-01 -4.3217E-01  2.7737E 00
 4.0000E-01 -2.0490E-01 -1.5468E-01  2.6877E 00
 5.0000E-01 -2.0755E-01  9.4468E-02  2.2628E 00
 6.0000E-01 -1.8768E-01  2.9370E-01  1.7087E 00
 7.0000E-01 -1.5077E-01  4.3440E-01  1.0991E 00
 8.0000E-01 -1.0289E-01  5.1257E-01  4.6061E-01
 9.0000E-01 -5.0416E-02  5.2580E-01 -1.9997E-01

DSL/360 SIMULATION TIME=    0.19 SECONDS.

***  RKS      INTEGRATION USED ***
 0.0              0.0              0.0          -2.0000E 01
 1.0000E-01 -5.4233E-02 -7.7908E-01 -8.0286E-01
 2.0000E-01 -1.2805E-01 -6.4492E-01  2.5024E 00
 3.0000E-01 -1.7907E-01 -3.7135E-01  2.7758E 00
 4.0000E-01 -2.0277E-01 -1.0836E-01  2.4442E 00
 5.0000E-01 -2.0213E-01  1.1353E-01  1.9846E 00
 6.0000E-01 -1.8166E-01  2.8766E-01  1.4957E 00
 7.0000E-01 -1.4624E-01  4.1243E-01  9.9926E-01
 8.0000E-01 -1.0083E-01  4.8743E-01  5.0043E-01
 9.0000E-01 -5.0418E-02  5.1248E-01  6.6757E-04

DSL/360 SIMULATION TIME=    0.54 SECONDS.

***  RKS      INTEGRATION USED ***
 0.0              0.0              0.0          -3.0000E 01
 1.0000E-01 -6.4174E-02 -8.2011E-01  1.0207E 00
 2.0000E-01 -1.3573E-01 -5.8483E-01  2.8146E 00
 3.0000E-01 -1.8038E-01 -3.1255E-01  2.5682E 00
 4.0000E-01 -1.9944E-01 -7.5242E-02  2.1731E 00
 5.0000E-01 -1.9677E-01  1.2175E-01  1.7665E 00
 6.0000E-01 -1.7644E-01  2.7803E-01  1.3589E 00
 7.0000E-01 -1.4252E-01  3.9353E-01  9.5126E-01
 8.0000E-01 -9.9093E-02  4.6828E-01  5.4362E-01
 9.0000E-01 -5.0227E-02  5.0225E-01  1.3607E-01

DSL/360 SIMULATION TIME=    0.57 SECONDS.

NPLOT= 1
```

APPENDIX D

COMPUTER PROGRAM SIMULATING A LAG-FREE, A SINGLE QUADRATIC LAG AND A BIQUADRATIC LAG SYSTEM FOR COMPARISON PURPOSES

INPUT FOR DSL/360 TRANSLATOR (VERSION 1)

```
TITLE * CLASSICAL P.N IMPLEMENTATION *
*     * COMPARISON OF    A) LAG FREE CONTROL SYSTEM
*     *                  B) BIQUADRATIC LAG WS=WA
*     *                  C) SINGLE QUADRATIC LAG  WS=00
INTGER NPLOT,L
CONST NPLOT=3,VCLOS=1500.0,WS=30.,WA=20.,MA=0.5,L=1
STORAG N(3)
TABLE N(1-3)=1.0,0.5,0.25
PARAM TENG=1.0,NAVC=2.5,UM=1.
PREPAR TPER,BX5
INTEG MILNE
*
*****************************************************************************
* BX5 MISDISTANCE IN FEET FOR BIQUADRATIC LAG SYSTEM                        *
* WS  SEEKER'S NATURAL FREQUENCY                                            *
* MS  SEEKER'S DAMPING                                                      *
* WA  AUTOPILOT'S NATURAL FREQUENCY                                         *
* MA  AUTOPILOT'S DAMPING                                                   *
* VCLOS CLOSING VELOCITY                                                    *
*****************************************************************************
*
*
DYNAMIC
********
*****************************************************************
* NAVC EFFECTIVE NAVIGATION CONSTANT                            *
*      TWO VALUES ARE USED TO COVER THE EXTREME CASES OF HIGH   *
*      AND LOW SIDES. THESE VALUES ARE 2.5  AND  4.5            *
* TENG TOTAL TIME OF ENGAGEMENT.                                *
*      TWO VALUES ARE USED TO COVER THE CASES OF RELATEVLYSORT   *
*      AND LONG ENGAGEMENTS. THESE VALUES ARE WS*TENG=10, 30     *
*      RESPECTIVELY.                                            *
* TPER PERCENTAGE OF ELLAPSED TIME (NORMALIZED TIME GONE)       *
*****************************************************************
*
      MS=N(L)
*
      TPER=TIME*WS
*
      TIMEGO=(TENG-TIME)
*
      RTM=VCLOS*TIMEGO
*
      K=VCLOS*NAVC
*
      FX3=NAVC*(1.-TIME)**(NAVC-2.)
*
*****************************************************************************
* RTM RELATIVE INSTANTANEOUS DISTANCE BETWEEN MISSILE + TARGET              *
*  X3   MISSILE'S ACTUAL ACCELERATION    *                                  *
*       B    STANTS FOR BIQUADRATIC LAG SYSTEM                             *
*       S    STANTS FOR SINGLE QUADRATIC LAG SYSTEM*                       *
*       F    STANTS FOR LAG FREE SYSTEM                                    *
*****************************************************************************
```

```
*
*
DERIVATIVE
**********
      BX1DOT=BX2
*
      BX1=INTGRL(C.0,BX1DOT)
*
      BX2DOT=-WS**2*BX1-2.*MS*WS*BX2-WS**2/RTM*BX5
*
      BX2=INTGRL(C.0,BX2DOT)
*
      BX3DOT=BX4
*
      BX3=INTGRL(0.0,BX3DOT)
*
      BX4DOT=WA**2*K*BX2-WA**2*BX3-2.*MA*WA*BX4
*
      BX4=INTGRL(0.0,BX4DOT)
*
      BX5DOT=BX6 - UM
*
* X5 ACTUAL MISDISTANCE

      BX5=INTGRL(0.0,BX5DOT)
*
      BX6DOT=BX3
*
* X6 RATE OF MISDISTANCE
      BX6=INTGRL(0.0,BX6DOT)
*
SAMPLE
      CALL   DRWG(1,L,TPER,BX5)
*
TERMINAL
      L=L+1
      IF  (L  .LE.  3)  CALL RERUN
      IF  (L  .GT.  3)  CALL ENDRUN(NPLOT)
PRINT 0.10,TPER,BX5
CONTRL FINTIM=01.0,DELT=0.005,DELS=0.01
END
PARAM NAVC=3.5
END
PARAM NAVC=4.5
END
```

```
        * CLASSICAL P.N IMPLEMENTATICN *
     TIME          TPER          BX5
 0.0           0.0              0.0
 1.0000E-01    3.0000E 00 -9.9575E-02
 2.0000E-01    6.0000E 00 -1.8994E-01
 3.0000E-01    9.0000E 00 -2.5379E-01
 4.0000E-01    1.2000E 01 -2.8481E-01
 5.0000E-01    1.5000E 01 -2.8545E-01
 6.0000E-01    1.8000E 01 -2.5989E-01
 7.0000E-01    2.1000E 01 -2.1221E-01
 8.0000E-01    2.4000E 01 -1.4730E-01
 9.0000E-01    2.7000E 01 -7.1536E-02
 1.0000E 00    3.0000E 01  4.8619E-03

DSL/360 SIMULATION TIME=    0.29 SECONDS.                          81.268

***  MILNE    INTEGRATION USED ***
 0.0           0.0              0.0
 1.0000E-01    3.0000E 00 -9.9446E-02
 2.0000E-01    6.0000E 00 -1.8631E-01
 3.0000E-01    9.0000E 00 -2.4063E-01
 4.0000E-01    1.2000E 01 -2.6303E-01
 5.0000E-01    1.5000E 01 -2.6113E-01
 6.0000E-01    1.8000E 01 -2.3830E-01
 7.0000E-01    2.1000E 01 -1.9662E-01
 8.0000E-01    2.4000E 01 -1.3933E-01
 9.0000E-01    2.7000E 01 -7.1197E-02
 1.0000E 00    3.0000E 01  3.9603E-04

DSL/360 SIMULATION TIME=    0.23 SECONDS.                          81.268

***  MILNE    INTEGRATION USED ***
 0.0           0.0              0.0
 1.0000E-01    3.0000E 00 -9.9349E-02
 2.0000E-01    6.0000E 00 -1.8328E-01
 3.0000E-01    9.0000E 00 -2.3123E-01
 4.0000E-01    1.2000E 01 -2.5153E-01
 5.0000E-01    1.5000E 01 -2.5086E-01
 6.0000E-01    1.8000E 01 -2.3009E-01
 7.0000E-01    2.1000E 01 -1.9086E-01
 8.0000E-01    2.4000E 01 -1.3641E-01
 9.0000E-01    2.7000E 01 -7.1433E-02
 1.0000E 00    3.0000E 01 -2.1550E-03

DSL/360 SIMULATION TIME=    0.26 SECONDS.                          81.268

NPLOT= 3
```

* CLASSICAL P.N IMPLEMENTATION *

TIME	TPER	BX5
0.0	0.0	0.0
1.0000E-01	3.0000E 00	-9.8587E-02
2.0000E-01	6.0000E 00	-1.6139E-01
3.0000E-01	9.0000E 00	-1.6131E-01
4.0000E-01	1.2000E 01	-1.5799E-01
5.0000E-01	1.5000E 01	-1.3951E-01
6.0000E-01	1.8000E 01	-1.1586E-01
7.0000E-01	2.1000E 01	-8.6436E-02
8.0000E-01	2.4000E 01	-5.8259E-02
9.0000E-01	2.7000E 01	-3.3942E-02
1.0000E 00	3.0000E 01	7.0637E-03

DSL/360 SIMULATION TIME= 0.17 SECONDS. 81.268 0

NPLOT= 1

* CLASSICAL P.N IMPLEMENTATION *

TIME	TPER	BX5
0.0	0.0	0.0
1.0000E-01	3.0000E 00	-9.8901E-02
2.0000E-01	6.0000E 00	-1.6939E-01
3.0000E-01	9.0000E 00	-1.8965E-01
4.0000E-01	1.2000E 01	-1.9642E-01
5.0000E-01	1.5000E 01	-1.8096E-01
6.0000E-01	1.8000E 01	-1.5650E-01
7.0000E-01	2.1000E 01	-1.2037E-01
8.0000E-01	2.4000E 01	-8.1762E-02
9.0000E-01	2.7000E 01	-4.3454E-02
1.0000E 00	3.0000E 01	-4.4601E-04

DSL/360 SIMULATION TIME= 0.19 SECONDS. 81.268 0

NPLOT= 2

APPENDIX E

COMPUTER PROGRAM SIMULATING THE SUGGESTED IN PART VII.C KINEMATIC HOMING LOOP, UTILIZING A FIRST ORDER AUTOPILOT

Utilized parameters: $\omega_o = 1.0$

$\omega_{ap} = 30.0$ rad/sec

$A = 1.6$

$T = 1$ sec

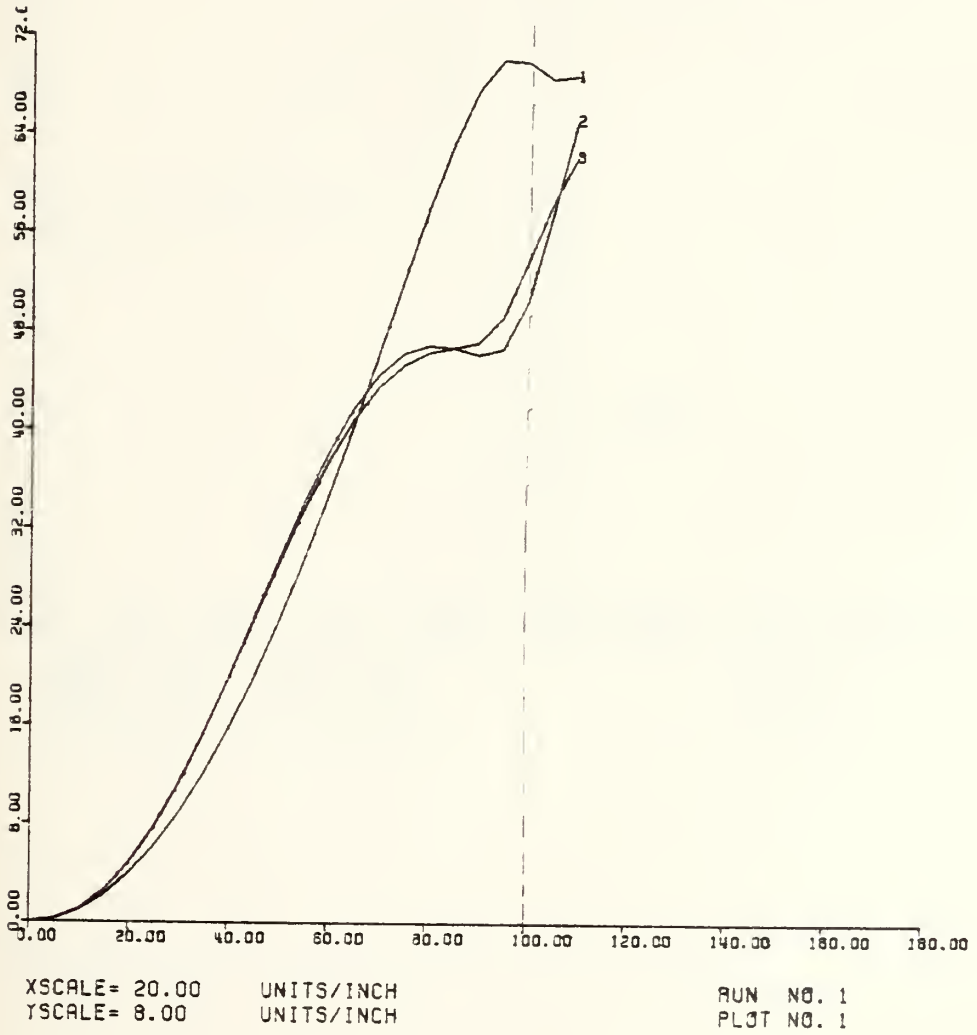

Fig. E-1. Misdistance vs normalized time. Comparison between PN, AP and MCG law.

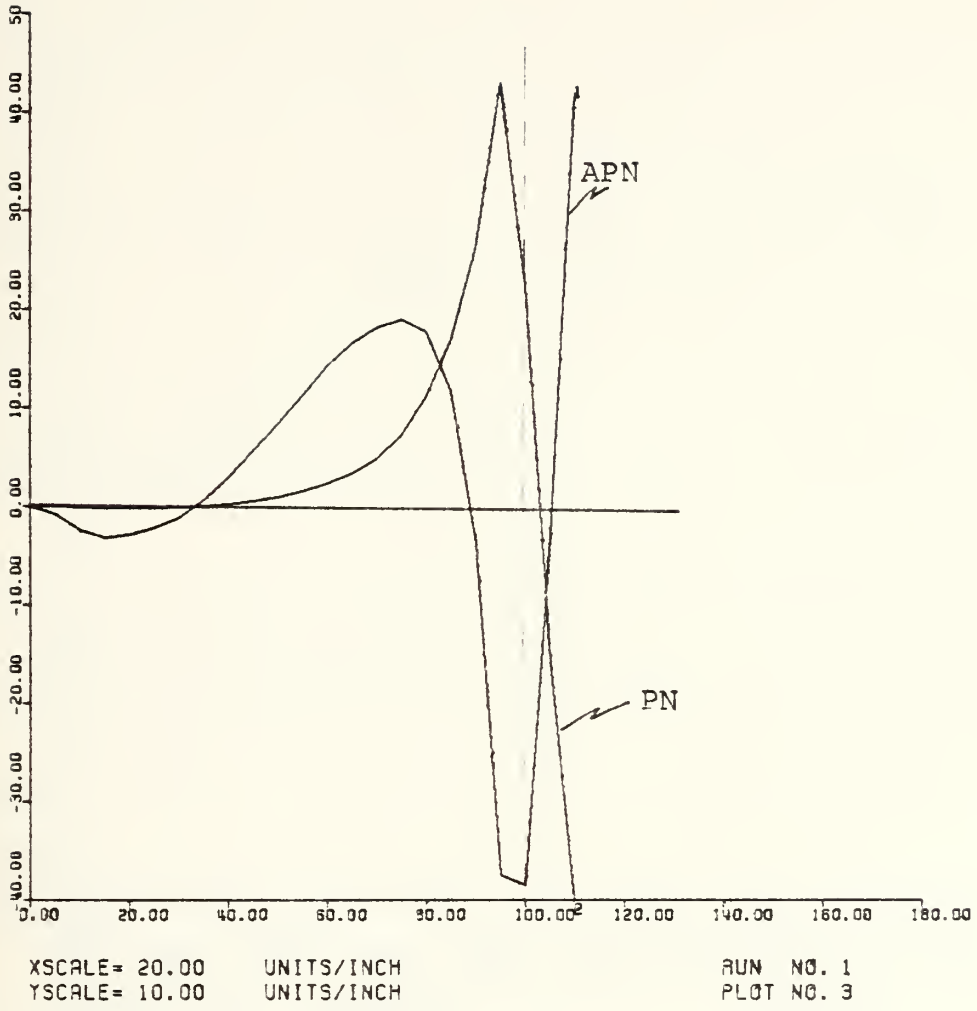

Fig. E-2. Required lateral acceleration in g's vs. time gone. Comparison between APN and PN

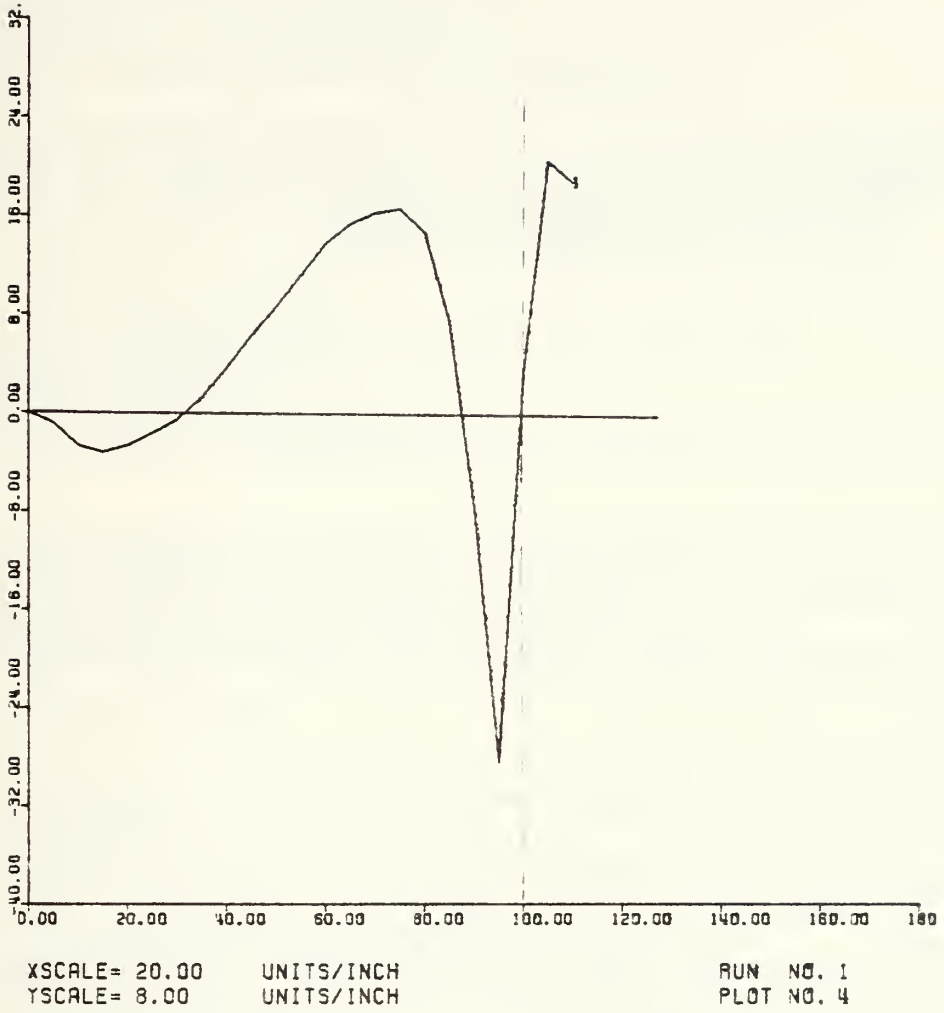

Fig. E-3. Required lateral acceleration in g's vs. time gone, in case of MCG law utilization.

INPUT FOR DSL/360 TRANSLATOR (VERSION 1)

```
TITLE * GUIDANCE LAWS COMPARISON *
INTGER NPLOT,K,SP1,NP1
CONST NPLOT=5,VCLOS=1500.0,NT=192.,TS=0.05,K=1
STORAG N(7)
TABLE N(1-7)=0.4,0.6,0.8,1.0,1.2,1.4,1.6
PARAM TENG=1.0,B=0.0,ICX5=0.0,OMEGAP=1.2,  ...
      SP1=3,SP2=0.0,SP3=.3,NP1=5,NP2=0.0,NP3=.586
PREPAR TPER,PX5,AX5,MX5,NAVCM,NAVC,NLPN,NLAPN,NLMCG,RTM
INTEG MILNE
*
*****************************************************************
* SP1,NP1 ARE THE SEEDS FOR THE RADOM NOISE GENERATION FUNCTION(NORMAL)*
* SP2,NP2 ARE THE  MEANS  OF S-SOURCE + N-GLINT NOISE RESPECTIVELY      *
* SP3,NP3 ARE THE STANDARD DEVIATIONS OF S-SOURCE + N-GLINT NOISE.      *
* X5 MISDISTANCE IN FEET. P  STANDS FOR PROPORTIONAL NAVIGATION         *
*                         A  STANDS FOR AUGMENT  P.N                    *
*                         M  STANDS FOR MODERN CONTROL GUIDANCE         *
* CMEGAP AUTOPILOT'S BANDWIDTH                                          *
* CMEGAZ                                                                *
* TENG TOTAL TIME OF ENGAGMENT                                          *
* A FRACTION OF ESTIMATED TIME TO GO OVER TRUE TIME TO GO               *
* B BIAS FACTOR IN ESTIMATED TIME TO GO                                 *
* VCLCS CLOSING VELOCITY                                                *
* NT TARGET'S ACCELERATION IN G'S                                       *
* TS SEEKER'S INVERCE OF TIME CONSTANT                                  *
*****************************************************************
*
*
DYNAMIC
********
*****************************************************************
* NAVC EFFECTIVE NAVIGATION CONSTANT (TIME INVARIED FOR PN + APN)  *
* NAVCM  EFFECTIVE NAVIGATION CONSTANT UTILIZED BY MODERN CONTROL  *
*        GUIDANCE.IT IS A TIME VARYING CONSTANT.                   *
* TPER PERCENTAGE OF ELLAPSED TIME (NORMALIZED TIME GONE)          *
*****************************************************************
*
*
      TPER=TIME*100./TENG
      A=N(K)
*     A=1.
*
*****************************************************************
* US SYSTEM'S NOISE                                                *
* UN GLINT NOISE                                                   *
* FOR RANDOM NOISE WE USE GAUSSIAN DISTRIBUTION.FOR THIS IMPLEMENTATION*
* WE USED THE D.S.L FUNCTION  Y=NORMAL(P1,P2,P3)  (SEE D.S.L MANUAL  *
*                                                  PAGE 6-12 )     *
* IF USE MULTIPLE RUNS THEN RE-ASSIGNTHE P1 VALUE                  *
* OMEGAZ IS A FUNCTION OF SIGNAL AND NOISE SPECTRALDENSITIES.THERFORE, *
*        OMEGAZ,+P3 FOR US AND UN MUST BE INTERELATED AND THEIR COR-  *
*        RESPONDING VALUES MUST BE ENTERED APPROPRIATELLY.           *
* IN CASE OF TESTING FOR NOISE EFFECTS IN THE SYSTEM, MULTIPLE RUNS  *
*        MUST BE CONDUCTED HAVING EXACTLY THE SAME SYSTEM'S PARAMETERS *
*        BUT DIFFERENT VALUES OF  P1 ,IN ORDER TO PRODUCE DEFFERENT  *
*        RANDOM SEQUENCE IN THE NOISE GENERATOR.                     *
*****************************************************************
*
      US=10.0*(NORMAL(SP1,SP2,SP3))
      UN=10.0*(NORMAL(NP1,NP2,NP3))
      OMEGAZ=(SP3/NP3)**(1./3.)
      TIMEGO=A*(TENG-TIME) + B
      IF   ( TIMEGO  .LT.  0.1 )   TIMEGO=0.1
      T=TIMEGO*OMEGAP
      IF   ( T   .LT.   0.1 )  T=0.1
*
*****************************************************************
*  THE BEST FOUND VALUE FOR  T  FOR AVOIDING OVERFLOW IS  T=0.1   *
*  DO NOT ERASE THE FOLLOWING  IF STATEMENT FOR  AA ,OTHERWISE*   *
*  OVERFLOW OCCURES AS IT IS BEYOND THE COMPUTER'S CAPABILITIES   *
*  THE CALCULATION OF EXPONENT BIGGER THAN  170. *                *
*****************************************************************
*
*
      AA=2.*T
      IF   ( AA  .GT.  170. )  AA=170.0
*
```

```
*************************************************************************
* NAVC  EFFECTIVE NAVIGATION CONSTANT UTILIZED BY CLASSICAL P.N +       *
*       AUGMENT P.N. IT IS TIME INVARIED                                *
* NAVCM EFFECTIVE NAVIGATION CONSTANT UTILIZED BY MODERN CONTROL        *
*       GUIDANCE. IT IS TIME VARYING                                    *
* NNAVCM,DNAVCM NUMERATOR + DENOMINATOR OF NAVCM.THESE ARE CALCULATED   *
*       SEPERATELLY TO AVOID UNDETERMINED FUNCTION OF THE FORM (0.0/0.0)*
*       CASE WHICH RESULTS AS T  GOES TO ZERO                           *
*************************************************************************
*
      NAVC=3.
      NNAVCM=6.*T**2*(EXP(-T)-1.+T)
      DNAVCM=2.*T**3.+3.+6.*T*(1.-T)-12.*T*EXP(-T)-3.*EXP(-AA)
      NAVCM=NNAVCM/DNAVCM
      RTM=VCLOS*TIMEGO
      IF   ( RTM  .LT.  1. )  RTM=1.
*
*************************************************************************
* RTM RELATIVE INSTANTANEOUS DISTANCE BETWEEN MISSILE + TARGET          *
* MX4DOT RATE OF MISSILE'S ACTUAL ACCELERATION IN CASE OF M.C.G  LAW    *
*                                                                       *
* C1,C2            RELATIONS IMPLEMENTING THE     P.N.   LAW           *
* C1,C2,C3         RELATIONS IMPLEMENTING THE  A.P.N.   LAW            *
* C1M,C2M,C3M,C4M  RELATIONS IMPLEMENTING THE  M.C.G.   LAW            *
*************************************************************************
*
      C1 = NAVC/(TIMEGO**2)
      C2 = NAVC/TIMEGO
      C3 = NAVC*0.5*NT
      C1M= NAVCM/(TIMEGO**2)
      C2M= NAVCM/TIMEGO
      C3M= NAVC1*0.5*NT
      C4M= NAVCM/(T**2)*(1.-T-EXP(-T))
*
*
DERIVATIVE
**********
      PX1DOT=PX2+2.*OMEGAZ*(RTM*PX8-PX1)
      AX1DOT=AX2+2.*OMEGAZ*(RTM*AX8-AX1)
      MX1DOT=MX2+2.*OMEGAZ*(RTM*MX8-MX1)
*
* X1 ESTIMATED MISDISTANCE
      PX1=INTGRL(0.0,PX1DOT)
      AX1=INTGRL(0.0,AX1DOT)
      MX1=INTGRL(0.0,MX1DOT)
*
      PX2DOT=PX3+2.*(RTM*PX8-PX1)*OMEGAZ**2-PX4
      AX2DOT=AX3+2.*(RTM*AX8-AX1)*OMEGAZ**2-AX4
      MX2DOT=MX3+2.*(RTM*MX8-MX1)*OMEGAZ**2-MX4
*
* X2 ESTIMATED RATE OF MISDISTANCE
      PX2=INTGRL(0.0,PX2DOT)
      AX2=INTGRL(0.0,AX2DOT)
      MX2=INTGRL(0.0,MX2DOT)
*
      PX3DOT=(OMEGAZ**3)*(RTM*PX8-PX1)
      AX3DOT=(OMEGAZ**3)*(RTM*AX8-AX1)
      MX3DOT=(OMEGAZ**3)*(RTM*MX8-MX1)
*
* X3 ESTIMATED RELATIVE ACCELERATION
      PX3=INTGRL(0.0,PX3DOT)
      AX3=INTGRL(0.0,AX3DOT)
      MX3=INTGRL(0.0,MX3DOT)
*
      PX4DOT=OMEGAP*(C1*PX1+C2*PX2-PX4)
      AX4DOT=OMEGAP*(C1*AX1+C2*AX2+C3*AX3-AX4)
      MX4DOT=OMEGAP*(C1M*MX1+C2M*MX2+C3M*MX3+(C4M-1.)*MX4)
*
* X4 COMMANDED ACCELERATION (NL)
      PX4=INTGRL(0.0,PX4DOT)
      AX4=INTGRL(0.0,AX4DOT)
      MX4=INTGRL(0.0,MX4DOT)
*
* NLPN,NLAPN,NLMCG  ACHIEVED ACCELERATION IN G S FOR CORRESPONDING CASES
      NLPN =PX4/32.17
      NLAPN=AX4/32.17
      NLMCG=MX4/32.17
*
      PX5DOT=PX6
      AX5DOT=AX6
      MX5DOT=MX6
*
```

```
* X5 ACTUAL MISDISTANCE
      PX5=INTGRL(0.0,PX5DOT)
      AX5=INTGRL(0.0,AX5DOT)
      MX5=INTGRL(0.0,MX5DOT)
*
      PX6DOT=NT-PX4+PX7
      AX6DOT=NT-AX4+AX7
      MX6DOT=NT-MX4+MX7
*
* X6 RATE OF MISDISTANCE
      PX6=INTGRL(0.0,PX6DOT)
      AX6=INTGRL(0.0,AX6DOT)
      MX6=INTGRL(0.0,MX6DOT)
*
      PX7DOT=US
      AX7DOT=US
      MX7DOT=US
*
* X7 RELATIVE ACCELERATION
      PX7=INTGRL(0.0,PX7DOT)
      AX7=INTGRL(0.0,AX7DOT)
      MX7=INTGRL(0.0,MX7DOT)
*
      PX8DOT=PX5/(TS*RTM)-PX8/TS+UN/TS/RTM
      AX8DOT=AX5/(TS*RTM)-AX8/TS+UN/TS/RTM
      MX8DOT=MX5/(TS*RTM)-MX8/TS+UN/TS/RTM
*
* X8 ESTIMATED L.O.S ANGLE IN RAD
      PX8=INTGRL(0.0,PX8DOT)
      AX8=INTGRL(0.0,AX8DOT)
      MX8=INTGRL(0.0,MX8DOT)
SAMPLE
TERMINAL
      K=K+1
      IF  (K  .GT.  7)    CALL ENDRW(NPLOT)
      IF  (K  .LE.  7)    CALL RERUN
PRINT 0.25,A,TPER,PX5,AX5,MX5,OMEGAZ,NLPN,NLAPN,NLMCG
CCNTRL FINTIM=01.10,DELT=0.005,DELS=0.05
END
PARAM K=1,SP1=3,NP1=5,NP3=.3
END
PARAM K=1,SP1=7,NP1=3,NP3=.174
END
PARAM K=1,SP1=11,NP1=13,NP3=.109
END
PARAM K=1,SP1=3,NP1=11,NP3=.07
END
```

APPENDIX F

COMPUTER PROGRAM SIMULATING THE SUGGESTED IN PART VII.C KINEMATIC HOMING LOOP, UTILIZING A 2ND ORDER AUTOPILOT

Utilized Parameters: $\omega_o = 1.0$

$\omega_{ap} = 3.0$ rad/sec

$A = 1.6$

$T = 1.0$ sec

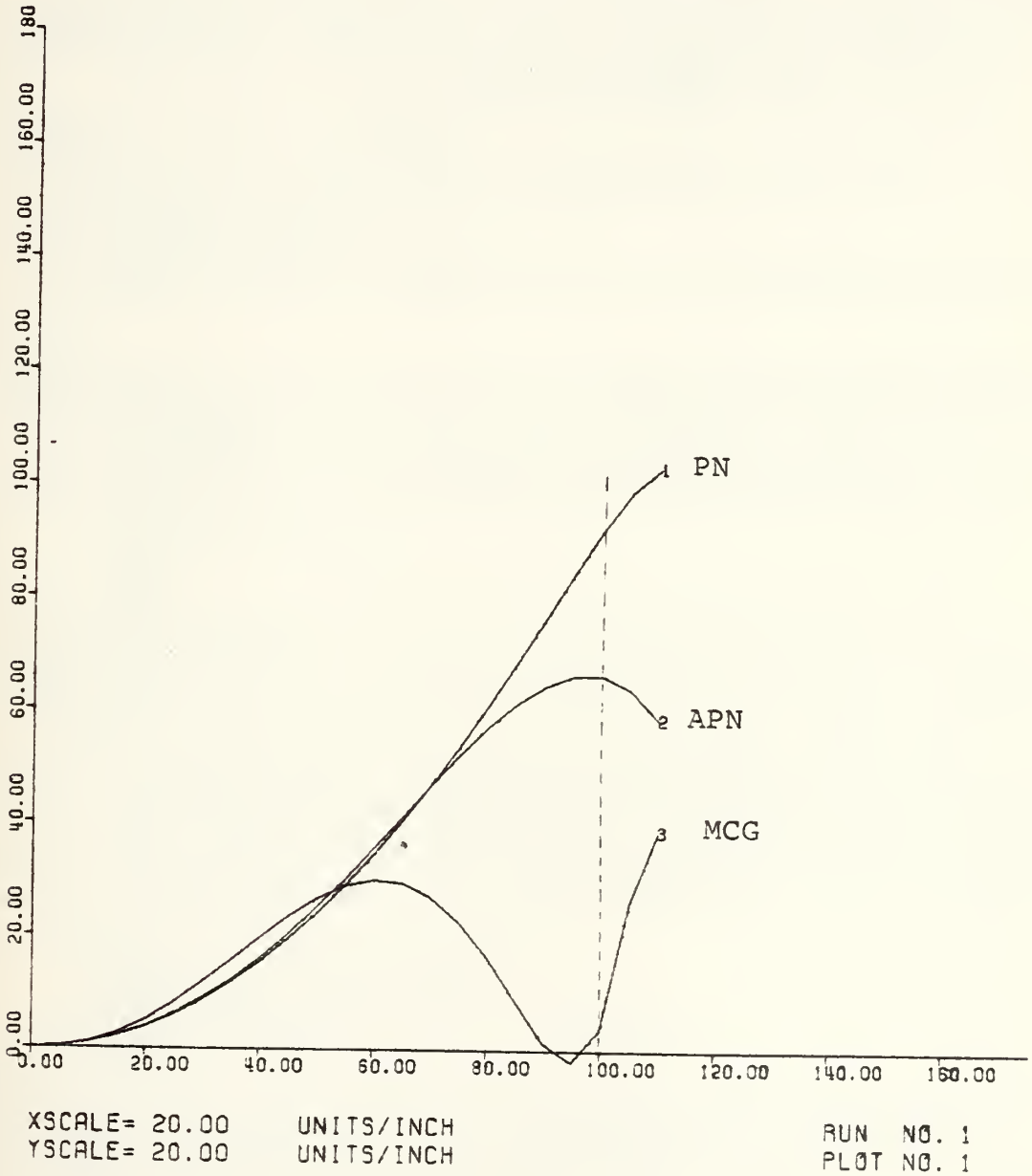

Fig. F-1. Misdistance vs. normalized time gone. Comparison between PN, APN and MCG law.

INPUT FOR CSL/360 TRANSLATOR (VERSION 1)

```
TITLE * GUIDANCE LAWS COMPARISON *
INTEGER NPLOT,K,SP1,NP1
CONST NPLOT=1,VCLOS=1500.0,NT=192.,TS=0.01,MA=0.5,K=1
STORAG N(7)
TABLE N(1-7)=0.4,0.6,0.8,1.0,1.2,1.4,1.6
PARAM TENG=1.0,B=0.0,IC>=0.0,OMEGAP=30.,   ...
      SP1=3,SP2=0.0,SP3=.3,NP1=5,NP2=0.0,NP3=.3
PREPAR TPER,PXS,AXS,MXS,NAVCM,NAVC,NLPN,NLAPN,NLMCG,RTM
INTEG MILNE
*
*****************************************************************
* SP1,NP1 ARE THE SEEDS FOR THE RADOM NOISE GENERATION FUNCTION(NORMAL)*
* SP2,NP2 ARE THE  MEANS  OF S-SOURCE + N-GLINT NOISE RESPECTIVELY  *
* SP3,NP3 ARE THE STANDARD DEVIATIONS OF S-SOURCE + N-GLINT NOISE.  *
* XS MISDISTANCE IN FEET. P  STANDS FOR PROPORTIONAL NAVIGATION     *
*                         A  STANDS FOR AUGMENT  P.N                *
*                         M  STANDS FOR MODERN CONTROL GUIDANCE     *
* OMEGAP AUTOPILOT'S BANDWIDTH                                      *
* OMEGAZ                                                            *
* TENG TOTAL TIME OF ENGAGMENT                                      *
* A FRACTION OF ESTIMATED TIME TO GO OVER TRUE TIME TO GO           *
* B BIAS FACTOR IN ESTIMATED TIME TO GO                             *
* VCLOS CLOSING VELOCITY                                            *
* NT TARGET'S ACCELERATION IN G'S                                   *
* TS SEEKER'S INVERSE OF TIME CONSTANT                              *
*****************************************************************
*
*
DYNAMIC
********
*****************************************************************
* NAVC EFFECTIVE NAVIGATION CONSTANT (TIME INVARIED FOR PN + APN) *
* NAVCM  EFFECTIVE NAVIGATION CONSTANT UTILIZED BY MODERN CONTROL *
*        GUIDANCE.IT IS A TIME VARYING CONSTANT.                  *
* TPER PERCENTAGE OF ELLAPSED TIME (NORMALIZED TIME SCALE)        *
*****************************************************************
*
*
      TPER=TIME*100./TENG
*     A=N(K)
      A=1.6
*
*****************************************************************
* LS SYSTEM'S NOISE                                               *
* LN GLINT NOISE                                                  *
* FOR RANDOM NOISE WE USE GAUSSIAN DISTRIBUTION.FOR THIS IMPLEMENTATION*
* WE USED THE C.S.L FUNCTION  Y=NORMAL(P1,P2,P3)  (SEE C.S.L MANUAL *
*                                                  PAGE 6-12 )    *
* IF USE MULTIPLE RUNS THEN RE-ASSIGNTHE P1 VALUE                 *
* OMEGAZ IS A FUNCTION OF SIGNAL AND NOISE SPECTRALDENSITIES.THEREFORE, *
*        OMEGAZ,+P3 FOR LS AND LN MUST BE INTERELATED AND THEIR CORR- *
*        RESPONDING VALUES MUST BE ENTERED APPROPRIATELLY.          *
* IN CASE OF TESTING FOR NOISE EFFECTS IN THE SYSTEM, MULTIPLE RUNS *
*        MUST BE CONDUCTED HAVING EXACTLY THE SAME SYSTEM'S PARAMETERS *
*        BUT DIFFERENT VALUES OF  P1 ,IN ORDER TO PRODUCE DEFFERENT *
*        RANDOM SEQUENCE IN THE NOISE GENERATOR.                    *
*****************************************************************
*
      LS=10.0*(NORMAL(SP1,SP2,SP3))
      LN=10.0*(NORMAL(NP1,NP2,NP3))
      OMEGAZ=(SP3/NP3)**(1./3.)
      TIMEGO=A*(TENG-TIME) + B
      IF   ( TIMEGO  .LT.  0.1 )   TIMEGO=0.1
      T=TIMEGO*OMEGAP
      IF   ( T   .LT.   0.1 )  T=0.1
*
*****************************************************************
*  THE BEST FOUND VALUE FOR  T  FOR AVOIDING OVERFLOW IS  T=0.1  *
*  DO NOT ERASE THE FOLLOWING  IF STATEMENT FOR  AA ,OTHERWISE*  *
*  OVERFLOW OCCURES AS IT IS BEYOND THE COMPUTER'S CAPABILITIES  *
*  THE CALCULATION OF EXPONENT BIGGER THAN  170. *               *
*****************************************************************
*
*
      AA=2.*T
      IF   ( AA  .GT.  170. )  AA=170.0
*
```

```
**********************************************************************
* NAVC  EFFECTIVE NAVIGATION CONSTANT UTILIZED BY CLASSICAL P.N +    *
*       AUGMENT P.N. IT IS TIME INVARIEC                             *
* NAVCM EFFECTIVE NAVIGATION CONSTANT UTILIZED BY MODERN CONTROL     *
*       GUIDANCE. IT IS TIME VARYING                                 *
* NNAVCM,DNAVCM NUMERATOR + DENOMINATOR OF NAVCM.THESE ARE CALCULATED*
*       SEPERATELLY TO AVOID UNDETERMINED FUNCTION OF THE FORM (0.0/0.0)*
*       CASE WHICH RESULTS AS T  GOES TO ZERO                        *
**********************************************************************
*
      NAVC=3.
      NNAVCM=6.*T**2*(EXP(-T)-1.+T)
      DNAVCM=2.*T**3.+3.+6.*T*(1.-T)-12.*T*EXP(-T)-3.*EXP(-2A)
      NAVCM=NNAVCM/DNAVCM
      RTM=VCLOS*TIMEGO
      IF   ( RTM  .LT.  1. )  RTM=1.
*
**********************************************************************
* RTM RELATIVE INSTANTANEOUS DISTANCE BETWEEN MISSILE + TARGET       *
* MISDCT RATE OF MISSILE'S ACTUAL ACCELERATION IN CASE OF M.C.G  LAW *
*                                                                    *
* C1,C2             RELATIONS IMPLEMENTING THE    P.N.  LAW         *
* C1,C2,C3          RELATIONS IMPLEMENTING THE  A.P.N.  LAW         *
* C1M,C2M,C3M,C4M   RELATIONS IMPLEMENTING THE  M.C.G.  LAW         *
**********************************************************************
*
      C1 = NAVC/(TIMEGO**2)
      C2 = NAVC/TIMEGO
      C3 = NAVC*0.5*NT
      C1M= NAVCM/(TIMEGO**2)
      C2M= NAVCM/TIMEGO
      C3M= NAVCM*0.5*NT
      C4M= NAVCM/(T**2)*(1.-T-EXP(-T))
*
*
DERIVATIVE
**********
      PX1DOT=PX2+2.*OMEGAZ*(RTM*PX5-PX1)
      AX1DOT=AX2+2.*OMEGAZ*(RTM*AX5-AX1)
      MX1DOT=MX2+2.*OMEGAZ*(RTM*MX5-MX1)
*
* X1 ESTIMATED MISDISTANCE
      PX1=INTGRL(0.0,PX1DOT)
      AX1=INTGRL(0.0,AX1DOT)
      MX1=INTGRL(0.0,MX1DOT)
*
      PX2DOT=PX3+2.*(RTM*PX5-PX1)*OMEGAZ**2-PX4
      AX2DOT=AX3+2.*(RTM*AX5-AX1)*OMEGAZ**2-AX4
      MX2DOT=MX3+2.*(RTM*MX5-MX1)*OMEGAZ**2-MX4
*
* X2 ESTIMATED RATE OF MISDISTANCE
      PX2=INTGRL(0.0,PX2DOT)
      AX2=INTGRL(0.0,AX2DOT)
      MX2=INTGRL(0.0,MX2DOT)
*
      PX3DOT=(OMEGAZ**3)*(RTM*PX5-PX1)
      AX3DOT=(OMEGAZ**3)*(RTM*AX5-AX1)
      MX3DOT=(OMEGAZ**3)*(RTM*MX5-MX1)
*
* X3 ESTIMATED RELATIVE ACCELERATION
      PX3=INTGRL(0.0,PX3DOT)
      AX3=INTGRL(0.0,AX3DOT)
      MX3=INTGRL(0.0,MX3DOT)
* X4 COMMANDED ACCELERATION (NL)
      PX4DOT=PX5
      AX4DOT=AX5
      MX4DOT=MX5
*
      PX4=INTGRL (0.0,PX4DOT)
      AX4=INTGRL (0.0,AX4DOT)
      MX4=INTGRL (0.0,MX4DOT)
*
      PX5DOT=OMEGAP*(C1*PX1+C2*PX2-PX4-2.*MA*PX5)
      AX5DOT=OMEGAP*(C1*AX1+C2*AX2+C3*AX3-AX4-2.*MA*AX5)
      MX5DOT=OMEGAP**2*(C1M*MX1+C2M*MX2+C3M*MX3+(C4M-1.)*MX4) ...
             -2.*MA*OMEGAP*MX5
*
* X5 RATE OF COMMANDED ACCELERATION (NL)
      PX5=INTGRL(0.0,PX5DOT)
      AX5=INTGRL(0.0,AX5DOT)
      MX5=INTGRL(0.0,MX5DOT)
*
```

```
* NLPN,NLAPN,NLMCG  ACHIEVED ACCELERATION IN G S FOR CORRESPONDING CASES
      NLPN =PX4/32.17
      NLAPN=AX4/32.17
      NLMCG=MX4/32.17
*
      PX6DOT=P*7
      AX6DOT=A*7
      MX6DOT=M*7
*
* X6 ACTUAL MISDISTANCE
      PX6=INTGRL(0.0,PX6DOT)
      AX6=INTGRL(0.0,AX6DOT)
      MX6=INTGRL(0.0,MX6DOT)
*
      PX7DOT=NT-PX4+P*8
      AX7DOT=NT-AX4+A*8
      MX7DOT=NT-MX4+M*8
*
* X7 RATE OF MISDISTANCE
      PX7=INTGRL(0.0,PX7DOT)
      AX7=INTGRL(0.0,AX7DOT)
      MX7=INTGRL(0.0,MX7DOT)
*
      PX8DOT=0.0
      AX8DOT=0.0
      MX8DOT=0.0
*
* X8 RELATIVE ACCELERATION
      PX8=INTGRL(0.0,PX8DOT)
      AX8=INTGRL(0.0,AX8DOT)
      MX8=INTGRL(0.0,MX8DOT)
*
      PX9DOT=PX6/(TS*RTM)-P*9/TS+LN/TS/RTM
      AX9DOT=AX6/(TS*RTM)-A*9/TS+LN/TS/RTM
      MX9DOT=MX6/(TS*RTM)-M*9/TS+LN/TS/RTM
*
* X9 ESTIMATED L.O.S ANGLE IN RAD
      PX9=INTGRL(0.0,PX9DOT)
      AX9=INTGRL(0.0,AX9DOT)
      MX9=INTGRL(0.0,MX9DOT)
SAMPLE
      CALL    DRWG(1,1,TPER,PX6)
      CALL    DRWG(1,2,TPER,AX6)
      CALL    DRWG(1,3,TPER,MX6)
      CALL    DRWG(2,1,TPER,NAVCM)
      CALL    DRWG(2,2,TPER,NAVC )
      CALL    DRWG(3,1,TPER,NLAPN)
      CALL    DRWG(3,2,TPER,NLPN )
      CALL    DRWG(3,3,TPER,NLMCG)
*
TERMINAL
***   K=K+1
***   IF  (K  .GT.  7)   CALL ENDRW(NPLOT)
***   IF  (K  .LE.  7)   CALL REPLN
      CALL ENDRW(NPLOT)
PRINT 0.10,TPER,PX5,AX5,MX5,OMEGAZ,NLPN,NLAPN,NLMCG,NAVCM
CONTRL FINTIM=01.10,DELT=0.005,DELS=0.05
*NC
*ARAM K=1,SP1=3,NP1=5,NP3=.3
*NC
*ARAM K=1,SP1=7,NP1=3,NP3=.174
*NC
*ARAM K=1,SP1=11,NP1=13,NP3=.109
*NC
*ARAM K=1,SP1=3,NP1=11,NP3=.07
END
```

LIST OF REFERENCES

1. Garnell, P., and East, D. J., Guided Weapon Control Systems, Pergamon Press Ltd., Headington Hill Hall, 1977.

2. Bryson, A. E., and Ho, Y. C., Applied Optimal Control, Blaisdell Publishing Co., Waltham, Massachusetts, 1969.

3. Northrop Corporation Division NORAIR, Dynamics of the Airframe, 1952.

4. Chin, S. S., Missile Configuration Design, McGraw-Hill, New York, 1961.

5. Nesline, F. William, and Zarchang, Paul, "A New Look at Classical vs Modern Homing Missile Guidance," Journal of Guidance and Control, Vol. 4, No. 1, pp. 78-85, Jul-Aug 1980.

6. Cottrell, R. G., "Optimal Intercept Guidance for Short-Range Tactical Missiles," AIAA Journal, Vol. 9, pp 1414-1415, July 1971.

7. Missile Systems Division, Raytheon Co., Bedford, Massachusetts, Report No. P247, Classical and Modern Guidance of Homing Interceptor Missiles, April 1976.

8. George, L. C., "Missile Guidance and Control System Design Trends," SAE paper, National Aerospace Engineering and Manufacturing Meeting 740873, 1974.

9. Gregory, P. C., "General Considerations in Guidance Control Technology," Guidance and Control of Tactical Missiles, AGARD Report L.S-52.

10. Wagner, J. T., and McAllister, D. F., "Simplified Performance Analysis of Space and Missile Guidance," American Astronautical Society and ORSA, June 1969.

11. I.I.T. Research Institute Report, GACIAC HB-78-01, Chicago, Illinois, Guidance Law Handbook for Classical Proportional Navigation, by L. O. Paarman, J. M. Farone and C. W. Smoots, June 1978.

12. Fitzgerall, R. G., and Zarchan, P., "Shaping Filters for Randomly Initiated Target Maneuvers," AIAA Guidance and Control Conference, Palo Alto, California, August 1978.

13. Wiener, N., Extrapolation, Interpolation and Smoothing of Stationary Time Series, MIT Press, Cambridge, Massachusetts, 1949.

14. Wong, T. W. J., "Guidance Systems for Air-to-Air Missiles," Interavia, pp. 1525-1528, November 1961.

15. Kalman, R. E., and Bucy, R., "New Results in Linear Filtering and Prediction," Journal of Basic Engineering, Vol. 83D, pp. 95-108, 1961.

16. Raytheon Memorandum SAD-1230, Bedford, Massachusetts, A Simple Derivation of Certain Optimal Control Laws, by I. Kliger, November 1970.

INITIAL DISTRIBUTION LIST

		No. Copies
1.	Defense Technical Information Center Cameron Station Alexandria, Virginia 22314	2
2.	Library, Code 0142 Naval Postgraduate School Monterey, California 93940	2
3.	Department Chairman, Code 62 Department of Electrical Engineering Naval Postgraduate School Monterey, California 93940	1
4.	Department Chairman, Code 67Pl Department of Aeronautical Engineering Naval Postgraduate School Monterey, California 93940	1
5.	Professor Daniel J. Collins, Code 67Co Department of Aeronautical Engineering Naval Postgraduate School Monterey, California 93940	3
6.	Professor George Thaler, Code 62Tr Department of Electrical Engineering Naval Postgraduate School Monterey, California 93940	2
7.	Hellenic General Naval Staff 2nd Branch, Educations Department Stratopedon Papagou Athens, Greece	3
8.	LT Gregory George Voulgarakis H.N. Thessalonikis 8, Holargos Athens, Greece	3
9.	LT Elias D. Gatsos H.N. 105 Brownell Circle Monterey, California 93940	1